

CATALYSIS IN BIOPOLYMER CHEMISTRY

by

Joseph Bartholomew Binder

A Dissertation Submitted in Partial Fulfillment
of the Requirements for the degree of

Doctor of Philosophy
(Chemistry)

at the

UNIVERSITY OF WISCONSIN-MADISON

2009

A dissertation entitled

CATALYSIS IN BIOPOLYMER CHEMISTRY

submitted to the Graduate School of the
University of Wisconsin-Madison
in partial fulfillment of the requirements for the
Degree of Doctor of Philosophy

by

Joseph Bartholomew Binder

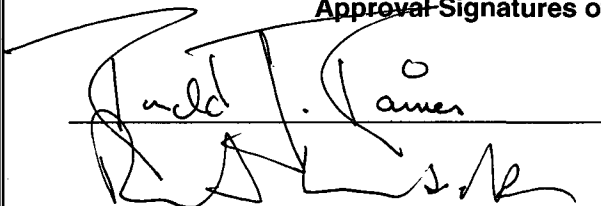


Date of Final Oral Examination: April 30, 2009

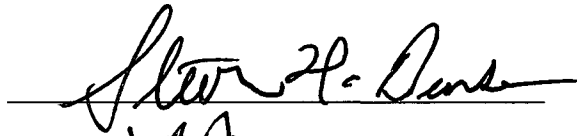
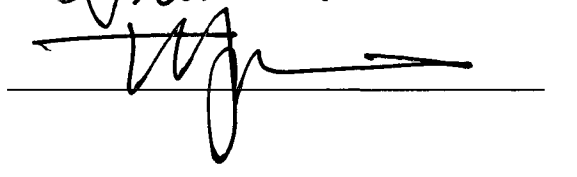
Month & Year Degree to be awarded: **December**

May 2009

August

Approval Signatures of Dissertation Committee

Signature, Dean of Graduate School

 A.W.

ABSTRACT

CATALYSIS IN BIOPOLYMER CHEMISTRY

Joseph Bartholomew Binder

Under the supervision of Professor Ronald T. Raines

At the University of Wisconsin–Madison

Biopolymers such as proteins and polysaccharides are challenging yet important targets for catalytic chemical modification. Proteins comprise as much as three-quarters of the human body when water and fat are excluded, while polysaccharides make up about two-thirds of plant dry mass. Consequently, proteins are critical targets for human health and polysaccharides are promising resources for renewable products. In this dissertation, I report my research on both olefin metathesis reactions for decoration of proteins in water and catalytic chemistry for conversion of biomass into fuels and chemicals.

Olefin metathesis is a revolutionary tool for chemical synthesis and water-tolerant metathesis catalysts hold promise for chemical biology. Chapter One reviews applications of olefin metathesis in chemical biology and the development of aqueous olefin metathesis catalysts. In its final sections, the chapter describes other researchers' recent use of metathesis in aqueous solvent mixtures to decorate a protein, vividly illustrating the utility of this method.

Chapter Two recounts my synthesis of olefin metathesis catalysts bearing both *N*-heterocyclic carbene and salicylaldimine ligands. Although this ligand pairing had been

previously reported in the literature, I was the first to prepare the authentic ruthenium complexes and confirm their structure using X-ray crystallographic analysis. These highly stable catalysts perform ring-closing metathesis of both dienes and enynes in high yields in protic media under air.

In Chapter Three, I describe my development of strategies for using conventional olefin metathesis catalysts in water–organic solvent mixtures. The combination of the second-generation Hoveyda–Grubbs complex and solvents such as 1,2-dimethoxyethane and acetone proved particularly efficacious, enabling ring-closing and cross metathesis in aqueous media, even in the presence of proteins.

My work on aqueous olefin metathesis laid the foundations for construction of modified biopolymers with novel structures and functions. In contrast, raw materials such as biomass usually must be chemically deconstructed for conversion into energy and materials to supply civilization. Production of renewable building blocks through such transformations is the focus of the second half of this dissertation. Chapter Four details my invention of a process for transformation of lignocellulosic biomass into simple furan molecules. The privileged pairing of chromium salts and halide additives produced extraordinarily high yields of 5-hydroxymethylfurfural (HMF) from not only fructose and glucose but also cellulose and corn stover. Furthermore, I demonstrated that hydrogenolysis of HMF from corn stover yields the liquid fuel 2,5-dimethylfuran, offering a two-step direct route from biomass to biofuels.

In the next chapters I explore more extensively the chromium-catalyzed synthesis of furans from mono- and polysaccharides. The disparate reactivity of mannose and

galactose, two monomers from hemicellulose, is the subject of Chapter Five. While mannose is readily converted into HMF, galactose performs poorly. These results and the behavior of other sugars provide support for a mechanism in which chromium ions catalyze the isomerization of aldoses into ketoses. Chapter Six examines specifically the synthesis of furfural from xylose and xylan. Using chromium salts, I accomplished the dehydration of xylose under more mild conditions than are typical, suggesting that chromium facilitates an alternative, low-energy pathway.

Traditional Brønsted acid catalysis was first reported in 1819 as a means to depolymerize cellulose *en route* to ethanol. Chapter Seven describes the synergy of this antique method with modern ionic liquid solvents for fast, efficient saccharification of biomass. Sugars produced from cellulose or corn stover by this method can be recovered with quantitative recycling of the ionic liquid and fermented by bacteria and yeasts to produce ethanol.

Finally, I use Chapter Eight to propose possible future directions for these projects. In particular, biomass transformation offers rich opportunities for the application of modern organic chemistry, such as designer solvents and transition metal catalysis. These possibilities and this dissertation reflect the power of organic chemistry for constructing and dismantling biological materials. Organic matter, whether the stuff of humans or the stuff of plants, is at the center of today's challenges in health and energy, and organic chemistry is the fundamental tool for its manipulation.

ACKNOWLEDGEMENT

When I raise my head from the computer screen long enough to consider it, I find that being on the brink of completing my dissertation has a surreal feel to it because I have been working toward this goal since my childhood. This document reflects the influence of the many people who have aided me along the journey from pre-school to grad school.

Foremost I am grateful to my family who have passed down the value of hard work and helped me throughout my education. In particular, my father and mother have been phenomenal role models and provided so much advice and support, and my sisters and brother have been invaluable companions.

If, as it has been said, the Biochemistry Addition has been my home in Madison, my lab has been my second family. I am deeply indebted to my advisor, Ron Raines, for his guidance in becoming a scientist and his encouragement in being fearless. The extraordinary freedom and responsibility which I enjoyed in his lab have enabled my professional growth and provided me with unique experiences, such as the opportunity to travel widely to represent our bioenergy research in the past year.

It has been a privilege to work with many gifted students and postdocs in Ron's group. My labmates' diverse expertise and helpful nature made challenging projects achievable, while their companionship enlivened the hours of flash chromatography and sample preparation. I was fortunate to join the lab with my classmate, Matt Shoulders, who has been an excellent source of advice, camaraderie, and competition through my time at Wisconsin. Frank Kotch cheerfully helped me get started when I first joined the

lab. Along with Matt and Frank, Matt Soellner, Annie Tam, Luke Lavis, Jia-Cherng “Jason” Horng, Daniel Gottlieb, Amit Choudhary, Sayani Chattopadhyay, and Ben Caes comprised the chemistry contingent of the Raines Lab and built an exciting and enjoyable environment for doing science. I am excited that Ben Caes has joined me on developing biomass conversion in the lab, while Rex Watkins has bravely collaborated with me on olefin metathesis. I have had the pleasure of working with Christine Bradford first on peptide cross metathesis during her rotation and then on synthesis of the “sulfate sponge,” and I am grateful that she is bringing these projects to life. My labmates on the biological side, including Rex, Greg Ellis, and Tom Rutkoski, were invaluable aids for my brief stint of fermentation.

It has truly been a joy to do research with Jackie Blank and Anthony Cefali over the past two years. I appreciate their patience through the travails of wild experiments, my travel schedule, and analytical balance drudgery, and the results of their motivation and hard work are evident in Chapters Five and Six. Jackie’s dedication and Anthony’s perspective invigorated our work together.

Among the freedoms Ron granted during my career was the career-changing opportunity to work at Pacific Northwest National Lab. My advisor there, Johnathan Holladay, as well as Heather Brown, Mike Gray, Rick Orth, Tom Peterson, Jim White, Conrad Zhang fostered my interest in biomass transformation and prepared me for my current research directions. I am grateful for the training I received there as well as John’s patience as we spent nearly two years preparing a manuscript for *Biomass & Bioenergy*.

I am also indebted to Paul Bloom at Archer Daniels Midland who introduced me to 5-hydroxymethylfurfural and has continued to offer professional guidance.

While in Madison I have been fortunate to meet many friends, including my chemistry classmates and my Wisconsin Track Club teammates, and I thank them for their support and advice. I have been very fortunate to train and compete with the men and women of WTC, and I am especially grateful to Jim Reardon for his coaching and perspective on running and science.

The University of Wisconsin exceeded my expectations for graduate training, in large part due to the excellent faculty and staff. I am grateful to my committee members for their guidance on my dissertation and to the many faculty members involved in my coursework, preliminary exams, and research. Among the staff who made my research possible are Ilia Guzei of the chemistry crystallography facility, Mark Anderson of NMRFAM and the administrative personnel of the Great Lakes Bioenergy Research Center (GLBRC). Participation in the Chemistry–Biology Interface program and the GLBRC has enabled research which would have otherwise been impossible and facilitated my scientific growth. The research opportunities and freedom I have enjoyed at Wisconsin would also not have been possible without funding from the Department of Defense, the Department of Energy, the National Institutes of Health, the National Science Foundation, and ultimately, the taxpayers of the United States of America.

CONTENTS

Abstract	i
Acknowledgement	iv
Contents	vii
List of Tables	xiii
List of Figures	xv
Chapter 1 Olefin Metathesis for Chemical Biology	1
1.1 Introduction	2
1.2 Applications of Olefin Metathesis in Chemical Biology	3
1.3 Olefin Metathesis Catalysts Designed for Water	7
1.3.1 Water-Soluble Phosphine Complexes	7
1.3.2 Polymeric Water-Soluble <i>N</i> -Heterocyclic Carbene Complexes	8
1.3.3 Small-Molecule Water-Soluble <i>N</i> -Heterocyclic Carbene Complexes ..	10
1.4 Olefin Metathesis in Homogeneous Aqueous Solvent Mixtures	12
1.5 Olefin Metathesis on Proteins	13
1.6 Conclusions	14
1.7 Thesis Summary	15
1.8 Acknowledgements	15
Chapter 2 Salicylaldimine Ruthenium Alkylidene Complexes: Metathesis Catalysts Tuned for Protic Solvents.....	16
2.1 Introduction	17
2.2 Results and Discussion.....	19
2.2.1 Synthesis of NHC-Salicylaldimine Complexes	19
2.2.2 Spectral and Structural Characterization of NHC–Salicylaldimine Complexes.....	21
2.2.3 Synthesis of Authentic 10a by Phosphine Displacement with H ₂ IMes ..	24

2.2.4	Ring-Closing Metathesis Activity of 10a–c	24
2.3	Conclusion.....	31
2.4	Acknowledgements	32
2.5	Experimental Section	32
2.5.1	General Considerations	32
2.5.2	Preparation of <i>N</i> -(4-Bromo-2,6-dimethylphenyl)-5-trimethylammoniumsalicylaldehyde Chloride (12c)	34
2.5.3	Preparation of NHC–Imine Complex 10a	34
2.5.4	Preparation of NHC–Imine Complex 10b	35
2.5.5	Preparation of NHC–Imine Complex 10c	36
2.5.6	Preparation of <i>N,N</i> -Di-3-butenyl-2-nitrobenzenesulfonamide (13g) ...	37
2.5.7	Preparation of <i>N</i> -(2-Propenyl)- <i>N</i> -(2-butenyl)-4-methylbenzenesulfonamide (13j).....	37
2.5.8	Preparation of Allyl 1,1-Diphenylpropargyl Ether (13k).....	38
2.5.9	Representative Procedure for RCM Reactions.....	38
2.5.10	Alternative Preparation of NHC–Imine Complex 10a	38
2.5.11	Preparation of Imine Complex 11c	39
2.5.12	Structure Determination of NHC–Imine Complex 10a	40
Chapter 3	Olefin Metathesis in Homogeneous Aqueous Media Catalyzed by Conventional Ruthenium Catalysts.....	55
3.1	Introduction	56
3.2	Results and Discussion.....	58
3.2.1	Solvent Screening.....	58
3.2.2	Catalyst Screening.....	60
3.2.3	Substrate Scope	62
3.3	Conclusion.....	64
3.4	Acknowledgments.....	65

3.5	Experimental Section	65
3.5.1	General Considerations	65
3.5.2	Methyl (<i>d,l</i>)- <i>N</i> -(Allyl)allylglycinate.....	67
3.5.3	Protein Solubility Measurements	68
3.5.4	Representative Procedures for Metathesis Reactions.....	68
Chapter 4	Simple Chemical Transformation of Lignocellulosic Biomass into Furans for Fuels and Chemicals.....	74
4.1	Introduction	75
4.2	Results and Discussion.....	78
4.2.1	Synthesis of HMF from Fructose in DMA with Halide Additives	78
4.2.2	Influence of Halides on the Formation of HMF from Fructose	82
4.2.3	Synthesis of HMF from Glucose in DMA	84
4.2.4	Synthesis of HMF from Cellulose.....	88
4.2.5	Synthesis of HMF and Furfural from Lignocellulosic Biomass	90
4.2.6	Conversion of Lignocellulosic Biomass into 2,5-Dimethylfuran	92
4.3	Conclusion.....	93
4.4	Acknowledgements	94
4.5	Experimental Section	95
4.5.1	General Considerations	95
4.5.2	Analytical Methods	96
4.5.3	Representative Procedure for Synthesis of HMF from Sugars	97
4.5.4	Kinetic Analysis of HMF Formation from Fructose.....	97
4.5.5	Representative Procedure for Synthesis of HMF from Cellulose and Lignocellulose	97
4.5.6	Ion-Exclusion Chromatographic Separation of HMF	98
4.5.7	Synthesis of DMF from Fructose	98
4.5.8	Synthesis of DMF from Corn Stover	99

4.6	Calculations of Energy Yields.....	100
4.6.1	Relevant Enthalpies of Combustion.....	100
4.6.2	Energy Yield for Cellulosic Ethanol Production.....	100
4.6.3	Energy Yield for Furan Production.....	101
Chapter 5	Mechanistic Insights on the Dehydration of Galactose, Lactose, and Mannose to Form HMF	104
5.1	Introduction	105
5.2	Results and Discussion.....	107
5.2.1	Synthesis of HMF from Mannose.....	107
5.2.2	Synthesis of HMF from Galactose and Lactose.....	109
5.2.3	Synthesis of HMF from Tagatose, Psicose, and Sorbose.....	111
5.3	Conclusions	115
5.4	Acknowledgements	116
5.5	Experimental	116
5.5.1	General Considerations	116
5.5.2	Analytical Methods	116
5.5.3	Representative Procedure for Synthesis of HMF from Sugars	117
5.5.4	Determination of L-Sorbose Tautomeric Equilibrium in DMSO.....	117
Chapter 6	Chromium Halide Catalysts for the Synthesis of Furfural from Xylose and Xylan 120	
6.1	Introduction	121
6.2	Results and Discussion.....	123
6.2.1	Conversion of Xylose into Furfural	123
6.2.2	Kinetics and Mechanism of Furfural Synthesis from Xylose	125
6.2.3	Conversion of Xylan into Furfural	127
6.3	Conclusions	131
6.4	Acknowledgements	132

6.5	Experimental	132
6.5.1	General Considerations	132
6.5.2	Analytic Methods	132
6.5.3	Representative Procedure for Synthesis of Furfural from Xylose	133
6.5.4	Representative Procedures for Synthesis of Furfural from Xylan	133
6.5.5	Kinetic Analysis of Furfural Formation from Xylose	134
Chapter 7	Sugars from Biomass in Ionic Liquids	135
7.1	Introduction	136
7.2	Results	139
7.2.1	Reaction of Glucose and Cellulose in [EMIM]Cl	139
7.2.2	Hydrolysis of Cellulose in Alternative Ionic Liquids	146
7.2.3	Hydrolysis of Lignocellulosic Biomass	147
7.2.4	Recovery and Fermentation of Hydrolyzate Sugars	149
7.3	Discussion	151
7.4	Acknowledgements	153
7.5	Experimental Section	154
7.5.1	General Considerations	154
7.5.2	Analytical Methods	155
7.5.3	Representative Procedure for Hydrolysis of Cellulose	155
7.5.4	Representative Reaction of Glucose in [EMIM]Cl	156
7.5.5	Hydrolysis of Xylan	156
7.5.6	Representative Procedure for Hydrolysis of Corn Stover	157
7.5.7	Representative Procedure for Recovery of Sugars and [EMIM]Cl from Hydrolyzates	158
7.5.8	Bacterial Growth Studies	159
7.5.9	Bacterial Fermentation Studies	160

7.5.10	Yeast Growth Studies.....	161
7.5.11	Yeast Fermentation Studies.....	161
Chapter 8	Future Directions.....	163
8.1	Aqueous Olefin Metathesis	164
8.2	Transformation of Renewable Resources into Furan Intermediates	164
8.3	Processing of Lignocellulosic Biomass.....	166
8.4	Conclusions	167
References	168

LIST OF TABLES

Table 2.1 ^1H NMR (CDCl_3) Data for 10a and Related Complexes.....	23
Table 2.2 RCM of Nonpolar Dienes Catalyzed by Ruthenium Complexes under Air.....	26
Table 2.3 RCM of Nonpolar Dienes under Air to Form Six- and Seven-Membered Rings	27
Table 2.4 RCM of Polar Dienes and Enynes Catalyzed by Ruthenium Complexes	29
Table 2.5 Solvent Dependence of RCM of <i>N</i> -Tosyl Diallylamine (13c) Catalyzed by Complex 10b	30
Table 3.1 RCM Catalyzed by 2 in Aqueous Media	59
Table 3.2 RCM of Representative Dienes Catalyzed by 4a in Aqueous Media under Air	63
Table 3.3 CM Catalyzed by 4a in an Aqueous Medium under Air	64
Table 3.4 Substrate and Product ^1H NMR Signals in RCM Reactions	70
Table 4.1 Synthesis of HMF from Fructose.....	79
Table 4.2 Synthesis of HMF from Fructose with [EMIM]Cl	81
Table 4.3 Synthesis of HMF from Fructose with Additives.....	82
Table 4.4 Synthesis of HMF from Glucose	85
Table 4.5 Synthesis of HMF from Glucose with Alternative Ionic Additives	86
Table 4.6 Synthesis of HMF from Glucose in Various Solvents.....	87
Table 4.7 Synthesis of HMF from Cellulose	89
Table 4.8 Synthesis of HMF from Corn Stover and Pine Sawdust	91
Table 5.1 Synthesis of HMF from Mannose.....	108

Table 5.2 Synthesis of HMF from Galactose.....	110
Table 5.3 Synthesis of HMF from Lactose.....	111
Table 5.4 Synthesis of HMF from Tagatose.....	113
Table 5.5 Synthesis of HMF from Psicose and Sorbose.....	115
Table 6.1 Synthesis of Furfural from Xylose.....	124
Table 6.2 Synthesis of Furfural from Xylan at 100 °C	128
Table 6.3 Synthesis of Furfural from Xylan at 120 °C	129
Table 6.4 Synthesis of Furfural from Xylan at 140 °C	129
Table 6.5 Synthesis of Furfural from Xylan after HCl Treatment.....	130
Table 7.1 Hydrolysis of Cellulose in [EMIM]Cl.....	141
Table 7.2 Acid-Catalyzed Degradation of Glucose in [EMIM]Cl.....	143
Table 7.3 Effect of Dissolution Time on Hydrolysis of Cellulose	145
Table 7.4 Hydrolysis of Cellulose in Ionic Liquids.....	147
Table 7.5 Hydrolysis of Corn Stover in [EMIM]Cl.....	148

LIST OF FIGURES

Figure 1.1 Conventional ruthenium catalysts for olefin metathesis.....	2
Figure 1.2 Olefin metathesis reactions and their application to chemical biology.....	6
Figure 1.3 Ruthenium catalysts for aqueous olefin metathesis.....	8
Figure 1.4 Olefin cross metathesis for site-specific protein modification at allyl sulfide substituents.....	14
Figure 2.1 Olefin metathesis catalysts.	19
Figure 2.2 Synthesis of NHC-imine complexes 10a–c by the reported route from 11a and our route from 9d	21
Figure 2.3 Solid-state molecular structure of complex 7a	23
Figure 2.4 ^1H NMR of <i>N</i> -(4-Bromo-2,6-dimethylphenyl)-5- trimethylammoniumsalicylaldimine chloride	42
Figure 2.5 ^{13}C NMR of <i>N</i> -(4-Bromo-2,6-dimethylphenyl)-5- trimethylammoniumsalicylaldimine chloride	43
Figure 2.6 ^1H NMR of NHC–Imine Complex 10a	44
Figure 2.7 ^{13}C NMR of NHC–Imine Complex 10a	45
Figure 2.8 ^1H NMR of NHC–Imine Complex 10b	46
Figure 2.9 ^{13}C NMR of NHC–Imine Complex 10b	47
Figure 2.10 ^1H NMR of NHC–Imine Complex 10c	48
Figure 2.11 ^{13}C NMR of NHC–Imine Complex 10c	49
Figure 2.12 ^1H NMR of Imine Complex 11c	50
Figure 2.13 ^1H NMR of <i>N,N</i> -Di-3-butenyl-2-nitrobenzenesulfonamide	51

Figure 2.14 ^{13}C NMR of <i>N,N</i> -Di-3-butenyl-2-nitrobenzenesulfonamide	52
Figure 2.15 ^1H NMR of Allyl 1,1-diphenylpropargyl ether	53
Figure 2.16 ^{13}C NMR of Allyl 1,1-diphenylpropargyl ether	54
Figure 3.1 Conventional ruthenium olefin metathesis catalysts.	56
Figure 3.2 Metathesis catalysts adapted to aqueous solvents.	58
Figure 3.3 RCM conversion of 0.05 M substrate 13c catalyzed by complexes 1–4a	60
Figure 3.4 Kinetics of RCM of 0.05 M substrate 13c catalyzed by complex 4a in acetone/water monitored by ^1H NMR spectroscopy.....	61
Figure 3.5 ^1H NMR of Methyl (<i>d,l</i>)- <i>N</i> -(Allyl)allylglycinate	71
Figure 3.6 ^{13}C NMR of Methyl (<i>d,l</i>)- <i>N</i> -(Allyl)allylglycinate	72
Figure 3.7 ^1H NMR of Methyl (<i>d,l</i>)- <i>N</i> -(Allyl)allylglycinate hydrochloride.....	73
Figure 4.1 Halide salts in DMA enable previously elusive yields of bio-based chemicals from a variety of carbohydrates.	77
Figure 4.2 Log-log plot of initial rates of HMF formation from fructose vs $[\text{LiI}]$	80
Figure 4.3 Putative mechanisms for the dehydration of fructose and isomerization of glucose.	83
Figure 4.4 Refractive index HPLC traces of representative reaction mixtures.	102
Figure 4.5 Refractive index HPLC trace of corn stover reaction mixture	103
Figure 5.1 Synthesis of HMF from sugars and lignocellulosic biomass.	106
Figure 5.2 Mono- and disaccharide precursors for HMF.....	107
Figure 5.3 Putative mechanism for chromium-catalyzed conversion of glucose and mannose into HMF	109

Figure 5.4 Putative mechanism for chromium-catalyzed conversion of galactose into HMF.....	112
Figure 5.5 ^{13}C NMR Spectrum of L-sorbose in DMSO-d_6	119
Figure 6.1 Synthesis of furfural.	122
Figure 6.2 Log-log plots of initial rates of furfural formation vs [xylose] (A) and $[\text{CrCl}_2]$ (B).....	126
Figure 6.3 Proposed mechanism of chromium-catalyzed dehydration of xylose.....	127
Figure 7.1 Hydrolysis reactions of cellulose and xylan.....	137
Figure 7.2 Acid-catalyzed degradation of glucose in $[\text{EMIM}]\text{Cl}$	142
Figure 7.3 Glucose, HMF, and cellobiose production during cellulose hydrolysis in $[\text{EMIM}]\text{Cl}$	145
Figure 7.4 Aerobic growth of ethanologenic microbes on corn stover hydrolyzate sugars.	150
Figure 7.5 Integrated process for biofuel production using ionic liquid biomass hydrolysis.....	152

CHAPTER 1*

OLEFIN METATHESIS FOR CHEMICAL BIOLOGY

Abstract: Chemical biology relies on effective synthetic chemistry for building molecules to probe and modulate biological function. Olefin metathesis in organic solvents is a valuable addition to this armamentarium, and developments during the previous decade are enabling metathesis in aqueous solvents for the manipulation of biomolecules. Functional group-tolerant ruthenium metathesis catalysts modified with charged moieties or hydrophilic polymers are soluble and active in water, enabling ring-opening metathesis polymerization, cross metathesis, and ring-closing metathesis. Alternatively, conventional hydrophobic ruthenium complexes catalyze a similar array of metathesis reactions in mixtures of water and organic solvents. This strategy has enabled cross metathesis on the surface of a protein. Continuing developments in catalyst design and methodology will popularize the bioorthogonal reactivity of metathesis.

*This chapter has been published, in part, under the same title. Reference: Binder, J. B.; Raines, R. T. *Current Opinion in Chemical Biology* **2008**, 12, 767–773.

1.1 Introduction

Olefin metathesis is a versatile, chemoselective means to create carbon–carbon bonds in a range of molecules including natural products, polymers, and biomolecules.¹⁻⁶ In the metathesis reaction, carbon–carbon multiple bonds are broken and made through the intermediacy of transition metal carbenes. This process requires no additional reagents beyond the alkene starting materials and a metal catalyst, and produces simple alkene byproducts, such as ethylene.

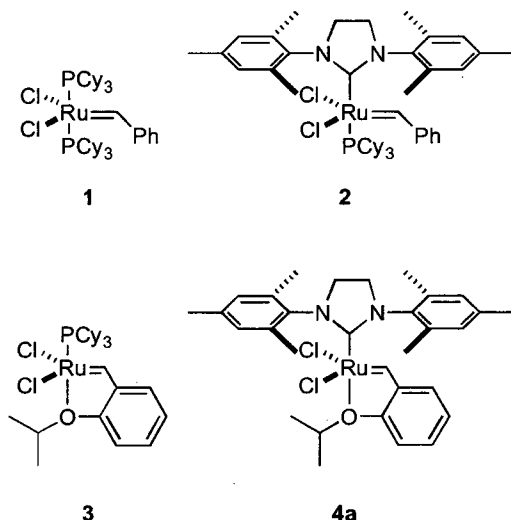


Figure 1.1 Conventional ruthenium catalysts for olefin metathesis

Modern ruthenium olefin metathesis initiators, such as complexes **1–4**, tolerate many functional groups common in biomolecules, including amides, alcohols, and carboxylic acids (**Figure 1.1**). Under some circumstances, metathesis occurs even in the presence of amines and sulfur-containing moieties. Moreover, olefin metathesis is highly chemoselective. Most functional groups other than alkenes and alkynes are not modified by ruthenium metathesis catalysts, and the reaction forms only carbon–carbon bonds.

These characteristics suggest that olefin metathesis is a candidate for a “bioorthogonal” reaction.⁷ Solvent-exposed alkenyl groups are uncommon in living systems, so biomolecules labeled with alkenes could be modified selectively by olefin metathesis.

As far back as 1975, olefin metathesis was exploited to create molecules to modulate biological function. The laboratories of Rossi and Streck independently recognized the opportunity of metathesis to create complex olefins and used primitive ill-defined metathesis catalysts to prepare insect pheromones from simple alkene precursors.^{8,9} Although these initial examples employed sensitive early-transition metal catalysts, major advances in catalyst development since 1975 have produced well-defined metathesis initiators such as air- and moisture-stable ruthenium complexes **1–4**. These user-friendly initiators have popularized metathesis among organic chemists and are being used to address biological questions. Nonetheless, olefin metathesis in biological contexts remains limited because of the difficulty of enacting the reaction in aqueous solvents. Conventional metathesis catalysts are insoluble in water, and metathesis with water-soluble complexes in water tends to be far less efficient than in organic solvents. After briefly surveying applications of metathesis in chemical biology, this review will focus on recent progress toward metathesis in homogenous aqueous solutions in order to modify biomolecules in their native environment.

1.2 Applications of Olefin Metathesis in Chemical Biology

One of the advantages of the metathesis reaction is the wide variety of structures which can be created through its many variations.^{1,2} Ring-opening metathesis polymerization (ROMP) converts a cyclic olefin into an unsaturated polymer (**Figure**

1.2a). Kiessling and coworkers were the first to use ROMP to synthesize bio-active polymers, including multivalent displays of carbohydrates and other bioactive ligands.¹⁰⁻¹² Such polymers have recently been used to modulate immune responses *in vivo*.¹³ Cross metathesis (CM) exchanges the linear alkene fragments, providing a means to connect two molecules (**Figure 1.2b**). The chemoselectivity and functional group tolerance of ruthenium metathesis catalysts enabled Diver and Schreiber to dimerize unprotected FK506 in a single step to form a small-molecule ligand that activated signal transduction and protein expression *in vivo*.¹⁴ More recently, Raines, Miller, and coworkers examined protein folding using a *trans* peptide bond mimic made by CM of two alkene-containing fragments (**Figure 1.2b**).^{15,16} Ring-closing metathesis (RCM) transforms a diene (or alkene–alkyne) into a cyclic alkene and has proven to be a potent method for creating macrocycles, including bio-active cyclic peptidomimetics (**Figure 1.2c**). Demonstrating the robustness of peptide RCM, Liskamp and coworkers have constructed alkene mimics of the five peptide-thioether rings of the lantibiotic nisin.^{17,18} Such carba analogs are anticipated to be more stable than native linkages such as disulfide bonds. Vederas and coworkers confirmed this prediction with the disulfide-bridged peptide macrocycle atosiban, finding that a carba-atosiban generated through RCM had a significantly longer half-life in placental tissue and only moderately lower activity as an oxytocin antagonist (**Figure 1.2c**).^{19,20} RCM offers an alternative approach to improve peptide stability by creating crosslinks between otherwise flexible portions of a peptide chain. Grubbs and coworkers were the first to demonstrate that RCM could be used to tether residues of helical peptides.²¹ From this initial report, the field of peptide “stapling” has blossomed

and is reviewed elsewhere.²² In one sense, the maturity of metathesis as a tool for chemical biology is evident in Aileron Therapeutics, which is seeking to commercialize bio-active peptides stabilized by RCM-crosslinks.²³ On the other hand, the use of aqueous metathesis for chemical biology is just beginning.

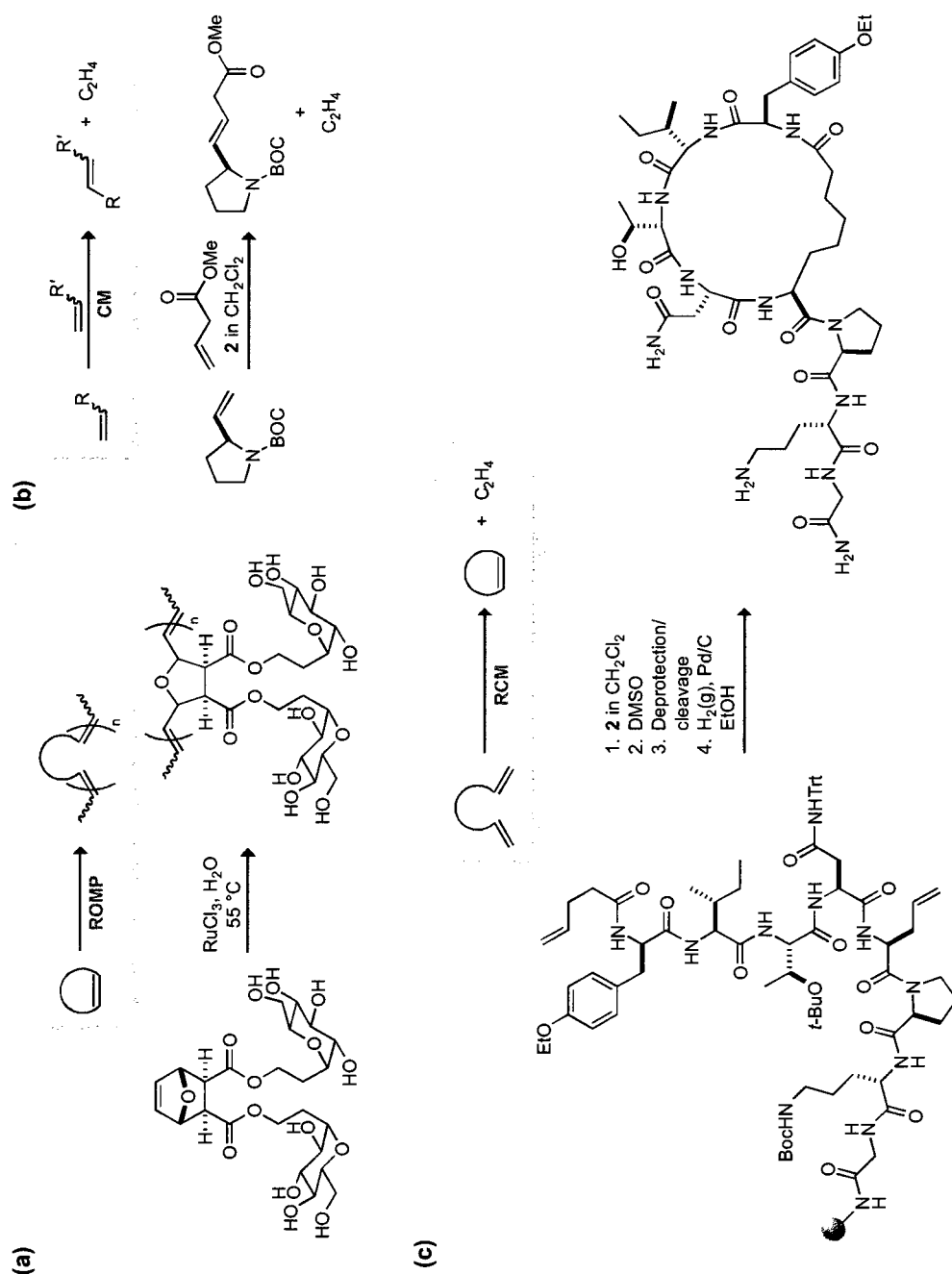


Figure 1.2 Olefin metathesis reactions and their application to chemical biology. (a) Ring-opening metathesis polymerization can produce highly functionalized and well-defined macromolecules, such as this carbohydrate-displaying polymer. (b) Cross metathesis links two alkene fragments to create increasingly complex molecules, including this proline-glycine dipeptide mimic. (c) Ring-closing metathesis is an effective reaction for producing cyclic molecules with constrained conformations, such as this oxytocin hormone mimic.

1.3 Olefin Metathesis Catalysts Designed for Water

1.3.1 Water-Soluble Phosphine Complexes

Grubbs and coworkers led the development of ruthenium olefin metathesis catalysts and recognized that the catalytic ruthenium species were actually water-tolerant, in contrast to other metathesis-active metals. In fact, they noted that ill-defined ruthenium ROMP catalysts initiated faster in water than in organic solvents.²⁴ These observations led to the subsequent development of well-defined ruthenium initiators such as **1**. Grubbs and coworkers returned to water by substituting the hydrophobic phosphines in **1** with electron-rich, cationic phosphines to create complexes such as **5**, which are capable of catalyzing ROMP and RCM in water (**Figure 1.3**). Notably, complex **5** accomplishes living ROMP in water when activated with one equivalent of hydrochloric acid. These phosphine-based catalysts, however, were highly air-sensitive, and required that one of the alkene partners in RCM be substituted with a terminal alkyl group.²⁵⁻²⁷ These problems limited the practicality of water-soluble phosphine-based initiators. More recently, Schanz and coworkers reported benzyldiene-functionalized catalysts, such as **6**, that catalyze ROMP in mixtures of 2,2,2-trifluoroethanol and water, but are also air-sensitive (**Figure 1.3**).²⁸

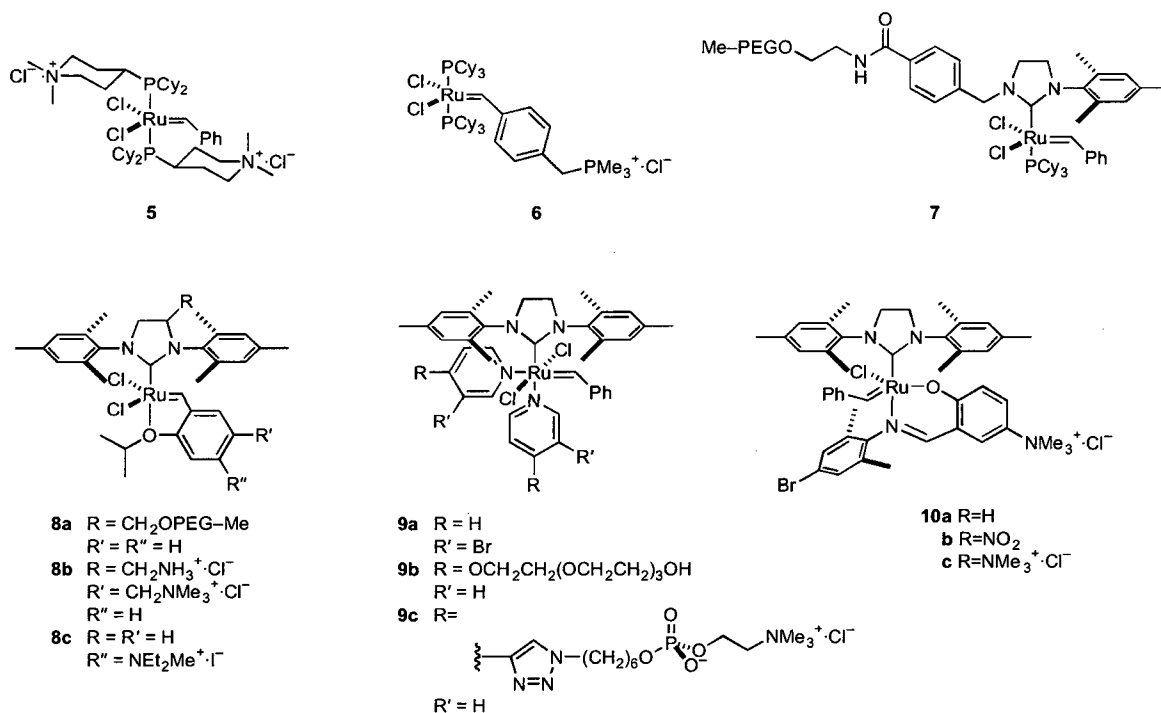


Figure 1.3 Ruthenium catalysts for aqueous olefin metathesis

1.3.2 Polymeric Water-Soluble *N*-Heterocyclic Carbene Complexes

Application of *N*-heterocyclic carbene (NHC) ligands to ruthenium olefin metathesis catalysts has led to remarkable increases in stability and activity in both organic solvents and water. The laboratories of Herrmann,²⁹ Nolan,³⁰ and Grubbs³¹ nearly concurrently reported ruthenium complexes bearing one tightly-bound NHC ligand and one labile phosphine, such as **2**. Although these complexes initiate more slowly than **1**, they transform much faster within the metathesis catalytic cycle. In addition, the NHC ligand increases the stability of the ruthenium complex. Hoveyda and coworkers reported another important advance in catalyst design with complexes **3** and **4a**.^{32,33} In these initiators, a chelating ether replaces the phosphine ligand, further decreasing the air-sensitivity of the catalyst and improving catalyst stability.^{34,35}

Many researchers have capitalized on these improvements in organic-soluble complexes to develop more effective metathesis catalysts for aqueous solution, chiefly by substituting complexes with poly(ethylene glycol) (PEG) or quaternary ammonium moieties. In an early development, Connon and Blechert immobilized a complex similar to **4a** on hydrophilic PEGA-NH₂ resin (amino-functionalized dimethylacrylamide and mono-2-acrylamidoprop-1-yl polyethyleneglycol).³⁶ This heterogeneous catalyst was capable of CM of a variety of alcohols in water but was less effective with charged substrates. In contrast, Grubbs and coworkers have developed soluble polymer-supported complexes. Complex **7**, in which PEG is attached to an *N*-benzyl NHC, is more active than **5** for ROMP of hindered cyclic olefins in water (**Figure 1.3**). Nonetheless, complex **7** is rather ineffective for RCM of simple unsubstituted dienes in methanol, and was not reported to catalyze RCM in water.³⁷ Despite these disappointing results with the first PEG-derivatized initiator, minor modifications led to much more efficient water-soluble catalysts. In particular, shifting the point of attachment of the PEG to the NHC backbone and replacing the phosphine with an ether chelate dramatically improved the activity of **8a** over that of **7** (**Figure 1.3**).³⁸ Complex **8a** is stable in water at room temperature for more than one week under inert atmosphere and is faster at ROMP than is complex **7**. Moreover, the modified complex enables both RCM of water-soluble α,ω -dienes in neat water in good yields and CM of allyl alcohol. Gratifyingly, complex **8a** accomplishes the challenging formation of trisubstituted olefins through RCM. Unfortunately, CM using this catalyst fails with some alkenes substituted with carboxylic acids or quaternary ammonium groups. The basis for the improved activity of this PEG-based initiator is

likely its maintaining the crucial 1,3-diaryl NHC structure while incorporating an ether chelate. Furthermore, the amphiphilic nature of the PEG-complex conjugate leads to aggregation of the complexes into micelle-like structures. The resulting sequestration in a PEG shell would protect the catalyst from water, but also have the deleterious consequence of preventing metathesis of bulky, water-soluble substrates such as proteins.

An additional problem with these early water-soluble complexes is that the NHC slows initiation of the complex, preventing the synthesis of well-defined polymers via ROMP. Grubbs and coworkers overcame this problem in organic solvents by creating the fast-initiating bis(3-bromopyridine) complex **9a**, and Emrick and coworkers have sought to do the same in water with water-soluble bis(pyridine) complexes such as **9b** and **9c** (**Figure 1.3**).^{39,40} *O*-Linked PEG initiator **9b** is capable of ROMP at in water low pH, which is presumably required for dissociation of the basic ligands. On the other hand, the phosphorylcholine-based **9c** is active under both neutral and acidic conditions, in part because of the increased basicity of the pyridine nitrogen. Unfortunately, these catalysts produce polymers with polydispersity indices (PDI) between 1.3 and 2.4, whereas well-controlled ROMP results in $\text{PDI} < 1.1$. Hence, the production of well-defined ROMP polymers in water remains challenging.

1.3.3 Small-Molecule Water-Soluble *N*-Heterocyclic Carbene Complexes

Small-molecule aqueous-soluble catalysts avoid the heterogeneity problems of PEG-based catalysts and, in fact, are typically as active as PEG-based catalysts. To date, most of these complexes have been made hydrophilic by the attachment of a quaternary ammonium groups. Taking advantage of the well-documented stability of ruthenium

salicylaldimine complexes, I reported complex **10c**, which is soluble and stable in 2:1 methanol/water (**Figure 1.3**).⁴¹ This robust initiator requires elevated temperatures for activation but enables RCM and ring-closing enyne metathesis of hydrophobic and hydrophilic substrates in methanol/water under air at 55 °C. I explain my synthesis and characterization of ruthenium salicylaldimine complexes in depth in Chapter 2.

The laboratories of both Grubbs⁴² and Grela⁴³⁻⁴⁶ have developed chelating ether complexes functionalized with a range of quaternary ammonium substituents. Jordan and Grubbs reported complex **8b**, which bears two cationic centers and is readily soluble in water (**Figure 1.3**). This initiator is as active as **8a** for aqueous ROMP, RCM, and CM of water-soluble substrates, but does display a greater propensity for promoting isomerization side reactions of challenging substrates. As with **8a**, the reported CM substrate scope of **8b** is limited to allylic alcohols.

Grela and coworkers examined the activity of complex **8c**^{43,46} as well other benzylidene-tagged initiators^{44,45} in water and water/alcohol mixtures (**Figure 1.3**). This diethylmethylammonium-substituted catalyst is moderately soluble in water and displays a substrate scope similar to that of **8a** and **8b** for RCM and CM, though this catalyst has not been reported to mediate RCM of water-soluble substituted dienes. Complex **8c** also accomplishes RCM and CM of a variety of substrates in homogeneous alcohol/water mixtures. Notably, metathesis by **8c** often can be achieved with lower catalyst loadings (1–2.5 mol% *versus* 5 mol%), a finding Grela and coworkers attribute to the electronic activation provided by the electron-withdrawing quaternary ammonium group. Nonetheless, the multiple water-soluble metathesis catalysts now available all have

similar activities and substrate scopes, which, though impressive, have not yet been shown to be sufficient for the synthesis of complex molecules in water.

1.4 Olefin Metathesis in Homogeneous Aqueous Solvent Mixtures

The intricate synthesis of water-soluble ligands presents a further limitation of specially-designed aqueous metathesis catalysts. The use of conventional hydrophobic ruthenium complexes in mixtures of organic solvents and water avoids this difficulty, yet effective metathesis reactions of water-soluble substrates typically require homogeneous conditions. Blechert and coworkers initially demonstrated the possibility of using chelating ether complexes under these conditions, finding that a complex similar to **4a** enabled RCM of a hydrophobic substrate in moderate yields in 3:1 *N,N*-dimethylformamide/water.⁴⁷ In work I describe in more detail in Chapter 3, I extended these results through a more comprehensive survey of reaction conditions.⁴⁸ By testing a variety of water-miscible aprotic solvents, I found that acetone, 1,2-dimethoxyethane (DME), and PEG are superior cosolvents for aqueous RCM. In addition, **4a** is superior to complexes **1–3** in DME/water, likely for the same reasons that NHC ligands and chelating ethers enhance water-soluble catalyst performance. In DME/water and acetone/water, complex **4a** enables RCM of a range of hydrophobic and hydrophilic substrates, as well as CM of allyl alcohol, and its performance in these mixed solvents is similar to that of the best water-soluble complexes in water. Thus, the main advantage of the specialized ligands of water-soluble complexes is their hydrophilicity rather than their effects on stability or activity. The efficiency of both catalyst systems is still far lower than that of conventional complexes in organic solvents. Further advances

in aqueous metathesis will likely require ligands that provide even greater water-tolerance.

1.5 Olefin Metathesis on Proteins

Using a similar strategy, Davis and coworkers have further developed aqueous CM and achieved metathesis on a protein.⁴⁹ Screening a variety of alkene partners for CM with allyl alcohol in 1:1 water/*t*-butyl alcohol, they found that alkenes with allylic heteroatoms are privileged participants in CM and that sulfur substitution is the most effective. The effectiveness of CM diminishes with butenyl and pentenyl sulfides, leading Davis and coworkers to hypothesize that the allylic heteroatom plays a role as a directing group, while the more distant sulfides form unproductive chelates. Incorporation of *S*-allylcysteine on the surface of a model protein, subtilisin *Bacillus lentus*, provides a potential protein CM partner.⁵⁰ Although CM fails with allyl alcohol and 200 equivalents of **4a** in 7:3 phosphate buffer/*t*-butyl alcohol, the addition of MgCl₂ (presumably to mask protein carboxylate groups) enables CM with allyl alcohol and allylic ethers in 50–90% conversion (**Figure 1.4**). This methodology allowed Davis and coworkers to functionalize the model protein with carbohydrate and PEG moieties while maintaining the enzymatic activity of subtilisin. It is noteworthy that *S*-allylcysteine can be incorporated genetically as a methionine surrogate.⁴⁹

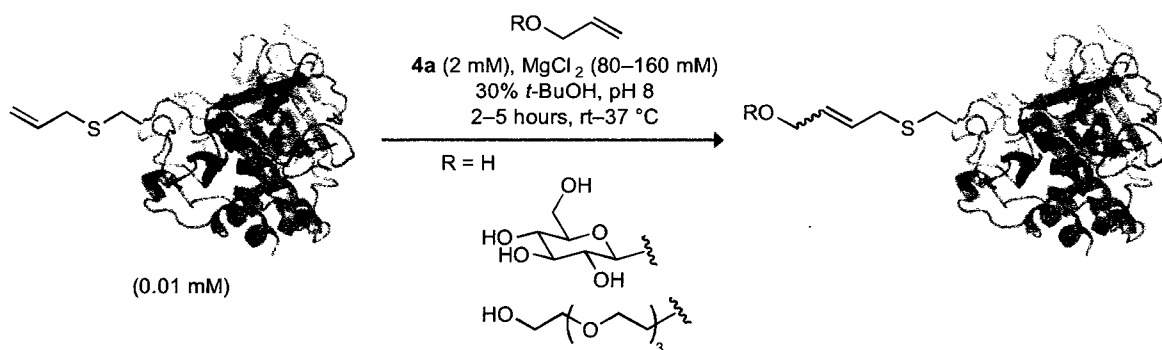


Figure 1.4 Olefin cross metathesis for site-specific protein modification at allyl sulfide substituents. The allyl group is appended to Cys156 of the S156C variant of subtilisin *Bacillus lentus*. The protein structure is based on the atomic coordinates in PDB entry 1st3.

1.6 Conclusions

The olefin metathesis reaction is a highly versatile tool for synthetic chemical biologists. Modern ruthenium-based catalysts are readily available and can be easily used in organic solution to construct molecules for probing and manipulating biological function. On the other hand, metathesis on biomolecules in water remains challenging. Advances in catalyst design during the past decade have enabled simple ROMP, RCM, and CM in water, but controlled ROMP to create low polydispersity polymers is still difficult and the CM of many substrates remains impossible. Many of the reactions made possible by water-soluble catalysts are also catalyzed by conventional complexes in aqueous–organic solutions amenable to biological substrates. This hybrid approach has enabled the first CM on the surface of a protein using complex **4a**, a success that heralds olefin metathesis in water as a method for chemical biology. Nonetheless, more complex applications of metathesis, such as demanding ROMP or CM in water, will likely require the endowment of ruthenium catalysts with additional stability and activity in aqueous environments.

1.7 Thesis Summary

Working in the swiftly-advancing field of aqueous olefin metathesis,⁵¹⁻⁵³ I developed both new water-adapted catalysts, which I describe in Chapter Two, and strategies for using traditional catalysts in aqueous solution, which I detail in Chapter Three. After the completion of this work I chose to apply my catalysis experience to the problem of developing renewable fuels and chemicals from abundant lignocellulosic biomass resources. In research explained in Chapter Four, I invented an efficient one-step process for production of the renewable platform chemical 5-hydroxymethylfurfural from lignocellulosic biomass, as well as fructose and glucose. In further development of this process, I explored the conversion of other sugars into HMF and furfural. Chapter Five details the synthesis of HMF from mannose and galactose, sugars which are minor components of plant biomass, and from lactose, tagatose, psicose, and sorbose. In work illustrated in Chapter Six, I examined the synthesis of furfural from xylose and xylan to develop more effective means for conversion of hemicellulose into furan chemicals. Through simple modifications, our transformation process also enables production of sugars from biomass. I found that acid catalysts in aqueous ionic liquids effect efficient cellulose and hemicellulose hydrolysis and that the resulting sugars can be fermented by both bacterial and yeast ethanologens. I explain this comprehensive process in Chapter Seven, while Chapter Eight highlights some potential future directions.

1.8 Acknowledgements

Work in our laboratory on olefin metathesis is supported by grant GM044783 (NIH). J.B.B. is supported by an NSF Graduate Research Fellowship.

CHAPTER 2***SALICYLALDIMINE RUTHENIUM ALKYLIDENE COMPLEXES:
METATHESIS CATALYSTS TUNED FOR PROTIC SOLVENTS**

Abstract: Tuning the electronic and steric environment of olefin metathesis catalysts with specialized ligands can adapt them to broader applications, including metathesis in aqueous solvents. Bidentate salicylaldimine ligands are known to stabilize ruthenium alkylidene complexes, as well as allow ring-closing metathesis in protic media. Here, we report the synthesis of exceptionally robust olefin metathesis catalysts bearing both salicylaldimine and *N*-heterocyclic carbene ligands, including a trimethylammonium-functionalized complex adapted for polar solvents. NMR spectroscopy and X-ray crystallographic analysis confirm the structures of the complexes. Although the *N*-heterocyclic carbene–salicylaldimine ligand combination limits the activity of these catalysts in nonpolar solvents, this pairing enables efficient ring-closing metathesis of both dienes and enynes in methanol and methanol–water mixtures under air.

Co-author contribution: I. A. G. collected X-ray diffraction data, solved the structure of **10a**, prepared the structure report, and composed the related experimental details.

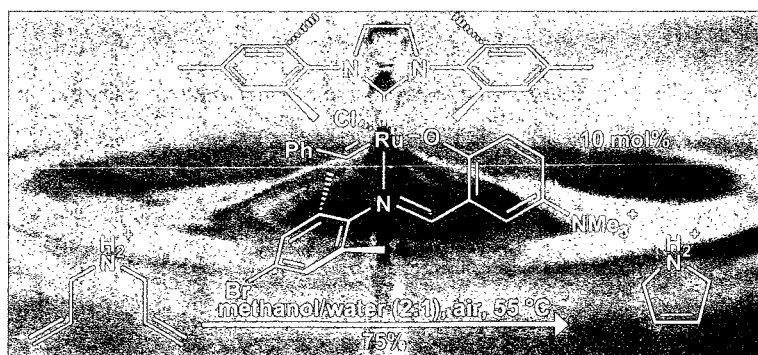
*This chapter has been published, in part, under the same title. Reference: Binder, J. B.; Guzei, I. A.; Raines, R. T. *Advanced Synthesis & Catalysis*. **2007**, 349, 395–404.

2.1 Introduction

As an efficient, selective means for forming carbon–carbon bonds, olefin metathesis has revolutionized organic synthesis and polymer chemistry.^{1,2,4} The high catalytic activity and functional group tolerance of well-defined ruthenium-based complexes **1–4a** allow extensive use of metathesis chemistry (**Figure 2.1**).^{54,32,55,33} Still more diverse utilization of metathesis necessitates catalysts tailored to specific applications.⁵⁶ For instance, aqueous olefin metathesis is attractive for carbon–carbon bond formation in biological applications^{10,57,11,58–64,16,20} and green chemistry,^{65–67,38} yet complexes **1–4a** are insoluble in water and soluble versions such as **5** have proven to be unstable to air and incompatible with internal olefins.^{25–27,37} Grubbs and coworkers have begun to address this challenge by modifying the local environment of the catalyst with a polyethylene glycol-bearing ligand, as in complex **8a**.³⁸ Here, our intent is to complement this approach by tuning the primary coordination sphere of the catalyst to the demands of aqueous media.

With the goal of creating designer catalysts for aqueous metathesis, we were attracted to reported ruthenium complexes containing bidentate salicylaldimine ligands, such as **11a–b** and **10a–b**.^{68–70} These complexes display impressive stability and activity, and their readily accessible imine ligands lend themselves to catalyst tuning.⁷¹ In addition, we were encouraged by the capacity of phosphine-bearing catalysts similar to **11a** to perform ring-closing metathesis (RCM) in methanol.⁷² Aware of the benefits that *N*-heterocyclic carbene (NHC) ligands provide other ruthenium metathesis catalysts, we chose to investigate salicylaldimine complexes such as **10a** and **b** reported by Verpoort

and coworkers.⁷³⁻⁷⁵ According to their work, this family of NHC-imine complexes efficiently catalyzes ring-opening metathesis polymerization (ROMP), RCM, and Kharasch addition. Imine-bearing ruthenium complexes are proposed to enter the olefin metathesis catalytic cycle with decoordination of the imine nitrogen rather than the phosphine dissociation observed for initiation of **1** and **2**.^{71,74} As a result, we expected that an NHC ligand such as 1,3-dimesityl-4,5-dihydroimidazol-2-ylidene (H₂IMes) could beneficially replace the spectator tricyclohexylphosphine of **11a-c**, leading to improved thermal stability and enhanced olefin metathesis activity.^{30,76} This report details our synthesis of NHC-imine metathesis catalysts and the first crystal structure of a member of this class, complex **10a**, as well as the activity of water-adapted complex **10c**.



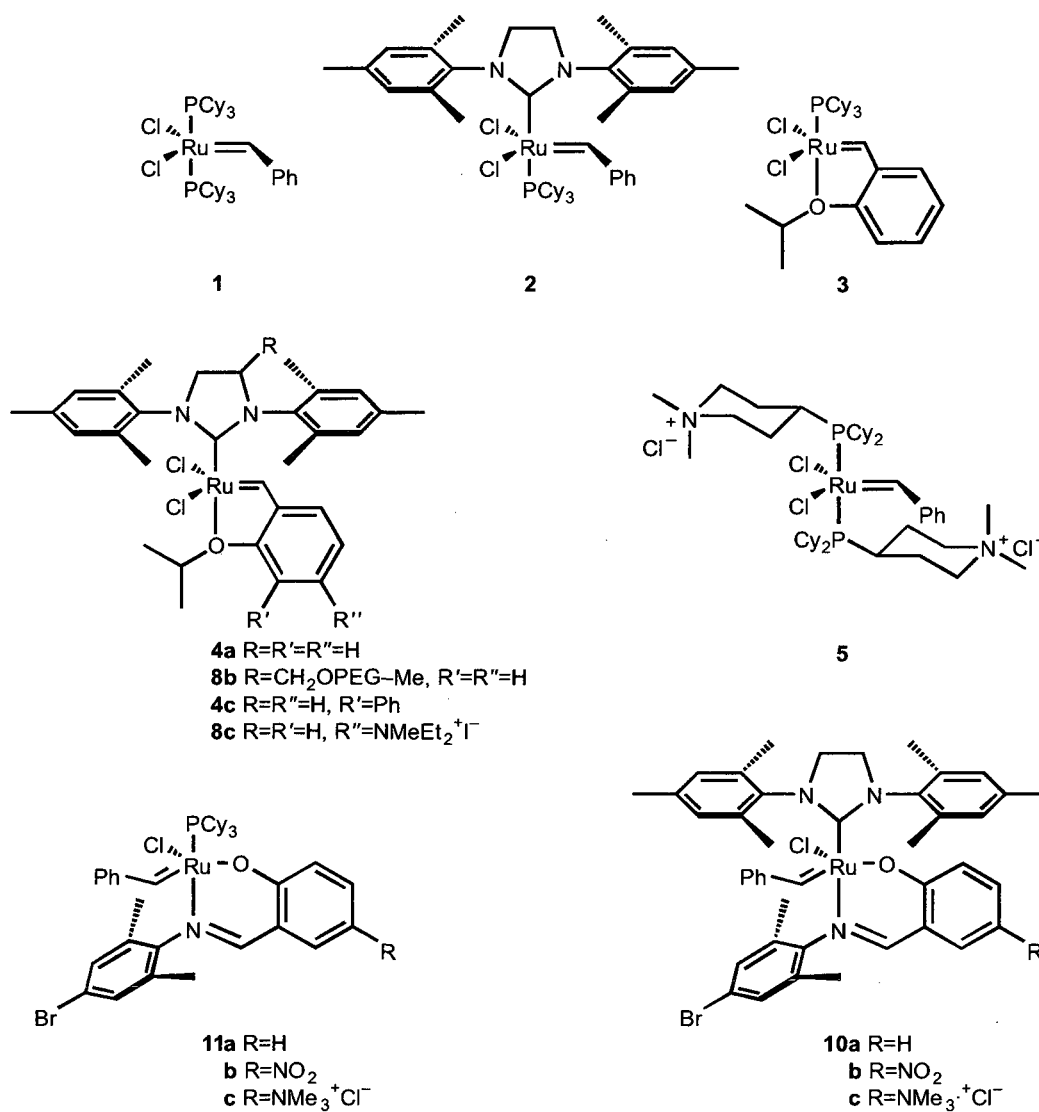


Figure 2.1 Olefin metathesis catalysts.

2.2 Results and Discussion

2.2.1 Synthesis of NHC-Salicylaldimine Complexes

As shown in **Figure 2.2**, our initial efforts concentrated on using the standard means for introducing the H_2IMes ligand, here, *in situ* formation of the free carbene from the imidazolium salt with potassium *tert*-butoxide and subsequent reaction with the phosphine-bearing ruthenium complex **11a**.⁷⁴ Attempts to prepare reported complex **10a**

by this published method resulted, however, in decomposition of the ruthenium benzylidene starting material. Faced with this roadblock, we chose to approach **10a–c** by introducing salicylaldimine ligands to a complex already bearing the H₂IMes ligand. Alkoxide and aryloxy ligands, as well as neutral donors, react readily with bis(pyridine) precursor **9d**.^{77–81} The chloride ligands in **9d** are far more labile than those in **2** and are displaced easily by incoming ligands, especially with the assistance of thallium ion. Accordingly, the thallium salts of salicylaldimine ligands **12a–c** were prepared *in situ* with thallium ethoxide and reacted with **9d** (Figure 2.2). Gratifyingly, the green hexacoordinate starting material quickly formed wine-red complexes **10a–c** as pyridine and chloride were displaced by the bidentate ligand. After the removal of thallium chloride and excess ligand, complexes **10a–c** were isolated in good (56–87%) yield. Notably, this robust route even allowed access to cationic complex **10c** with polar ligand **12c** in DMF.

Manipulation of the NHC–imine complexes **10a–c** revealed their dramatic stability to air, heat, and water. These complexes tolerate storage for months as solids under vacuum without degradation as judged by ¹H NMR spectroscopy. Although **2** decomposes completely in less than 1 d in C₆D₆ at 55 °C under air, ≥95% of complex **10b** is intact after 8 d according to ¹H NMR spectroscopy. Complex **10c** tolerates water, and remains <40% intact after 2 d in CD₃OD/D₂O (3:1) under air at 20 °C (according to integration of Ar–CH₃ and alkylidene ¹H NMR signals). In contrast, previous catalysts bearing ligands with cationic functional groups (such as **5**²⁷) decompose in minutes when exposed to traces of oxygen in solution.

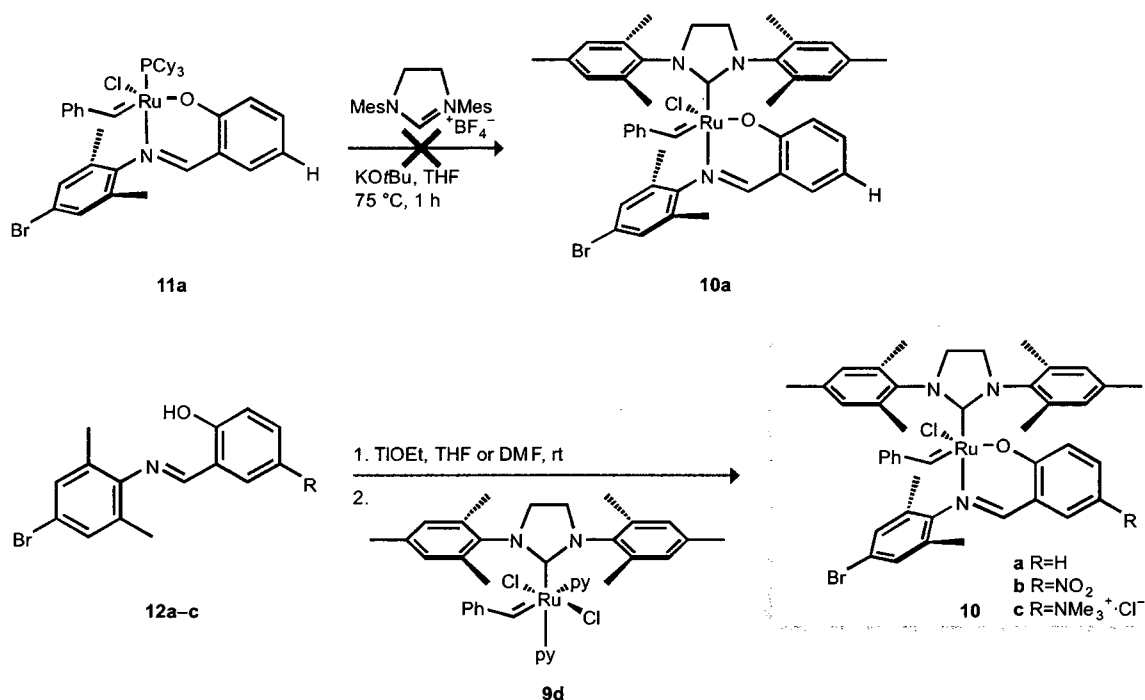


Figure 2.2 Synthesis of NHC-imine complexes **10a–c** by the reported route from **11a** and our route from **9d**.

Interestingly, no exchange of the alkylidene proton of complex **10c** with solvent deuterons is observed in CD₃OD/D₂O (3:1). Such H/D exchange is observed for ruthenium alkylidene and vinylidene complexes without NHC ligands, including **5** and **11a–b**,⁸² but not for complex **8a**.³⁸ Ligand electronics are known to affect the rate of alkylidene H/D exchange,⁸² and the presence of the NHC ligands could slow this process.

2.2.2 Spectral and Structural Characterization of NHC–Salicylaldimine Complexes

¹H and ¹³C NMR spectral data for complexes **10a–b** synthesized by the route in **Figure 2.2** were consistent with their putative structures, but surprisingly did not match those previously reported for these complexes.⁷⁴ As listed in Table 2.1, the benzylidene proton resonance appears at δ 18.56 for **10a** while the literature reports δ 19.42, which is

nearly the same as that reported for the parent phosphine-bearing complex **11a**.⁷¹ Evidenced by ¹H and ¹³C NMR spectra of **1–4a**, replacement of the tricyclohexylphosphine ligand with H₂IMes typically results in a shielding effect on the alkylidene proton that shifts its resonance approximately 0.9 ppm upfield.^{54,32,55,33} In addition, the observed ¹H spectrum of **10a** includes eight distinct Ar–CH₃ singlets, consistent with the asymmetry of the putative structure, while the literature spectrum reveals only six Ar–CH₃ resonances, including an aliphatic three-proton doublet. No coalescence of the methyl resonances of **10a** was observed at elevated temperature (55 °C in CDCl₃ or 70 °C in C₆D₆). Spectra for **10b–c** agree with these findings, with both complexes displaying benzyldiene proton resonances about 0.9 ppm upfield from those of the parent complexes⁷² and eight distinct methyl resonances.

To resolve this conflict, we sought crystallographic evidence. Suitable crystals of complex **10a** were grown by slow diffusion of pentane into a concentrated benzene solution over a few days. The crystalline material both displayed a ¹H NMR spectrum that was indistinguishable from that of complex **10a** prior to crystallization and retained RCM activity (*vide infra*). The X-ray data confirmed the structure of **10a**, as shown in **Figure 2.3**. Both **10a** and phosphine-bearing complexes similar to **11a–b** adopt a distorted trigonal-bipyramidal geometry; the common bond lengths and angles in the two classes of complex are virtually identical.⁷² As in the phosphine-bearing complexes, the anionic moieties are *trans* with an O–Ru–Cl bond angle of 172.5° in NHC–imine complex **10a**. Just as in oxygen-ligated complex **4a**,³³ the Ru–C16 bond is shorter than

compound	δ (ppm), Ru=CHAr	δ (ppm), ArCH ₃
10a	18.56 (s, 1H)	2.60 (s, 3H), 2.41 (s, 3H), 2.28 (s, 3H), 2.25 (s, 3H), 2.19 (s, 3H), 2.00 (s, 3H), 1.46 (s, 3H), 1.04 (s, 3H)
10a ⁷⁴	19.42 (s, 1H)	2.49 (s, 6H), 2.31 (s, 3H), 2.20 (s, 6H), 2.09 (s, 3H), 1.76 (s, 3H), 1.72 (d, 3H)
11a ⁷¹	19.45 (d, 1H)	2.45 (q, 3H), 2.33 (s, 3H), 1.78 (d, 3H), 1.71–1.14 (m, 30H)
1 ^{[a] 54}	20.02 (s, 1H)	2.62–1.15 (m, 66H)
2 ^{[a] 55}	19.16 (s, 1H)	2.56–0.15 (m, 51H)
3 ³²	17.44 (d, 1H)	2.37–1.20 (m, 33H), 1.80 (d, 6H)
4a ³³	16.56 (s, 1H)	2.48 (s, 12H), 2.40 (s, 6H), 1.27 (d, 6H)

The ORTEP diagram shows the molecular structure of the Ru(II) complex. The central ruthenium atom (Ru) is coordinated by a bidentate ligand through its nitrogen atoms (N1, N2) and an oxygen atom (O). The ruthenium atom is also coordinated by a chloride ligand (Cl) and a water molecule (O). The structure is shown with thermal ellipsoids at the 50% probability level. The labels for the atoms are: Ru, Cl, N1, C7, N2, C16, N3, C37, and C38.

Figure 2.3 Solid-state molecular structure of complex **7a**. Hydrogen atoms omitted for clarity. Thermal ellipsoids are shown at 50% probability. Selected bond lengths (Å) and angles (°): Ru–C37 1.838(2), Ru–C16 2.032(2), Ru–Cl 2.0530(15), Ru–O 2.1080(18), Ru–N1 2.3976(6), C16–N2 1.347(3), C16–N3 1.346(3), C7–N1 1.301(3), C37–H37 0.9500, C37–C38 1.476(3); C37–Ru–C16 98.28(9), C37–Ru–O 98.70(9), C16–Ru–N1 158.34(8), O–Ru–N1 89.40(6), C37–Ru–Cl 88.79(8), C16–Ru–O 83.79(7), C37–Ru–N1 103.07(8), C16–Ru–Cl 94.73(6), O–Ru–Cl 172.50(4), N1–Ru–Cl 89.35(5).

2.2.3 Synthesis of Authentic **10a** by Phosphine Displacement with H_2IMes

Returning to the original synthesis of complex **10a**, we sought to reproduce the published results by using the improved method for introducing the H_2IMes ligand reported by Nolan and coworkers.⁸⁵ Switching the reaction solvent to hexanes and the base to the more soluble potassium *tert*-amylate enhanced the synthesis, enabling the clean conversion of **11a** to **10a** as confirmed by 1H NMR. Once again, spectral characterization failed to reveal the signals of the proposed imine complex reported by De Clercq & Verpoort,⁷⁴ Although these results confirm that **10a** is the authentic product of both our synthesis from H_2IMes complex **9d** and the preparation from **10a**, the identity of the product reported previously⁷⁴ still remains unclear.

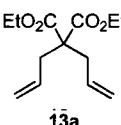
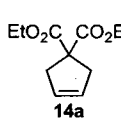
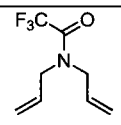
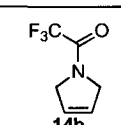
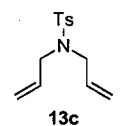
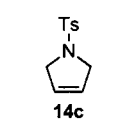
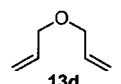

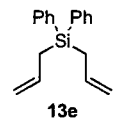
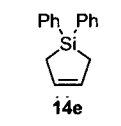
After we submitted this manuscript, Verpoort and coworkers reported the synthesis of complex **10b** and three similar NHC–imine complexes by a route similar to ours.^{86,87} These workers found the RCM activity of their NHC–imine complexes in nonpolar solvents to be similar to that of the NHC–imine complexes reported herein (*vide infra*). Although they confirmed the structure of these complexes by X-ray crystallographic analysis, they did not comment on the discrepancies with their earlier paper⁷⁴ nor did they examine RCM catalysis in an aqueous environment.

2.2.4 Ring-Closing Metathesis Activity of **10a–c**

Having confirmed the structure of the NHC–imine complexes, we investigated their activity for diene RCM. In contrast to previous reports,⁷³ complexes **10a–c** are dramatically less active in nonpolar solvents (*e.g.*, benzene and CH_2Cl_2) than their phosphine-bearing counterpart, **11a** (Table 2.2 and Table 2.3). Elevated temperatures are

necessary for metathesis. Even at 55 °C, complexes **10a** and **10b** require 40–72 h to achieve a high conversion of most substrates in toluene or benzene, but standard complexes **2**, **4a**, and **4c** and phosphine-bearing complexes such as **11a** achieve such transformations in a few hours or less.^{72,71} Cationic complex **10c** shows similarly low activity in benzene, requiring 40 h for high conversions.

Table 2.2 RCM of Nonpolar Dienes Catalyzed by Ruthenium Complexes under Air

substrate	product	solvent (substrate conc. [M])	complex (mol%)	time (h)	conversion (%) ^[a]
 13a	 14a	CH ₂ Cl ₂ (0.01)	2 (1)	1.5	99 ^[b]
		CH ₂ Cl ₂ (0.01)	4c (1)	0.16	99 ^[b]
		C ₆ D ₅ Cl (0.1)	11a (5)	4	100 ^[c]
		C ₆ D ₆ (0.1)	10a (5)	4	100 ^[d]
		C ₆ D ₆ (0.1)	10a (5)	72	90
		C ₇ D ₈ (0.05)	10b (5)	70	76
		CD ₃ OD (0.025)	10b (5)	23	94
		C ₆ D ₆ (0.05)	10c (5)	40	>95
		CD ₃ OD (0.05)	10c (5)	12	>95
		2:1 CD ₃ OD/D ₂ O (0.025)	10c (10)	6	60
 13b	 14b	CD ₃ OD (0.025)	10b (5)	9	36
		CD ₃ OD (0.05)	10c (5)	9	34
		2:1 CD ₃ OD/D ₂ O (0.025)	10c (5)	6	29
 13c	 14c	CH ₂ Cl ₂ (0.01)	4a (1)	4.5	91 ^[e]
		C ₆ D ₆ (0.05)	10a (5)	6	8
		C ₆ D ₆ (0.05)	10a (5)	26	68
		C ₆ D ₆ (0.05)	10b (5)	24	10
		C ₇ D ₈ (0.05)	10b (5)	6	43 (+ 8) ^[f]
		C ₇ D ₈ (0.05)	10b (5)	70	92
		CD ₃ OD (0.025)	10b (5)	9	>95
		C ₆ D ₆ (0.05)	10c (5)	6	7
		CD ₃ OD (0.05)	10c (5)	6	>95
		2:1 CD ₃ OD/D ₂ O (0.025)	10c (5)	6	93
 13d	 14d	C ₇ D ₈ (0.05)	10b (5)	40	45
		CD ₃ OD (0.025)	10b (5)	9	94
		C ₆ D ₆ (0.05)	10c (5)	40	65
		CD ₃ OD (0.05)	10c (5)	9	>95
		2:1 CD ₃ OD/D ₂ O (0.025)	10c (5)	6	57
 13e	 14e	C ₇ D ₈ (0.05)	10a (5)	70	41
		C ₇ D ₈ (0.05)	10b (5)	40	10
		CD ₃ OD (0.025)	10b (5)	9	<5
		C ₆ D ₆ (0.05)	10c (5)	40	77
		CD ₃ OD (0.05)	10c (5)	9	<5

^[a] Conditions for RCM catalyzed by complexes **10a–c**: 55 °C, air. Conversions determined by ¹H NMR..

^[b] 20 °C, ref ⁸⁸.


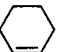
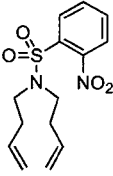
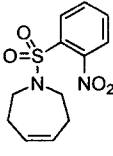
^[c] 55 °C, ref ⁷¹.

^[d] 55 °C, ref ⁷³.

^[e] Room temperature, ref ⁸⁹.

^[f] 80 °C.

Table 2.3 RCM of Nonpolar Dienes under Air to Form Six- and Seven-Membered Rings

Substrate	product	solvent (substrate conc. [M])	complex (mol%)	time (h)	conversion (%) ^[a]
 13f	 14f	C ₇ D ₈ (0.05)	10a (5)	40	>95
		C ₇ D ₈ (0.05)	10b (5)	40	>95
		CD ₃ OD (0.025)	10b (5)	5	95
		C ₆ D ₆ (0.05)	10c (5)	40	>95
		CD ₃ OD (0.05)	10c (5)	7	>95
		2:1 CD ₃ OD/D ₂ O (0.025)	10c (5)	6	85
 13g	 14g	C ₇ D ₈ (0.05)	10a (5)	40	90
		C ₇ D ₈ (0.05)	10b (5)	40	90
		CD ₃ OD (0.025)	10b (5)	9	93
		C ₆ D ₆ (0.05)	10c (5)	40	89
		CD ₃ OD (0.05)	10c (5)	7	>95
		2:1 CD ₃ OD/D ₂ O (0.025)	10c (10)	6	>95

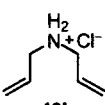
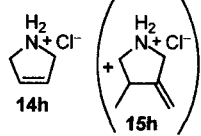
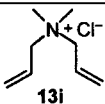
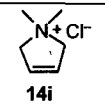
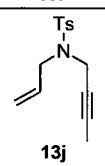
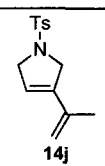
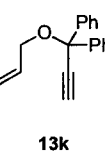
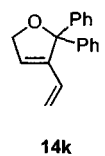
^[a] Conditions for RCM catalyzed by complexes **10a–c**: 55 °C, air. Conversions determined by ¹H NMR.

Yet, under similar conditions in methanol, complexes **10b** and **10c** catalyze the complete ring-closing of both polar and nonpolar substrates to form five-, six-, and seven-membered cyclic products in only 6–12 h. Although complex **10b** is less soluble in methanol than complex **10c**, these two catalysts display similar activity, demonstrating that the trimethylammonium substituent influences solubility more than reactivity. Unlike other metathesis catalysts adapted to protic solvents, complex **10c** does not require inert atmosphere conditions for catalysis of RCM. In addition, complex **10c** is effective for RCM of *N,N*-dimethyl-*N,N*-diallylammonium chloride (**13i**), which has proven to be recalcitrant for other catalysts (Table 2.4).^{90,91} This specialized catalyst is also active in methanol–water mixtures, with 10 mol% of **10c** achieving the highest conversion of *N,N*-diallylamine hydrochloride (**13h**) to RCM product **14d** yet reported in an aqueous environment.^{26,36,91,92,38} Moreover, **10c** accomplishes this transformation cleanly. For

comparison, Grubbs and coworkers reported 67% ring-closing of **13h** along with 28% conversion to cycloisomer **15h** using 5 mol% of complex **8a** in water at room temperature over 36 h.³⁸ With a variety of nonpolar dienes **10c** also achieves good to excellent conversions to five-, six-, and seven-membered rings in methanol–water mixtures (Table 2.2 and Table 2.3). In contrast to RCM with complexes **10a–c** in nonpolar solvents or methanol, RCM in the aqueous environment is limited by decomposition of the catalyst or intermediates—in the former solvents the intact complex is observable by NMR spectroscopy throughout the timecourse of the reaction, but in methanol–water the resonances of the complex disappear.

Enyne metathesis by salicylaldimine alkylidene ruthenium complexes has not been reported previously. We found that complexes **10a–c** are efficient catalysts of enyne RCM (Table 2.4). Substrate **13k** is smoothly transformed in nonpolar solvents (5–36 h) and in protic media (2–6 h). For comparison, Grela and coworkers recently reported metathesis of **13k** with complex **8c** in 92% conversion in an aqueous solvent.⁴³ With **10a–c**, the more difficult substrate **13j** also undergoes ring closure to a moderate extent.

Table 2.4 RCM of Polar Dienes and Enynes Catalyzed by Ruthenium Complexes

substrate	product	solvent (substrate conc. [M])	complex (mol%)	time (h)	conversion (%) ^[a]
 13h	 14h + 15h	2:1 CD ₃ OD/D ₂ O (0.05)	10c (5)	6	59
		2:1 CD ₃ OD/D ₂ O (0.025)	10c (10)	9	75
		D ₂ O (0.2)	8a (5)	36	67 (+28) ^[b]
 13i	 14i	CD ₃ OD (0.05)	10c (5)	12	79
		2:1 CD ₃ OD/D ₂ O (0.025)	10c (10)	6	40
 13j	 14j	C ₇ D ₈ (0.05)	10a (5)	36	7
		C ₇ D ₈ (0.05)	10b (5)	36	7
		CD ₃ OD (0.025)	10b (5)	36	25
		C ₆ D ₆ (0.05)	10c (5)	36	42
		CD ₃ OD (0.05)	10c (5)	36	32
 13k	 14k	C ₇ D ₈ (0.05)	10a (5)	36	93
		C ₇ D ₈ (0.05)	10b (5)	18	>95
		CD ₃ OD (0.025)	10b (5)	2	90
		C ₆ D ₆ (0.05)	10c (5)	5	>95
		CD ₃ OD (0.05)	10c (5)	2	>95
		5:2 CD ₃ OD/D ₂ O (0.02)	10c (10)	6	>95
		5:2 CH ₃ OH/H ₂ O (0.02)	8c (5)	0.5	92 ^[c]

^[a] Conditions for RCM catalyzed by complexes **10a–c**: 55 °C, air. Conversions determined by ¹H NMR.

^[b] Room temperature, ref³⁸.

^[c] 25 °C, ref⁴³.

The solvent dependence of ring-closing metathesis with the NHC–imine complexes offers an explanation for their low activity. Catalysts bearing the H₂IMes ligand are typically more active in aromatic solvents than in CH₂Cl₂.^{93,94} In contrast, complex **10b** is more active in more polar solvents (Table 2.5). This solvent dependence is consistent with the initiation rate trend for catalysis by **2**, wherein switching from toluene to CH₂Cl₂ increased the initiation rate by 30%.⁷⁶ Together, these data suggest that the activity of NHC–imine complexes **10a–c** is limited by their rate of initiation. Direct observations of metathesis reaction mixtures by ¹H NMR also support this conclusion. For both NHC–

imine catalysts and several other chelated catalysts,⁹⁵ propagating alkylidene species are not detected during metathesis, and, in nonpolar solvents, the ¹H NMR signals for the complexes are typically unchanged upon completion. These results imply that the ligand combination in **10a–c** allows only a small fraction of the complex species to participate in metathesis. Although NHC ligands improve metathesis propagation activities for ruthenium complexes, they tend to decrease their initiation rates drastically.⁷⁶ Switching from a tricyclohexylphosphine spectator ligand to an NHC could likewise decrease the initiation rate for imine complexes, such that they remain largely dormant as 16-electron species.⁷⁶ Increasing the temperature and solvent polarity apparently enables the complexes to surmount this hurdle, resulting in the high RCM activity of **10b–c** in a polar solvent. Thus, ruthenium NHC–imine complexes are rare examples of complexes that are more active as metathesis catalysts in methanol than in nonpolar solvents.³⁶

Table 2.5 Solvent Dependence of RCM of *N*-Tosyl Diallylamine (**13c**) Catalyzed by Complex **10b**

solvent	dielectric constant (ϵ)	conversion (%)
C ₆ D ₆	2.28	14
CD ₂ Cl ₂	8.9	36
CD ₃ OD	32.6	69

Reaction conditions: 5 mol% **10b**, 0.025 M substrate **13c**, 40 °C, 24 h, under air.

These characteristics of high stability and slow initiation suit salicylaldimine-based catalysts to specific applications. For example, complexes **10b–c** could enable ROMP in protic media, though their slow initiation rates are likely to result in large polydispersities

that could be inappropriate for some applications.⁹⁶⁻⁹⁸ Similarly, the low concentrations of propagating alkylidene species produced by salicylaldimine catalysts prevent them from supporting cross-metathesis. Nonetheless, these same qualities make NHC-salicylaldimine catalysts promising for RCM in aqueous environments. Slow initiation appears to protect the complex from water while providing a steady supply of active species with which to accomplish RCM. These advantages could be combined with the protective local environment provided by polyethylene glycol-functionalized ligands³⁸ to provide even more efficient catalysts for aqueous RCM.

2.3 Conclusion

Specialized ligands can tune the characteristics of olefin metathesis catalysts, adapting them to demanding applications, including metathesis in aqueous environments. We prepared ruthenium complexes bearing both NHC and salicylaldimine ligands, and confirmed their structure by NMR spectroscopy and X-ray crystallographic analysis. These new complexes initiate slowly, but are highly effective catalysts for diene and enyne RCM in protic media. The enhanced stability engendered by the salicylaldimine ligands allows trimethylammonium-functionalized complex **10c** to achieve clean RCM of *N,N*-diallylamine hydrochloride (**13h**) with the highest conversion yet reported in an aqueous environment. Further investigations will address the potential of these catalysts for RCM of more complex substrates as well as the possible enhancement of salicylaldimine-based catalysts with polyethylene glycol-bearing ligands.

2.4 Acknowledgements

We are grateful to H. E. Blackwell, L. L. Kiessling, D. M. Lynn, and M. Kim for contributive discussions. J.B.B. was supported by an NDSEG Fellowship sponsored by the Air Force Office of Scientific Research. This work was supported by grant GM44783 (NIH). NMRFAM was supported by grant P41RR02301 (NIH).

2.5 Experimental Section

2.5.1 General Considerations

Commercial chemicals were of reagent grade or better, and were used without further purification. Anhydrous THF, DMF, and CH_2Cl_2 were obtained from CYCLETAINER[®] solvent delivery systems (J.T. Baker, Phillipsburg, NJ). Other anhydrous solvents were obtained in septum-sealed bottles. In all reactions involving anhydrous solvents, glassware was either oven- or flame-dried. Manipulation of organometallic compounds was performed using standard Schlenk techniques under an atmosphere of dry Ar(g) , except as noted otherwise.

The term “concentrated under reduced pressure” refers to the removal of solvents and other volatile materials using a rotary evaporator at water aspirator pressure (<20 torr) while maintaining the water-bath temperature below 40 °C. In other cases, solvent was removed from samples at high vacuum (<0.1 torr). The term “high vacuum” refers to vacuum achieved by a mechanical belt-drive oil pump.

NMR spectra were acquired with a Bruker DMX-400 Avance spectrometer (^1H , 400 MHz; ^{13}C , 100.6 MHz), Bruker Avance DMX-500 spectrometer (^1H , 500 MHz; ^{13}C , 125.7 MHz), or Bruker Avance DMX-600 spectrometer (^1H , 600 MHz) at the National

Magnetic Resonance Facility at Madison (NMRFAM). NMR spectra were obtained at ambient temperature unless indicated otherwise. Coupling constants J are given in Hertz.

Mass spectrometry was performed with a Micromass LCT (electrospray ionization, ESI) in the Mass Spectrometry Facility in the Department of Chemistry. Elemental analyses were performed at Midwest Microlabs (Indianapolis, IN).

N-(4-Bromo-2,6-dimethylphenyl)-salicylaldehyde (**12a**), *N*-(4-bromo-2,6-dimethylphenyl)-5-nitrosalicylaldehyde (**12b**), and ruthenium imine complex **11a** were prepared according to the methods of De Clercq & Verpoort.⁷¹ (3-Formyl-4-hydroxyphenyl)-trimethylammonium iodide was prepared according to the method of Ando & Emoto⁹⁹ and converted to the chloride salt by anion exchange. $(\text{H}_2\text{IMes})(\text{C}_5\text{H}_5\text{N})_2(\text{Cl})_2\text{Ru}=\text{CHPh}$ (**9d**) was synthesized by the method of Grubbs and coworkers.⁷⁷

The following RCM substrates were obtained from commercial sources and used without further purification: diethyl diallylmalonate (**13a**), *N,N*-diallyl-2,2,2-trifluoroacetamide (**13b**), allyl ether (**13d**), and 1,7-octadiene (**13f**) from Aldrich (Milwaukee, WI); *N,N*-diallyl-*N,N*-dimethylammonium chloride (**13i**) from Fluka (Buchs, Switzerland); and diallyldiphenylsilane (**13e**) from Acros Organics (Geel, Belgium).

N,N-Diallyl-4-methylbenzenesulfonamide (**13c**) was prepared by the method of Lamaty and coworkers.¹⁰⁰ Diallylamine hydrochloride (**13h**) was prepared from the corresponding amine (Aldrich) by treatment with ethereal HCl. *N*-(2-Propenyl)-4-methylbenzenesulfonamide was prepared by the method of Pagenkopf and coworkers.¹⁰¹

2.5.2 Preparation of *N*-(4-Bromo-2,6-dimethylphenyl)-5-

trimethylammoniumsalicylaldimine Chloride (12c)

4-Bromo-2,6-dimethylaniline (1.003 g, 5.02 mmol) and (3-formyl-4-hydroxyphenyl)-trimethylammonium chloride (1.082 g, 5.02 mmol) were dissolved in ethanol (25 mL), and the resulting solution was stirred at reflux for 16 h. The reaction mixture was allowed to cool and concentrated under reduced pressure. The residue was treated with hexanes (15 mL), removed by filtration, and dried under high vacuum to afford **12c** (1.544 g, 3.88 mmol, 77% yield) as a yellow powder. ^1H NMR (CD_3OD) δ : 8.61 (s, 1H), 8.20 (s, 1H), 8.00 (d, $J = 8.5$ Hz, 1H), 7.31 (s, 2H), 7.22 (d, $J = 8.5$ Hz, 1H), 3.70 (s, 9H), 2.18 (s, 6H). ^{13}C NMR (CD_3OD) δ : 168.5, 163.0, 148.4, 140.1, 132.2, 131.9, 126.3, 125.6, 120.4, 120.0, 119.3, 58.2, 18.5. HRMS-ESI (m/z): $[\text{M}-\text{Cl}]^+$ calcd for $\text{C}_{18}\text{H}_{22}\text{BrN}_2\text{O}$, 361.0916; found 361.0906.

2.5.3 Preparation of NHC-Imine Complex **10a**

N-(4-Bromo-2,6-dimethylphenyl)-salicylaldimine **12a** (60 mg, 197 μmol) was dissolved in anhydrous THF (5 mL). Thallium(I) ethoxide (14 μL , 197 μmol) was added to this solution, and the resulting yellow mixture was stirred for 1.5 h. The green complex **9d** (114 mg, 158 μmol) was added as a solid, resulting in a rapid color change of the solution from yellow to red. After 1.5 h, the solvent was removed by high vacuum. The residue was dissolved in benzene (5 mL), and the resulting solution was filtered through a glass wool plug to remove the thallium chloride byproduct. The solvent was removed under high vacuum, and pentane (10 mL) was added to the residue to make a slurry. The red solid was removed by filtration, washed with pentane (3×5 mL), and dried under

high vacuum to afford **10a** (101 mg, 121 μ mol, 76% yield) as a red powder. Crystals suitable for X-ray diffraction analysis were obtained by layering pentane over a solution of **10a** in benzene. ^1H NMR (CD_2Cl_2) δ : 18.47 (s, 1H), 7.50 (s, 1H), 7.48 (d, $J = 8.0$ Hz, 2H), 7.34 (t, $J = 7.5$ Hz, 1H), 7.26 (t, $J = 7.7$ Hz, 1H), 7.01–6.95 (m, 6H), 6.91 (s, 1H), 6.77 (s, 1H), 6.48 (t, $J = 7.3$ Hz, 1H), 6.40 (s, 1H), 6.36 (s, 1H), 4.14–3.94 (m, 4H), 2.56 (s, 3H), 2.44 (s, 3H), 2.36 (s, 3H), 2.25 (s, 3H), 2.11 (s, 3H), 1.97 (s, 3H), 1.42 (s, 3H), 1.06 (s, 3H). ^{13}C NMR (CD_2Cl_2) δ : 298.7, 220.7, 170.3, 167.5, 152.2, 151.7, 140.2, 139.5, 138.2, 137.6, 137.4, 137.0, 136.9, 135.1, 134.3, 132.7, 129.6, 129.4, 128.6, 128.2, 123.8, 119.1, 117.7, 114.0, 51.8, 51.2, 21.1, 21.0, 20.1, 18.8, 18.3, 18.2, 17.9, 17.8. HRMS–ESI (m/z): $[\text{M}]^+$ calcd for $\text{C}_{43}\text{H}_{45}\text{BrClN}_3\text{ORu}$, 829.1511; found 829.1517. Anal. Calc. for $\text{C}_{43}\text{H}_{45}\text{BrClN}_3\text{ORu}$: C, 61.76; H, 5.42; N, 5.02. Found: C, 61.70; H, 5.43; N, 4.90.

2.5.4 Preparation of NHC–Imine Complex **10b**

Complex **10b** was prepared in 79% yield from **12b** and **9d** by using a procedure similar to that for the preparation of **10a**. ^1H NMR (CD_2Cl_2) δ : 18.43 (s, 1H), 8.06 (dd, $J = 9.4$ Hz, 2.5 Hz, 1H), 8.02 (d, $J = 2.5$ Hz, 1H), 7.58 (s, 1H), 7.49 (b, 2H), 7.40 (t, $J = 7.4$ Hz, 1H), 7.07–7.00 (m, 4H), 6.96 (d, $J = 9.4$ Hz, 1H), 6.93 (s, 1H), 6.76 (s, 1H), 6.42 (s, 1H), 6.37 (s, 1H), 4.17–3.96 (m, 4H), 2.53 (s, 3H), 2.41 (s, 3H), 2.34 (s, 3H), 2.25 (s, 3H), 2.07 (s, 3H), 1.99 (s, 3H), 1.45 (s, 3H), 1.04 (s, 3H). ^{13}C NMR (CD_2Cl_2) δ : 297.2, 214.4, 170.2, 163.0, 147.4, 146.0, 135.6, 134.9, 134.4, 134.0, 133.1, 132.4, 131.9, 131.1, 130.6, 129.9, 129.1, 127.5, 125.9, 125.2, 125.1, 125.0, 124.9, 124.8, 123.8, 123.5, 119.6,

113.8, 113.6, 47.2, 46.6, 16.4, 16.3, 15.4, 14.3, 13.7, 13.5, 13.3, 13.1. HRMS–ESI (m/z): $[M]^+$ calcd for $C_{43}H_{44}BrClN_4O_3Ru$, 874.1361; found 874.1324.

2.5.5 Preparation of NHC–Imine Complex **10c**

N-(4-Bromo-2,6-dimethylphenyl)-5-trimethylammoniumsalicylaldehyde chloride **12c** (71 mg, 180 μ mol) was dissolved in anhydrous DMF (3 mL). Thallium(I) ethoxide (12.7 μ L, 180 μ mol) was added to the solution, and the resulting yellow mixture was stirred for 1 h. The green complex **9d** (119 mg, 164 μ mol) was added to this mixture as a solution in THF (0.5 mL), resulting in a rapid color change from yellow to red. After 1 h the solvent was removed under high vacuum. The residue was dissolved in CH_2Cl_2 (20 mL), and the resulting solution was filtered to remove the thallium chloride byproduct. Subsequent manipulations were performed under air with reagent-grade solvents. The filtrate was washed twice with deionized water (20 mL) and once with brine (20 mL), and the organic layer was concentrated under reduced pressure. The residue was dissolved in CH_2Cl_2 (1 mL), and the resulting solution was transferred into pentane (20 mL) to precipitate a red-brown solid. The precipitate was removed by filtration, washed with pentane (10 mL), and dried under high vacuum to yield **10c** (132 mg, 142 μ mol, 87% yield) as a red-brown powder. 1H NMR (CD_2Cl_2) δ : 18.37 (s, 1H), 7.90 (d, J = 8.7 Hz, 1H), 7.64 (s, 1H), 7.46–7.59 (m, 3H), 7.38 (t, J = 6.8 Hz, 1H), 7.14 (d, J = 8.7 Hz, 1H), 7.02 (m, 4H), 6.94 (s, 1H), 6.78 (s, 1H), 6.44 (s, 1H), 6.32 (s, 1H), 3.94–4.16 (m, 4H), 3.79 (s, 9H), 2.52 (s, 3H), 2.44 (s, 3H), 2.39 (s, 3H), 2.26 (s, 3H), 2.03 (s, 3H), 1.97 (s, 3H), 1.42 (s, 3H), 1.09 (s, 3H). ^{13}C NMR (CD_2Cl_2) δ : 300.7, 219.4, 170.3, 166.9, 152.1, 151.0, 140.3, 139.3, 139.2, 138.5, 137.7, 137.1, 136.7, 134.6, 134.1, 133.7, 132.2, 130.6, 130.5, 129.8, 129.7,

129.4, 129.3, 128.4, 127.6, 126.1, 124.9, 118.3, 118.0, 58.4, 51.8, 51.3, 21.1, 21.0, 20.0, 18.8, 18.3, 18.1, 18.0, 17.9. HRMS–ESI (m/z): $[M-Cl]^+$ calcd for $C_{46}H_{53}BrClN_4ORu$, 887.2167; found 887.2125.

2.5.6 Preparation of *N,N*-Di-3-butenyl-2-nitrobenzenesulfonamide (13g)

A procedure from the literature¹⁰² was modified as follows. 2-Nitrobenzenesulfonamide (1.01 g, 5.00 mmol) and 4-bromo-1-butene (4.05 g, 30.0 mmol) were dissolved in acetone (25 mL), and potassium carbonate (1.73 g, 12.5 mmol) was added to this solution. The resulting mixture was stirred for 5 d. After filtration, the reaction mixture was acidified with formic acid until no additional evolution of $CO_2(g)$ was observed, and then concentrated under reduced pressure. The residue was dissolved in EtOAc, washed once with 1 M HCl (50 mL), twice with saturated aqueous $NaHCO_3$ (50 mL), and once with brine (50 mL). The organic layer was dried with $MgSO_4(s)$ and concentrated under reduced pressure. The crude product was purified by flash chromatography (20% EtOAc v/v in hexane) to afford **13g** (180 mg, 0.580 mmol, 11.6%) as a yellow oil. 1H NMR ($CDCl_3$) δ : 8.07–8.01 (m, 1H), 7.72–7.61 (m, 3H), 5.77–5.64 (m, 2H), 5.13–4.98 (m, 4H), 3.39 (t, $J = 7.6$ Hz, 4H), 2.31 (q, $J = 7.6$ Hz, 4H). ^{13}C NMR ($CDCl_3$) δ : 148.2, 134.3, 133.9, 133.6, 131.8, 131.0, 124.3, 117.6, 46.9, 32.8. HRMS–ESI (m/z): $[M+Na]^+$ calcd for $C_{14}H_{18}N_2O_4SNa$, 333.0885; found 333.0891.

2.5.7 Preparation of *N*-(2-Propenyl)-*N*-(2-butyne)-4-methylbenzenesulfonamide (13j)

Following the procedure of Pagenkopf and coworkers,¹⁰¹ *N*-(2-propenyl)-4-methylbenzenesulfonamide (2.00 g, 9.51 mmol), 1-bromo-2-butyne (3.79 g, 28.5 mmol),

and potassium carbonate (1.58 g, 11.41 mmol) yielded **13j** (1.15 g, 4.36 mmol, 46%) as a yellow oil following silica gel flash chromatography (10% EtOAc v/v in hexane). ¹H NMR data were in agreement with those reported by Buchwald and coworkers.¹⁰³

2.5.8 Preparation of Allyl 1,1-Diphenylpropargyl Ether (**13k**)

Allyl 1,1-diphenylpropargyl ether was prepared by the method of Dixneuf and coworkers.¹⁰⁴ $R_f = 0.52$ (silica gel, 5% EtOAc v/v in hexane). ¹H NMR (CDCl₃) δ : 7.58 (d, $J = 7.6$ Hz, 4H), 7.30 (t, $J = 7.4$ Hz, 4H), 7.23 (t, $J = 7.2$ Hz, 2H), 6.05–5.93 (m, 1H), 5.36 (d, $J = 17.5$, 1H), 5.16 (d, $J = 10.4$ Hz, 1H), 4.04 (d, $J = 5.1$ Hz, 2H), 2.86 (s, 1H). ¹³C NMR (CDCl₃) δ : 143.3, 134.9, 128.4, 127.9, 126.7, 116.3, 83.4, 80.2, 77.8, 66.1. HRMS–ESI (m/z): $[M+Na]^+$ calcd for C₁₈H₁₆ONa, 271.1099; found 271.1106.

2.5.9 Representative Procedure for RCM Reactions

On the benchtop under air, the ruthenium complex **10a** (1.6 mg, 1.9 μ mol) was dissolved in non-distilled, non-degassed C₆D₆ (0.75 mL) in an NMR tube, and substrate **13c** (8.1 μ L, 38 μ mol) was added to this solution. The tube was capped, wrapped with parafilm, shaken, and placed in a temperature-controlled water bath at 55 °C. Product formation was monitored by ¹H NMR integration of the allylic methylene signals.

2.5.10 Alternative Preparation of NHC–Imine Complex **10a**

A flame-dried Schlenk flask was charged with 1,3-bis(2,4,6-trimethylphenyl)-4,5-dihydroimidazolium tetrafluoroborate (12.2 mg, 30.9 μ mol) and anhydrous hexanes (5 mL). After the addition of 1.7 M potassium *t*-amylate in toluene (18.2 μ L, 30.9 μ mol), the

suspension was stirred for 5 min. Complex **11a** (5.0 mg, 6.2 μmol) was added as a solid, and the resulting reddish mixture was heated to 75 $^{\circ}\text{C}$ for 1 h, after which the solvent was removed under high vacuum. The crude product was analyzed by ^1H NMR in CD_2Cl_2 .

2.5.11 Preparation of Imine Complex **11c**

N-(4-Bromo-2,6-dimethylphenyl)-5-trimethylammoniumsalicylaldehyde chloride **12c** (199 mg, 500 μmol) was dissolved in anhydrous DMF (10 mL). Thallium(I) ethoxide (35 μL , 500 μmol) was added to the solution, and the resulting yellow mixture was stirred for 3 h. The purple complex **1** (329 mg, 400 μmol) was added to this mixture as a solution in anhydrous THF (7 mL), resulting in a rapid color change from yellow to red. After 2.5 h the solvent was removed under high vacuum. The residue was treated with pentane (15 mL) and the pink pentane solution was filtered from the brown residue. The residue was dissolved in CH_2Cl_2 (5 mL), and the resulting solution was filtered to remove the thallium chloride byproduct. The filtrate was evaporated under high vacuum and redissolved in CH_2Cl_2 (1.5 mL). Pentane (15 mL) was added to precipitate the desired complex, and the pentane supernatant was decanted. This process was repeated twice more until the pentane supernatant was colorless. The solids were filtered out, washed with copious pentane, and dried under high vacuum to afford **11c** (249 mg, 276 μmol , 68.9%) as a red-brown powder. ^1H NMR (CD_2Cl_2) δ : 19.47 (d, $J_{\text{PH}} = 4.6$ Hz, 1H), 8.14 (d, $J = 5.5$ Hz, 1H), 7.99 (d, $J = 7.7$ Hz, 2H), 7.87 (br. s, 2H), 7.57 (t, $J = 7.3$ Hz, 1H), 7.31–7.23 (m, 3H), 7.21–7.14 (m, 2H), 3.82 (s, 9H), 2.49 (q, $J = 11.4$ Hz, 3H), 2.38 (s,

3H), 1.88–1.15 (br. m). $^{31}\text{P}\{^1\text{H}\}$ NMR (CD_2Cl_2) δ : 50.02. ^{13}C NMR (CD_2Cl_2) δ : 283.8.

LRMS–ESI (m/z): $[\text{M}–\text{Cl}]^+$ calcd for $\text{C}_{43}\text{H}_{60}\text{BrClN}_2\text{OPRu}$, 867.2; found 867.5, 847.5.

2.5.12 Structure Determination of NHC–Imine Complex 10a

A red crystal of complex **10a** with approximate dimensions $0.36 \times 0.31 \times 0.30 \text{ mm}^3$ was selected under oil under ambient conditions and attached to the tip of a nylon loop. The crystal was mounted in a stream of cold $\text{N}_2(\text{g})$ at 100(2) K and centered in the X-ray beam by using a video camera.

The crystal evaluation and data collection were performed on a Bruker CCD-1000 diffractometer with Mo K_α ($\lambda = 0.71073 \text{ \AA}$) radiation and a diffractometer to crystal distance of 4.9 cm.

The initial cell constants were obtained from three series of ω scans at different starting angles. Each series consisted of 20 frames collected at intervals of 0.3° in a 6° range about ω with the exposure time of 15 s per frame. A total of 141 reflections was obtained. The reflections were indexed successfully with an automated indexing routine built in the SMART program. The final cell constants were calculated from a set of 13907 strong reflections from the actual data collection.

Diffraction data were collected by using the hemisphere data collection routine. The reciprocal space was surveyed to the extent of a full sphere to a resolution of 0.80 \AA . A total of 27059 data were harvested by collecting three sets of frames with 0.3° scans in ω and ϕ with an exposure time 45 s per frame. These highly redundant datasets were corrected for Lorentz and polarization effects. The absorption correction was based on

fitting a function to the empirical transmission surface as sampled by multiple equivalent measurements.¹⁰⁵

The systematic absences in the diffraction data were consistent for the space groups $P\bar{1}$ and $P1$. The E -statistics strongly suggested the centrosymmetric space group $P\bar{1}$ that yielded chemically reasonable and computationally stable results of refinement.¹⁰⁵

A successful solution by the direct methods provided most non-hydrogen atoms from the E -map. The remaining non-hydrogen atoms were located in an alternating series of least-squares cycles and difference Fourier maps. All non-hydrogen atoms were refined with anisotropic displacement coefficients. All hydrogen atoms were included in the structure factor calculation at idealized positions and were allowed to ride on the neighboring atoms with relative isotropic displacement coefficients.

The final least-squares refinement of 459 parameters against 7597 data resulted in residuals R (based on F^2 for $I \geq 2\sigma$) and wR (based on F^2 for all data) of 0.0262 and 0.0739, respectively. The final difference Fourier map was featureless.

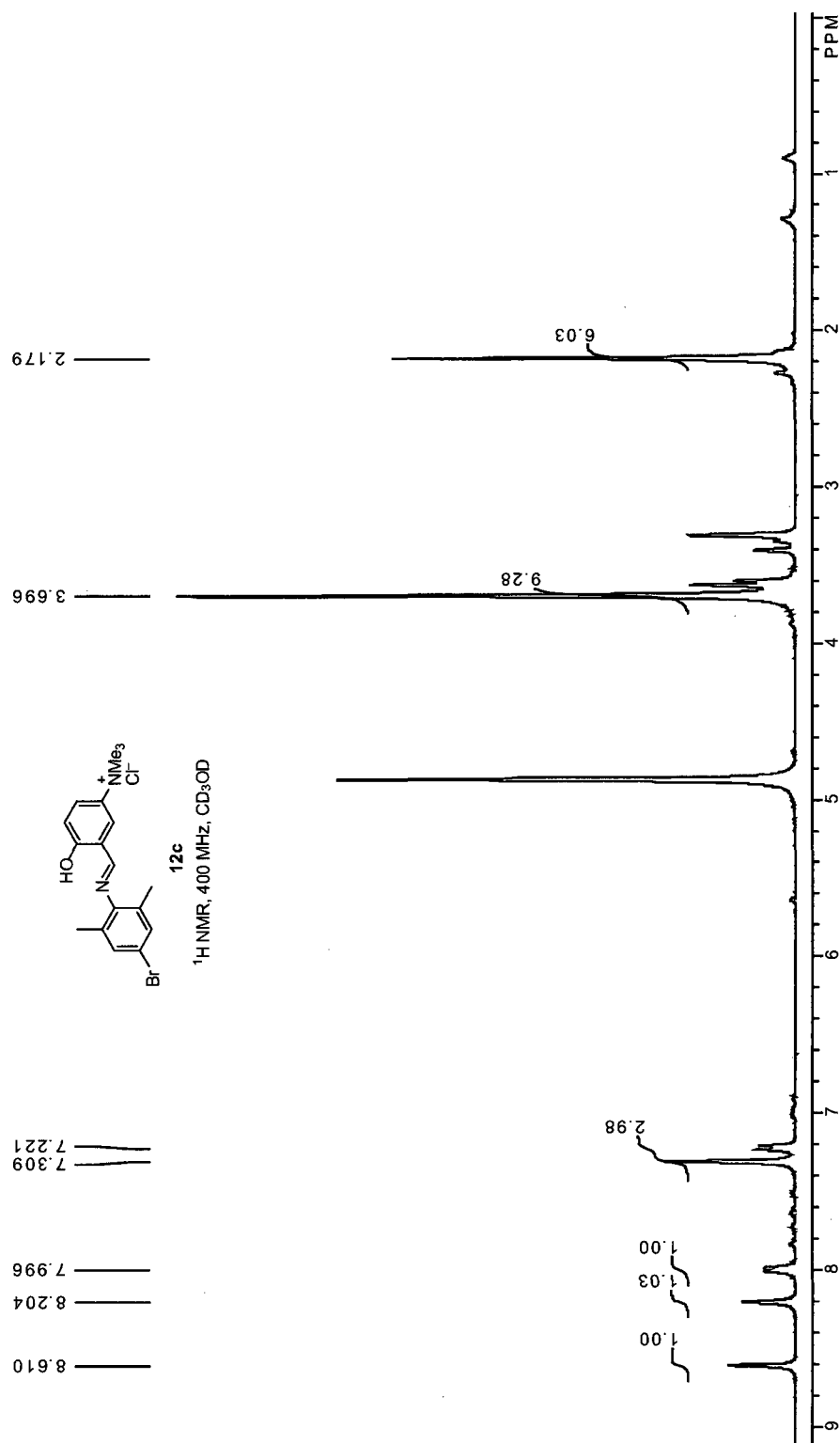


Figure 2.4 ^1H NMR of *N*-(4-Bromo-2,6-dimethylphenyl)-5-trimethylammoniumsalicylaldimine chloride

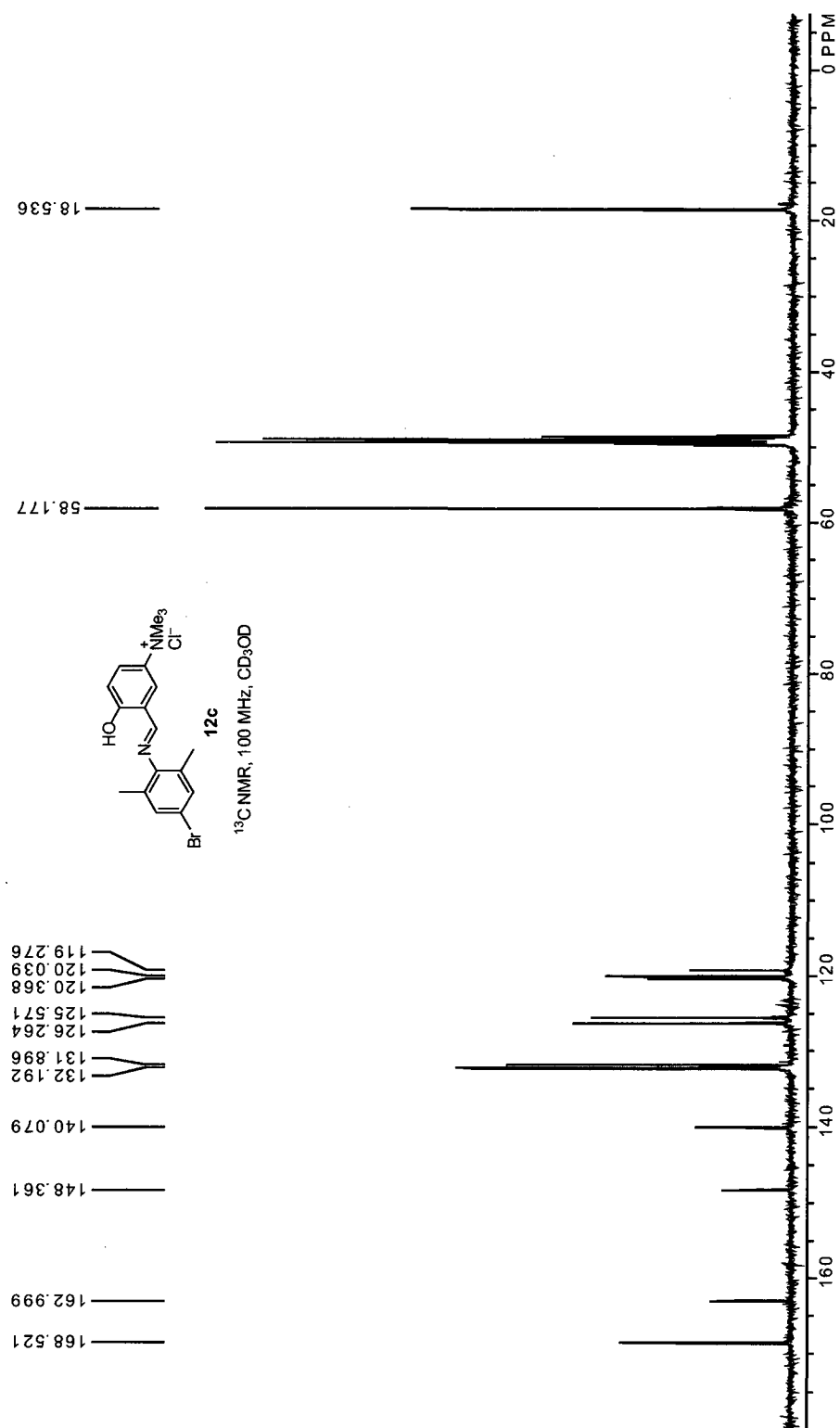


Figure 2.5 ¹³C NMR of *N*-(4-Bromo-2,6-dimethylphenyl)-5-trimethylammoniumsalicylaldehyde chloride

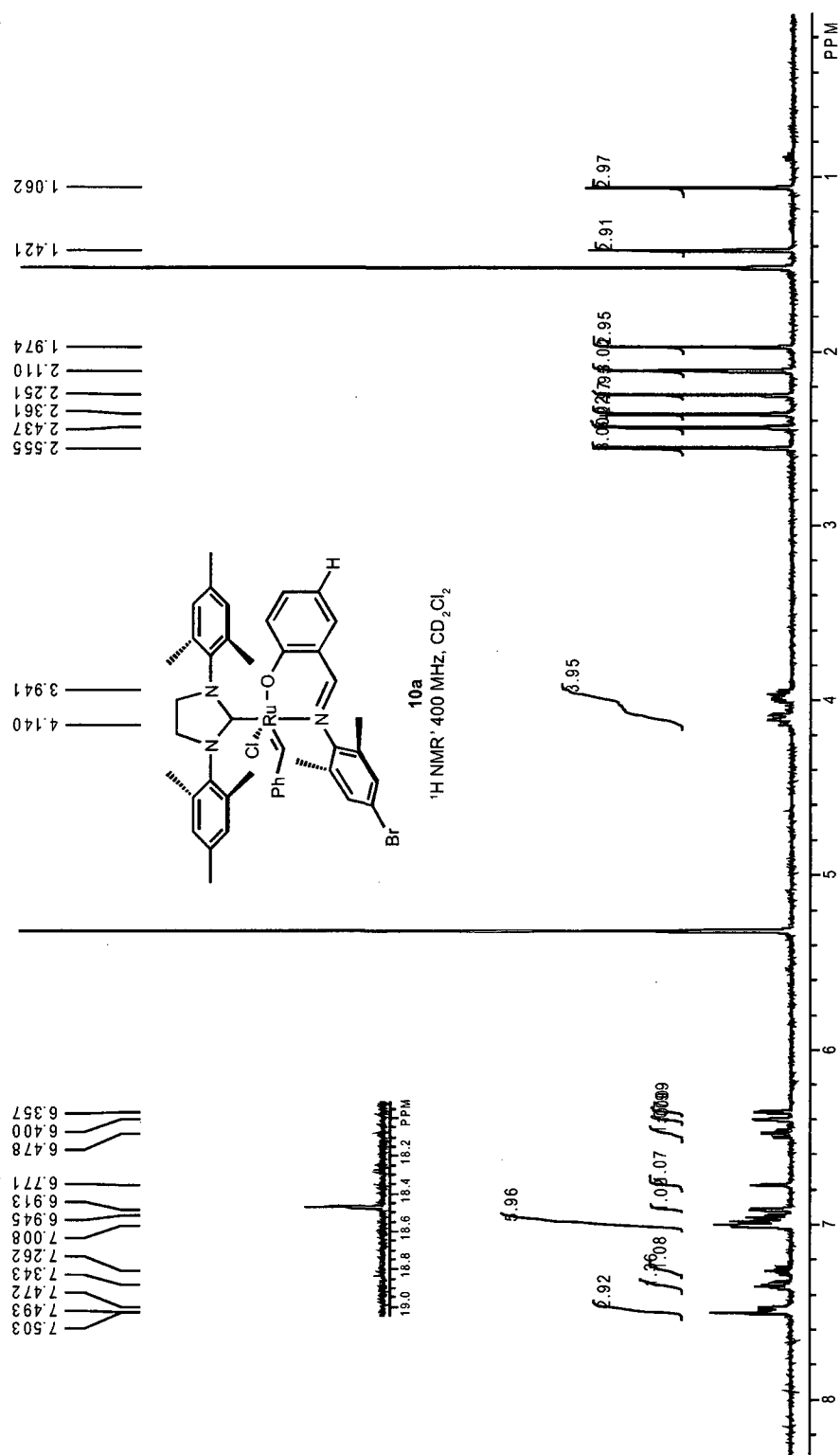


Figure 2.6 ¹H NMR of NHC-Imine Complex 10a

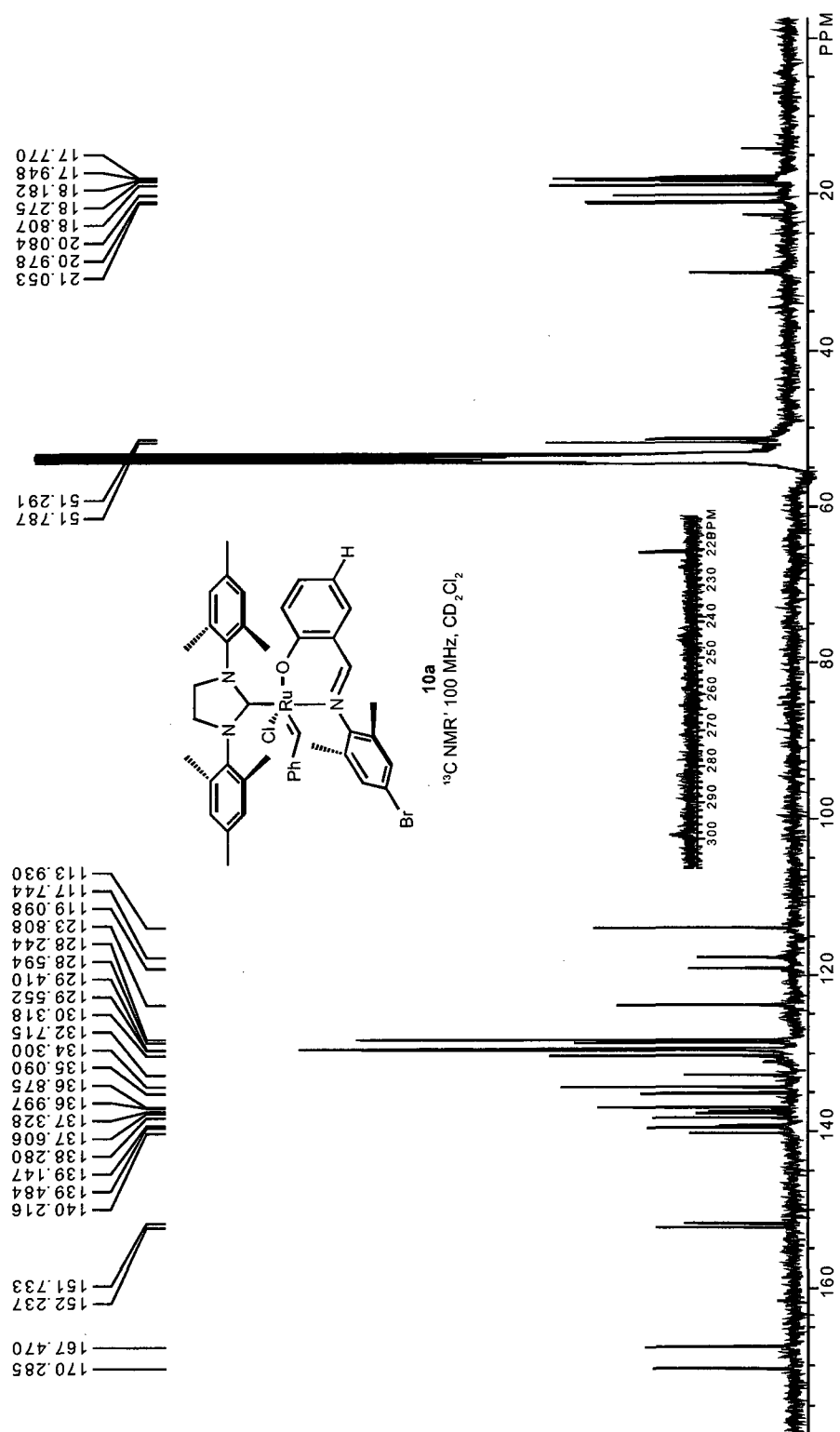


Figure 2.7 ¹³C NMR of NHC-Imine Complex 10a

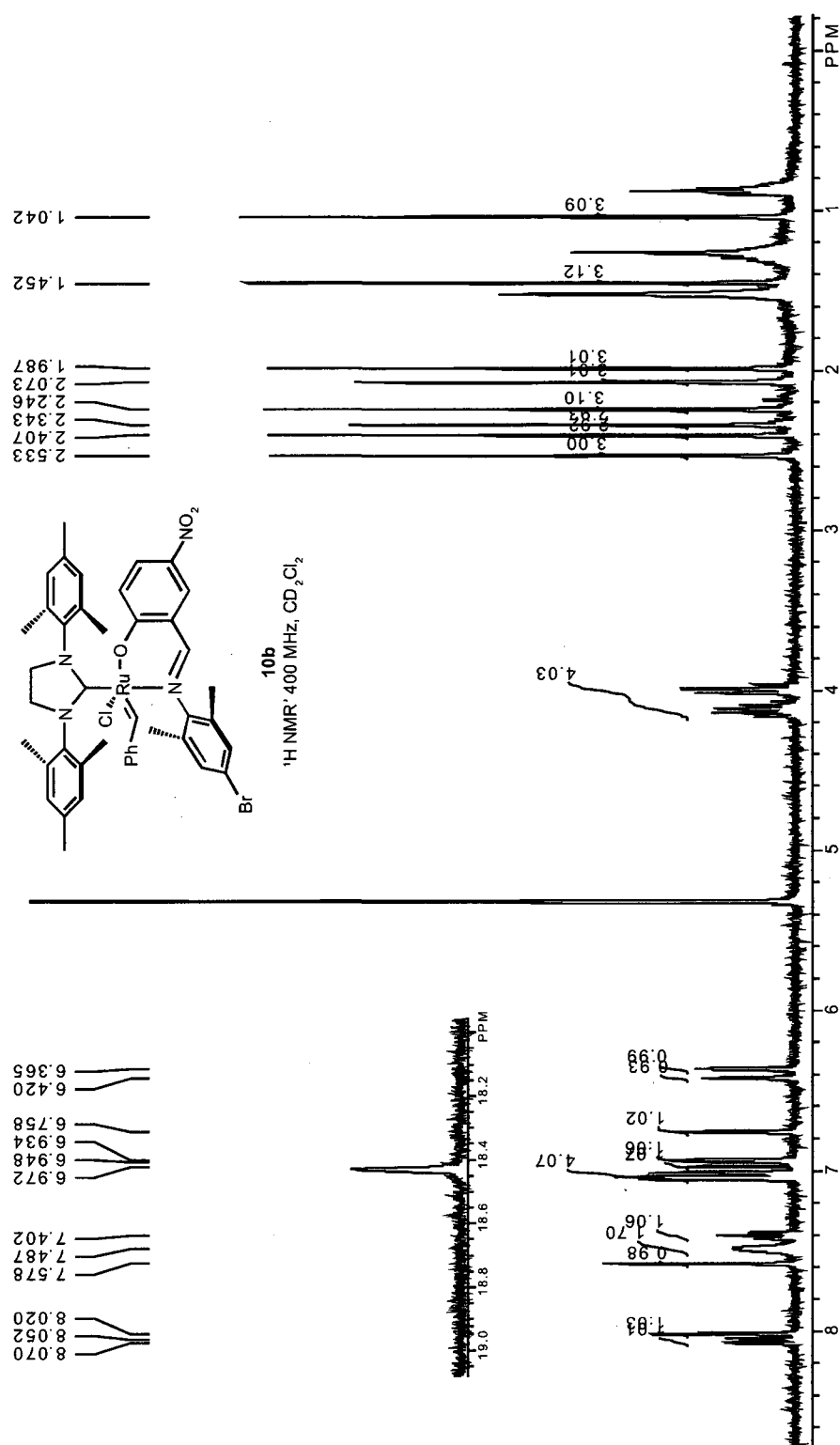


Figure 2.8 ¹H NMR of NHC–Imine Complex **10b**

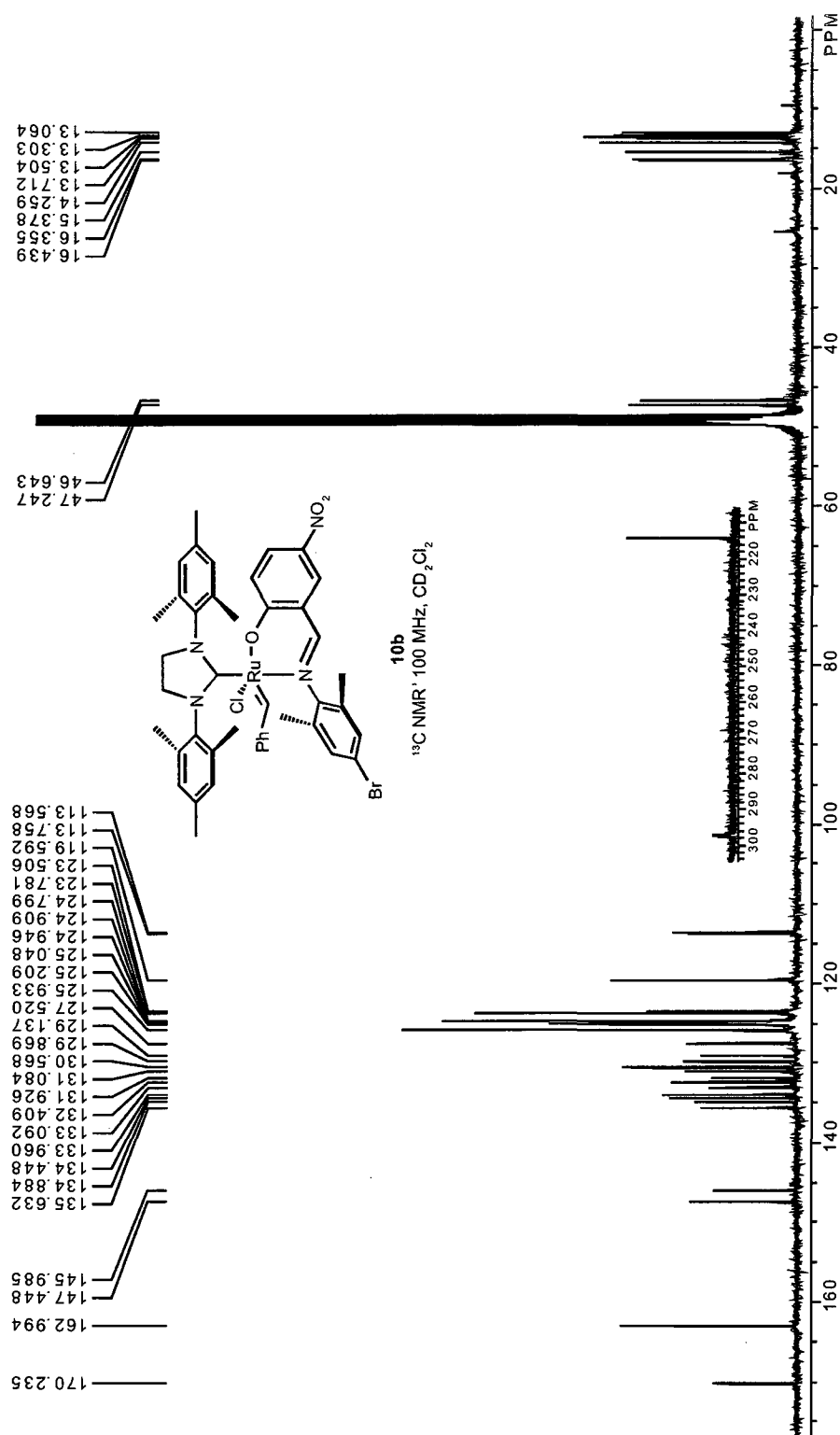


Figure 2.9 ^{13}C NMR of NHC-Imine Complex **10b**

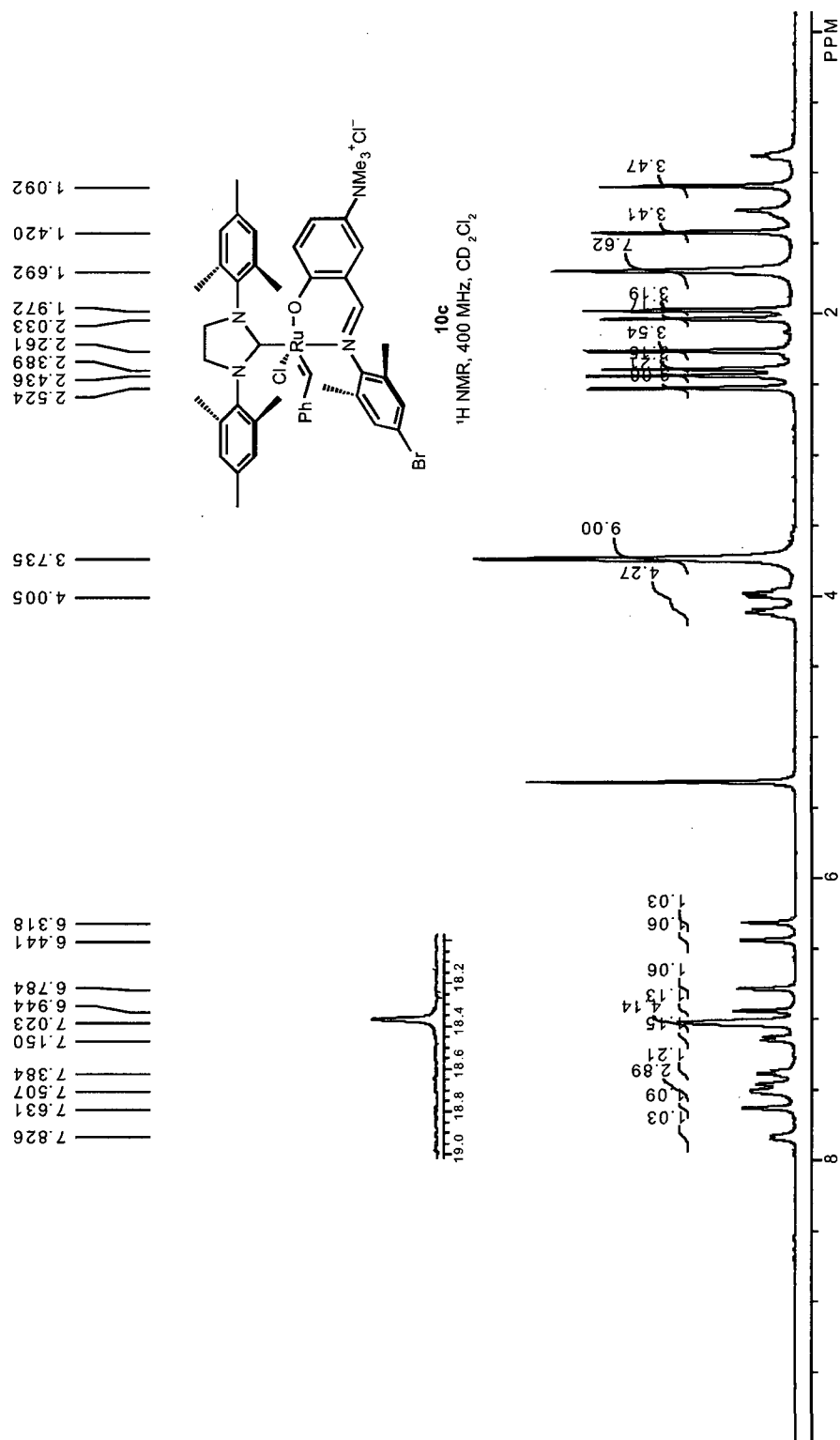


Figure 2.10 ¹H NMR of NHC–Imine Complex **10c**

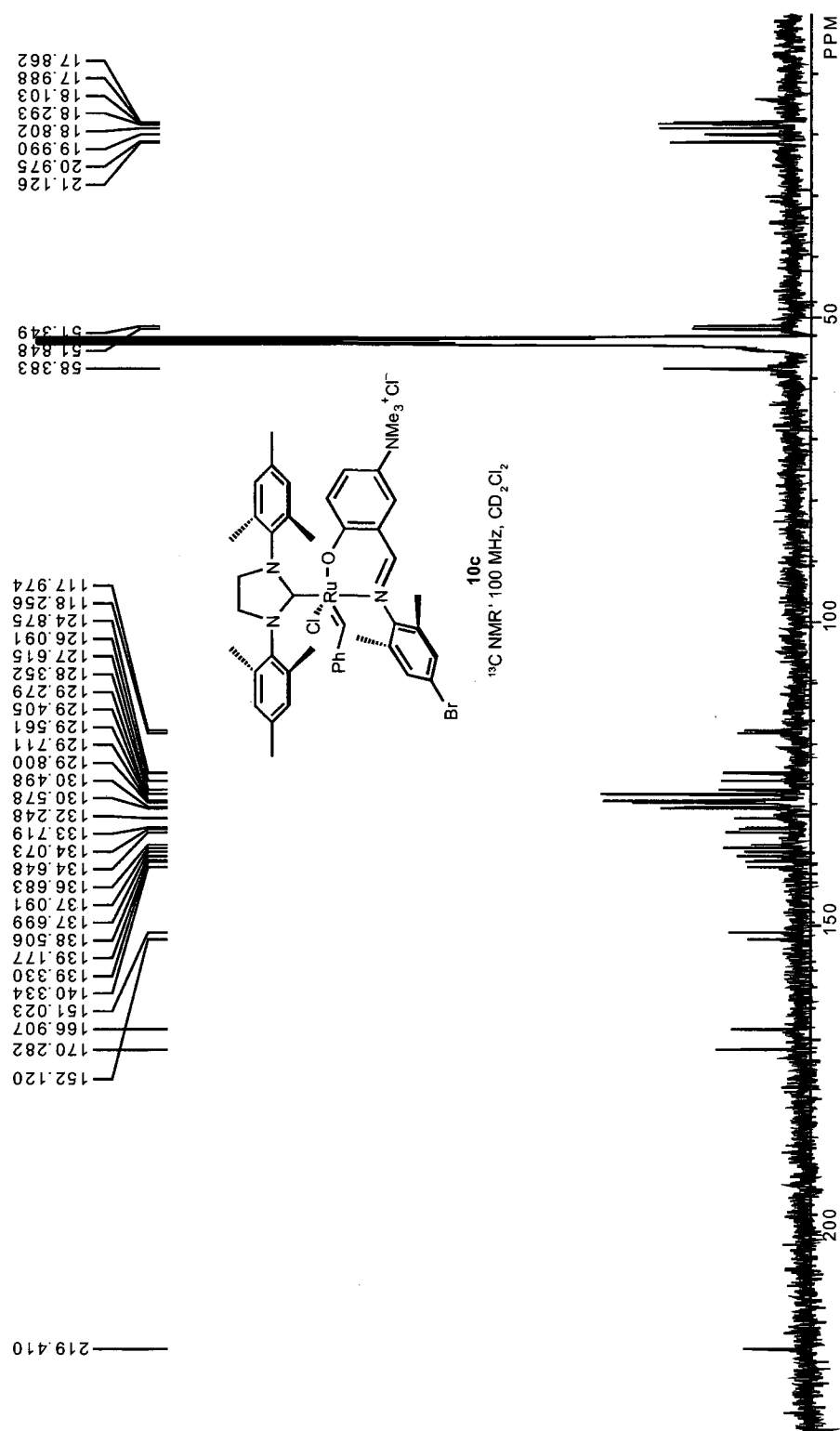


Figure 2.11 ^{13}C NMR of NHC-Imine Complex **10c**

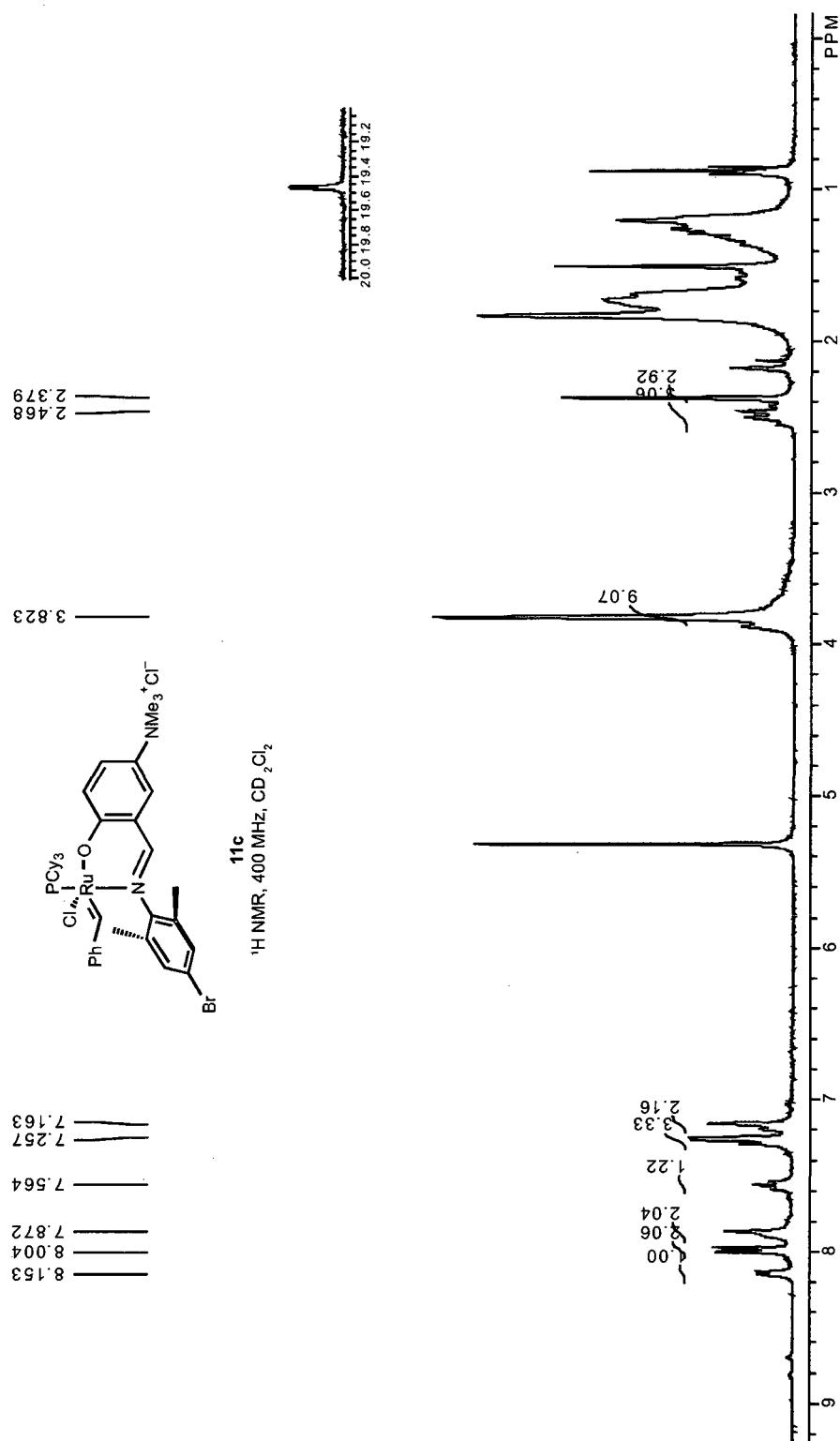


Figure 2.12 ^1H NMR of Imine Complex **11c**

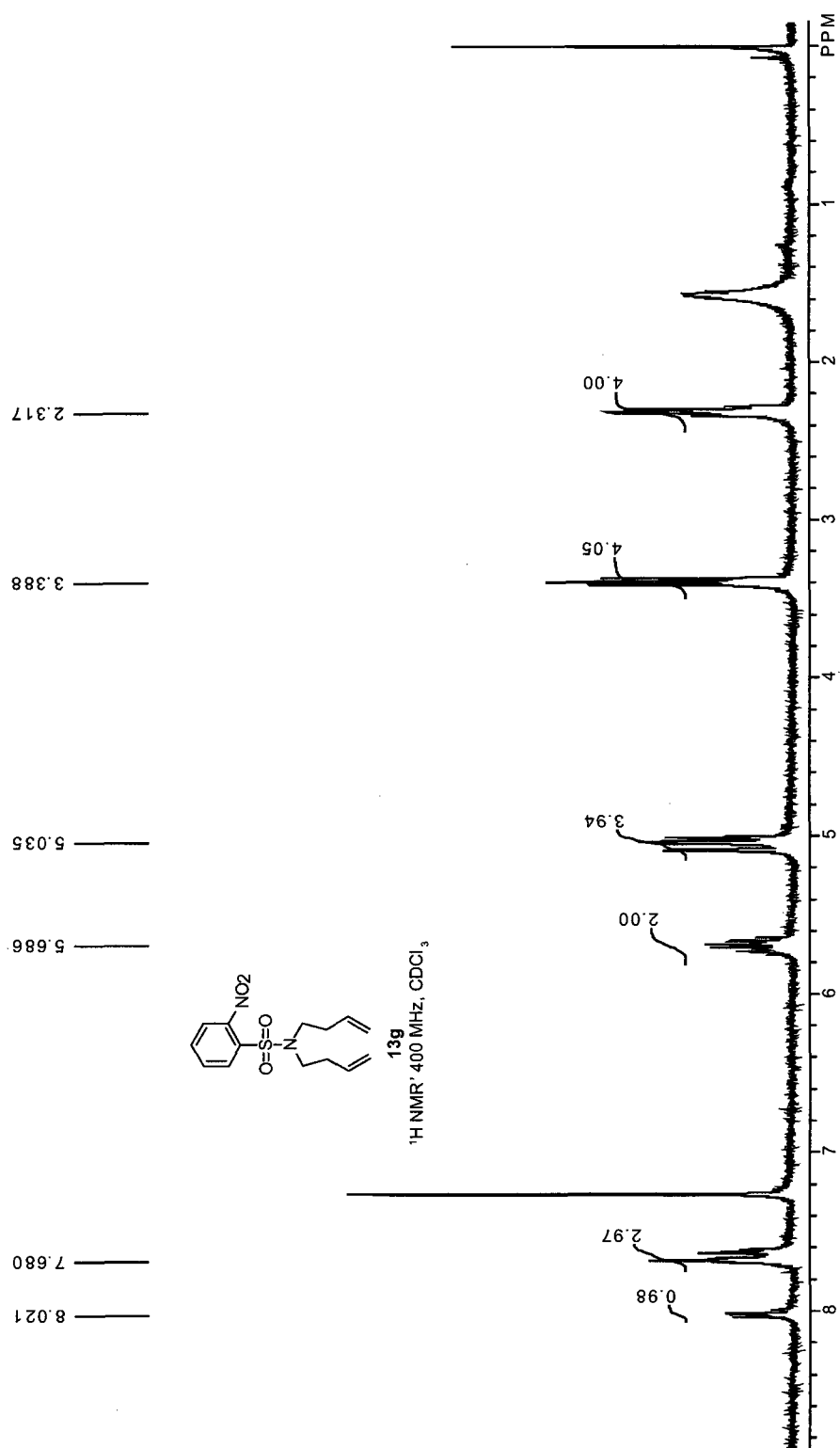


Figure 2.13 ¹H NMR of *N,N*-Di-3-butenyl-2-nitrobenzenesulfonamide

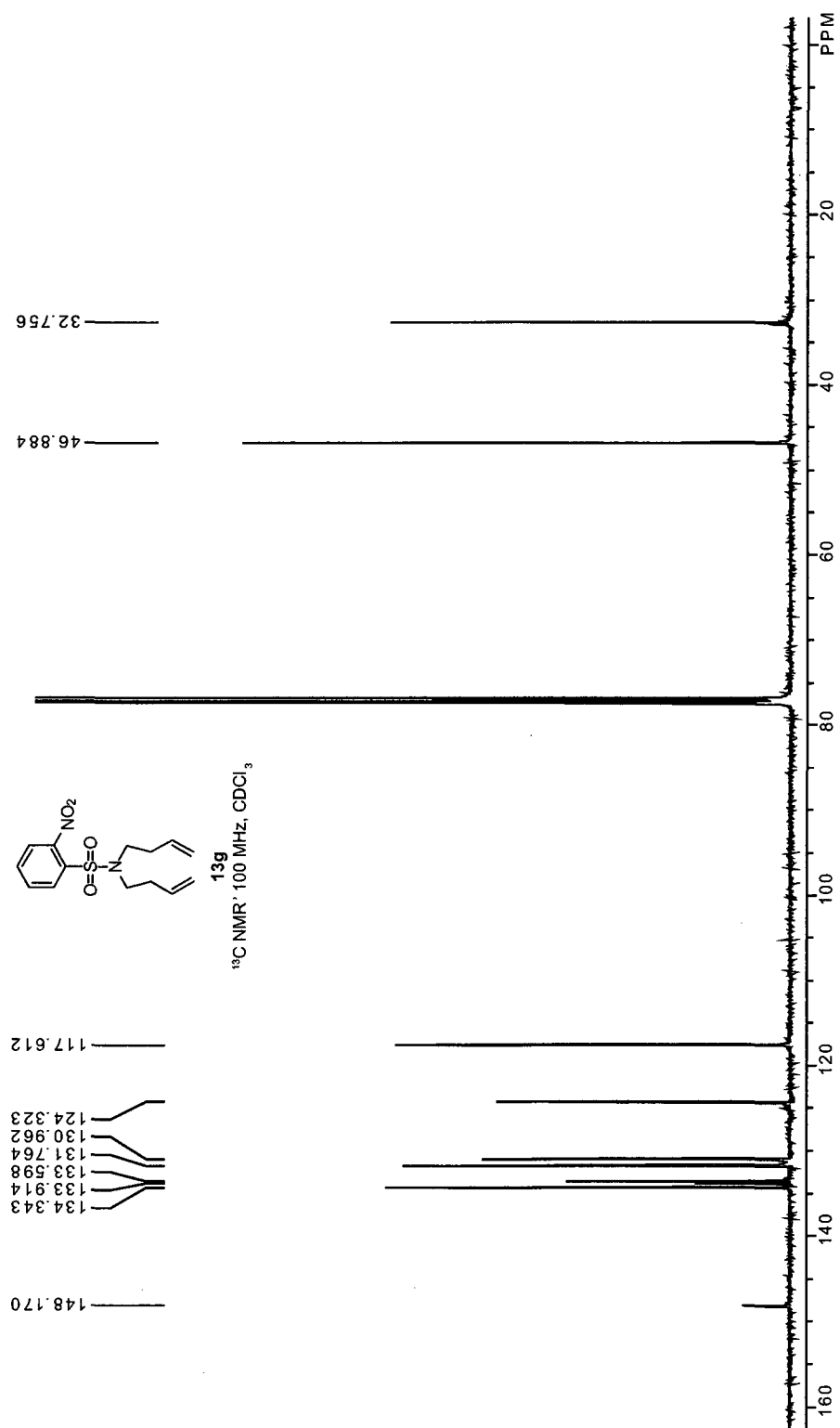


Figure 2.14 ^{13}C NMR of *N,N*-Di-3-butenyl-2-nitrobenzenesulfonamide

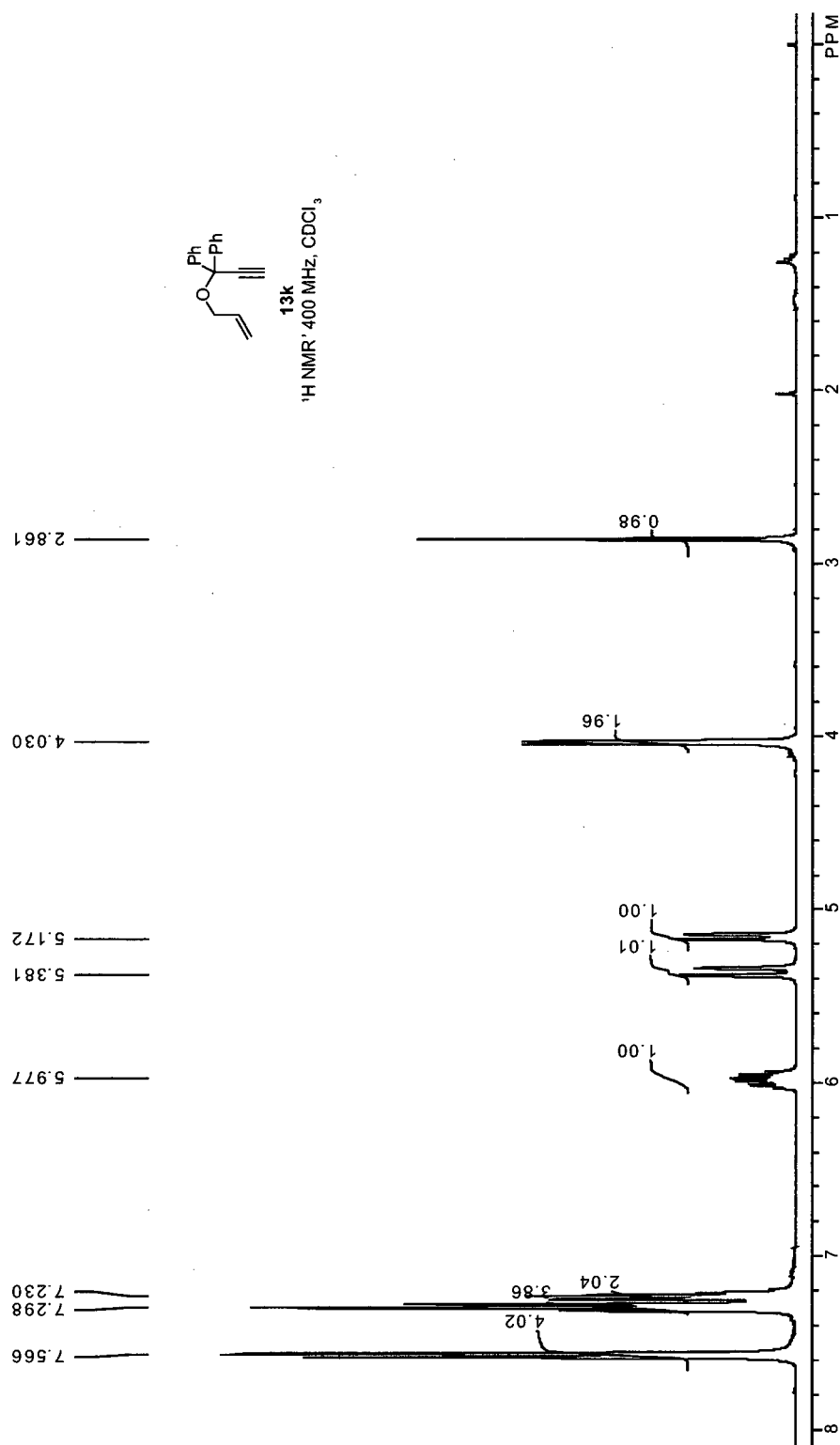


Figure 2.15 ¹H NMR of Allyl 1,1-diphenylpropargyl ether

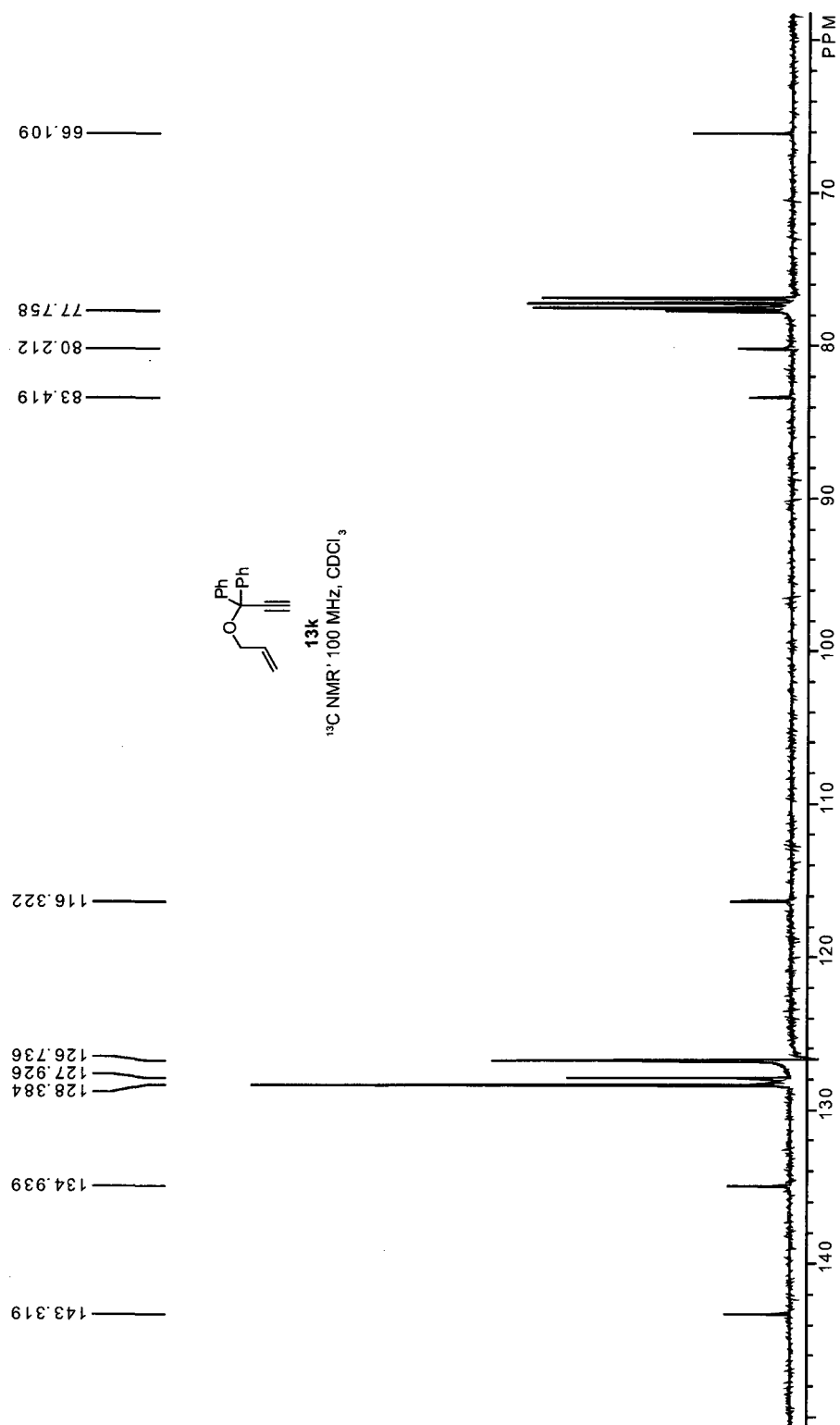
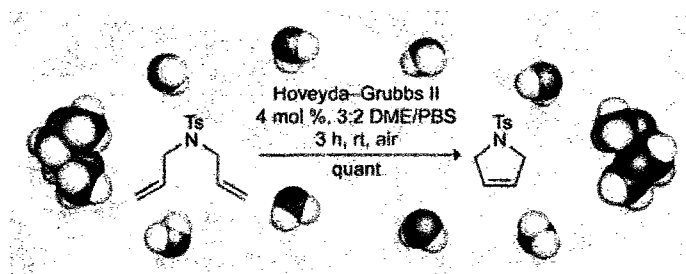


Figure 2.16 ^{13}C NMR of Allyl 1,1-diphenylpropargyl ether

CHAPTER 3*

**OLEFIN METATHESIS IN HOMOGENEOUS AQUEOUS MEDIA
CATALYZED BY CONVENTIONAL RUTHENIUM CATALYSTS**

Abstract: Olefin metathesis in aqueous solvents is sought for applications in green chemistry and with the hydrophilic substrates of chemical biology, such as proteins and polysaccharides. Most demonstrations of metathesis in water, however, utilize exotic complexes. We have examined the performance of conventional catalysts in homogeneous water–organic mixtures, finding that the second-generation Hoveyda–Grubbs catalyst has extraordinary efficiency in aqueous dimethoxyethane and aqueous acetone. High (71–95%) conversions are achieved for ring-closing and cross metathesis of a variety of substrates in these solvent systems.



Co-author contribution: J. J. B. performed and analyzed some of the olefin metathesis and protein solubility experiments herein.

*This chapter has been published, in part, under the same title. Reference: Binder, J. B.; Blank, J. J.; Raines, R. T. *Organic Letters* **2007**, 9, 4885–4888.

3.1 Introduction

As a highly effective means for creating carbon–carbon bonds, olefin metathesis is a privileged reaction in the armamentarium of synthetic and polymer chemists.^{1–4} Readily available and highly active ruthenium catalysts **1–4a** have popularized metathesis chemistry in organic solvents (**Figure 3.1**).^{54,32,55,33} On the other hand, metathesis in aqueous solvents largely remains the domain of catalysts designed expressly for use in water (**Figure 3.2**).^{25,36,38,41,42} Despite the allure of aqueous olefin metathesis for biological applications^{106,10,107,57,19,16,20} and green chemistry,^{65–67,108} the synthesis of these water-soluble ligands and complexes imposes barriers to their wider use.

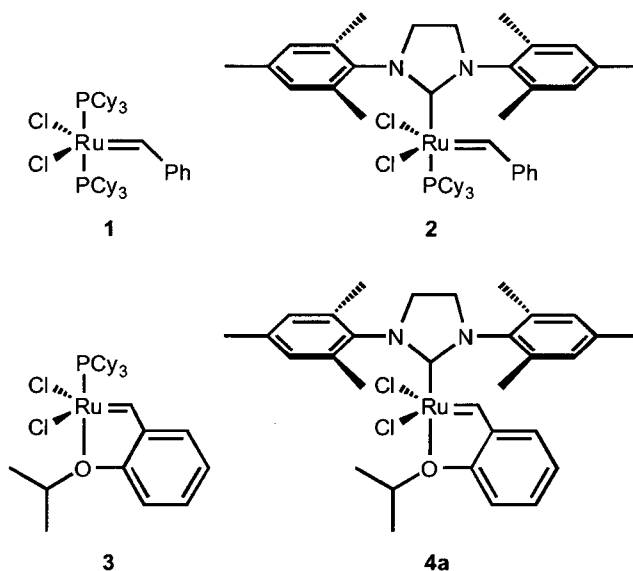


Figure 3.1 Conventional ruthenium olefin metathesis catalysts.

Developing aqueous reaction conditions suitable for catalysts such as **1–4a** is an alternative approach. In the initial work with well-defined catalysts in aqueous systems, Grubbs and coworkers performed ring-opening metathesis polymerization (ROMP) with

1 in aqueous emulsions,¹⁰⁹⁻¹¹¹ a method that allowed Kiessling and coworkers to synthesize biologically active glycopolymers.^{112,113} For ring-closing metathesis (RCM) and cross metathesis (CM), Blechert and coworkers employed commercially-available **2** and complex **8e**, a relative of commercially-available **4a**, in water-methanol and water-DMF mixtures.⁴⁷ Although they achieved high conversion in the ring-closure of N-tosyldiallylamine (**13c**) in 3:1 water/methanol and 3:1 water/DMF over an extended reaction time of 12 h, these reactions were not accomplished in homogenous systems: neither the substrate nor the catalyst was dissolved completely in the aqueous phase. In most cases detailed in their report, the ruthenium complex was only sparingly soluble in the aqueous reaction mixture.

Metathesis in homogeneous aqueous systems would likely be faster and more versatile than in these heterogeneous systems. An effective system for metathesis with commercially available catalysts in homogeneous aqueous media would not only make this chemistry more accessible, but also highlight the limitations of the standard catalysts in water, informing catalyst-design efforts. Yet, reports of the use of common metathesis catalysts in an aqueous context are limited. For these reasons, we chose to test the capabilities of catalysts **1–4a** in homogeneous aqueous media, and we report the results of our exploration herein.

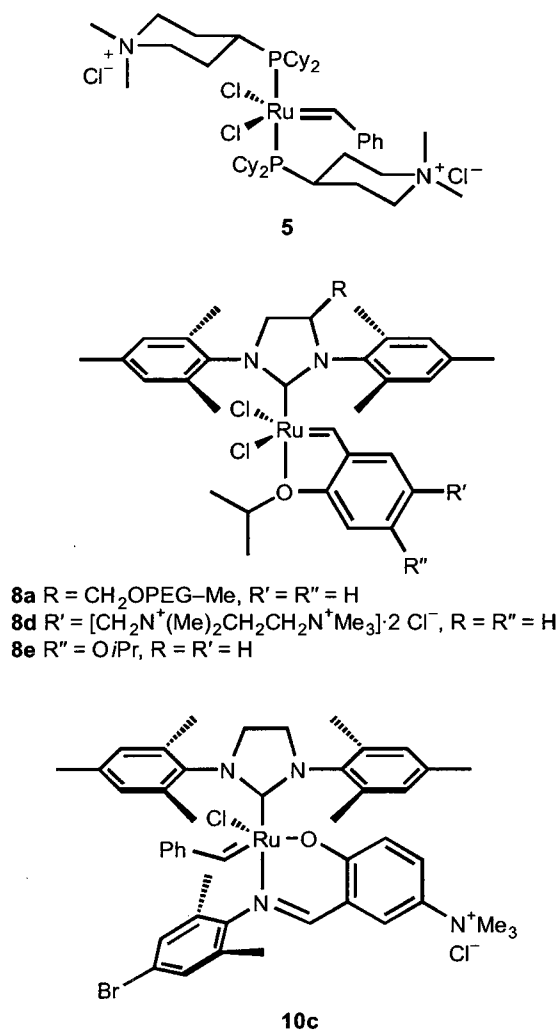


Figure 3.2 Metathesis catalysts adapted to aqueous solvents.

3.2 Results and Discussion

3.2.1 Solvent Screening

First, we screened various organic solvents as co-solvents for RCM of **13c** in a homogeneous aqueous solution (Table 3.1). The solvents typically used for olefin metathesis reactions, such as CH_2Cl_2 , 1,2-dichloroethane, and toluene, are immiscible with water, so we resorted to water-miscible solvents. Tetrahydrofuran (THF), used

previously as a solvent for ROMP and acyclic diene metathesis with varying success,^{114,115} failed as a cosolvent for RCM. On the other hand, the ethylene glycol ether-based solvents dimethoxyethane (DME or glyme) and poly(ethylene glycol) (PEG) were excellent co-solvents. Their improved results with respect to THF and dioxane could relate to their better coordinating ability.^{116,117} Able to coordinate the tetracoordinate ruthenium complexes of the metathesis catalytic cycle, these ethers could more ably protect them from detrimental coordination by water. Grubbs and coworkers suggest that decomposition of metathesis intermediates in water results from water coordination at ruthenium in the methyldiene-propagating species.¹¹⁸ Interestingly, these results show that the protective environment of the PEG-bearing ligand in **8a** can also be provided by ethylene glycol ethers in the bulk solvent.

Table 3.1 RCM Catalyzed by **2** in Aqueous Media

Reaction scheme: 13c (a 5-membered ring with a Ts group and two vinyl groups) reacts with **2** (5 mol %) in 0.024 M, 24 h, rt, air to form a 5-membered ring product with a Ts group and one vinyl group.

13c	
solvent ^a	conversion (%)
4:1 THF/H ₂ O	3
4:1 1,4-dioxane/H ₂ O	5
4:1 DMF/H ₂ O	75
4:1 (CH ₃) ₂ CO/H ₂ O	>95
4:1 DME/H ₂ O	>95
3:1 PEG-500 dimethyl ether/H ₂ O	>95

^a Mass:mass ratio.

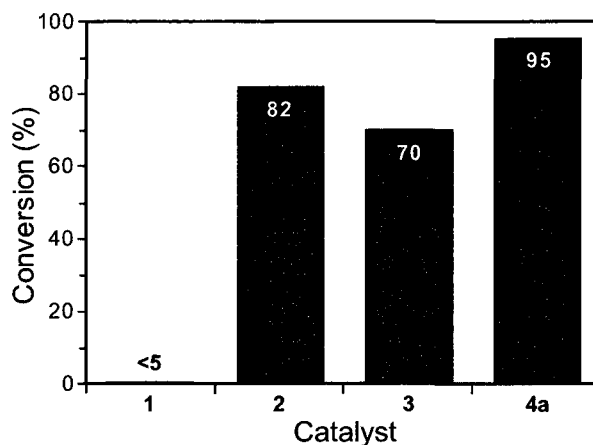


Figure 3.3 RCM conversion of 0.05 M substrate **13c** catalyzed by complexes **1–4a**: 1 mol % [Ru], 2:1 DME/water, 24 h, rt, under air.

3.2.2 Catalyst Screening

Next, we studied the performance of different commercially available catalysts in the DME–water solvent system with substrate **13c** (**Figure 3.3**). Phosphine-free complex **4a** displayed the highest turnover, with both N-heterocyclic carbene (NHC) complexes outperforming the 1st-generation catalysts. The more σ -donating NHC ligand could aid olefin coordination over attack by water, favoring metathesis with the 2nd-generation catalysts as opposed to decomposition. The advantage of **4a** over **2** is more difficult to rationalize because both complexes produce the same propagating species. The improved performance of **4a** could be due to the presence of the chelating isopropoxy moiety, which could potentially protect the catalyst from decomposition in water prior to entry into the catalytic cycle, as suggested by Blechert and coworkers for metathesis in organic solvents.³⁴ Although the ether ligand binds more loosely than does the phosphine of **2** (**4a** initiates >800-fold faster at 25 °C),¹¹⁹ its rebinding to ruthenium prior to metathesis is unimolecular. As a result, the ether ligand is more likely to rebind the coordinatively

unsaturated intermediate, protecting it from water to preserve the complex in solution.³⁴ In addition to helping select known catalysts for use in water–organic systems, these results can inform the design of water-soluble catalysts. The combination of a chelate and an NHC produces a more effective catalyst for aqueous metathesis, as borne out by complexes **8a**, **8d**, and **10c**. Future catalyst designs should incorporate these features.

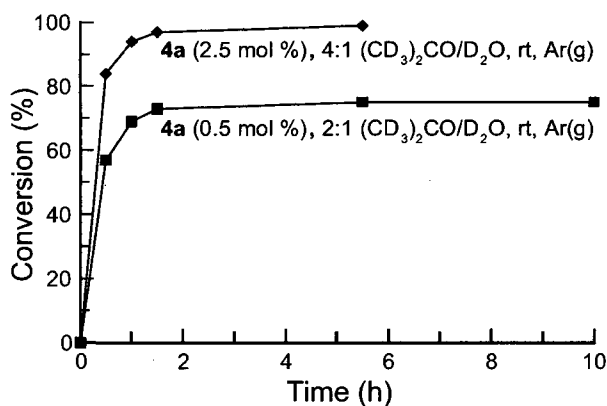


Figure 3.4 Kinetics of RCM of 0.05 M substrate **13c** catalyzed by complex **4a** in acetone/water monitored by ¹H NMR spectroscopy.

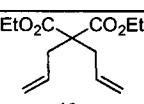
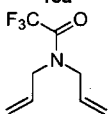
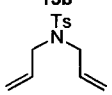
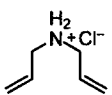
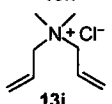
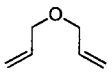
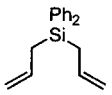

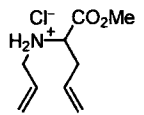
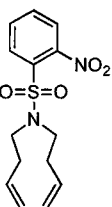
Following the identification of **4a** as the superior catalyst in the water–DME system, the progress of RCM in acetone–water was monitored to evaluate the rate of the reaction and the lifetime of catalytically-active species (**Figure 3.4**). The majority of RCM occurred within 90 min of the beginning of the reaction, as is typical for RCM of **13c** with this catalyst and temperature.⁸⁹ Notably, this reaction is far faster than the 12-h reaction time reported by Blechert and coworkers for their heterogeneous systems.⁴⁷ Nevertheless, catalyst decomposition also proceeds quickly in the aqueous solvent, with the results of the trial with 0.5 mol % catalyst indicating that the majority of the

catalytically-active species is destroyed within 90 min. In organic solvents, on the other hand, complex **4a** can be recovered after RCM reactions requiring several hours.³³

3.2.3 Substrate Scope

With optimized reaction conditions established, we probed the RCM of a variety of dienes using complex **4a** in aqueous DME and acetone solutions. Under these homogeneous conditions, substrates with a variety of substituents were metathesized to form five-, six-, and seven-membered cyclic products (Table 3.2). High conversion was consistently achieved with traditional non-polar substrates, except for diallyldiphenylsilane (**13e**). Water-soluble substrates such as **13h** and **16**—a putative model for peptide substrates—were more challenging, requiring increased catalyst loading and organic cosolvent concentrations for high conversion. As it has with many other metathesis systems, diallyldimethylammonium chloride (**13i**) resisted RCM.^{90,38,42}

Table 3.2 RCM of Representative Dienes Catalyzed by **4a** in Aqueous Media under Air

substrate	solvent ([substrate], M)	mol % 4	conversion (%) (time, h)	
 13a	2:1 (CD ₃) ₂ CO/D ₂ O (0.05)	3	>95	(2)
	2:1 DME/H ₂ O (0.05)	3	85	(3)
 13b	2:1 (CD ₃) ₂ CO/D ₂ O (0.05)	3	90	(2)
	2:1 DME/H ₂ O (0.05)	3	>95	(3)
 13c	2:1 (CD ₃) ₂ CO/D ₂ O (0.05)	3	>95	(2)
	2:1 DME/H ₂ O (0.05)	1	95	(24)
 13h	2:1 (CD ₃) ₂ CO/D ₂ O (0.01)	10	>95	(48)
	4:1 DME/H ₂ O (0.05)	10	77	(24)
 13i	2:1 (CD ₃) ₂ CO/D ₂ O (0.05)	3	0	(2)
 13d	2:1 (CD ₃) ₂ CO/D ₂ O (0.05)	3	>95	(2)
 13e	2:1 (CD ₃) ₂ CO/D ₂ O (0.05)	3	0	(2)
	2:1 DME/H ₂ O (0.05)	3	0	(3)
 13f	2:1 (CD ₃) ₂ CO/D ₂ O (0.05)	3	>95	(2)
 16	4:1 DME/H ₂ O (0.02)	40	>95	(24)
 13g	2:1 (CD ₃) ₂ CO/D ₂ O (0.05)	3	>95	(2)
	2:1 DME/H ₂ O (0.05)	3	75	(4)

Complex **4a** is also capable of homodimerization of allyl alcohol (**17**) in acetone–water, achieving good conversion over several hours (Table 3.3). Nevertheless, CM of other substrates in aqueous solvents has proven elusive for us as well as others.^{36,38,42}

Table 3.3 CM Catalyzed by **4a** in an Aqueous Medium under Air

10 mol % **4a**, 0.1 M substrate **17**
2:1 (CD₃)₂CO/D₂O, rt, air

time (h)	conversion (%)
2	71
6	75

3.3 Conclusion

The effectiveness of **4a** for RCM and CM in aqueous–organic solution is comparable to that of complex **8d**, which is among the best catalysts for metathesis in pure water. Two conclusions can be drawn: homogeneous aqueous–organic mixtures could be advantageous for some olefin metathesis reactions, and the principle advantage of current aqueous metathesis catalysts is merely water solubility. Conventional catalysts such as **4a** are active in aqueous solvents, and hence can be used for metathesis of polar molecules if the substrate is amenable to aqueous DME, PEG, or acetone. For instance, some enzymes and polysaccharides are compatible with aqueous DME,^{120–123} suggesting that these biomolecules might be suitable for a metathesis strategy that avoids the synthesis of specialized complexes. Moreover, we have found that ribonuclease A is >90% soluble in 3:2 DME/phosphate-buffered saline (PBS). In this solution, complex **4a** is not only

soluble, but also catalyzes the quantitative RCM of N-tosyldiallylamine (**13c**), even in the presence of ribonuclease A (*Reaction conditions*: 4 mol % **4a**, 0.025 M substrate **13c**, 0.2 mg/mL ribonuclease A, 3:2 DME/PBS, 24 h, rt, under air). It is noteworthy that water comprises 80% of the molecules in this reaction mixture. Thus, apart from its insolubility in pure water, **4a** is nearly as effective in the presence of water as are specialized complexes like **8d**. Hence, additional advances in aqueous metathesis will require enhanced ligands that not only provide water solubility but also improve upon the NHC and isopropoxy chelate in protecting the complex from water.

3.4 Acknowledgments

We are grateful to A. Choudhary (University of Wisconsin–Madison) for critical review of this manuscript. J.B.B. was supported by an NDSEG Fellowship sponsored by the Air Force Office of Scientific Research. This work was supported by grant GM44783 (NIH). NMRFAM was supported by grant P41RR02301 (NIH).

3.5 Experimental Section

3.5.1 General Considerations

Commercial chemicals were of reagent grade or better, and were used without further purification. The term “concentrated under reduced pressure” refers to the removal of solvents and other volatile materials using a rotary evaporator at water aspirator pressure (<20 torr) while maintaining the water-bath temperature below 40 °C. NMR spectra were acquired with a Bruker DMX-400 Avance spectrometer (¹H, 400 MHz; ¹³C, 100.6 MHz) or a Bruker Avance DMX-500 spectrometer (¹H, 500 MHz;

^{13}C , 125.7 MHz) at the National Magnetic Resonance Facility at Madison (NMRFAM). NMR spectra were obtained at ambient temperature unless indicated otherwise. Coupling constants J are given in Hertz. Mass spectrometry was performed with a Micromass LCT (electrospray ionization, ESI) in the Mass Spectrometry Facility in the Department of Chemistry. Absorption spectra were recorded in 1-cm path length cuvettes on a Cary model 50 spectrometer from Varian.

Complexes **1–4a** were obtained from Aldrich (Milwaukee, WI) and used without further purification. Bovine pancreatic ribonuclease A (RNase A type III-A, >85%) was obtained from Sigma (St. Louis, MO). Phosphate-buffered saline (PBS), pH 7.4, contained (in 1.00 L) KCl (0.20 g), KH_2PO_4 (0.20 g), NaCl (8.0 g), and $\text{Na}_2\text{HPO}_4 \cdot 7\text{H}_2\text{O}$ (2.16 g). The following metathesis substrates were obtained from commercial sources and used without further purification: diethyl diallylmalonate (**13a**), *N,N*-diallyl-2,2,2-trifluoroacetamide (**13b**), diallyl ether (**13d**), 1,7-octadiene (**13f**), and allyl alcohol (**17**) from Aldrich (Milwaukee, WI); *N,N*-diallyl-*N,N*-dimethylammonium chloride (**13i**) from Fluka (Buchs, Switzerland); and diallyldiphenylsilane (**13e**) from Acros Organics (Geel, Belgium). *N,N*-Diallyl-4-methylbenzenesulfonamide (**13c**) was prepared by the method of Lamaty and co-workers.¹⁰⁰ Diallylamine hydrochloride (**13h**) was prepared from the corresponding amine (Aldrich) by treatment with ethereal HCl. *N,N*-Di-3-butenyl-2-nitrobenzenesulfonamide (**13g**) was prepared as previously reported.⁴¹ Methyl (D,L)-allylglycinate hydrochloride was prepared by the method of Creighton and coworkers.¹²⁴

3.5.2 Methyl (*d,l*)-*N*-(Allyl)allylglycinate

Methyl (*D,L*)-allylglycinate hydrochloride (1.35 g, 8.15 mmol) and triethylamine (3.41 mL, 24.5 mmol) were dissolved in CH₂Cl₂ (50 mL), and 2-nitrobenzenesulfonylchloride (1.84 g, 8.31 mmol) was added. After stirring overnight, the resulting solution was washed twice with 1 M aqueous HCl (50 mL), twice with saturated aqueous NaHCO₃ (50 mL), and once with brine (50 mL). The organic layer was dried over MgSO₄(s) and concentrated under reduced pressure. The yellow residue was taken up in DMF (10 mL), and combined with allyl bromide (0.848 mL, 9.78 mmol) and potassium carbonate (2.53 g, 18.3 mmol). After the reaction mixture was stirred for 24 h, mercaptoacetic acid (1.25 mL, 17.9 mmol) was added, followed after 30 min by DBU (9.75 mL, 65.2 mmol). After stirring for 3 h, the resulting mixture was diluted with EtOAc (75 mL) and mixed with saturated aqueous NaHCO₃ (50 mL). The organic layer was separated and washed twice with saturated aqueous NaHCO₃ (50 mL). The aqueous washes were combined and extracted with EtOAc (100 mL). The organic extracts were combined, washed with brine (50 mL), and concentrated under reduced pressure. The crude product was purified by flash chromatography (10% EtOAc v/v in hexane with 0.1% triethylamine to elute byproducts followed by 15-20% EtOAc v/v in hexane with 0.1% triethylamine) to afford methyl (*D,L*)-*N*-(allyl)allylglycinate (0.477 g, 2.82 mmol, 35%) as a colorless oil. R_f = 0.30 (20% EtOAc in hexanes with 1% triethylamine). ¹H NMR (400 MHz, CDCl₃) δ 5.92–5.69 (m, 2H), 5.22–5.02 (m, 4H), 3.72 (s, 3H), 3.37 (X of ABX, J = 6.2, 5.8 Hz, 1H), 3.28 (A of ABX, J = 13.8, 5.8 Hz, 1H), 3.13 (B of ABX, J = 13.8, 6.2 Hz, 1H), 2.42 (t, J = 6.7 Hz, 2H), 1.84 (br. s, 1H); ¹³C NMR (100 MHz,

CDCl₃) δ 174.9, 136.1, 133.5, 118.0, 116.4, 60.0, 51.5, 50.6, 37.5; HRMS–ESI (m/z): [M+H]⁺ calcd for C₉H₁₆NO₂, 170.1181; found 170.1179. Methyl (D,L)-*N*-(allyl)allylglycinate hydrochloride (**16**) was prepared from methyl (D,L)-*N*-(allyl)allylglycinate by treatment with ethereal HCl. ¹H NMR (400 MHz, CD₃OD) δ 5.99–5.87 (m, 1H), 5.82–5.69 (m, 1H), 5.59–5.50 (m, 2H), 5.34–5.25 (m, 2H), 4.19 (t, J = 5.8, 1H), 3.86 (s, 3H), 3.72 (d, J = 6.9 Hz, 2H), 2.85–2.66 (m, 2H).

3.5.3 Protein Solubility Measurements

Ribonuclease A (RNase A; 4 mg) was dissolved in PBS (4 mL). To prepare solutions with four different DME concentrations, this solution was mixed in the following proportions with DME: 0:1, 1:1, 6:4, and 2:1 DME/PBS. After thorough mixing, the solutions were subjected to centrifugation (13,000 rpm, 10 min) and their absorbances at 277.5 nm were measured. A sharp decrease in absorbance was apparent between the 6:4 and 2:1 DME:PBS solutions, indicating that RNase A is soluble at 0.4 mg/mL in 6:4 DME:PBS. Observation of RNase A precipitation at DME concentrations above this threshold corroborated this result.

3.5.4 Representative Procedures for Metathesis Reactions

3.5.4.1 Non-Deuterated Solvents.

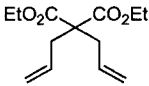
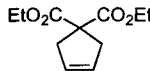
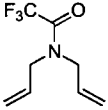
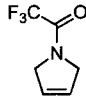
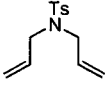
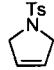
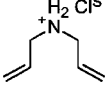
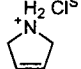
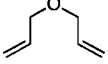


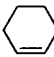
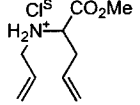
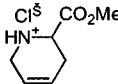
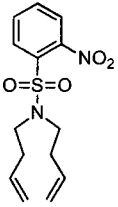
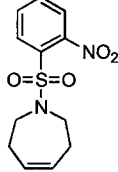
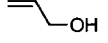
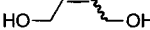
The ruthenium complex **2** (1.0 mg, 1.2 μ mol) was dissolved in DME (0.67 g), and deionized water (0.33 g) was added to this solution, followed by *N*-tosyl diallylamine **13c** (5.0 μ L, 24 μ mol). The reaction mixture was shaken at room temperature for 1 day before it was quenched by addition of ethyl vinyl ether (1 mL). This mixture was concentrated

under reduced pressure, and the residue was analyzed by ^1H NMR spectroscopy of its CDCl_3 or D_2O solution. Conversion was determined by the ratio of the integrals of the substrate and product signals (*vide infra*).

3.5.4.2 Acetone- d_6 / D_2O solvent.

Diallylamine hydrochloride (**13h**) (1.3 mg, 10 μmol) was dissolved in acetone- d_6 (0.617 mL) and D_2O (0.333 mL) in an NMR tube. The ruthenium complex **4a** (0.63 mg, 1 μmol) was added as a solution in acetone- d_6 (50 μL), and the NMR tube was capped. The reaction mixture was shaken at room temperature, and the reaction was monitored by ^1H NMR spectroscopy. Conversion was determined by the ratio of the integrals of the signals described in Table 3.4.

Table 3.4 Substrate and Product ^1H NMR Signals in RCM Reactions

 13a methylene doublet at 2.6 ppm	versus	 product singlet at 3.0 ppm
 13b substrate methylene signals at 4.0 ppm	versus	 product signals at 4.4 and 4.5 ppm
 13c methylene doublet at 3.8 ppm	versus	 product singlet at 4.1 ppm
 13h methylene doublet at 3.6 ppm	versus	 product singlet at 4.0 ppm
 13d methylene doublet at 4.0 ppm	versus	 product singlet at 4.3 ppm
 13f substrate vinylic signals at 5.0 ppm	versus	 product olefin singlet at 5.6 ppm
 16 vinylic signals at 5.2 and 5.4 ppm	versus	 signals at 5.7 and 5.9 ppm
 13g vinylic signals at 5.0 and 5.7 ppm	versus	 product singlet at 5.8 ppm
 17 vinylic signals at 5.0 and 5.9 ppm	versus	 product olefinic signal at 5.8 ppm

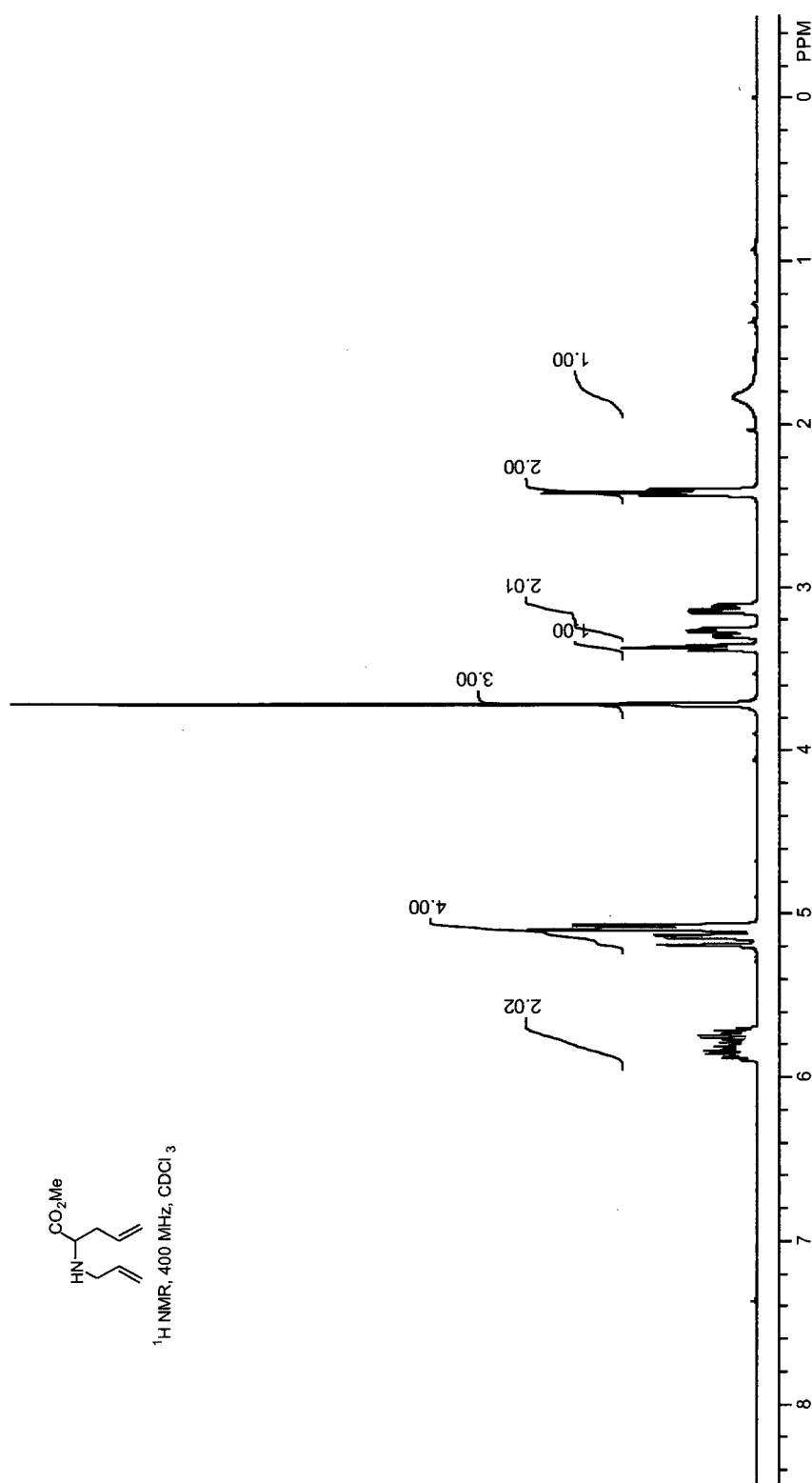


Figure 3.5 ^1H NMR of Methyl (*d,l*)-*N*-(Allyl)allylglycinate

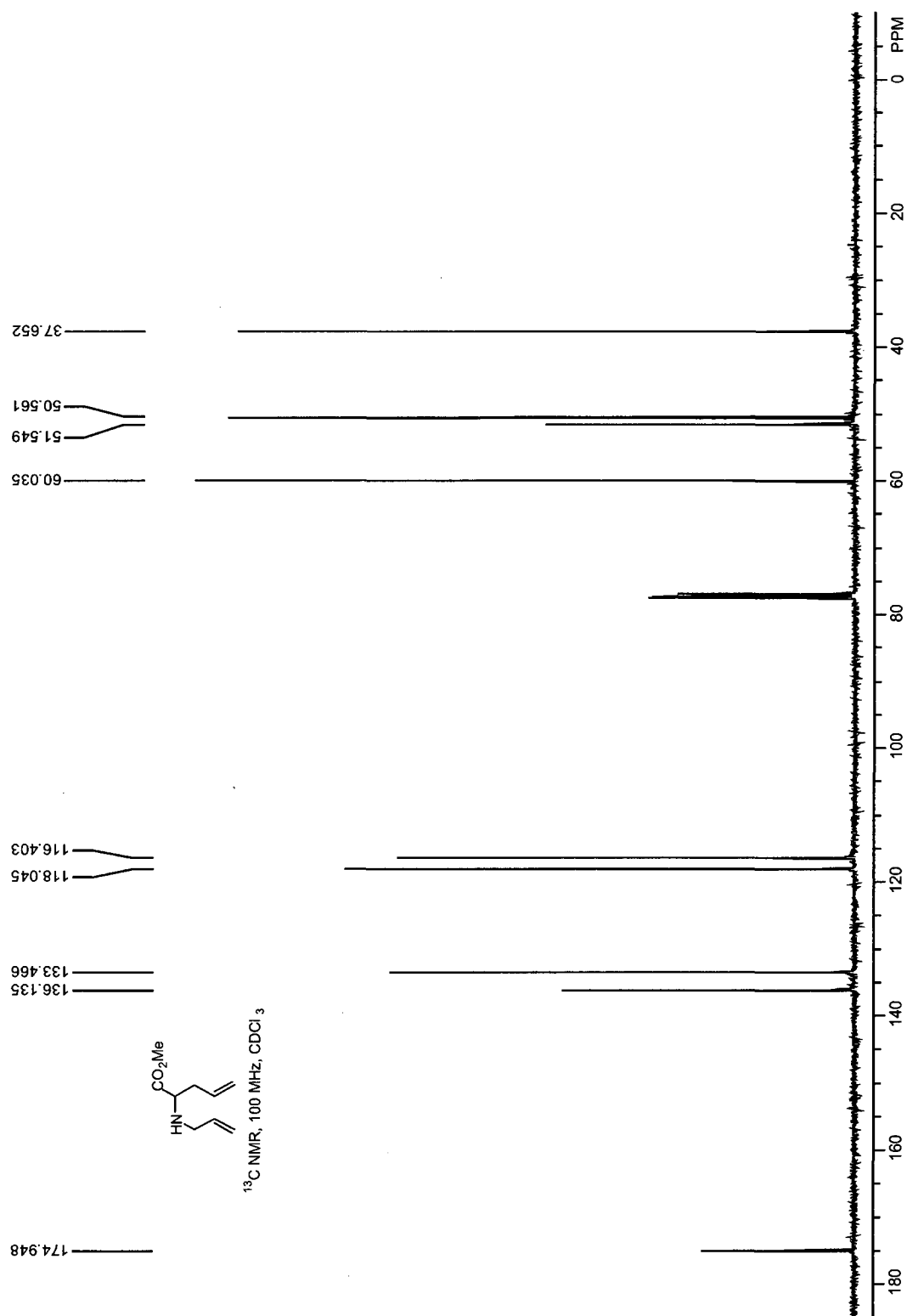


Figure 3.6 ¹³C NMR of Methyl (*d,l*)-*N*-(Allyl)allylglycinate

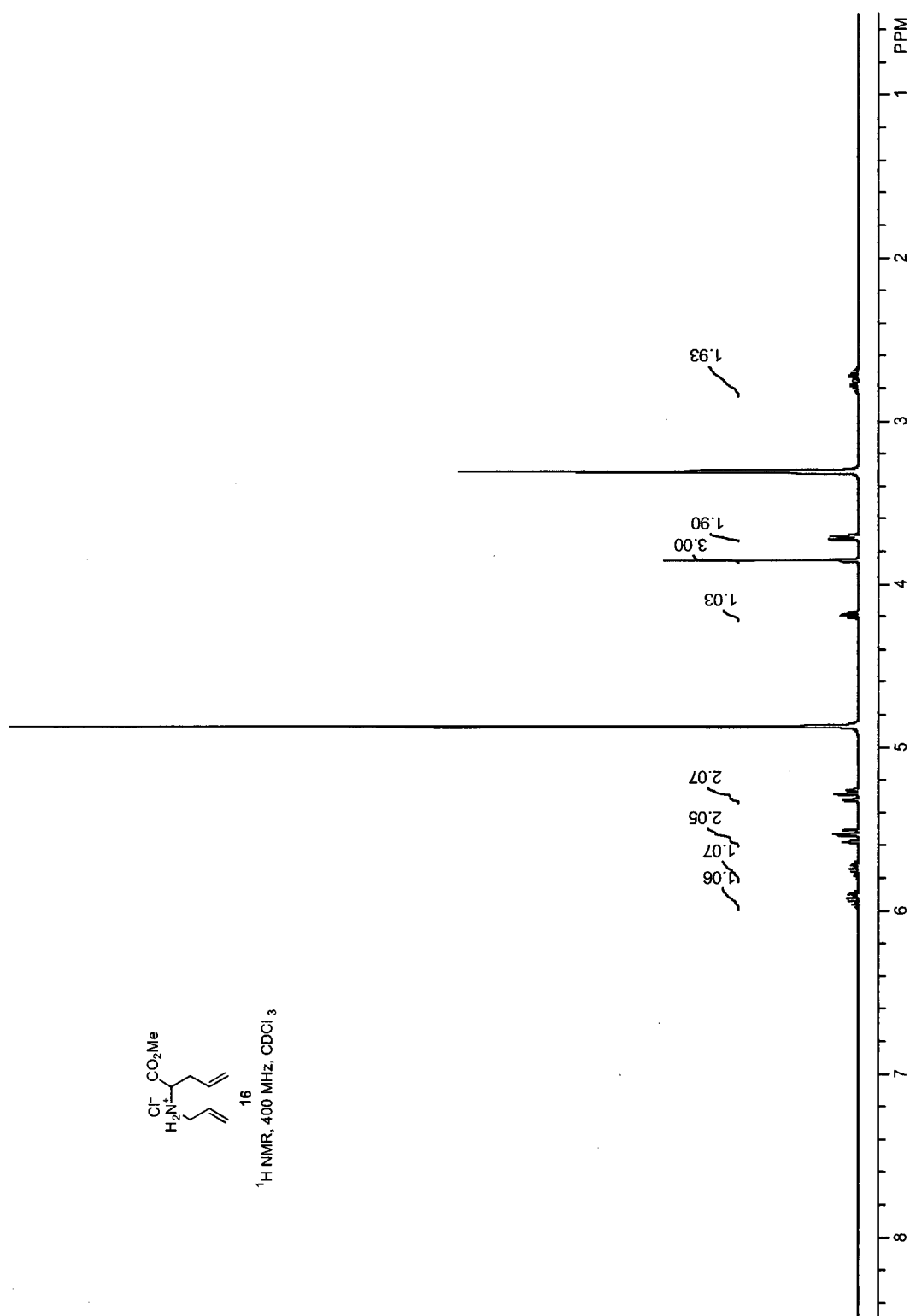


Figure 3.7 ¹H NMR of Methyl (*d,l*)-*N*-(Allyl)allylglycinate hydrochloride

CHAPTER 4*

SIMPLE CHEMICAL TRANSFORMATION OF LIGNOCELLULOSIC
BIOMASS INTO FURANS FOR FUELS AND CHEMICALS

Abstract: Lignocellulosic biomass is a plentiful and renewable resource for fuels and chemicals. Despite this potential, nearly all renewable fuels and chemicals are now produced from edible resources, such as starch, sugars, and oils; the challenges imposed by notoriously recalcitrant and heterogeneous lignocellulosic feedstocks have made their production from nonfood biomass inefficient and uneconomical. Here, we report that *N,N*-dimethylacetamide (DMA) containing lithium chloride (LiCl) is a privileged solvent that enables the synthesis of the renewable platform chemical 5-hydroxymethylfurfural (HMF) in a single step and unprecedented yield from untreated lignocellulosic biomass, as well as from purified cellulose, glucose, and fructose. The conversion of cellulose into HMF is unabated by the presence of other biomass components, such as lignin and protein. Mechanistic analyses reveal that loosely ion-paired halide ions in DMA-LiCl are critical for the remarkable rapidity (1-5 h) and yield (up to 92%) of this low-temperature (≤ 140 °C) process. The simplicity of this chemical transformation of lignocellulose contrasts markedly with the complexity of extant bioprocesses and provides a new paradigm for the use of biomass as a raw material for renewable energy and chemical industries.

* This chapter has been published, in part, under the same title. Reference: Binder, J. B.; Raines, R. T. *Journal of the American Chemical Society* **2009**, *131*, 1979–1985.

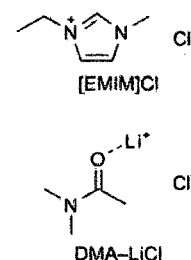
4.1 Introduction

Throughout most of human history, renewable biomass resources have been the primary industrial and consumer feedstocks. Only in the past 150 years have coal, natural gas, and petroleum grown into their dominant roles as sources for energy and chemicals.¹²⁵ Today these fossil resources supply approximately 86% of energy and 96% of organic chemicals, but in as soon as two decades petroleum production is unlikely to meet the world's growing needs and natural gas resources will be increasingly inaccessible.¹²⁶ Moreover, consumers and governments concerned about CO₂ emissions and other environmental impacts are demanding renewable power and products.

With advances in conversion technology, plentiful biomass resources have the potential to regain their central position as feedstocks for civilization, particularly as renewable carbon sources for transportation fuels and chemicals.¹²⁷⁻¹²⁹ A hexose dehydration product, the platform chemical 5-hydroxymethylfurfural (HMF) will be a key player in the bio-based renaissance. This six-carbon analogue of commodity chemicals like terephthalic acid and hexamethylenediamine can be converted by straightforward methods into a variety of useful acids, aldehydes, alcohols, and amines, as well as the promising fuel, 2,5-dimethylfuran (DMF).^{130,131} The energy content of DMF (31.5 MJ/L) is similar to that of gasoline (35 MJ/L), and 40% greater than that of ethanol (23 MJ/L).^{132,133} Moreover, DMF (bp 92–94 °C) is less volatile than ethanol (bp 78 °C) and is immiscible with water. These attributes bode well for the use of DMF as an alternative liquid fuel for transportation.

Despite the potential for HMF-based fuels and chemicals, most efforts toward HMF production have used edible starting materials, primarily fructose and glucose. In fact, almost all renewable fuels and chemicals are usually based on food resources such as starch, sugars, and oils. These simple starting materials are easy to convert into valuable products, while inedible lignocellulosic biomass is relatively recalcitrant and heterogeneous, making its conversion typically inefficient and uneconomical.¹³⁴ In the case of HMF, its formation by the dehydration of fructofuranose is straightforward, and has been demonstrated in water, traditional organic solvents,¹³⁵ multiphase systems,^{136,137} and ionic liquids.^{138,134,139} Zhao and coworkers reported that chromium catalysts in alkylimidazolium chloride ionic liquids, such as 1-ethyl-3-methylimidazolium chloride ([EMIM]Cl), enable synthesis of HMF from glucose, a less expensive feedstock, in good yield.¹³⁴ While promising, this method depends on expensive ionic liquid solvents and still uses starch-derived glucose. In our research, we sought to address these concerns, by *both* minimizing the use of ionic liquids *and* utilizing authentic lignocellulosic biomass as the starting material for HMF production.

Noting that the chloride counterions in [EMIM]Cl form only weak ion pairs,¹⁴⁰⁻¹⁴² we reasoned that other non-aqueous solvents containing a high concentration of chloride ions could be as effective as [EMIM]Cl for HMF synthesis. We were aware that DMA containing LiCl is one of few solvents that can dissolve cellulose without modifying its chemical structure and can do so to a concentration of up to 15 wt%, and that DMA-LiCl can also dissolve simple sugars.^{143,144} These useful properties likely stem from the association of lithium ions with



DMA to form $\text{DMA} \cdot \text{Li}^+$ macrocations, resulting in a high concentration of weakly ion-paired chloride ions (2.0 M in saturated anhydrous DMA-LiCl *versus* 6.8 M in $[\text{EMIM}]\text{Cl}$). These chloride ions can form hydrogen bonds with the hydroxyl groups of cellulose, disrupting its otherwise extensive network of intra- and interchain hydrogen bonds. Here, we report that using DMA-LiCl as a solvent enables the efficient synthesis of HMF in a single step from cellulose and even lignocellulosic biomass, as well as fructose and glucose (**Figure 4.1**). This discovery facilitates access to fuels and chemicals derived from HMF.

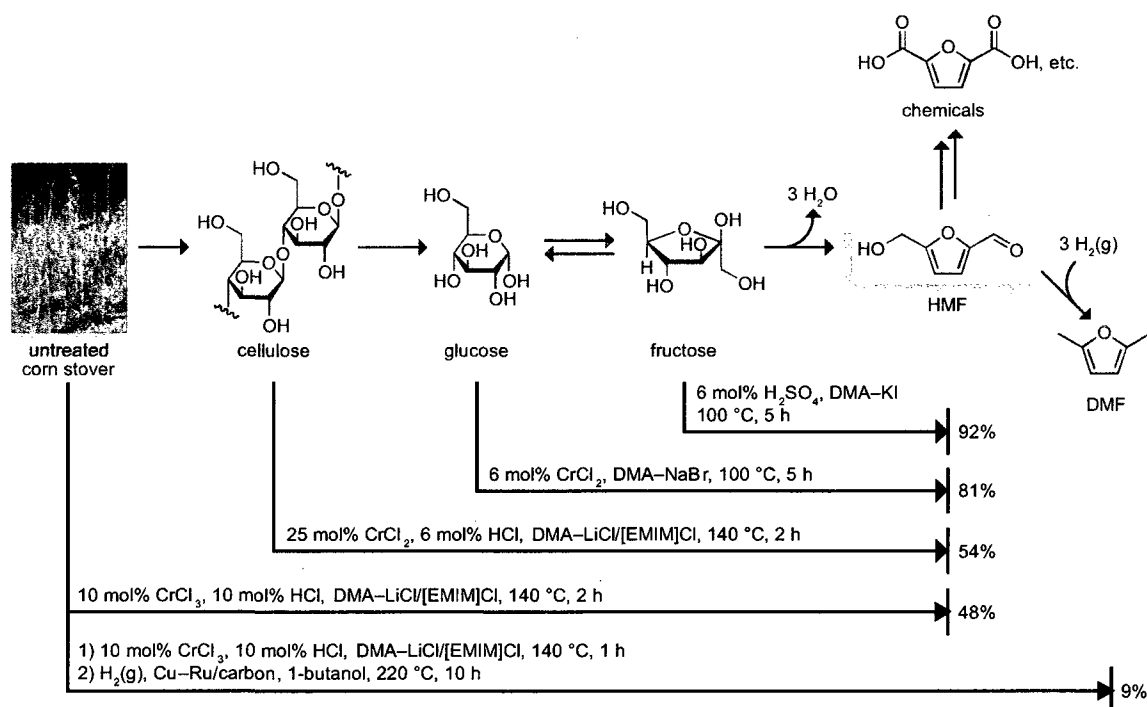


Figure 4.1 Halide salts in DMA enable previously elusive yields of bio-based chemicals from a variety of carbohydrates. Conditions are optimized for the conversion of carbohydrates into HMF (1 step) and DMF (2 steps). (Photograph courtesy of Department of Energy/National Renewable Energy Laboratory.)

4.2 Results and Discussion

4.2.1 *Synthesis of HMF from Fructose in DMA with Halide Additives*

We began by exploring the reactivity of fructose in DMA–LiCl, both alone and with added catalysts. When mixed with DMA–LiCl and heated to sufficiently high temperatures (80–140 °C), fructose is converted to HMF in moderate yields (55–65%; Table 4.1). Increased yields up to 71% can be obtained through catalysis by Brønsted acids (*e.g.*, H₂SO₄) and metal chlorides (*e.g.*, CuCl, CuCl₂, and PdCl₂). Nonetheless, these yields of HMF are moderate when compared to the yields of up to 85% achieved in solvents such as DMSO and [EMIM]Cl.^{135,134} In an effort to favor the formation of HMF, we added increasing amounts of [EMIM]Cl to the DMA–LiCl medium (Table 4.2). In general, the addition of ionic liquid improved yields. For example, [EMIM]Cl in combination with CuCl bolstered the yield of HMF up to 83%.

Table 4.1 Synthesis of HMF from Fructose

sugar	solvent	catalyst (mol%)	additives (wt%)	<i>T</i> (°C)	time (h)	molar yield (%)
fructose	DMA–LiCl (10%)			80	5	58
fructose	DMA–LiCl (10%)			100	4	62
fructose	DMA–LiCl (10%)			120	2	65
fructose	DMA–LiCl (10%)			140	0.5	55
fructose	DMA–LiCl (10%)	H ₂ SO ₄ , 6		80	4	66
fructose	DMA–LiCl (10%)	CuCl ₂ , 6		80	4	66
fructose	DMA–LiCl (10%)	RuCl ₃ , 6		80	4	58
fructose	DMA–LiCl (10%)	PdCl ₂ , 6		80	5	60
fructose	DMA–LiCl (10%)	CuCl, 6		80	5	62
fructose	DMA–LiCl (1%)	H ₂ SO ₄ , 6		80	1	57
fructose	DMA	H ₂ SO ₄ , 6		80	1	16
fructose	DMA–LiCl (10%)	H ₂ SO ₄ , 6		100	5	63
fructose	DMA–LiCl (10%)	CuCl ₂ , 6		100	4	55
fructose	DMA–LiCl (10%)	RuCl ₃ , 6		100	5	65
fructose	DMA–LiCl (10%)	PdCl ₂ , 6		100	4	62
fructose	DMA–LiCl (10%)	CuCl, 6		100	5	62
fructose	DMA–LiCl (10%)	CrCl ₂ , 6		100	5	66
fructose	DMA–LiCl (10%)	H ₂ SO ₄ , 6		120	1	68
fructose	DMA–LiCl (10%)	CuCl, 6		120	3	71
fructose	DMA–LiCl (10%)	RuCl ₃ , 6		120	1.5	61
fructose	DMA–LiCl (10%)	PtCl ₂ , 6		120	3	66
fructose	DMA–LiCl (10%)	CuCl ₂ , 6		120	3	65
fructose	DMA–LiCl (10%)	H ₂ SO ₄ , 6		140	0.5	66
fructose	DMA–LiCl (10%)	CuCl, 6		140	0.5	58
fructose	DMA–LiCl (10%)	PtCl ₂ , 6		140	0.5	58
fructose	DMA–LiCl (10%)	CuCl ₂ , 6		140	0.5	62

Fructose was reacted at a concentration of 10 wt% relative to the total mass of the reaction mixture. The solvent composition is indicated by the wt% of LiCl relative to DMA with additive concentrations relative to the total mass of the reaction mixture. Catalyst loading is relative to fructose. Yields are based on HPLC analysis.

Intrigued by the effect of [EMIM]Cl, we investigated the influence of other additives on the dehydration of fructose in DMA as catalyzed by H₂SO₄ (Table 4.3). The trifluoromethanesulfonate and tetrafluoroborate salts of EMIM delivered modest HMF yields, which were increased by the addition of LiCl. Adding ionic liquids with a variety of cationic counterions for chloride delivered HMF in yields around 80%. These results

suggested that chloride ion mediated the crucial advantage of [EMIM]Cl as an additive. Furthermore, the reaction appeared to proceed better with the loosely ion-paired chloride afforded by ionic liquids than with lithium chloride. We also observed that the potassium-complexing agent 18-crown-6 increased the yield of HMF in reactions utilizing potassium chloride. These results indicate that weakly ion-paired halide ions¹⁴⁵ favor the reaction.

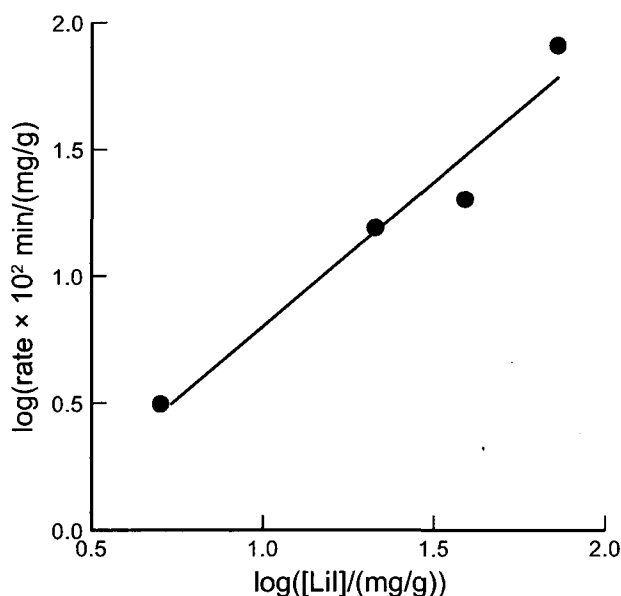


Figure 4.2 Log-log plot of initial rates of HMF formation from fructose vs [LiI]. Linear regression analysis of the data (shown) gives a slope of 1.1, which is consistent with a first-order dependence of the rate of HMF formation on $[I^-]$.

We found distinct differences in the ability of halide ions to mediate the formation of HMF from fructose in DMA containing H_2SO_4 . As expected from their low nucleophilicity and high basicity, fluoride ions were completely ineffective. On the other hand, bromide and iodide ions, which tend to be less ion-paired than fluoride or chloride, enabled exceptionally high HMF yields in DMA. For example, adding 10 wt% lithium

bromide or potassium iodide enabled the conversion of 92% of fructose to HMF in 4–5 h at 100 °C (**Figure 4.1**). These reactions were highly selective, resulting in only low levels of the colored byproducts and insoluble polymeric products (*i.e.*, humins) often formed concurrently with HMF.¹³⁰ Kinetic analyses indicate that the rate of HMF formation has a first-order dependence on halide concentration (**Figure 4.2**).

Table 4.2 Synthesis of HMF from Fructose with [EMIM]Cl

sugar	solvent	catalyst (mol%)	additives (wt%)	<i>T</i> (°C)	time (h)	molar yield (%)
fructose	DMA–LiCl (10%)	CuCl ₂ , 6	[EMIM]Cl, 5	80	5	74
fructose	DMA–LiCl (10%)	CuCl ₂ , 6	[EMIM]Cl, 10	80	5	64
fructose	DMA–LiCl (10%)	CuCl ₂ , 6	[EMIM]Cl, 20	80	5	74
fructose	DMA–LiCl (10%)	CuCl ₂ , 6	[EMIM]Cl, 40	80	5	78
fructose	DMA–LiCl (10%)	H ₂ SO ₄ , 6	[EMIM]Cl, 5	80	4	70
fructose	DMA–LiCl (10%)	H ₂ SO ₄ , 6	[EMIM]Cl, 10	80	4	72
fructose	DMA–LiCl (10%)	H ₂ SO ₄ , 6	[EMIM]Cl, 20	80	4	78
fructose	DMA–LiCl (10%)	H ₂ SO ₄ , 6	[EMIM]Cl, 40	80	4	75
fructose	DMA–LiCl (10%)	CuCl ₂ , 6	[EMIM]Cl, 5	120	1	62
fructose	DMA–LiCl (10%)	CuCl ₂ , 6	[EMIM]Cl, 10	120	1.5	68
fructose	DMA–LiCl (10%)	CuCl ₂ , 6	[EMIM]Cl, 20	120	1	64
fructose	DMA–LiCl (10%)	CuCl ₂ , 6	[EMIM]Cl, 40	120	1	67
fructose	DMA–LiCl (10%)	H ₂ SO ₄ , 6	[EMIM]Cl, 5	120	1	61
fructose	DMA–LiCl (10%)	H ₂ SO ₄ , 6	[EMIM]Cl, 10	120	1	67
fructose	DMA–LiCl (10%)	H ₂ SO ₄ , 6	[EMIM]Cl, 20	120	1	69
fructose	DMA–LiCl (10%)	H ₂ SO ₄ , 6	[EMIM]Cl, 40	120	1	75
fructose	DMA–LiCl (10%)	CuCl, 6	[EMIM]Cl, 5	120	1.5	62
fructose	DMA–LiCl (10%)	CuCl, 6	[EMIM]Cl, 10	120	1.5	70
fructose	DMA–LiCl (10%)	CuCl, 6	[EMIM]Cl, 20	120	1	67
fructose	DMA–LiCl (10%)	CuCl, 6	[EMIM]Cl, 40	120	1.5	83

Fructose was reacted at a concentration of 10 wt% relative to the total mass of the reaction mixture. The solvent composition is indicated by the wt% of LiCl relative to DMA with additive concentrations relative to the total mass of the reaction mixture.

Table 4.3 Synthesis of HMF from Fructose with Additives

sugar	solvent	catalyst (mol%)	additives (wt%)	<i>T</i> (°C)	time (h)	molar yield (%)
fructose	DMA	H ₂ SO ₄ , 6	LiF, 10	80	2	0
fructose	DMA	CuCl ₂ , 6	LiF, 10	80	2	0
fructose	DMA	H ₂ SO ₄ , 6	NaCl, 10	80	1	71
fructose	DMA	H ₂ SO ₄ , 6	NaI, 10	80	1	80
fructose	DMA	H ₂ SO ₄ , 6	CsF, 10	80	2	0
fructose	DMA	CuCl ₂ , 6	CsF, 10	80	2	0
fructose	DMA	H ₂ SO ₄ , 6	KCl, 1.5; 18-crown-6, 5.6	80	2	63
fructose	DMA	H ₂ SO ₄ , 6	KCl, 1.5	80	2	56
fructose	DMA	H ₂ SO ₄ , 6	KI, 10	100	5	92
fructose	DMA	H ₂ SO ₄ , 6	NaI, 10	100	5	91
fructose	DMA	H ₂ SO ₄ , 6	LiI, 10	100	6	89
fructose	DMA	H ₂ SO ₄ , 6	KBr, 10	100	2	92
fructose	DMA	H ₂ SO ₄ , 6	NaBr, 10	100	2	93
fructose	DMA	H ₂ SO ₄ , 6	LiBr, 10	100	4	92
fructose	DMA	H ₂ SO ₄ , 6	NaI, 8	120	0.2	84
fructose	DMA	H ₂ SO ₄ , 6	NaI, 0.5	120	0.2	52
fructose	DMA	H ₂ SO ₄ , 6	LiI, 8	120	0.2	85
fructose	DMA	H ₂ SO ₄ , 6	LiI, 0.5	120	0.2	62
fructose	DMA	H ₂ SO ₄ , 6	LiBr, 10	120	0.25	85
fructose	DMA		LiI, 10	120	3	16
fructose	DMA		LiBr, 10	120	3	63
fructose	DMA-LiCl (10%)	H ₂ SO ₄ , 6	[EMIM]BF ₄ , 20	100	2	71
fructose	DMA	H ₂ SO ₄ , 6	[EMIM]BF ₄ , 20	100	4	59
fructose	DMA-LiCl (10%)	H ₂ SO ₄ , 6	[EMIM]OTf, 20	100	1	71
fructose	DMA	H ₂ SO ₄ , 6	[EMIM]OTf, 20	100	2	48
fructose	DMA	H ₂ SO ₄ , 6	[EMIM]Cl, 20	100	2	84
fructose	DMA	H ₂ SO ₄ , 6	[EMIM]Br, 20	100	1	94
fructose	DMA	H ₂ SO ₄ , 6	[PMIM]I, 20	100	2	81
fructose	DMA	H ₂ SO ₄ , 6	[EtPy]Cl, 20	100	2	81
fructose	DMA	H ₂ SO ₄ , 6	[MBPy]Cl, 20	100	2	78
fructose	DMA	H ₂ SO ₄ , 6	[MMEIM]Cl, 20	100	2	79

Fructose was reacted at a concentration of 10 wt% relative to the total mass of the reaction mixture. The solvent composition is indicated by the wt% of LiCl relative to DMA with additive concentrations relative to the total mass of the reaction mixture. Catalyst loading is relative to fructose. Yields are based on HPLC analysis.

4.2.2 Influence of Halides on the Formation of HMF from Fructose

Our results provide mechanistic insights regarding the conversion of fructose into HMF. In most depictions of this process,¹⁴⁶ a fructofuranosyl oxocarbenium ion forms

first, and then deprotonates spontaneously at C-1 to form an enol. To account for the dramatic influence of halide on yield and rate, we propose two variations on this mechanism (**Figure 4.3A**). In one, a halide ion (X^-) attacks the oxocarbenium ion to form a 2-deoxy-2-halo intermediate that is less prone to side reactions as well as reversion to fructose. This intermediate then loses HX to form the enol (nucleophile pathway). Alternatively, a halide ion could form the enol merely by acting as a base that deprotonates C-1 (base pathway).

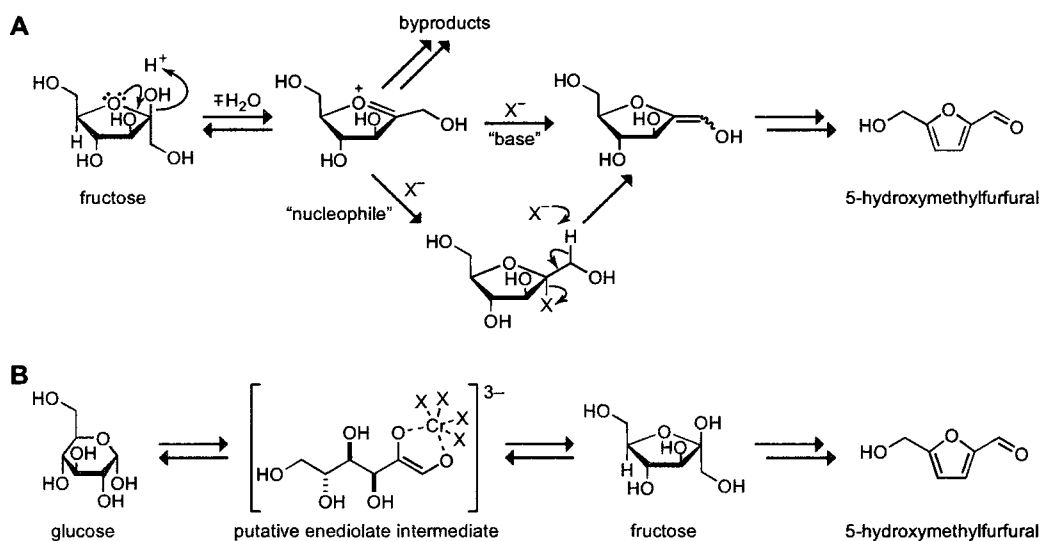


Figure 4.3 Putative mechanisms for the dehydration of fructose and isomerization of glucose. (A) Putative nucleophilic and basic mechanisms for halide participation in the conversion of fructose into HMF. X^- represents a halide ion. (B) Putative mechanism for the chromium-catalyzed transformation of glucose into HMF. Chromium species, depicted here as a hexacoordinate chromium(II) complex, catalyze the isomerization of glucose into fructose through a putative enediolate intermediate. Fructose is then converted rapidly into HMF.

The known reactivity of sugars as well as our observations of fructose reactivity support the nucleophile pathway. The fructofuranosyl oxocarbenium ion is known to be attacked readily by alcohols,¹⁴⁷ borohydrides,¹⁴⁸ and even fluoride,¹⁴⁹ so it is reasonable

to expect its being attacked by chloride, bromide, and iodide. Bromide and iodide, which are better nucleophiles and leaving groups than chloride, are also more effective as ionic additives. A mechanism that required the halide ion to act only as a base would invert the order of halide reactivity.

4.2.3 *Synthesis of HMF from Glucose in DMA*

Next, we sought to utilize the DMA–halide system to convert glucose into HMF. As in [EMIM]Cl, CrCl₂ and CrCl₃ in DMA enable the conversion of glucose into HMF in yields up to 69% (Table 4.4 and Table 4.5). We found negligible HMF yields (<1%) from glucose in the absence of chromium salts. With the addition of CrCl₂ to DMA or DMA–LiCl, we obtained substantial yields of HMF (47–60%), which were improved further by adding [EMIM]Cl to the reaction mixture. Supplementing the solvent with up to 20% [EMIM]Cl allows HMF yields up to 69%, comparable to those obtained by Zhao and coworkers in [EMIM]Cl alone.¹³⁴ As with fructose, we observed a marked halide effect. Although addition of iodide salts to the chromium chloride reaction mixture did not greatly change the HMF yield, using 10 wt% lithium or sodium bromide increased the HMF yield to 79–81% after 5–6 h at 100 °C (Table 4.5). These yields of HMF from glucose exceed those reported previously, approach typical yields of HMF from fructose, and do not require ionic liquid solvents. Moreover, glucose syrups like those readily available from corn are also excellent feedstocks for HMF synthesis using our methods.

Table 4.4 Synthesis of HMF from Glucose

Sugar	solvent	catalyst (mol%)	additives (wt%)	<i>T</i> (°C)	time (h)	molar yield (%)
glucose	DMA–LiCl (10%)	—	—	100	6	<1
glucose	DMA–LiCl (10%)	—	[EMIM]Cl, 20	100	6	<1
glucose	DMA	CrCl ₂ , 6	—	100	4	60
glucose	DMA	CrCl ₂ , 6	—	120	3	47
glucose	DMA	CrCl ₂ , 6	[EMIM]Cl, 8	120	3	57
glucose	DMA	CrCl ₂ , 6	[EMIM]Cl, 5	100	6	64
glucose	DMA	CrCl ₂ , 6	[EMIM]Cl, 10	100	6	67
glucose	DMA	CrCl ₂ , 6	[EMIM]Cl, 20	100	6	67
glucose	DMA–LiCl (10%)	CrCl ₂ , 6	—	100	5	60
glucose	DMA–LiCl (10%)	CrCl ₂ , 6	—	120	3	53
glucose	DMA–LiCl (10%)	CrCl ₂ , 6	TMEDA, 1	120	3	28
glucose	DMA–LiCl (10%)	CrCl ₂ , 6	pyridine, 1	120	3	43
glucose	DMA–LiCl (10%)	CrCl ₂ , 6	[EMIM]Cl, 5	100	6	58
glucose	DMA–LiCl (10%)	CrCl ₂ , 6	[EMIM]Cl, 10	100	6	61
glucose	DMA–LiCl (10%)	CrCl ₂ , 6	[EMIM]Cl, 20	100	6	62
glucose	DMA	CrCl ₂ , 6	[EMIM]Cl, 5	120	5	67
glucose	DMA	CrCl ₂ , 6	[EMIM]Cl, 10	120	3	62
glucose	DMA	CrCl ₂ , 6	[EMIM]Cl, 20	120	3	63
glucose	DMA–LiCl (10%)	CrCl ₂ , 6	[EMIM]Cl, 5	120	3	64
glucose	DMA–LiCl (10%)	CrCl ₂ , 6	[EMIM]Cl, 10	120	5	70
glucose	DMA–LiCl (10%)	CrCl ₂ , 6	[EMIM]Cl, 20	120	5	66
glucose	DMA–LiCl (10%)	CrCl ₃ , 6	—	120	2	55
glucose	DMA	CrCl ₃ , 6	[EMIM]Cl, 5	100	6	59
glucose	DMA	CrCl ₃ , 6	[EMIM]Cl, 10	100	6	63
glucose	DMA	CrCl ₃ , 6	[EMIM]Cl, 20	100	6	67
glucose	DMA–LiCl (10%)	CrCl ₃ , 6	[EMIM]Cl, 5	100	6	57
glucose	DMA–LiCl (10%)	CrCl ₃ , 6	[EMIM]Cl, 10	100	6	69
glucose	DMA–LiCl (10%)	CrCl ₃ , 6	[EMIM]Cl, 20	100	3	65
glucose	DMA	CrCl ₃ , 6	[EMIM]Cl, 5	120	3	62
glucose	DMA	CrCl ₃ , 6	[EMIM]Cl, 10	120	4	60
glucose	DMA	CrCl ₃ , 6	[EMIM]Cl, 20	120	3	64
glucose	DMA–LiCl (10%)	CrCl ₃ , 6	[EMIM]Cl, 5	120	3	61
glucose	DMA–LiCl (10%)	CrCl ₃ , 6	[EMIM]Cl, 10	120	3	61
glucose	DMA–LiCl (10%)	CrCl ₃ , 6	[EMIM]Cl, 20	120	2	62
glucose, 45% in water	DMA–LiCl (10%)	CrCl ₂ , 6	[EMIM]Cl, 20	100	6	62

Glucose was reacted at a concentration of 10 wt% relative to the total mass of the reaction mixture. The solvent composition is indicated by the wt% of LiCl relative to DMA with additive concentrations relative to the total mass of the reaction mixture. Catalyst loading is relative to glucose. Yields are based on HPLC analysis.

Table 4.5 Synthesis of HMF from Glucose with Alternative Ionic Additives

sugar	solvent	catalyst (mol%)	additives (wt%)	<i>T</i> (°C)	time (h)	molar yield (%)
glucose	DMA–LiCl (10%)	CrCl ₂ , 6	[EMIM]OTf, 20	100	2	59
glucose	DMA	CrCl ₂ , 6	[EMIM]OTf, 20	100	4	54
glucose	DMA	CrCl ₂ , 6	[EMIM]Br, 20	100	2	78
glucose	DMA	CrCl ₂ , 6	[PMIM]I, 20	100	1	55
glucose	DMA	CrCl ₂ , 6	[EtPy]Cl, 20	100	1	64
glucose	DMA	CrCl ₂ , 6	[MBPy]Cl, 20	100	2	63
glucose	DMA	CrCl ₂ , 6	[MMEIM]Cl, 20	100	1	76
glucose	DMA	CrCl ₂ , 6	LiBr, 10	100	4	79
glucose	DMA–LiCl (5%)	CrCl ₂ , 6	LiBr, 5	100	4	56
glucose	DMA	CrCl ₂ , 6	LiI, 10	100	4	54
glucose	DMA	CrCl ₃ , 6	LiBr, 10	100	6	79
glucose	DMA	CrBr ₃ , 6	LiBr, 10	100	6	80
glucose	DMA	CrBr ₃ , 2	LiBr, 10	100	6	76
glucose	DMA	CrBr ₃ , 1	LiBr, 10	100	6	66
glucose	DMA	CrCl ₂ , 6	NaBr, 10	100	5	77
glucose	DMA	CrCl ₃ , 6	NaBr, 10	100	5	81
glucose	DMA	CrCl ₂ , 6	[EMIM]Br, 20	100	5	78

Glucose was reacted at a concentration of 10 wt% relative to the total mass of the reaction mixture. The solvent composition is indicated by the wt% of LiCl relative to DMA with additive concentrations relative to the total mass of the reaction mixture. Catalyst loading is relative to glucose. Yields are based on HPLC analysis.

Further investigation of the generality of chromium-catalyzed HMF synthesis revealed that a wide range of polar aprotic solvents afforded HMF from glucose in yields higher than those commonly achieved (Table 4.6).¹³⁷ On the other hand, some coordinating classes of solvents prevent formation of HMF, such as amines and alcohols, perhaps because of their interactions with the chromium salts. No HMF was formed upon reaction of glucose in pyridine, and adding several equivalents (based on chromium) of pyridine or *N,N,N,N*-tetramethylethylenediamine markedly decreased HMF formation in DMA–LiCl (Table 4.4). The basicity of these amines might also disfavor HMF

formation. Although Zhao and coworkers reported that CrCl_2 was markedly less effective than CrCl_3 , we found that chromium in either oxidation state gave a similar yield.

Table 4.6 Synthesis of HMF from Glucose in Various Solvents

sugar	solvent	catalyst (mol%)	T (°C)	time (h)	molar yield (%) ^a
glucose	DMA	CrCl_2 , 6	120	3.25	45
glucose	<i>N,N</i> -dimethylformamide	CrCl_2 , 6	120	3.25	36
glucose	<i>N</i> -methylpyrrolidone	CrCl_2 , 6	120	3.25	45
glucose	sulfolane	CrCl_2 , 6	120	3.25	35
glucose	dimethylsulfoxide	CrCl_2 , 6	120	3.25	46
glucose	acetonitrile	CrCl_2 , 6	120	3.25	0
glucose	dioxane	CrCl_2 , 6	120	3.25	13
glucose	1-butanol	CrCl_2 , 6	120	3.25	4
glucose	pyridine	CrCl_2 , 6	120	3.25	0
glucose	1-ethyl-2-pyrrolidinone	CrCl_2 , 6	120	3.25	32
glucose	<i>N</i> -methylcaprolactam	CrCl_2 , 6	120	3.25	38
glucose	<i>N,N</i> -diethylacetamide	CrCl_2 , 6	120	3.25	28
glucose	1-formylpyrrolidine	CrCl_2 , 6	120	3.25	33
glucose	<i>N,N</i> -dimethylpropionamide	CrCl_2 , 6	120	3.25	29

Glucose was reacted at a concentration of 10 wt% relative to the total mass of the reaction mixture. Catalyst loading is relative to glucose. Yields are based on HPLC analysis.

^aAverage of two trials.

Chromium likely enables conversion of glucose to HMF by catalyzing the isomerization of glucose into fructose (**Figure 4.3B**).¹³⁴ The fructose is then converted to HMF. Our observations suggest that the yield of HMF from glucose in reactions utilizing chromium correlates with metal coordination. Highly coordinating ligands such as amines decrease the yield of HMF. On the other hand, halide ligands enhance HMF yields, with bromide being the most effective. Our data suggest that the halide additives must balance two roles in the conversion of glucose into HMF—serving as ligands for

chromium and facilitating the selective conversion of fructose. Although iodide excels in the latter role, its large size or low electronegativity could compromise its ability as a ligand. In contrast, bromide potentially offers the optimal balance of nucleophilicity and coordinating ability, enabling unparalleled transformation of glucose into HMF.

4.2.4 *Synthesis of HMF from Cellulose*

HMF has been traditionally obtained from monosaccharides. Cellulosic biomass is, however, an especially promising source because of its inexpensive availability from non-food resources. Unfortunately, the typical aqueous acid hydrolysis methods for producing HMF from cellulose rely on high temperatures and pressures (250–400 °C, 10 MPa) and result in yields of 30%, at most.¹⁵⁰ We suspected that the solubility of cellulose in DMA–LiCl and the efficient conversion of glucose into HMF with chromium would enable superior results. Dissolution of purified cellulose in a mixture of DMA–LiCl and [EMIM]Cl and addition of CrCl₂ or CrCl₃ produced HMF from cellulose in up to 54% yield within 2 h at 140 °C (Table 4.7). These yields compare well with reports of HMF synthesis from cellulose in the patent literature using aqueous acid and ionic liquids.^{150,139} Neither lithium iodide nor lithium bromide alone produced high yields of HMF because these salts in DMA do not dissolve cellulose.¹⁴³ Using lithium bromide along with DMA–LiCl did enable modest improvements in yield. Likewise, using hydrochloric acid as a co-catalyst boosted yields.

Table 4.7 Synthesis of HMF from Cellulose

biomass	solvent	catalyst (mol%)	additives (wt%)	<i>T</i> (°C)	time (h)	molar yield (%)
cellulose	DMA–LiCl (10%)		[EMIM]Cl, 40	140	2	4
cellulose	DMA–LiCl (10%)	CrCl ₂ , 25; HCl, 10		140	2	22
cellulose	DMA–LiCl (10%)	CrCl ₃ , 25; HCl, 10		140	2	33
cellulose	DMA–LiCl (10%)	CrCl ₂ , 25		140	6	15
cellulose	DMA–LiCl (15%)	CrCl ₃ , 36		140	6	17
cellulose	DMA–LiCl (10%)	CrCl ₂ , 25	[EMIM]Cl, 10	140	4	18
cellulose	DMA–LiCl (10%)	CrCl ₂ , 25	[EMIM]Cl, 20	140	4	24
cellulose	DMA–LiCl (10%)	CrCl ₂ , 25	[EMIM]Cl, 40	140	4	33
cellulose	DMA–LiCl (10%)	CrCl ₂ , 25; HCl, 6	[EMIM]Cl, 10	140	4	21
cellulose	DMA–LiCl (10%)	CrCl ₂ , 25; HCl, 6	[EMIM]Cl, 20	140	4	33
cellulose	DMA–LiCl (10%)	CrCl ₂ , 25; HCl, 6	[EMIM]Cl, 40	140	1	43
cellulose	DMA–LiCl (10%)	CrCl ₂ , 25; HCl, 6	[EMIM]Cl, 60	140	2	54
cellulose	DMA–LiCl (10%)	CrCl ₂ , 25; HCl, 6	[EMIM]Cl, 80	140	2	47
cellulose	DMA–LiCl (10%)	CrCl ₃ , 25; HCl, 6	[EMIM]Cl, 10	140	4	22
cellulose	DMA–LiCl (10%)	CrCl ₃ , 25; HCl, 6	[EMIM]Cl, 20	140	4	30
cellulose	DMA–LiCl (10%)	CrCl ₃ , 25; HCl, 6	[EMIM]Cl, 40	140	4	38
cellulose	[EMIM]Cl	CrCl ₂ , 25; HCl, 6		140	1	53
cellulose	DMA	CrCl ₂ , 25; HCl, 10	LiI, 10	140	3	<1
cellulose	DMA	CrCl ₂ , 25; HCl, 10	LiBr, 10	140	3	<1
cellulose	DMA–LiCl (10%)	CrCl ₃ , 25; HCl, 10	LiI, 2	140	1	27
cellulose	DMA–LiCl (10%)	CrCl ₃ , 25; HCl, 10	LiBr, 1	140	2	34
cellulose	DMA–LiCl (10%)	CrCl ₃ , 25; HCl, 10	LiI, 5	140	1	23
cellulose	DMA–LiCl (10%)	CrCl ₃ , 25; HCl, 10	LiBr, 3	140	2	37

Cellulose was reacted at a concentration of 4 wt% relative to the total mass of the reaction mixture. The solvent composition is indicated by the wt% of LiCl relative to DMA with additive concentrations relative to the total mass of the reaction mixture. Catalyst loading and yield are relative to moles of glucose monomers contained in the cellulose. Yields are based on HPLC analysis.

Recently, Mascal and Nitikin reported an alternative method for producing furanic products, chiefly 5-chloromethylfurfural (CMF), from purified cellulose.¹⁵¹ Heating a solution of highly purified cellulose in concentrated hydrochloric acid and lithium chloride, and extracting the products with 1,2-dichloroethane yielded this chlorinated relative of HMF in 71% isolated yield. CMF can be converted subsequently to potential fuels like DMF and 5-ethoxymethylfurfural. Although this process avoids the use of

chromium and results in higher yields (84% isolated yield of furanic products *versus* 54%), it has notable drawbacks relative to our DMA–LiCl system. Mascal and Nitikin use chloride stoichiometrically and produce potentially hazardous chlorinated organic products,¹⁵² which are not observed in our system. In addition, the weight of their reaction mixture is nearly 150-fold greater than that of the cellulose reactant. Their 1,2-dichloroethane extractant, which is likewise used in a large excess relative to cellulose, is a possible carcinogen, and the concentrated hydrochloric acid presents its own hazards.¹⁵² By comparison, DMA–LiCl is a common industrial solvent that enables the processing of cellulose at far higher concentrations (15 *versus* 0.7 wt %).

4.2.5 *Synthesis of HMF and Furfural from Lignocellulosic Biomass*

We discovered another desirable attribute of our process—the ready conversion of lignocellulosic biomass. Efficient production of fuels or chemicals from crude biomass often requires pretreatment processes.^{153,154} In contrast, HMF can be produced readily from untreated lignocellulosic biomass such as corn stover or pine sawdust under conditions similar to those used for cellulose (Table 4.8). Yields of HMF from corn stover subjected to ammonia fiber expansion (AFEX) pretreatment¹⁵³ were nearly identical to those for untreated stover. Other biomass components, such as lignin and protein, did not interfere substantially in the process, as yields of HMF based on the cellulose content of the biomass were comparable to those from purified cellulose. To be highly efficient, a process for biomass conversion should also utilize the pentoses present in hemicellulose. Notably, the industrial chemical furfural is formed from the

hemicellulose component of biomass under our reaction conditions in yields similar to those obtained in industrial processes (34–37% *versus* ~50%).¹⁵⁵

Table 4.8 Synthesis of HMF from Corn Stover and Pine Sawdust

biomass	solvent	catalyst (mol%)	additives (wt%)	<i>T</i> (°C)	time (h)	HMF yield (%) ^a
pine sawdust	DMA–LiCl (10%)	CrCl ₂ , 33	[EMIM]Cl, 15	140	5	19
pine sawdust	DMA–LiCl (10%)	CrCl ₃ , 33	[EMIM]Cl, 15	140	5	17
corn stover	DMA–LiCl (10%)	CrCl ₂ , 19	[EMIM]Cl, 10	140	6	8
corn stover	DMA–LiCl (10%)	CrCl ₂ , 38	[EMIM]Cl, 10	140	6	16
AFEX corn stover	DMA–LiCl (10%)	CrCl ₂ , 19	[EMIM]Cl, 10	140	6	10
AFEX corn stover	DMA–LiCl (10%)	CrCl ₂ , 38	[EMIM]Cl, 10	140	6	16
corn stover	DMA–LiCl (10%)	CrCl ₃ , 19	[EMIM]Cl, 10	140	6	10
AFEX corn stover	DMA–LiCl (10%)	CrCl ₃ , 19	[EMIM]Cl, 10	140	6	11
corn stover	DMA–LiCl (10%)	CrCl ₂ , 10; HCl, 10	[EMIM]Cl, 20	140	3	23
corn stover	DMA–LiCl (10%)	CrCl ₂ , 10; HCl, 10	[EMIM]Cl, 40	140	3	24
corn stover	DMA–LiCl (10%)	CrCl ₂ , 10; HCl, 10	[EMIM]Cl, 60	140	3	36
corn stover	DMA–LiCl (10%)	CrCl ₂ , 10; HCl, 10	[EMIM]Cl, 80	140	3	31
corn stover	[EMIM]Cl	CrCl ₂ , 10; HCl, 10		140	3	29
corn stover	DMA–LiCl (10%)	CrCl ₃ , 10; HCl, 10	[EMIM]Cl, 20	140	3	26
corn stover	DMA–LiCl (10%)	CrCl ₃ , 10; HCl, 10	[EMIM]Cl, 40	140	1	39
corn stover	DMA–LiCl (10%)	CrCl ₃ , 10; HCl, 10	[EMIM]Cl, 60	140	2	48 ^b
corn stover	DMA–LiCl (10%)	CrCl ₃ , 10; HCl, 10	[EMIM]Cl, 80	140	2	47 ^c
corn stover	[EMIM]Cl	CrCl ₃ , 10; HCl, 10		140	1	42

Biomass was reacted at a concentration of 10 wt% relative to the total mass of the reaction mixture. The solvent composition is indicated by the wt% of LiCl relative to DMA with additive concentrations relative to the mass of the reaction mixture. Catalyst loading and yield are relative to moles of glucose monomers contained in the cellulose in the biomass. Yields are based on HPLC analysis.

^aYield from pine sawdust assumes a typical cellulose content of 40%; yields from corn stover are based on cellulose analysis of 34.4% for both AFEX-treated and untreated stover and xylan analysis of 22.8% for untreated stover.

^bFurfural was obtained in 34% molar yield from the xylan contained in the stover.

^cFurfural was obtained in 37% molar yield from the xylan contained in the stover.

We propose that the formation of HMF from cellulose in DMA–LiCl occurs via saccharification followed by isomerization of the glucose monomers into fructose and dehydration of fructose to form HMF. The saccharification of cellulose in water is thought to occur via Brønsted acid-catalyzed hydrolysis of its glycosidic bonds.¹⁵⁶ A similar Lewis acid-catalyzed process could be responsible for the hydrolysis activity of chromium halides. Additionally, the improved HMF yield with addition of hydrochloric acid suggests that Brønsted acid catalysis also occurs in DMA–LiCl. This area of cellulose chemistry offers rich opportunities for mechanistic understanding in addition to enabling HMF synthesis and possibly offering an alternative to enzymatic or aqueous acid-catalyzed hydrolysis for saccharification of lignocellulosic biomass.

4.2.6 Conversion of Lignocellulosic Biomass into 2,5-Dimethylfuran

The conversion of lignocellulosic biomass to HMF in a single step offers straightforward access to a wide variety of useful HMF derivatives, such as DMF. Dumesic and coworkers have shown that DMF, a promising HMF-derived fuel,^{132,133} can be prepared by hydrogenolysis of fully-purified HMF using copper catalysts.¹⁵⁷ We sought instead a process to synthesize DMF in two chemical reactions from lignocellulosic biomass.

In the first step of our process, we formed HMF from untreated corn stover in DMA–LiCl. We then removed the chloride ions from the crude HMF by ion-exclusion chromatography in water.^{158,159} This separation step prevented the chloride from poisoning the copper hydrogenolysis catalyst. Finally, we subjected the crude HMF from corn stover to hydrogenolysis in 1-butanol with a carbon-supported copper–ruthenium

catalyst, and obtained a 49% molar yield of DMF, similar to that obtained by Dumesic and coworkers using HMF that contained trace chloride.¹³³ The overall molar yield of DMF based on the cellulose content of the stover was 9% (**Figure 4.1**). We expect that optimization of the process could readily improve upon this result.

4.3 Conclusion

Our two-step process represents a low-temperature (<250 °C), non-enzymic route from lignocellulosic biomass to fuels. Most other chemical methods for the conversion of lignocellulosic biomass to fuels use extreme temperatures to produce pyrolysis oil or synthesis gas, incurring substantial energy costs. Our low-temperature chemical conversion also has inherent advantages over bioprocessing for cellulosic fuels and chemicals. Fermentation of lignocellulosic feedstocks requires saccharification through extensive pretreatment, fragile enzymes, and engineered organisms. In contrast, our chemical process uses simple, inexpensive catalysts to transform cellulose into a valuable product in an ample yield. In addition, our privileged solvents enable rapid biomass conversion at useful solid loadings (10 wt%). Under our best conditions, we transform 42% of the dry weight of cellulose into HMF and 19% of the dry weight of corn stover into HMF and furfural in one step. For comparison, cellulosic ethanol technology, which has been optimized extensively, enables the conversion of 24% of the dry weight of corn stover into ethanol in a complex process involving multiple chemical, biochemical, and microbiological steps.¹⁵⁴

Our process is also competitive on the basis of energy yield. The HMF and furfural products contain 43% of the combustion energy available from cellulose and xylan in the

corn stover starting material, whereas ethanol from corn stover preserves 62% of the sugar combustion energy (see: Supporting Information). Biomass components that cannot be converted into HMF, such as lignin, could be reformed to produce H_2 for HMF hydrogenolysis (**Figure 4.1**) or burned to provide process heat.¹⁶⁰

Realizing all of the intrinsic advantages of our process requires additional improvements. The high loading of the chromium catalyst and the toxicity of this metal could be barriers to its large-scale use. To address this issue, we have already found that decreasing chromium loading by two-thirds decreases the yield of HMF from glucose only slightly (Table 4.5). Additionally, the yields of HMF from cellulose and lignocellulosic biomass are still modest. Finally, methods for recycling solvents and salts would make the process more economical. We also anticipate that further mechanistic studies of this fascinating reaction cascade will enable the design of enhanced, chromium-free catalysts that can accomplish the transformation of cellulose into HMF in higher yield. With these types of improvements, this selective chemistry could become a highly attractive process for the conversion of lignocellulosic biomass into an array of fuels and chemicals.

4.4 Acknowledgements

This work was supported by the Great Lakes Bioenergy Research Center, a DOE Bioenergy Research Center. J.B.B. was supported by an NSF Graduate Research Fellowship. We are grateful to H. Brown, J. E. Holladay, and Z. Zhang for helpful conversations on biomass chemistry in ionic liquids, B. R. Caes, L. Summers, and R. Landick for contributive discussions, J. J. Blank and A. V. Cefali for experimental

assistance, S. Stahl for access to a Parr reactor, B. E. Dale and B. Venkatesh for corn stover samples, and K. Bersch for pine sawdust samples.

4.5 Experimental Section

4.5.1 General Considerations

Commercial chemicals were of reagent grade or better, and were used without further purification. With the exception of hydrogenolysis, reactions were performed in glass vessels heated in a temperature-controlled oil bath with magnetic stirring. The term “concentrated under high vacuum” refers to the removal of solvents and other volatile materials using a rotary evaporator at vacuum attained by a mechanical belt-drive oil pump while maintaining the water-bath temperature below 30 °C. Conductivity was measured using an Extech Instruments ExStik II conductivity meter.

1-Ethyl-3-methylimidazolium chloride (99.5%, [EMIM]Cl) was from Solvent-Innovation (Cologne, Germany). 1-Ethyl-3-methylimidazolium tetrafluoroborate (97%, [EMIM]BF₄), 5-hydroxymethylfurfural, and 2,5-dimethyl furan, and were from Aldrich (Milwaukee, WI). 1-Ethyl-3-methylimidazolium triflate (98.5%, [EMIM]OTf), 1-butyl-3-methylpyridinium chloride (97%, [BMPy]Cl), 1-ethyl-3-methylimidazolium bromide (97%, [EMIM]Br), and 1-propyl-3-methylimidazolium iodide (97%, [PMIM]I) were from Fluka (Geel, Belgium). 1-Ethylpyridinium chloride (98%, [EtPy]Cl), 1-ethyl-2,3-dimethylimidazolium chloride (98%, [MMEIM]Cl), and furfural were from Acros (Buchs, Switzerland). Cu–Ru/carbon catalyst (3:2 mole ratio Cu:Ru) was prepared by the method of Dumesic and coworkers using 5% Ru/carbon from Aldrich (Milwaukee, WI).¹³³ Cellulose (medium cotton linters, #C6288) was from Sigma (St. Louis, MO).

Milled and sieved corn stover and AFEX-treated corn stover were generously provided by B. E. Dale and coworkers (Michigan State University).¹⁵³ Cellulose and corn stover were dried to constant weight at 120 °C prior to use.

4.5.2 Analytical Methods

All reaction products were analyzed by HPLC and quantified using calibration curves generated with commercially-available standards. Following a typical reaction, the product mixture was diluted with a known mass of deionized water, centrifuged to sediment insoluble products, and analyzed. The concentrations of products were calculated from HPLC-peak integrations and used to calculate molar yields. HPLC was performed with either a Waters system equipped with two 515 pumps, a 717 Plus autosampler, and a 996 photodiode array detector or an Agilent 1200 system equipped with refractive index and photodiode array detectors. HMF and furfural were analyzed either by reversed-phase chromatography using a Varian MicrosorbTM-MV 100-5 C18 column (250 × 4.6 mm; 93:7 water/acetonitrile, 1 mL/min, 35 °C) or by ion-exclusion chromatography using a Bio-Rad Aminex[®] HPX-87H column (300 × 7.8 mm; 5 mM H₂SO₄, 0.6 or 0.9 mL/min, 65 °C). DMF was analyzed by reversed-phase chromatography using a Varian MicrosorbTM-MV 100-5 C18 column (250 × 4.6 mm; 55:45 water/acetonitrile, 1 mL/min, 35 °C). Representative ion-exclusion HPLC traces for HMF and furfural analysis are shown in **Figure 4.4** and **Figure 4.5**.

4.5.3 Representative Procedure for Synthesis of HMF from Sugars

Fructose (27.1 mg, 150 μ mol) and LiCl (24 mg) were mixed in DMA (203 mg). Following addition of concd H_2SO_4 (0.5 μ L, 9 μ mol), the reaction mixture was stirred at 80 $^\circ\text{C}$ for 5 h. At 1-h intervals, aliquots of the reaction mixture were removed for HPLC analysis. For reactions of glucose using [EMIM]Cl, chromium salts were mixed with a portion of the ionic liquid (25 mg) before addition to the reaction mixture. HMF yields for optimized reactions of sugars were reproduced to within 2–3%.

4.5.4 Kinetic Analysis of HMF Formation from Fructose

Fructose (425.6 mg, 2.362 mmol) and concd sulfuric acid (7.9 μ L, 142 μ mol) were dissolved in DMA (3.8185 g). Four known weights of this stock solution (approx. 0.5 g) were combined with four different mixtures of LiI and LiBF₄ (added to maintain constant salt concentration of 0.55 mmol/g) with LiI concentrations from 72.7 mg/g to 5.1 mg/g. After the salts were dissolved completely, the solutions were heated at 75 $^\circ\text{C}$ for 10 min and cooled rapidly on ice prior to HPLC analysis.

4.5.5 Representative Procedure for Synthesis of HMF from Cellulose and Lignocellulose

Cellulose (21.2 mg, 131 μ mol glucose units in cellulose), LiCl (26 mg), [EMIM]Cl (159 mg), and DMA (252 mg) were mixed at 50 $^\circ\text{C}$ for 24 h to form a viscous solution. To this cellulose solution were added concd HCl (1 μ L, 12 μ mol) and CrCl₂ (4 mg, 30 μ mol) in [EMIM]Cl (50 mg), and the reaction mixture was heated to 140 $^\circ\text{C}$ with vigorous stirring for 2 h. At 1-h intervals aliquots of the reaction mixture were removed for HPLC analysis. Reactions using lignocellulose were similar except that the

dissolution step was performed at 75 °C and the biomass was added at a concentration of 10 wt%. In other cases the cellulose was dissolved according to the methods of McCormick and coworkers.¹⁴³ HMF yields for optimized reactions of cellulose were reproduced to within 2–3%.

4.5.6 Ion-Exclusion Chromatographic Separation of HMF

Fructose (1.20 g, 6.67 mmol) and LiCl (600 mg) were mixed in DMA (6.0 g) and stirred at 140 °C for 1 h. Deionized water (1.0 g) was mixed with a portion of this reaction mixture (3.87 g) containing HMF (127 mg). This solution was loaded on to a column of ion-exclusion resin (Dowex 50X8-200, Li⁺ form, 70 × 1.5 cm) and eluted with deionized water at a rate of 3 cm/min. Fractions (25 mL) were collected and analyzed by HPLC. HPLC analysis indicated that >75% of the HMF was recovered in the HMF-containing fractions.

4.5.7 Synthesis of DMF from Fructose

Fructose (1.805 g, 10 mmol) and LiCl (1.690 g) were dissolved in DMA (14.67 g). Following addition of concd H₂SO₄ (33 µL, 0.6 mmol), the reaction mixture was stirred at 120 °C for 1 h. A portion of the reaction mixture (3.01 g, 16.5%) was then diluted with deionized water (2 g), loaded onto a column of ion-exclusion resin (Dowex 50X8-200, Li⁺ form, 70 × 1.5 cm), and eluted with deionized water at a rate of 2 cm/min. HMF-containing fractions with conductivity <50 µS were pooled and concentrated under high vacuum. The residue was taken up in 1-butanol (45 g) and placed in a Parr reactor with Cu–Ru/carbon catalyst (100 mg). The reactor was purged three times with H₂(g),

pressurized with 6.8 bar $\text{H}_2(\text{g})$, and heated to 220 °C with stirring. After 10 h, the reactor was cooled and vented. The contents were analyzed by HPLC for DMF (51.6 mg, 537 μmol , 32.5% based on fructose).

4.5.8 *Synthesis of DMF from Corn Stover*

Corn stover (1.504 g, 3.19 mmol glucose units in cellulose), LiCl (0.755 g), [EMIM]Cl (5.630 g), and DMA (6.756 g) were mixed at 75 °C for 24 h. To this viscous mixture were added concd HCl (26 μL , 310 μmol) and CrCl_3 (50.5 mg, 319 μmol) in [EMIM]Cl (0.55 g), and the reaction mixture was heated with 140 °C with vigorous stirring. After 2 h, the reaction mixture was cooled to room temperature, diluted with deionized water (7 g), and subjected to centrifugation to sediment insoluble material. After removal of the supernatant, the pellet was resuspended in deionized water (3 g), and the process repeated. The combined supernatant solutions were loaded onto a column of ion-exclusion resin (Dowex 50X8-200, Li^+ form, 70×1.5 cm), and eluted with deionized water at a rate of 3 cm/min. HMF-containing fractions with conductivity <50 μS were pooled and concentrated under high vacuum. After they were concentrated under high vacuum, the pooled HMF-containing fractions with conductivity >50 μS were loaded a second time on the ion-exchange column and eluted with deionized water. HMF-containing fractions from the second pass with conductivity <50 μS were pooled, concentrated under high vacuum, and combined with the earlier HMF concentrate. This residue was taken up in 1-butanol (45 g) and placed in a Parr reactor with Cu–Ru/carbon catalyst (79 mg). The reactor was purged three times with $\text{H}_2(\text{g})$, pressurized with 6.8 bar $\text{H}_2(\text{g})$, and heated to 220 °C with stirring. After 10 h, the reactor was cooled and vented.

The contents were analyzed by HPLC for DMF (27.7 mg, 288 μ mol, 9.0% based on cellulose).

4.6 Calculations of Energy Yields

4.6.1 Relevant Enthalpies of Combustion

glucose¹⁶¹ 669.9 kcal/mol

xylose¹⁶¹ 559.0 kcal/mol

ethanol¹⁶¹ 326.7 kcal/mol

HMF¹⁶² 664.8 kcal/mol

furfural¹⁶¹ 559.5 kcal/mol

Note: Below, the mannose and galactose enthalpies of combustion are approximated by that of glucose (which is also a hexose); the arabinose enthalpy of combustion is approximated by that of xylose (which is also a pentose).

4.6.2 Energy Yield for Cellulosic Ethanol Production

Corn stover starting material (100 g) in previous work contains:^{163,154}

cellulose 37.4 g

xylan 21.1 g

arabinan 2.9 g

galactan 2.0 g

mannan 1.6 g

$$\frac{37.4 \text{ g} + 2.0 \text{ g} + 1.6 \text{ g}}{162.14 \text{ g/mol hexose units}} = 0.253 \text{ mol hexose units}$$

$$\frac{21.1 \text{ g} + 1.9 \text{ g}}{132.12 \text{ g/mol pentose units}} = 0.182 \text{ mol pentose units}$$

Theoretical combustion energy available from sugar content:

$$(0.253 \text{ mol} \times 669.9 \text{ kcal/mol}) + (0.182 \text{ mol} \times 559.0 \text{ kcal/mol}) = 271.2 \text{ kcal}$$

Ethanol yield is 72 gal/dry ton stover:^{163,154} 0.237 g/g stover

Actual combustion energy attainable from ethanol product:

$$100 \text{ g stover} \times (0.237 \text{ g ethanol/g stover}) \times (\text{mol}/46.07 \text{ g ethanol}) \times 326.7 \text{ kcal/mol} = 168.1 \text{ kcal}$$

Combustion-energy yield = 168.1 kcal/271.2 kcal = **62%**

4.6.3 Energy Yield for Furan Production

Corn stover starting material (100 g) in this work contains:

cellulose 34.4 g

xylan 22.8 g

$$\frac{34.4 \text{ g}}{162.14 \text{ g/mol hexose units}} = 0.212 \text{ mol glucose}$$

$$\frac{22.8 \text{ g}}{162.14 \text{ g/mol hexose units}} = 0.173 \text{ mol xylose}$$

Theoretical combustion energy available from glucose and xylose:

$$(0.212 \text{ mol} \times 669.9 \text{ kcal/mol}) + (0.173 \text{ mol} \times 559.0 \text{ kcal/mol}) = 238.7 \text{ kcal}$$

Actual combustion energy attainable from furanic products (HMF and furfural):

$$47.2\% \text{ yield} \times (0.212 \text{ mol} \times 664.8 \text{ kcal/mol}) + 36.6\% \text{ yield} \times (0.173 \text{ mol} \times 559.5 \text{ kcal/mol}) = 101.9 \text{ kcal}$$

Combustion-energy yield = 102.4 kcal/238.7 kcal = **43%**

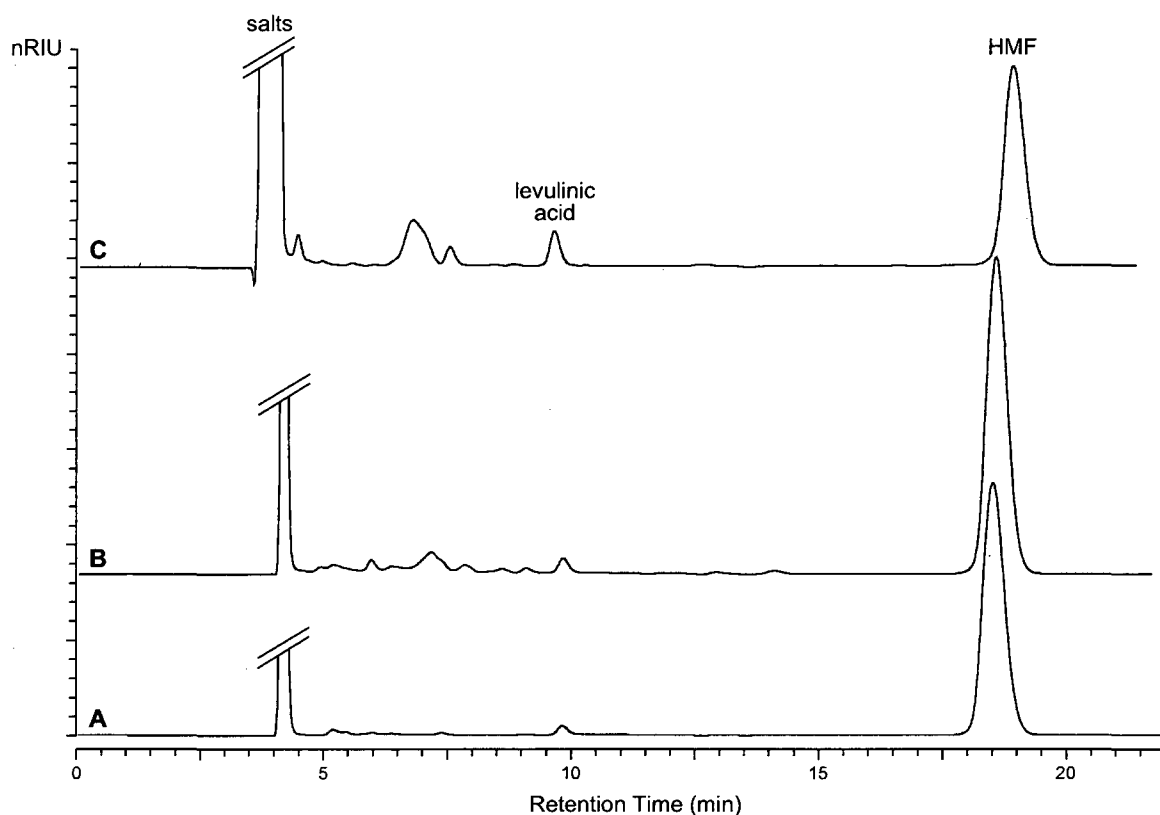


Figure 4.4 Refractive index HPLC traces of representative reaction mixtures. Analyses were performed with a Bio-Rad Aminex® HPX-87H column and a flow rate of 0.9 mL/min. (A) Synthesis of HMF from fructose with halide additives in DMA. (B) Synthesis of HMF from glucose with lithium bromide in DMA. (C) Synthesis of HMF from cellulose.

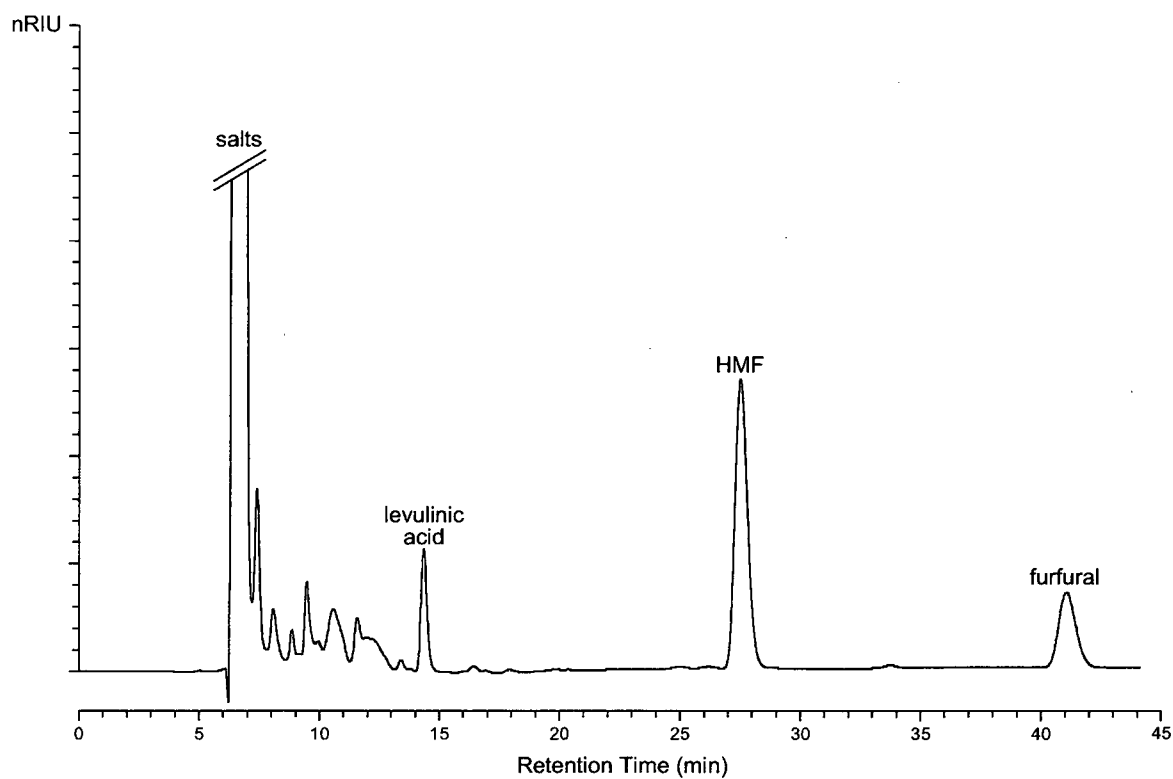


Figure 4.5 Refractive index HPLC trace of corn stover reaction mixture. Analyses were performed with a Bio-Rad Aminex® HPX-87H column and a flow rate of 0.6 mL/min. Major components are indicated.

CHAPTER 5***MECHANISTIC INSIGHTS ON THE DEHYDRATION OF GALACTOSE,
LACTOSE, AND MANNOSE TO FORM HMF**

Abstract: Efficient utilization of all of the components of biomass will enable a sustainable bio-economy. Sugars such as D-mannose and D-galactose comprise much of hemicellulose, while lactose is a common dairy byproduct. Here, we demonstrate new chemistry for conversion of these sugars into 5-hydroxymethylfurfural, an intermediate for renewable fuels and chemicals. Chromium salts enable the efficient conversion of mannose into HMF but are less effective for transformation of galactose, lactose, and the related hexulose, D-tagatose. Along with studies of the reactivity of D-psicose and L-sorbose, these results provide support for a mechanism of HMF formation involving chromium-catalyzed isomerization of aldoses into ketoses such as fructose and tagatose. Consequently, these minor sugars not only offer opportunities for renewable products and but also help uncover the mechanism of chromium-catalyzed HMF synthesis.

Co-author contributions: Anthony V. Cefali designed and performed experiments, analyzed data, and prepared drafts of the tables, results, and discussion. Jacqueline J. Blank performed experiments and edited the manuscript.

5.1 Introduction

Readily available fossil energy has fueled the dramatic growth of human society in the recent past. In 1850, when the world population was just over 1 billion, global energy production was about 2×10^{19} J, primarily from biomass such as wood.¹⁶⁴⁻¹⁶⁶ Since then, exponential growth of fossil fuel use has mirrored expanding population and production, and today human energy production is roughly 5×10^{20} J, with 85% from fossil fuels and under 10% from biomass.¹²⁶ As a result, civilization may face a major challenge in a few decades from declining petroleum supplies, inaccessible natural gas resources, and carbon-constrained coal usage. Advanced technology for chemical and biological biomass conversion may enable it to return to an important role in energy production and provide a replacement for diminishing fossil resources.

The hexose dehydration product, 5-hydroxymethylfurfural (HMF), is an important intermediate in the chemical transformation of biomass.¹³¹ This bifunctional, six-carbon molecule can be easily converted into a variety of useful derivatives,¹³⁰ incorporated into a variety of polymers,¹⁶⁷⁻¹⁷⁰ or upgraded into fuels.^{132,133} While HMF has long been synthesized in high yield from fructose,¹³⁰ we and others have recently demonstrated that HMF can be produced in high yield from glucose and in moderate yield from cellulose and lignocellulosic biomass using chromium salts in the presence of halide ions (**Figure 5.1**).^{134,139,171,172} High concentrations of chloride ions in solvents like the ionic liquid 1-ethyl-3-methylimidazolium chloride ([EMIM]Cl)^{173,142} or *N,N*-dimethylacetamide–lithium chloride (DMA–LiCl)¹⁴³ dissolve cellulose, and chromium ions likely catalyze the isomerization of glucose into fructose for rapid HMF formation. Together, these

features enable remarkably high yields of HMF from glucan in heterogeneous and recalcitrant lignocellulosic biomass.

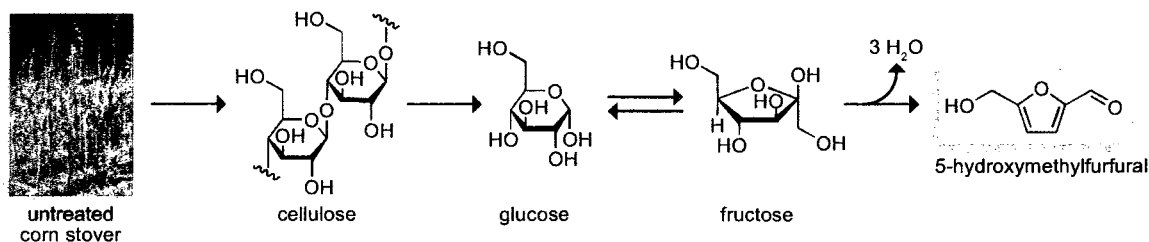


Figure 5.1 Synthesis of HMF from sugars and lignocellulosic biomass.

Despite these advances in the synthesis of HMF from glucose and glucose polysaccharides, the conversion of other hexoses into HMF has not been extensively studied. Because of our interest in the conversion of lignocellulosic biomass into HMF, we chose to study the transformation of D-mannose and D-galactose, minor hexose components of biomass, into HMF (**Figure 5.2**). Mannose-containing polymers may account for 10% of the dry weight of pine wood, while galactose may be as much as 2% of the carbohydrate in corn stover.^{174,153,175} Moreover, lactose, because of its poor digestibility, is an underutilized product of the dairy industry which has potential as a chemical or energy feedstock.¹⁷⁶⁻¹⁷⁸ None of these sugars have previously been converted into HMF in high yield. Ishida and coworkers studied lanthanide(III) ions as catalysts for HMF synthesis in both water and organic solvents, but achieved 6% yield from mannose and 7% yield from galactose, at most.^{179,180} In other cases, HMF formation from these sugars has primarily been examined as a side reaction or intermediary process during pretreatment or pyrolysis.^{181,175} Because chromium chlorides are efficient catalysts for conversion of glucose into HMF, we hypothesized that these catalysts would also

facilitate high yields of HMF from other aldoses such as mannose and galactose. To test this hypothesis, we studied HMF synthesis from not only mannose and galactose but also lactose and related hexuloses, such as D-tagatose (**Figure 5.2**). Our investigation revealed that mannose can be efficiently transformed into HMF and provided mechanistic insights into the role of chromium and hexose structure in HMF formation.

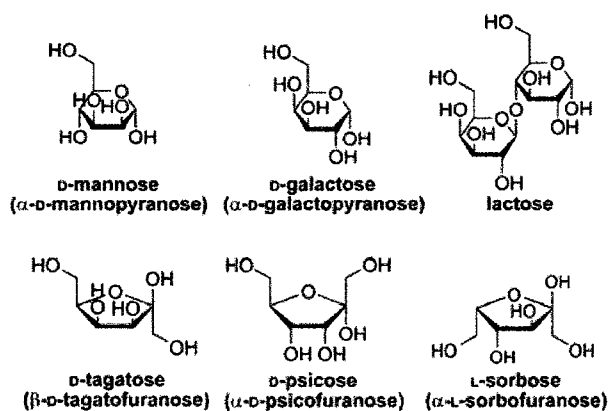


Figure 5.2 Mono- and disaccharide precursors for HMF.

5.2 Results and Discussion

5.2.1 Synthesis of HMF from Mannose.

The reactivity of mannose in DMA–LiCl and [EMIM]Cl was similar to that of glucose (Table 5.1).¹⁷² In the absence of chromium(II) or chromium(III), little HMF was formed and nearly all mannose was recovered unchanged at 100 °C. On the other hand, the addition of catalytic chromium enabled HMF yields of 43–54% in DMA–LiCl at 100–120 °C. Higher HMF yields were obtained in either DMA–LiBr or [EMIM]Cl, with a maximum yield of 69% achieved at 100 °C. These trends are comparable to those with glucose, suggesting that these two epimeric aldoses form HMF through a similar mechanism.

Table 5.1 Synthesis of HMF from Mannose

sugar	solvent	catalyst (mol%)	additives (wt%)	temp. (°C)	time (h)	molar yield (%)
mannose	DMA		LiCl, 10	120	2	2
mannose	[EMIM]Cl			120	2	1
mannose	DMA	CrCl ₂ , 6	LiCl, 10	120	2	54
mannose	DMA	CrCl ₃ , 6	LiCl, 10	120	2	43
mannose	DMA	CrCl ₂ , 6	LiBr, 10	120	2	51
mannose	DMA	CrCl ₃ , 6	LiBr, 10	120	2	64
mannose	[EMIM]Cl	CrCl ₂ , 6		120	2	57
mannose	[EMIM]Cl	CrCl ₃ , 6		120	2	56
mannose	DMA	CrCl ₂ , 6	LiCl, 10	100	2	54
mannose	DMA	CrCl ₃ , 6	LiCl, 10	100	2	47
mannose	DMA	CrCl ₂ , 6	LiBr, 10	100	2	69
mannose	DMA	CrCl ₃ , 6	LiBr, 10	100	2	60
mannose	[EMIM]Cl	CrCl ₂ , 6		100	2	68
mannose	[EMIM]Cl	CrCl ₃ , 6		100	2	52
glucose	DMA	CrCl ₂ , 6	LiCl, 10	120	3	53 ^a
glucose	DMA	CrCl ₂ , 6	LiBr, 10	100	4	79 ^a

Mannose was reacted at a concentration of 10 wt% relative to the total mass of the reaction mixture.

Additive concentrations are relative to the total mass of the reaction mixture. Catalyst loading is relative to mannose. Yields are based on HPLC analysis.

^a From reference ¹⁷².

Indeed, the proposed mechanism for chromium-catalyzed HMF formation from aldoses suggests that glucose and mannose share fructose as a common intermediate (**Figure 5.3**). In this mechanism, the aldo form of either glucose or mannose complexes with a chromium ion and forms an enediolate intermediate upon deprotonation. This deprotonation destroys the C-2 stereochemistry which differentiates mannose and glucose, and protonation of the enediolate at C-1 produces fructose. The common fructose intermediate is then readily dehydrated into HMF, likely via formation of a fructofuranosyl oxocarbenium ion.^{146,172} The similar reactivity of glucose and mannose is consistent with this mechanism, if the ease of chromium-catalyzed isomerization of glucose and mannose is comparable or does not affect the overall reaction.

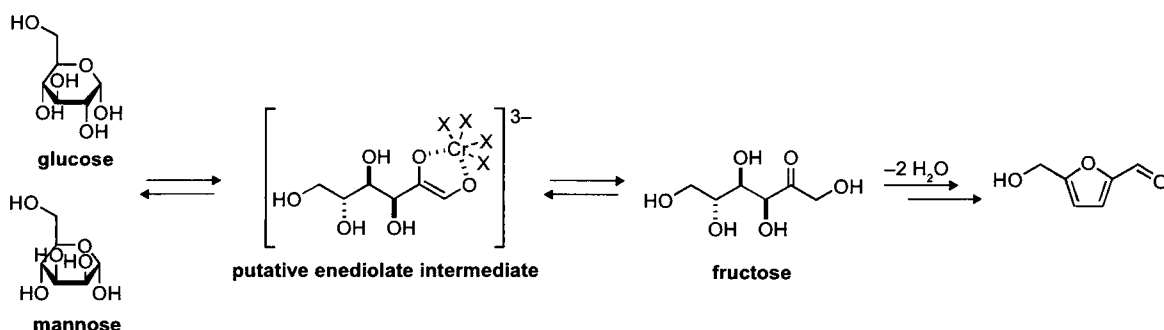


Figure 5.3 Putative mechanism for chromium-catalyzed conversion of glucose and mannose into HMF. Chromium species, depicted here as a hexacoordinate chromium(III) complex, catalyze the isomerization of these aldoses into fructose through a putative enediolate intermediate.

5.2.2 Synthesis of HMF from Galactose and Lactose.

Although we expected that galactose, a C-4 epimer of glucose, would readily be converted into HMF by chromium catalysts in DMA–LiCl, high yields of HMF from this sugar were elusive under a range of reaction conditions (Table 5.2). As anticipated, no HMF was produced from galactose in the absence of chromium salts. With CrCl₂ or CrCl₃ in DMA–LiCl at 120 °C, HMF was produced in 10% yield, far lower than the yields observed with glucose and mannose. Adding H₂SO₄ as a co-catalyst resulted in lower yields, while use of [EMIM]Cl as the solvent in place of DMA did not greatly improve the results. On the other hand, switching to non-chloride solvents increased HMF yields. Substituting LiBr for LiCl raised the HMF yield to 18%, and using CrBr₃ without a halide additive allowed a yield of 33%. Still, these yields are far lower than those observed for other aldoses, and reveal an unexpected deleterious effect from halide additives.

Table 5.2 Synthesis of HMF from Galactose

sugar	solvent	catalyst (mol%)	additives (wt%)	temp. (°C)	time (h)	molar yield (%)
galactose	DMA		LiCl, 10	120	2	1
galactose	[EMIM]Cl			120	2	1
galactose	[EMIM]Cl	H ₂ SO ₄ , 6		120	2	1
galactose	DMA	CrCl ₂ , 6	LiCl, 10	120	2	10
galactose	DMA	CrCl ₃ , 6	LiCl, 10	120	2	10
galactose	DMA	CrCl ₂ , 6; H ₂ SO ₄ , 6	LiCl, 10	120	2	9
galactose	DMA	CrCl ₃ , 6; H ₂ SO ₄ , 6	LiCl, 10	120	2	7
galactose	[EMIM]Cl	CrCl ₂ , 6		120	2	14
galactose	[EMIM]Cl	CrCl ₃ , 6		120	2	4
galactose	DMA	CrCl ₂ , 6	LiBr, 10	120	2	18
galactose	DMA	CrCl ₃ , 6	LiBr, 10	120	2	17
galactose	DMA	CrCl ₂ , 6; H ₂ SO ₄ , 6	LiBr, 10	120	2	9
galactose	DMA	CrCl ₃ , 6; H ₂ SO ₄ , 6	LiBr, 10	120	2	9
galactose	DMA	CrCl ₂ , 6		120	2	22
galactose	DMSO	CrCl ₂ , 6		120	2	22
galactose	DMA	CrBr ₃ , 6		120	3	33
galactose	DMSO	CrBr ₃ , 6		120	3	24
galactose	DMA	Cr(NO ₃) ₃ , 6		120	3	9
galactose	DMSO	Cr(NO ₃) ₃ , 6		120	3	5

Galactose was reacted at a concentration of 10 wt% relative to the total mass of the reaction mixture.

Additive concentrations are relative to the total mass of the reaction mixture. Catalyst loading is relative to galactose. Yields are based on HPLC analysis.

Transformation of lactose into HMF was also challenging (Table 5.3). Use of chloride-containing solvents resulted in yields of about 20%, which are far lower than achieved with most other sugars. Slightly higher yields were obtained in DMA without LiCl, and DMA containing bromide salts such as CrBr₃ enabled the highest yields. HMF yields from lactose parallel roughly the average of the yields from glucose and galactose under the same conditions. The likely mechanism of HMF formation from lactose provides a rationale for these results. Lactose can be cleaved into glucose and galactose units through acid catalysis, and H₂SO₄ probably aids in this process. The resulting

glucose is efficiently converted into HMF through chromium catalysis, with the galactose unit forming HMF less readily.

Table 5.3 Synthesis of HMF from Lactose

sugar	solvent	catalyst (mol%)	additives (wt%)	temp. (°C)	time (h)	molar yield (%)
lactose	[EMIM]Cl			120	2	3
lactose	[EMIM]Cl	H ₂ SO ₄ , 6		120	2	3
lactose	DMA	CrCl ₂ , 6	LiCl, 10	120	2	23
lactose	DMA	CrCl ₃ , 6	LiCl, 10	120	2	19
lactose	DMA	CrCl ₂ , 6; H ₂ SO ₄ , 6	LiCl, 10	120	2	19
lactose	DMA	CrCl ₃ , 6; H ₂ SO ₄ , 6	LiCl, 10	120	2	22
lactose	[EMIM]Cl	CrCl ₂ , 6		120	2	17
lactose	[EMIM]Cl	CrCl ₂ , 6; H ₂ SO ₄ , 6		120	2	21
lactose	DMA	CrCl ₂ , 6		120	3	23
lactose	DMSO	CrCl ₂ , 6		120	2	23
lactose	DMA	CrCl ₂ , 6; H ₂ SO ₄ , 6		120	3	26
lactose	DMSO	CrCl ₂ , 6; H ₂ SO ₄ , 6		120	3	11
lactose	DMA	CrCl ₂ , 6	LiBr, 10	120	2	27
lactose	DMA	CrCl ₃ , 6	LiBr, 10	120	2	29
lactose	DMA	CrCl ₂ , 6; H ₂ SO ₄ , 6	LiBr, 10	120	2	39
lactose	DMA	CrCl ₃ , 6; H ₂ SO ₄ , 6	LiBr, 10	120	2	35
lactose	DMA	Cr(NO ₃) ₃ , 6		120	3	4
lactose	DMSO	Cr(NO ₃) ₃ , 6		120	3	13
lactose	DMA	CrBr ₃		120	3	41

Lactose was reacted at a concentration of 10 wt% relative to the total mass of the reaction mixture.

Additive concentrations are relative to the total mass of the reaction mixture. Catalyst loading is relative to lactose. Yields are based on HPLC analysis.

5.2.3 Synthesis of HMF from Tagatose, Psicose, and Sorbose

Just as the differential reactivity of glucose and galactose predicts lactose yields, the stereochemical differences of these sugars may explain the difficulty of galactose conversion. Although glucose and mannose share fructose as a common intermediate on the pathway to HMF, isomerization of galactose into a ketose results in tagatose, the C-4

epimer of fructose (**Figure 5.4**). Inefficient dehydration of tagatose into HMF would prevent high HMF yields from galactose.

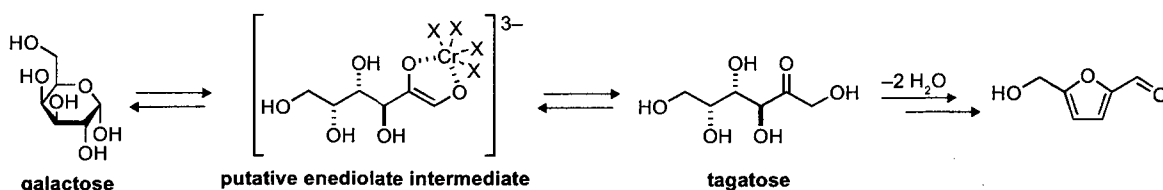


Figure 5.4 Putative mechanism for chromium-catalyzed conversion of galactose into HMF. In analogy to the proposed mechanism for glucose transformation, galactose isomerizes into tagatose. Dehydration of tagatose forms HMF in low yield.

Experimental results confirmed our hypothesis that poor tagatose reactivity limits HMF production from galactose. In chloride-containing solvents with chromium or H_2SO_4 catalysts, yields of HMF from tagatose were typically less than 20% (Table 5.4). Just as was observed with galactose, the highest yields of HMF were achieved in the absence of chloride ions. Moreover, the maximal yield from tagatose was 61%, which is significantly lower than the 80–90% yields commonly achieved with fructose.^{130,137,172} Our results suggest that transformation of tagatose into HMF is both more challenging than conversion of fructose and detrimentally affected by halide ions.

Table 5.4 Synthesis of HMF from Tagatose

sugar	solvent	catalyst (mol%)	additives (wt%)	temp. (°C)	time (h)	molar yield (%)
tagatose	DMA			120	2	0
tagatose	DMA		LiCl, 10	120	2	9
tagatose	[EMIM]Cl			120	2	15
tagatose	DMA	CrCl ₂ , 6	LiCl, 10	120	2	10
tagatose	DMA	CrCl ₃ , 6	LiCl, 10	120	2	8
tagatose	DMA	H ₂ SO ₄ , 6	LiCl, 10	120	2	7
tagatose	DMA	CrCl ₂ , 6; H ₂ SO ₄ , 6	LiCl, 10	120	2	11
tagatose	[EMIM]Cl	CrCl ₂ , 6		120	2	14
tagatose	[EMIM]Cl	CrCl ₃ , 6		120	2	10
tagatose	[EMIM]Cl	H ₂ SO ₄ , 6		120	2	12
tagatose	[EMIM]Cl	CrCl ₂ , 6; H ₂ SO ₄ , 6		120	2	9
tagatose	DMSO	CrCl ₂ , 6	LiCl, 10	120	2	20
tagatose	DMSO	H ₂ SO ₄ , 6	LiCl, 10	120	2	13
tagatose	DMSO		LiCl, 10	120	2	14
tagatose	DMA	H ₂ SO ₄ , 6		120	2	45
tagatose	DMSO			120	2	52
tagatose	DMSO	Dowex		120	2	55
tagatose	DMSO	H ₂ SO ₄ , 6		120	2	61
tagatose	DMA	CrCl ₂ , 6		120	2	21
tagatose	DMSO	CrCl ₂ , 6		120	2	27
tagatose	DMA	CrCl ₂ , 6	LiBr, 10	120	2	13
tagatose	DMA	CrCl ₃ , 6	LiBr, 10	120	2	12
tagatose	DMA	H ₂ SO ₄ , 6	LiBr, 10	120	3	26

Tagatose was reacted at a concentration of 10 wt% relative to the total mass of the reaction mixture.

Additive concentrations are relative to the total mass of the reaction mixture. Catalyst loading is relative to tagatose. Yields are based on HPLC analysis.

The disparity in fructose and tagatose reactivity might result from their tautomeric composition. Dehydration of ketoses into HMF probably proceeds through the equilibrium protonation and dehydration of furanose form of the sugar to form an oxocarbenium intermediate.¹⁴⁶ Increased concentrations of the furanose form would increase the rate of this reaction. As a result, fructose is poised for conversion into HMF in polar aprotic organic solvents because it exists primarily in furanose forms (48% β -furanose, 20% α -furanose, and 27% β -pyranose in DMSO at 27 °C).¹⁸² Tagatose, on the

other hand, preferentially forms pyranose tautomers in both water and organics (76% α -pyranose, 17% β -pyranose, 4% α -furanose and 3% β -furanose in DMSO at 27 °C).¹⁸² As a result, it may be less likely to undergo dehydration to produce HMF and more likely to participate in deleterious side reactions.

For further evidence, we examined the reactivity of the other epimeric hexuloses, D-psicose and L-sorbose (Table 5.5). Psicose is the C-3 epimer of fructose and exists as 50% furanose tautomers in DMSO (15% β -furanose, 35% α -furanose, 24% α -pyranose, and 26% β -pyranose at 27 °C),¹⁸² while sorbose is a C-5 epimer which is primarily pyranose (93% α -pyranose and 7% α -furanose in DMSO at 25 °C). The yield of HMF from psicose with H_2SO_4 in DMSO was higher than that of either tagatose or sorbose and similar to those obtained with fructose, which is consistent with the relatively high furanose preference of psicose. Nonetheless, yields of HMF from psicose and sorbose were similar under other conditions. In DMA and in the presence of LiCl both sugars formed HMF in 30–45% yields. In particular, sorbose and psicose delivered significantly higher yields than tagatose in the presence of lithium chloride. These results suggest that the interplay of hexulose structure and reactivity is subtle.

Table 5.5 Synthesis of HMF from Psicose and Sorbose

sugar	solvent	catalyst (mol%)	additives (wt%)	temp. (°C)	time (h)	molar yield (%)
psicose	DMA		LiCl, 10	120	3	35
psicose	DMA	H ₂ SO ₄ , 6	LiCl, 10	120	3	33
psicose	DMA	H ₂ SO ₄ , 6		120	3	30
psicose	DMSO		LiCl, 10	120	3	39
psicose	DMSO	H ₂ SO ₄ , 6	LiCl, 10	120	3	37
psicose	DMSO	H ₂ SO ₄ , 6		120	3	82
sorbose	DMA		LiCl, 10	120	3	39
sorbose	DMA	H ₂ SO ₄ , 6	LiCl, 10	120	3	38
sorbose	DMA	H ₂ SO ₄ , 6		120	3	37
sorbose	DMSO		LiCl, 10	120	3	45
sorbose	DMSO	H ₂ SO ₄ , 6	LiCl, 10	120	3	37
sorbose	DMSO	H ₂ SO ₄ , 6		120	3	60

Psicose and sorbose were reacted at a concentration of 10 wt% relative to the total mass of the reaction mixture. Additive concentrations are relative to the total mass of the reaction mixture. Catalyst loading is relative to sugar. Yields are based on HPLC analysis.

5.3 Conclusions

Although hemicellulose monomers such as mannose and galactose are relatively minor components of lignocellulose, methods for converting these sugars into chemicals and fuels are crucial for efficient utilization of biomass resources. Through our investigations of the chromium-catalyzed transformation of these and related sugars we discovered that HMF may be efficiently produced from mannose. This result is consistent with a mechanism in which mannose and glucose share a common intermediate, fructose. Galactose, lactose, and tagatose, the hexulose expected from isomerization of galactose, were both only poorly converted into HMF, which provides further mechanistic support. Additionally, we found that among fructose and its three epimers, the highest HMF yields could be obtained from fructose and psicose, the sugars with the highest furanose propensity, suggesting that tautomeric equilibria may explain the poor yield of HMF

from tagatose. Accordingly, minor sugars not only offer opportunities for production of renewable chemicals and fuels but also help illuminate the mechanism of HMF formation.

5.4 Acknowledgements

This work was supported by the Great Lakes Bioenergy Research Center, a DOE Bioenergy Research Center. J.B.B. was supported by an NSF Graduate Research Fellowship. We are grateful to J. E. Holladay and B. R. Caes for contributive discussions.

5.5 Experimental

5.5.1 General Considerations

Commercial chemicals were of reagent grade or better and were used without further purification. Reactions were performed in glass vessels heated in a temperature-controlled oil bath with magnetic stirring.

1-Ethyl-3-methylimidazolium chloride (99.5%, [EMIM]Cl) was from Solvent-Innovation (Cologne, Germany). 5-hydroxymethylfurfural, D-mannose, D-galactose, D-psicose, and Dowex® 50WX4 (200-400 mesh, H⁺ form) were from Aldrich (Milwaukee, WI). D-Tagatose was from Acros (Geel, Belgium). L-Sorbose was a gift from H. Lardy (University of Wisconsin–Madison).

5.5.2 Analytical Methods

All reaction products were analyzed by HPLC and quantified using calibration curves generated with commercially-available standards. Following a typical reaction, the

product mixture was diluted with a known mass of deionized water, centrifuged to sediment insoluble products, and analyzed. The concentrations of products were calculated from HPLC-peak integrations and used to calculate molar yields. HPLC was performed with either a Waters system equipped with two 515 pumps, a 717 Plus autosampler, and a 996 photodiode array detector or an Agilent 1200 system equipped with refractive index and photodiode array detectors. HMF was analyzed either by reversed-phase chromatography using a Varian Microsorb™-MV 100-5 C18 column (250 × 4.6 mm; 93:7 water/acetonitrile, 1 mL/min, 35 °C) or by ion-exclusion chromatography using a Bio-Rad Aminex® HPX-87H column (300 × 7.8 mm; 5 mM H₂SO₄, 0.6 or 0.9 mL/min, 65 °C).

5.5.3 Representative Procedure for Synthesis of HMF from Sugars

Tagatose (18.2 mg, 101 μmol) and LiCl (16 mg) were dissolved in DMA (200 mg), and the reaction mixture was stirred at 120°C for 2 hours. After the reaction, the solution was diluted with H₂O (300 mg) and analyzed by HPLC. Except where otherwise mentioned, reactions proceeded to high conversion and low yields indicate high byproduct formation.

5.5.4 Determination of L-Sorbose Tautomeric Equilibrium in DMSO

L-Sorbose (100 mg) was dissolved in DMSO-d₆ (1 mL) and equilibrated at ambient temperature for 8 d. A broadband ¹H-decoupled ¹³C NMR spectrum was recorded at 25 °C using a Bruker DMX-500 Avance spectrometer (¹³C, 125.7 MHz) at the National Magnetic Resonance Facility at Madison (NMRFAM). An inverse-gated pulse program

was used with a relaxation delay of 10 s. The spectrum was referenced to the DMSO- d_6 signal at 39.52 ppm. Signals from the α -pyranose and α -furanose tautomers were identified by comparison with chemical shifts in D_2O .¹⁸³ Other tautomers were not observed. Integrations of all signals for each tautomer were averaged to calculate tautomeric ratios.

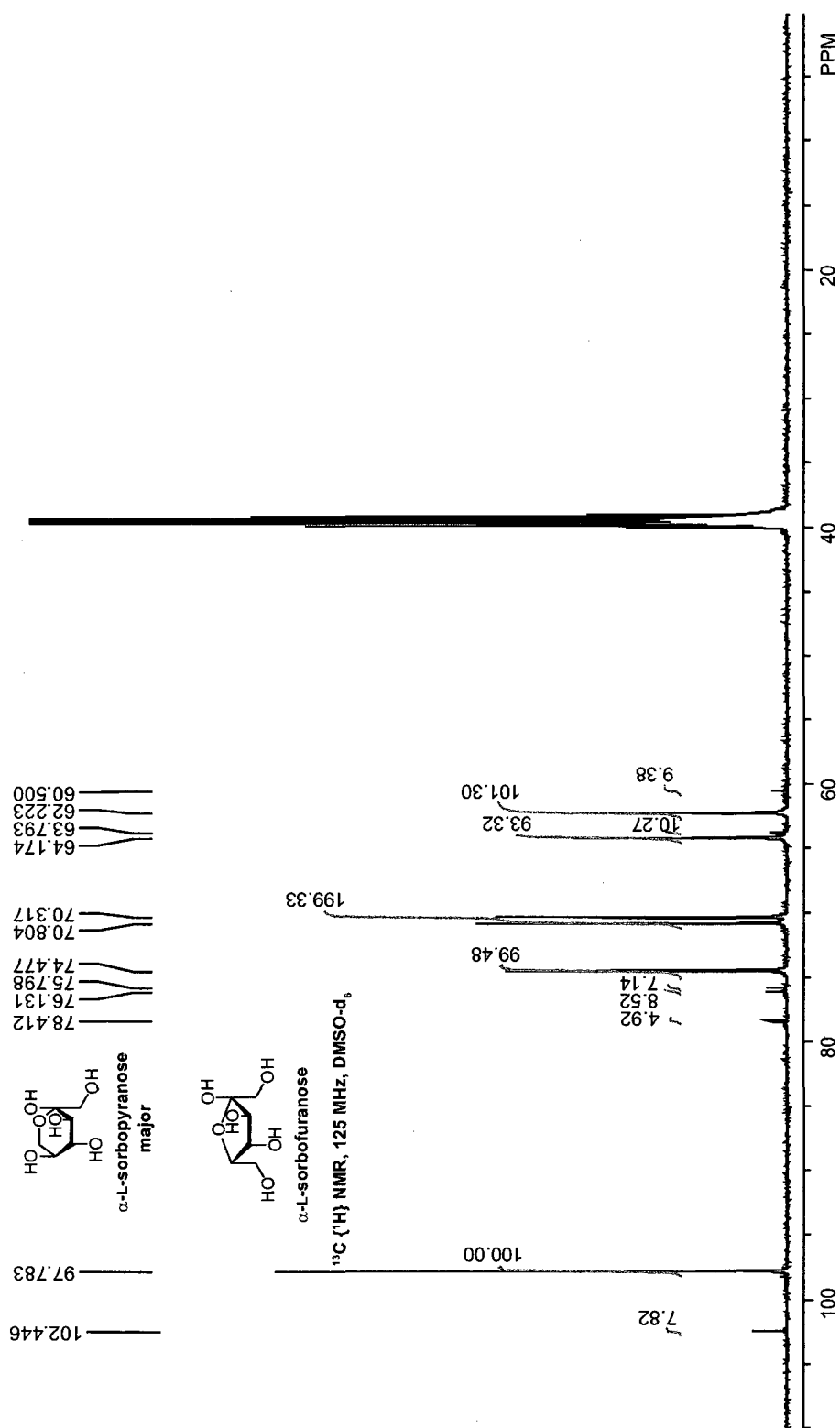


Figure 5.5 ^{13}C NMR Spectrum of L-sorbose in DMSO-d_6 .

CHAPTER 6***CHROMIUM HALIDE CATALYSTS FOR THE SYNTHESIS OF FURFURAL
FROM XYLOSE AND XYLAN**

Abstract: Renewable fuels and chemicals such as pentose-derived furfural can reduce the dependence of humanity on fossil resources. While furfural is produced industrially using high temperatures and strong acid catalysts, we have found that chromium halide catalysts enable furfural synthesis from xylose in *N,N*-dimethylacetamide and ionic liquids at moderate temperatures. Mechanistic investigations suggest that these catalysts isomerize xylose into xylulose, a reactive ketose intermediate which readily dehydrates into furfural. We have also investigated the transformation of xylan into furfural under similar conditions. Our chromium-based process offers an alternative route from pentoses to renewable furfural-derived fuels and chemicals.

Co-author contributions: Jacqueline J. Blank designed and performed experiments, analyzed data, and drafted the manuscript. Anthony V. Cefali assisted with experiments and edited the manuscript.

6.1 Introduction

Rising fossil energy prices and environmental preservation call for alternative sources of energy such as renewable fuels based on biomass.¹²⁶ Biofuels could reduce carbon dioxide emissions and decrease fuel prices, particularly if derived from non-food biomass resources such as agricultural, forest, and landfill wastes. Hemicellulose, a mixture of polysaccharides containing xylose, arabinose, glucose, galactose, mannose, and other sugars, is typically the second most abundant component of biomass after cellulose.¹⁷⁴ In grasses and hardwoods, xylan, a polymer of xylose, is often the primary hemicellulose. As a result, xylan conversion is critical for utilization of important biomass feedstocks like bagasse, corn stover, *Miscanthus*, switchgrass, and poplar.

Both xylan and xylose can be dehydrated into furfural, a biofuel precursor and industrial chemical (**Figure 6.1**).^{155,184} Indeed, furfural is perhaps the most common industrial chemical derived from lignocellulosic biomass with annual production of more than 200,000 t.^{185,125} The commercial utility of furfural was first discovered at Quaker Oats Company in 1921.¹⁸⁶ The company had produced vast quantities of oat hulls from the manufacture of oatmeal. At one point, Quaker Oats had amassed so much of this byproduct that the leftover oat hulls were stored in a circus tent. Though they could be used as livestock feed, the hulls were only partially digestible. Quaker Oats tested a variety of processes to valorize the hulls and found that treating them with dilute acid yielded useful amounts of furfural.

Since this initial discovery, many others have examined the conversion of pentoses into furfural.¹⁸⁷⁻¹⁹⁰ The process used by Quaker Oats employs a dilute sulfuric acid

catalyst and steam pressure, achieving 50% molar yields of furfural from xylan.¹⁵⁵

Most industrial processes achieve similar yields, likely limited by side reactions such as homopolymerization and condensation with unreacted xylose. Moreau and coworkers have converted xylose into furfural in about 50% yield using acidic dealuminated zeolites in water along with toluene as an extracting solvent.¹⁸⁸ Sulfated zirconia has also been used as a catalyst for xylose dehydration, producing yields of around 50%.¹⁹⁰ In all of these cases, Brønsted acidic catalysts were used in aqueous solution at temperatures greater than 150 °C. While questions remain about the mechanism for furfural formation from xylose under these conditions, recent computational work by Nimlos and coworkers¹⁹¹ supports the mechanism proposed by Antal and coworkers (**Figure 6.1**).¹⁹² In this mechanism, the C-2 hydroxyl group is displaced to form a xylose-2,5-anhydride. Subsequent dehydration steps produce furfural.

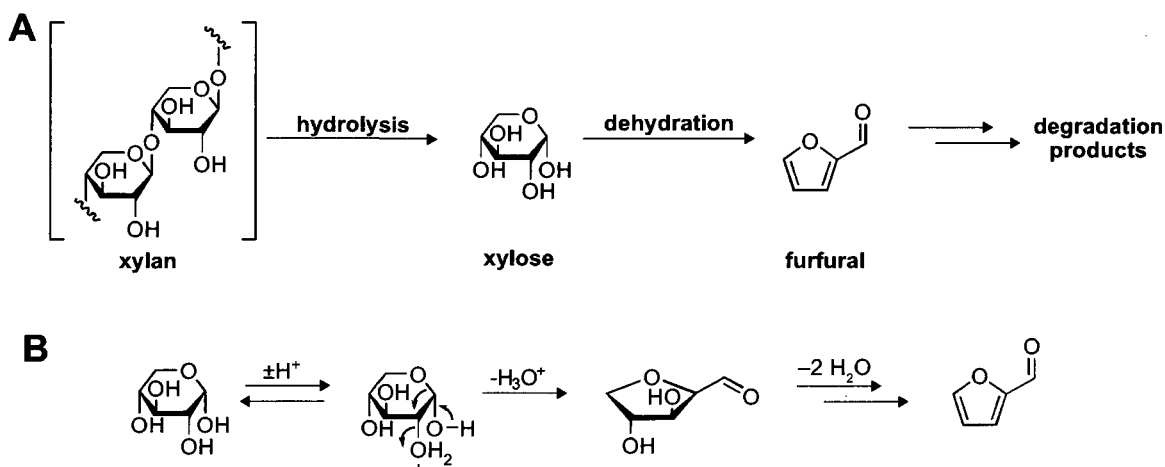


Figure 6.1 Synthesis of furfural. (A) Furfural may be produced from xylan by hydrolysis into xylose and subsequent dehydration. (B) In the most likely mechanism for acid-catalyzed dehydration of xylose, displacement of the C-2 hydroxyl group leads to a 2,5-anhydride intermediate which readily loses water to form furfural.

Recently, we and others have investigated the conversion of sugars^{134,171} and biomass¹⁷² into 5-hydroxymethylfurfural (HMF) in ionic liquids and *N,N*-dimethylacetamide containing lithium chloride (DMA–LiCl). In these initial studies, we found that the pentosans in biomass were dehydrated into furfural in moderate yields using a combination of chromium salts and HCl. These reaction conditions using non-aqueous solvents and chromium catalysts contrast with the aqueous Brønsted acid catalysis typical for furfural production. Consequently, we chose to investigate the reactions of xylose and xylan in DMA–LiCl and related solvents and report our findings herein.

6.2 Results and Discussion

6.2.1 *Conversion of Xylose into Furfural*

We began by investigating the reactivity of xylose in DMA with acid and chromium catalysts and halide additives at 100 °C (Table 6.1). Only low yields of furfural and moderate conversions of xylose were observed in DMA both alone and with HCl. For instance, 12 mol % HCl in DMA accomplished 47% conversion of xylose with only 6% yield of furfural. Although Brønsted acids such as HCl are typically used to produce furfural, these reactions are commonly carried out at temperatures greater than 150 °C. Under our more mild reaction conditions acids alone were less effective for rapid xylose conversion.

Table 6.1 Synthesis of Furfural from Xylose

sugar	solvent	catalyst (mol%)	additives (wt%)	temp. (°C)	time (h)	molar yield (%)
xylose	DMA			100	2	<5
xylose	DMA	CrCl ₃ , 6		100	2	37
xylose	DMA	CrCl ₃ , 6		100	4	38
xylose	DMA	CrCl ₃ , 6		100	6	37
xylose	DMA	HCl, 3		100	2	3
xylose	DMA	HCl, 6		100	2	1
xylose	DMA	HCl, 12		100	2	6
xylose	DMA	HCl, 24		100	2	9
xylose	DMA	HCl, 3	[EMIM]Cl, 5	100	2	1
xylose	DMA	HCl, 6	[EMIM]Cl, 5	100	2	2
xylose	DMA	HCl, 12	[EMIM]Cl, 5	100	2	3
xylose	DMA	CrCl ₃ , 6	[EMIM]Cl, 5	100	2	37
xylose	DMA	CrCl ₃ , 6	[EMIM]Cl, 5	100	4	37
xylose	DMA	CrCl ₃ , 6	[EMIM]Cl, 5	100	6	34
xylose	DMA	CrCl ₃ , 6	[EMIM]Cl, 10	100	2	37
xylose	DMA	CrCl ₃ , 6	[EMIM]Cl, 10	100	4	37
xylose	DMA	CrCl ₃ , 6	[EMIM]Cl, 10	100	6	38
xylose	DMA	CrCl ₃ , 6	[EMIM]Cl, 20	100	2	40
xylose	DMA	CrCl ₂ , 6	[EMIM]Cl, 5	100	2	45
xylose	DMA	CrCl ₂ , 6	[EMIM]Cl, 10	100	2	38
xylose	DMA	CrCl ₂ , 6	[EMIM]Cl, 20	100	2	41
xylose	DMA–LiCl (10%)	CrCl ₃ , 6	[EMIM]Cl, 5	100	2	40
xylose	DMA–LiCl (10%)	CrCl ₃ , 6	[EMIM]Cl, 10	100	2	30
xylose	DMA–LiCl (10%)	CrCl ₃ , 6	[EMIM]Cl, 20	100	2	37
xylose	DMA–LiCl (10%)	CrCl ₂ , 6	[EMIM]Cl, 5	100	2	24
xylose	DMA–LiCl (10%)	CrCl ₂ , 6	[EMIM]Cl, 10	100	2	33
xylose	DMA–LiCl (10%)	CrCl ₂ , 6	[EMIM]Cl, 20	100	2	36
xylose	DMA	CrCl ₃ , 6	LiBr, 10	100	4	47
xylose	DMA	CrBr ₃ , 6	LiBr, 10	100	4	50
xylose	DMA	CrCl ₂ , 6	NaBr, 10	100	4	54
xylose	DMA	CrCl ₂ , 6	[BMIM]Br, 20	100	4	55
xylose	DMA	CrCl ₂ , 6	LiBr, 10	100	4	56

Xylose was reacted at a concentration of 10 wt% relative to the total mass of the reaction mixture. The solvent composition is indicated by the wt% of LiCl relative to DMA with additive concentrations relative to the total mass of the reaction mixture. Catalyst loading is relative to xylose. Yields are based on HPLC analysis.

Conversely, xylose was converted into furfural in 30–40% yield in DMA using CrCl₂ and CrCl₃. With these catalysts, we observed no consistent effect of 1-ethyl-3-

methylimidazolium ([EMIM]) chloride or lithium chloride additives on the furfural yield. Bromide additives such as 1-butyl-3-methylimidazolium ([BMIM]) bromide and lithium bromide improved furfural yields up to 56%. Yields in these reactions are probably reduced by reactions of furfural with itself and with xylose to form oligomeric species.¹⁵⁵ The contrast between furfural yields using acid and chromium catalysts suggests that an alternative mechanism of xylose dehydration may occur in the presence of chromium salts.

6.2.2 Kinetics and Mechanism of Furfural Synthesis from Xylose

To further illuminate the mechanism of this reaction, we examined the initial rates of furfural appearance in DMA–LiCl with CrCl₂ (**Figure 6.2**). These analyses revealed that the rate of furfural formation has a first-order dependence on xylose concentration and a half-order dependence on chromium(II) concentration. These results indicate that chromium is directly involved in the mechanism of conversion prior to the rate-determining step, perhaps in a complex fashion. There appeared to be no correlation with lithium chloride concentration.

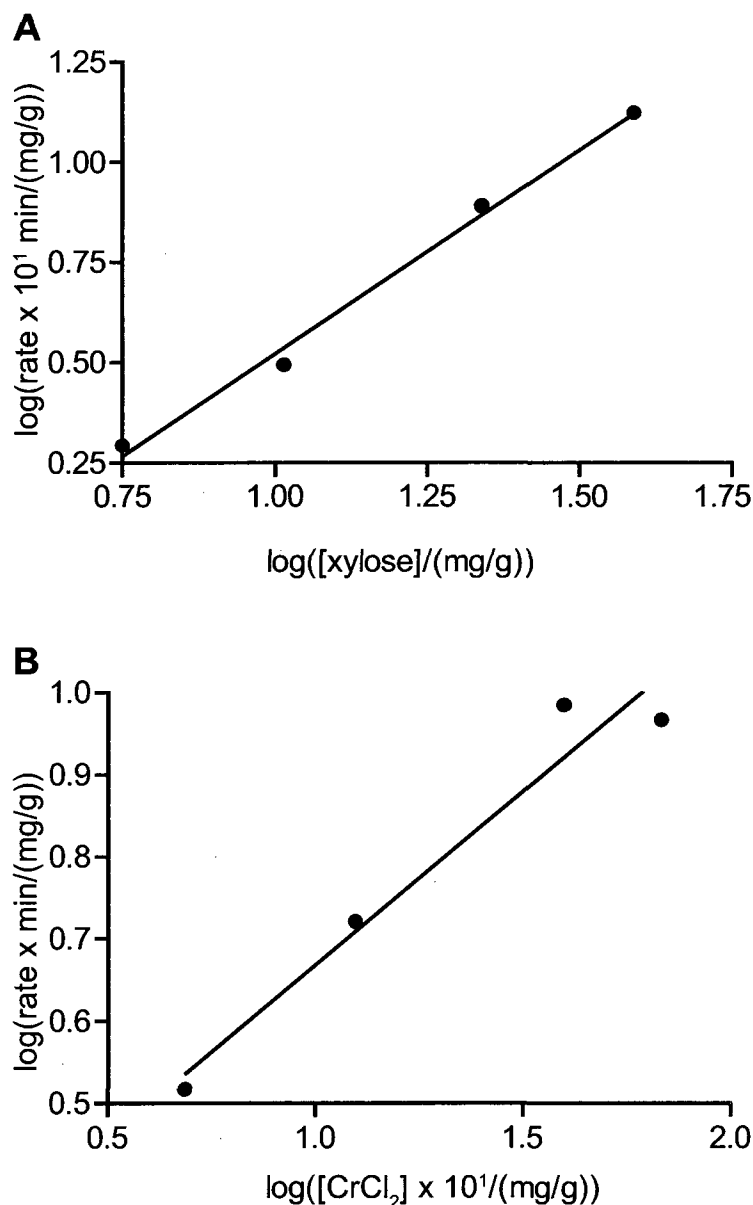


Figure 6.2 Log-log plots of initial rates of furfural formation vs [xylose] (A) and [CrCl₂] (B). (A) Linear regression analysis of the data gives a slope of 1.0, which is consistent with a first-order dependence of the rate of furfural formation on [xylose]. (B) Linear regression analysis of the data gives a slope of 0.4, which is consistent with a half-order dependence of the rate of furfural formation on [CrCl₂].

Based on these results and on the differences between chromium and HCl catalysts, we propose that chromium may effect the transformation of xylose into xylulose to

achieve xylose dehydration at lower temperatures (**Figure 6.3**). In this mechanism, which is analogous to that of chromium-catalyzed conversion of glucose into HMF,^{134,172} chromium catalyzes xylose isomerization through an enediolate intermediate. Acting as a Lewis acid, the chromium salt can convert the resulting xylulose into an oxocarbenium ion. Deprotonation of this species produces an enol, which loses two molecules of water to form furfural. This mechanism is consistent with our observations of carbohydrate reactivity. Aldohexoses likely form HMF through this isomerization mechanism, implying that xylose may do so as well.^{134,172} In addition, xylulose is far more predisposed to form furfural than xylose at 100 °C in water¹⁹³ and in DMA (68% yield vs. 6% yield from xylose after 2 h using 12 mol% HCl), suggesting that transformation of xylose into xylulose would facilitate efficient furfural formation.

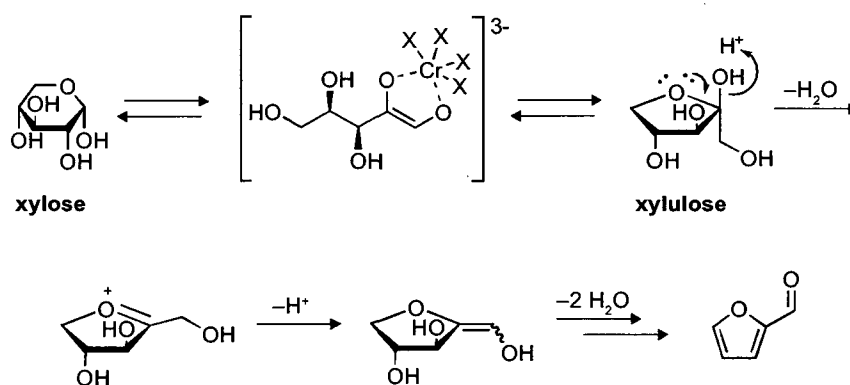


Figure 6.3 Proposed mechanism of chromium-catalyzed dehydration of xylose

6.2.3 Conversion of Xylan into Furfural

Conversion of xylan into furfural was significantly more challenging than dehydration of xylose, probably because of the polymeric nature of this feedstock. Birchwood xylan, the typical material used in these studies, was not readily soluble in

DMA. Instead, it was solubilized by heating and stirring in DMA with LiCl or LiBr at 80–120 °C for several hours. Xylan dissolved in DMA–LiCl precipitated by addition of water, indicating that it was not fully depolymerized into xylose under these conditions. Initially, we attempted conversion of xylan at 100 °C using conditions similar to those used successfully with xylose (Table 6.2). With xylan, however, only trace yields of fufural were obtained. Slightly higher yields were possible from reactions performed at 120 °C (Table 6.3), suggesting that these conditions were too mild to accomplish the depolymerization of xylan into xylose.

Table 6.2 Synthesis of Furfural from Xylan at 100 °C

biomass	solvent	catalyst (mol%)	additives (wt%)	time (h)	molar yield (%)
xylan	DMA–LiCl (10%)	HCl, 3		4	0
xylan	DMA–LiCl (10%)	HCl, 6		4	1
xylan	DMA–LiCl (10%)	HCl, 12		4	0
xylan	DMA–LiCl (10%)	CrCl ₂ , 6	[EMIM]Cl, 5	4	0
xylan	DMA–LiCl (10%)	CrCl ₂ , 6	[EMIM]Cl, 10	4	0
xylan	DMA–LiCl (10%)	CrCl ₂ , 6	[EMIM]Cl, 20	4	0
xylan	DMA–LiCl (10%)	CrCl ₃ , 6	[EMIM]Cl, 5	4	0
xylan	DMA–LiCl (10%)	CrCl ₃ , 6	[EMIM]Cl, 10	4	1
xylan	DMA–LiCl (10%)	CrCl ₃ , 6	[EMIM]Cl, 20	4	0
xylan	DMA–LiCl (10%)	HCl, 3	[EMIM]Cl, 10	4	0
xylan	DMA–LiCl (10%)	HCl, 6	[EMIM]Cl, 10	4	0
xylan	DMA–LiCl (10%)	HCl, 12	[EMIM]Cl, 10	4	1

Xylan was reacted at a concentration of 5 wt% relative to the total mass of the reaction mixture. The solvent composition is indicated by the wt% of LiCl relative to DMA with additive concentrations relative to the mass of the reaction mixture. Catalyst loading and yield are relative to moles of xylose monomers contained in xylan. Yields are based on HPLC analysis.

Table 6.3 Synthesis of Furfural from Xylan at 120 °C

biomass	solvent	catalyst (mol%)	additives (wt%)	time (h)	molar yield (%)
xylan	DMA–LiCl (10%)	CrCl ₂ , 6		4	0
xylan	DMA–LiCl (10%)	CrCl ₃ , 6		4	4
xylan	DMA–LiCl (10%)	CrCl ₂ , 6	[EMIM]Cl, 10	4	0
xylan	DMA–LiCl (10%)	CrCl ₂ , 6	[EMIM]Cl, 20	4	3
xylan	DMA–LiCl (10%)	CrCl ₃ , 6	[EMIM]Cl, 10	4	3
xylan	DMA–LiCl (10%)	CrCl ₃ , 6	[EMIM]Cl, 20	4	0

Xylan was reacted at a concentration of 5 wt% relative to the total mass of the reaction mixture. The solvent composition is indicated by the wt% of LiCl relative to DMA with additive concentrations relative to the mass of the reaction mixture. Catalyst loading and yield are relative to moles of xylose monomers contained in xylan. Yields are based on HPLC analysis.

Table 6.4 Synthesis of Furfural from Xylan at 140 °C

biomass	solvent	catalyst (mol%)	additives (wt%)	time (h)	molar yield (%)
xylan	DMA–LiCl (10%)	CrCl ₂ , 6	[EMIM]Cl, 5	2	8
xylan	DMA–LiCl (10%)	CrCl ₂ , 6	[EMIM]Cl, 10	2	7
xylan	DMA–LiCl (10%)	CrCl ₃ , 6	[EMIM]Cl, 20	2	1
xylan	[EMIM]Cl	CrCl ₂ , 10; HCl, 10		2	18
xylan (oat)	[EMIM]Cl	CrCl ₂ , 10; HCl, 10		2	25
xylan (beech)	[EMIM]Cl	CrCl ₂ , 10; HCl, 10		2	11
corn stover	[EMIM]Cl	CrCl ₂ , 10; HCl, 10		2	22

Xylan was reacted at a concentration of 5 wt% relative to the total mass of the reaction mixture. Birch xylan was used in all cases except where noted. The solvent composition is indicated by the wt% of LiCl relative to DMA with additive concentrations relative to the mass of the reaction mixture. Catalyst loading and yield are relative to moles of xylose monomers contained in xylan. Yield from corn stover is based on xylan content of 22.8%. Yields are based on HPLC analysis.

By increasing the reaction temperature to 140 °C, 7–8% yields of furfural were obtained using CrCl₂, although CrCl₃ was less effective (Table 6.4). Adding HCl to the reaction mixture as a co-catalyst for xylan saccharification and using [EMIM]Cl as the

solvent improved the yield of furfural to 18%. Disparate yields under these conditions were obtained with each xylan sources suggesting significant differences in xylan recalcitrance among biomass sources. These results imply that the depolymerization is a major barrier for chromium-catalyzed furfural production from xylan.

Table 6.5 Synthesis of Furfural from Xylan after HCl Treatment

biomass	solvent	catalyst (mol%)	additives (wt%)	time (h)	molar yield (%)
xylan	DMA	HCl, 25		2	7
xylan	DMA	CrCl ₃ , 6		2	0
xylan	DMA	CrCl ₃ , 6; HCl, 25		2	11
xylan	DMA	HCl, 25	[EMIM]Cl, 5	2	10
xylan	DMA	CrCl ₃ , 6	[EMIM]Cl, 10	2	3
xylan	DMA	CrCl ₃ , 6; HCl, 25	[EMIM]Cl, 20	2	15
xylan	DMA-LiCl (10%)	CrCl ₂ , 6; HCl, 25		2	7
xylan	DMA-LiCl (10%)	CrCl ₃ , 6; HCl, 25		2	4
xylan	DMA-LiCl (10%)	CrCl ₂ , 6; HCl, 25		2	6
xylan	DMA-LiCl (10%)	CrCl ₃ , 6; HCl, 25		2	6
xylan	DMA-LiCl (5%)	CrCl ₂ , 6; HCl, 25		2	6
xylan	DMA-LiCl (5%)	CrCl ₃ , 6; HCl, 25		2	6
xylan	DMA-LiCl (5%)	CrCl ₂ , 6; HCl, 25	[EMIM]Cl, 5	2	8
xylan	DMA-LiCl (5%)	CrCl ₂ , 6; HCl, 25	[EMIM]Cl, 10	2	4
xylan	DMA-LiCl (5%)	CrCl ₃ , 6; HCl, 25	[EMIM]Cl, 5	2	0
xylan	DMA-LiCl (5%)	CrCl ₃ , 6; HCl, 25	[EMIM]Cl, 10	2	8
xylan	DMA	CrCl ₂ , 6; HCl, 25	[BMIM]Br, 20	2	6
xylan	DMA	CrCl ₂ , 6; HCl, 25	LiBr, 10	2	11

Xylan was reacted at a concentration of 5 wt% relative to the total mass of the reaction mixture. The solvent composition is indicated by the wt% of LiCl relative to DMA with additive concentrations relative to the mass of the reaction mixture. Catalyst loading and yield are relative to moles of xylose monomers contained in xylan. Yields are based on HPLC analysis.

We attempted to address this problem by using acid for xylan saccharification prior to furfural synthesis. To do so, we treated xylan with HCl at 140 °C prior to addition of the chromium catalyst and reaction at 120 °C (Table 6.5). This process enabled furfural yields similar to those obtained at 140 °C. Use of HCl during the solubilization step was

essential for furfural production, while HCl alone did not result in yields as high as those obtained with both chromium and HCl. The effects of other additives such as LiCl, LiBr, and ionic liquids were modest. These data suggest that pre-treatment of xylan to form xylose improves furfural yields. We anticipate that improved methods for xylan depolymerization under our reaction conditions would enable improved overall furfural yields at lower temperatures. Using HCl in aqueous–ionic liquid mixtures, we have demonstrated that birchwood xylan can be hydrolyzed in up to 77% yield. A combination of this hydrolysis process with chromium catalysts for mild conversion of xylose into furfural may allow efficient transformation of xylan into furfural.

6.3 Conclusions

Furfural is among the most common industrial chemicals produced today from lignocellulosic biomass and is likely to become even more important as an intermediate for fuel and chemical production with the development of a bio-based economy. We have found that chromium catalysts enable efficient synthesis of furfural from xylose at unusually moderate temperatures in DMA and ionic liquid solvents. Mechanistic studies suggest that this reaction proceeds by an alternative pathway in which chromium catalyzes the isomerization of xylose into xylulose, which is easily dehydrated into furfural. At higher temperatures, chromium and HCl also enable the synthesis of furfural from xylan, albeit in lower yields. Our results provide new means for conversion of pentoses and hemicellulose into valuable chemicals.

6.4 Acknowledgements

This work was supported by the Great Lakes Bioenergy Research Center, a DOE Bioenergy Research Center. J.B.B. was supported by an NSF Graduate Research Fellowship. We are grateful to B. R. Caes for contributive discussions, A. V. Cefali for experimental assistance, and B. E. Dale and B. Venkatesh for corn stover samples.

6.5 Experimental

6.5.1 General Considerations

Commercial chemicals were of reagent grade or better and were used without further purification. Reactions were performed in glass vessels heated in a temperature-controlled oil bath with magnetic stirring.

1-Ethyl-3-methylimidazolium chloride (99.5%, [EMIM]Cl) was from Solvent-Innovation (Cologne, Germany). Birchwood xylan (X0502, 98% xylose residues, ~95% dry solids) and beechwood xylan (X4252, 95% xylose residues, ~95% dry solids) were from Aldrich (Milwaukee, WI). Furfural was from Acros (Buchs, Switzerland). Oat hull xylan (X0011, 70.2% xylose residues, ~95% dry solids) was from TCI (Tokyo, Japan). Milled and sieved corn stover (~95% dry solids) was generously provided by B. E. Dale and co-workers (Michigan State University)¹⁵³ and was passed through a 40 mesh screen prior to use.

6.5.2 Analytic Methods

All reaction products were analyzed by HPLC and quantified using calibration curves generated with commercially-available standards. Following a typical reaction, the

product mixture was diluted with a known mass of deionized water, centrifuged to sediment insoluble products, and analyzed. The concentrations of products were calculated from HPLC-peak integrations and used to calculate molar yields. HPLC was performed with an Agilent 1200 system equipped with refractive index and photodiode array detectors. Furfural was analyzed by ion-exclusion chromatography using a Bio-Rad Aminex[®] HPX-87H column (300 × 7.8 mm; 5 mM H₂SO₄, 0.6 or 0.9 mL/min, 65 °C).

6.5.3 Representative Procedure for Synthesis of Furfural from Xylose

Xylose (25.5 mg, 170 μmol) was mixed with DMA (225 mg) and CrCl₂ (2.5 mg, 20 μmol), and the reaction mixture was stirred at 100 °C for 4 h. For reactions of xylose using [EMIM]Cl, chromium salts were mixed with a portion of the ionic liquid (25 mg) before addition to the reaction mixture.

6.5.4 Representative Procedures for Synthesis of Furfural from Xylan

Xylan (10.2 mg, 72 μmol) and concd HCl (1.6 μL, 19 μmol) were stirred in DMA (240 mg) at 140 °C for 2 h. Following addition of CrCl₃ (1 mg, 6 μmol), the reaction mixture was stirred at 120 °C for 2 h.

In an alternative procedure, xylan (6.0 mg, 43.5 μmol) and [EMIM]Cl (266.9 mg) were stirred at 85 °C for 24 h. Following addition of HCl (0.33 μL, 4 μmol) and CrCl₂ (0.8 mg, 6.5 μmol), the reaction mixture was stirred at 140 °C for 2 h.

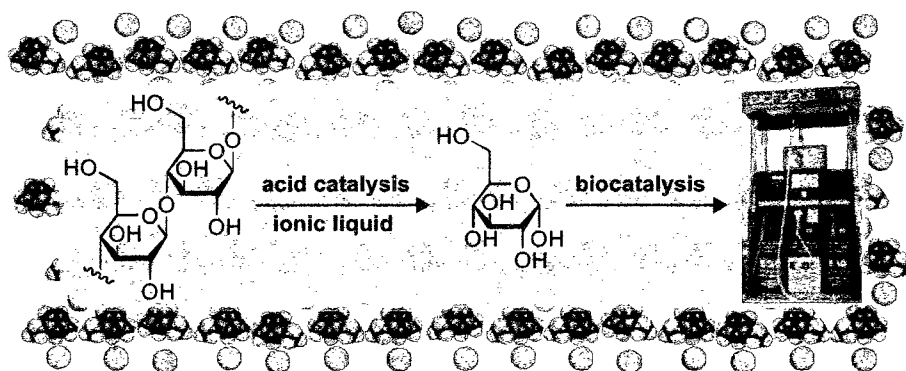
6.5.5 Kinetic Analysis of Furfural Formation from Xylose

Xylose (250.7 mg, 1.67 mmol) and LiCl (227.8 mg) were added to DMA (2.0427 g) and dissolved at 100 °C for 5 min. Five known weights of this stock solution (approx. 0.4 g) were combined with CrCl₂ (five different weights from 0 mg/g to 15 mg/g). The solutions were heated at 100 °C for 10 min and cooled rapidly on ice prior to HPLC analysis.

CHAPTER 7*

SUGARS FROM BIOMASS IN IONIC LIQUIDS

Abstract: Abundant plant biomass could become a sustainable source of fuels and chemicals. Unlocking this potential requires the economical conversion of recalcitrant lignocellulose into useful intermediates, such as sugars. We report a high-yielding process for the chemical hydrolysis of lignocellulose into monosaccharides. Adding water gradually to a chloride ionic liquid containing catalytic acid leads to a nearly 90% yield of glucose from cellulose and 70–80% yield of sugars from untreated corn stover. Ion-exclusion chromatography allows recovery of the ionic liquid and delivers sugar feedstocks that support the vigorous growth of ethanologenic microbes. Hence, a simple chemical process enables crude biomass to be the sole source of carbon for a scalable biorefinery.



* This chapter has been submitted for publication, in part, under the same title.

Reference: Binder, J. B.; Raines, R. T. *Nature Chemistry* **2009**.

7.1 Introduction

As the primary components of lignocellulosic biomass, the sugar polymers cellulose and hemicellulose are among the most abundant organic compounds on earth and have the potential to be renewable sources for energy and chemicals. The estimated global annual production of biomass is 1×10^{11} tons, sequestering 2×10^{21} J.^{126,194} For comparison, annual petroleum production amounts to 2×10^{20} J, while the technically recoverable endowment of conventional crude oil is 2×10^{22} J.¹²⁶ Hence, in only one decade, Earth's plants can renew in the form of cellulose, hemicellulose, and lignin all of the energy stored as conventional crude oil. The challenge for chemists is to access these polymers and convert them into fuels and building blocks for civilization.

Sugars are natural intermediates in the biological and chemical conversion of lignocellulosic biomass^{174,195,196,129,197,198}, but access to sugars is hindered by the recalcitrance of plant cell walls^{174,199}. The majority of glucose in lignocellulose is locked into highly crystalline cellulose polymers. Hemicellulose—a branched polymer of glucose, xylose, and other sugars—and lignin—a complex aromatic polymer—encase the cellulose, fortifying and protecting the plant. Deriving sugars from this heterogeneous feedstock requires both physical and chemical disruption. Enzymatic methods of saccharification are the most common, and use physical and chemical pretreatment processes²⁰⁰ followed by hydrolysis with cellulases to produce sugars. The proper combination of pretreatment and enzymes for a given feedstock enables high yields of sugars from both hemicellulose and cellulose components²⁰¹. Nonetheless, the costs of both pretreatment and enzymes (estimated to be as much as one-third of the cost of

ethanol production from cellulose¹⁶³) and low rates of hydrolysis are potential drawbacks to enzymatic hydrolysis.

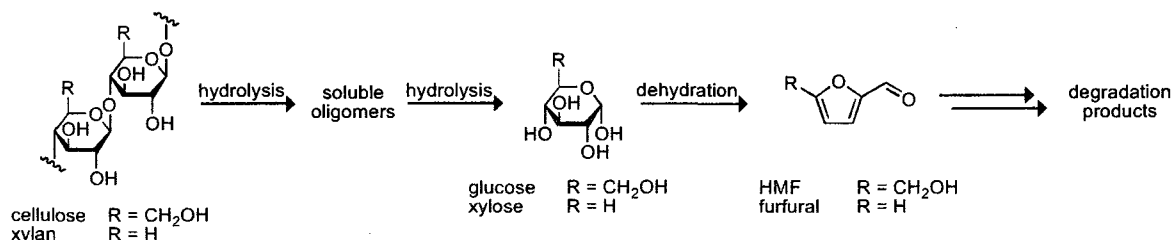


Figure 7.1 Hydrolysis reactions of cellulose and xylan. Chemical hydrolysis of cellulose and hemicellulose into monomeric sugars proceeds through oligomers and is accompanied by side reactions that form furans and other degradation products.

Exclusively chemical technologies for biomass hydrolysis have also been developed. As early as 1819, Braconnot demonstrated that linen dissolved in concentrated H₂SO₄, diluted with water, and heated was transformed into a fermentable sugar^{202,203}. As in this example, concentrated acid can play a dual role in biomass hydrolysis. By disrupting its network of intra- and interchain hydrogen bonds, strong acids decrystallize cellulose and make it accessible to reagents²⁰⁴; and by catalyzing the hydrolysis of glycosidic bonds, strong acids cleave cellulose and hemicellulose into sugars (**Figure 7.1**)¹⁷⁴. Bergius took advantage of these attributes of HCl in the development of a commercial process that operated in Germany from 1935 to 1948^{205,206}. In the United States, several related processes using H₂SO₄ have been developed, typically with 80–90% conversion of cellulose and hemicellulose into sugars^{207–211}. In a recent example, Cuzens and Farone used concentrated aqueous H₂SO₄ to hydrolyze agricultural residues via the Arkenol process²¹², which is being commercialized by BlueFire Ethanol. In this method, biomass is decrystallized with 77% H₂SO₄, diluted to a water content of about 40 wt%, and

hydrolyzed at 100 °C. This first stage hydrolyzes nearly all of the hemicellulose and some of the cellulose. The solid residue is then subjected to a second-stage hydrolysis to release the remaining glucose. Concentrated acid hydrolysis methods produce high sugar yields, use simple catalysts, and require only short reaction times. Despite these advantages, the hazards of handling concentrated acids and the complexities of recycling them have limited the adoption of this technology.

Less hazardous and more tractable cellulose solvents would facilitate lignocellulose hydrolysis. Ionic liquids, salts with melting points near or below ambient temperature, show promise as cellulose solvents for nonwoven fiber production²¹³ and chemical derivatization^{214,142}. Like concentrated acids, ionic liquids comprised of chloride, acetate, and other moderately basic anions disrupt the hydrogen bond network of cellulose and enable its dissolution^{173,214,142}. Recognizing these properties, Zhao and coworkers attempted to hydrolyze cellulose in 1-butyl-3-methylimidazolium chloride ([BMIM]Cl)²¹⁵. Using 11 wt% H₂SO₄ and 1.75 equiv of water relative to the glucose monomer units of the cellulose (about 1 wt% of the reaction mixture), they obtained a 43% molar yield of glucose after 9 h at 100 °C. They also reported a 77% yield of total reducing sugars (TRS) based on a 3,5-dinitrosalicylic acid (DNS) assay, but did not discuss what sugars other than glucose (which is the expected cellulose hydrolysis product) comprised TRS. Zhao and coworkers also reacted biomass materials such as corn stover and rice straw under similar conditions, obtaining TRS yields of 66–81% but not reporting glucose yields²¹⁶. Most likely, glucose yields from lignocellulose were no higher than those obtained with purified cellulose. Several reports from other researchers

have followed those of Zhao and coworkers. Schüth and coworkers used solid acid catalysts to depolymerize cellulose in [BMIM]Cl, obtaining mainly water-insoluble oligomers rather than glucose²¹⁷. Recently, Jones and coworkers hydrolyzed pine wood in [BMIM]Cl under low-water conditions, obtaining molar yields of monosaccharides that were typically <20%²¹⁸. Seddon and coworkers studied the reactivity of cellobiose in 1-ethyl-3-methylimidazolium chloride ([EMIM]Cl) and then applied their optimized conditions to pure cellulose and *Miscanthus* grass, obtaining 50% and 30% glucose yields, respectively^{219,220}.

These low glucose yields obtained in ionic liquids contrast with the nearly quantitative yields of glucose attainable from cellulose in concentrated acids and other cellulose solvents²²¹. Noting that these highly efficient hydrolyses employ much higher water concentrations than the Zhao process (Arkenol's 40% *versus* 1%), we reasoned that water could play an important role in delivering high glucose yields. Our investigation of the reactivity of glucose and cellulose in mixtures of an ionic liquid and water confirmed this hypothesis and enabled a high-yielding process for the hydrolysis of cellulose and lignocellulosic biomass. Moreover, this process generates easily recovered sugars that are superb feedstocks for microbial growth and biocatalytic ethanol production.

7.2 Results

7.2.1 Reaction of Glucose and Cellulose in [EMIM]Cl

Seeking a more effective hydrolysis process, we first investigated the fundamental reactivity of cellulose and sugars under acidic conditions in ionic liquids. To understand the results of Zhao and coworkers, we began by reacting cellulose under similar

conditions²¹⁵ with H_2SO_4 and HCl in $[\text{EMIM}]\text{Cl}$. Interestingly, we observed the production of 5-hydroxymethylfurfural (HMF) as well as moderate yields of glucose (Table 7.1). The aldehyde functionality of this sugar dehydration product interferes with the DNS assay used by Zhao and coworkers²²², and likely caused their TRS yields to be far higher than their actual sugar yields. The production of HMF at the expense of glucose suggested that either cellulose was being transformed directly into HMF or glucose from hydrolysis was being dehydrated to form HMF. To examine these alternatives, we reacted glucose in $[\text{EMIM}]\text{Cl}$ with varying water content (**Figure 7.2** and Table 7.2). In the absence of both acid and water, glucose was recovered unchanged. On the other hand, H_2SO_4 caused rapid glucose decay into HMF and other products in ionic liquid with little or no added water. Increasing the water content to 33 wt% decreased the rate of glucose disappearance so that nearly 90% of glucose remained after 1 h. These results suggest that glucose produced by cellulose hydrolysis degrades rapidly under non-aqueous conditions in $[\text{EMIM}]\text{Cl}$ but that high water concentrations prevent glucose loss.

Table 7.1 Hydrolysis of Cellulose in [EMIM]Cl

cellulose (wt %)	HCl (wt %)	water content (wt %)						time (h)	glucose yield (%)	HMF yield (%)
		0'	5'	10'	20'	30'	60'			
5	20 ^a	5	5	5	5	5	5	1	40	19
5	20	5	5	5	5	5	5	1	45	17
5	20	5	33	33	33	33	33	1	14	n.d.
								2	29	n.d.
5	20	5	5	20	20	20	20	1	31	n.d.
								2	64	19
								3	51	25
								4	36	30
5	20	5	5	20	20	33	33	1	40	n.d.
								2	84	7
								3	81	10
								4	77	8
5	20	5	5	20	25	33	33	1	44	n.d.
								2	86	7
								3	83	10
								4	77	13
5	20	5	5	20	25	33	43	1	38	n.d.
								2	85	5
								3	87	6
								4	89	7
10	10	5	5	20	25	33	43	3	71	n.d.

Cellulose was reacted in [EMIM]Cl at 105°C after dissolving at 105°C for 12 h. HCl loading is relative to cellulose weight. Yields are molar yields based on HPLC analysis and are relative to the glucose monomers contained in the cellulose. ^a H₂SO₄.

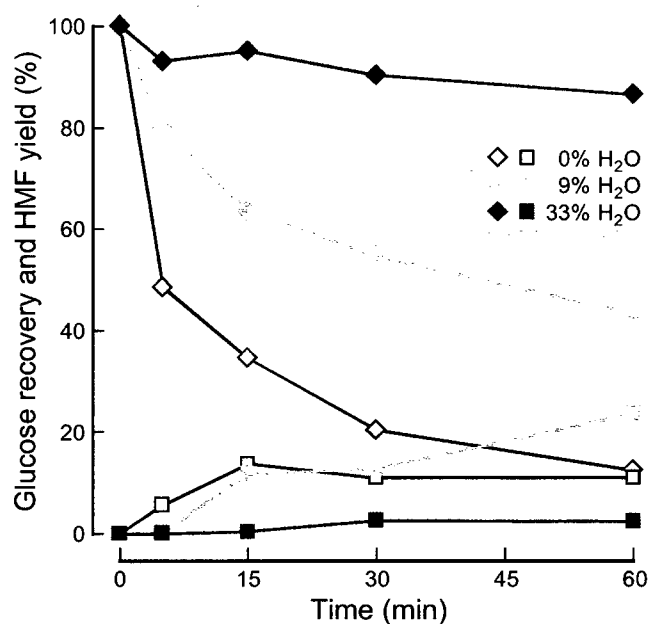


Figure 7.2 Acid-catalyzed degradation of glucose in [EMIM]Cl. In acidic [EMIM]Cl, glucose (diamonds) disappears rapidly at 100°C, forming HMF (squares) and other degradation products. Increased water content slows glucose loss. Reaction conditions: Glucose, 10 wt%; H₂SO₄, 4 wt% relative to glucose.

Table 7.2 Acid-Catalyzed Degradation of Glucose in [EMIM]Cl

H ₂ O (wt %)	time (min)	glucose recovery (%)	HMF yield (%)
0 ^a	0	100	0
	5	100	0
	15	97	0
	30	103	0
	60	101	0
0	0	100	0
	5	49	6
	15	35	14
	30	20	11
	60	13	11
9	0	100	0
	5	80	0
	15	63	12
	30	55	13
	60	43	24
20	0	100	0
	5	92	4
	15	82	2
	30	76	5
	60	65	11
33	0	100	0
	5	93	0
	15	95	0
	30	90	3
	60	87	2

Glucose was reacted in [EMIM]Cl at 100 °C with an initial concentration of 10 wt% and a H₂SO₄ loading of 4 wt % relative to glucose. The water content is relative to the total mass of the reaction mixture. Glucose recovery is based on HPLC analysis and is normalized to the initial glucose concentration. HMF molar yield is based on HPLC analysis. ^aNo H₂SO₄.

Accordingly, we expected that increasing the water concentration in the [EMIM]Cl hydrolysis mixture would enhance glucose yields from cellulose. Yet, water precipitates cellulose from ionic liquids¹⁷³. We observed that a 5 wt% solution of cellulose in [EMIM]Cl formed an intractable gel when the solution was diluted to achieve 10 wt% water, making homogeneous hydrolysis of cellulose in aqueous–ionic liquid solutions impossible. Instead, we attempted to balance cellulose solubility and glucose stability by

adding water *gradually* during hydrolysis, expecting that cellulose solubility would increase as the reaction progresses. For these experiments, we chose to use HCl so as to match the acid anion with that of the ionic liquid. [EMIM]Cl containing 5 wt% cellulose was first treated with HCl and a small amount of water at 105 °C to allow hydrolysis of the cellulose into shorter, more soluble segments (Table 7.1). After a delay, additional water was added to stabilize the glucose product.

The timing of water addition was critical for high glucose yields. When the reaction mixture was diluted to 33% water after 5 min, cellulose precipitated, resulting in low yields. Delaying dilution until after 10 min prevented cellulose precipitation, and gradually increasing the water content to 43% within 60 min allowed glucose yields of nearly 90% in 2–4 h. These yields are nearly twice as high as the previous best in ionic liquids and approach those achieved through enzymatic hydrolysis. We also examined the effect of the time for dissolution of cellulose in the ionic liquid prior to hydrolysis, finding that 6 h was optimal (Table 7.3). Longer times probably led to increased byproduct formation^{223,224}, which was indicated by discoloration of the reaction mixture, whereas shorter times were insufficient for complete solvation of the cellulose. With this optimized procedure, more concentrated cellulose solutions (10 wt%) could be hydrolyzed in high yields. Tiny cellulose fibers visible in these reaction mixtures suggest that glucose yields were slightly lower due to incomplete cellulose breakdown prior to water addition. It is likely that cellulose is converted into a mixture of glucose and soluble oligomers within the first 30–60 min of reaction, and that these oligomers hydrolyze subsequently into glucose. Monitoring glucose and cellobiose (a glucose

dimer) concentrations during hydrolysis revealed that cellobiose concentrations peaked at 1 h and decayed as glucose concentrations increased (**Figure 7.3**).

Table 7.3 Effect of Dissolution Time on Hydrolysis of Cellulose

dissolution time (h)	HCl (wt%)	water content (wt%)					time (h)	glucose yield (%)	HMF yield (%)
		0'	10'	20'	30'	60'			
3	20	5	20	25	33	43	2	86	3
							3	90	5
							4	92	7
6	20	5	20	25	33	43	2	89	4
							3	93	6
							4	92	8
9	20	5	20	25	33	43	2	83	4
							3	86	5
							4	87	7

Cellulose was reacted in [EMIM]Cl at 105 °C with an initial concentration of 5 wt%. HCl loading is relative to cellulose mass. Yields are molar yields based on HPLC analysis and are relative to the glucose monomers contained in the cellulose.

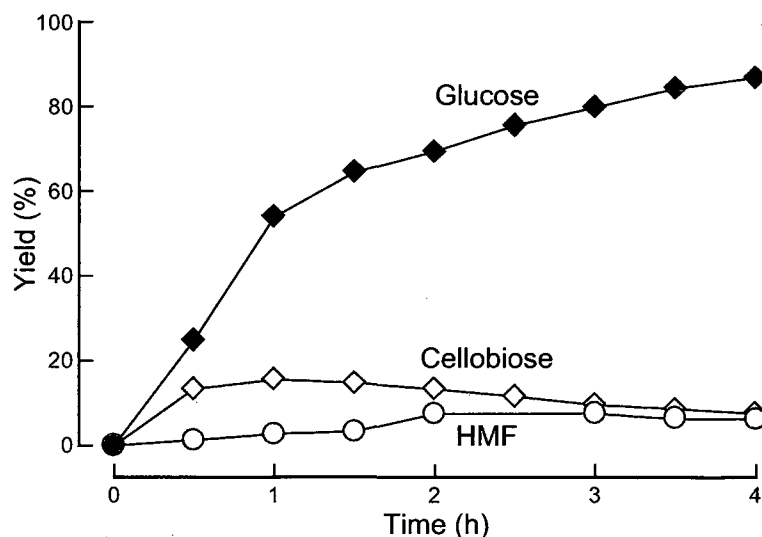


Figure 7.3 Glucose, HMF, and cellobiose production during cellulose hydrolysis in [EMIM]Cl. Glucose concentrations increase over four hours as cellulose oligomers, such as cellobiose, hydrolyze. Cellulose was reacted under standard optimized reaction conditions.

7.2.2 Hydrolysis of Cellulose in Alternative Ionic Liquids

Alternative ionic liquids were investigated as solvents for hydrolysis under conditions optimized with [EMIM]Cl (Table 7.4). Ionic liquids that did not dissolve cellulose produced poor glucose yields. [EMIM]NO₃ and [EMIM]BF₄ failed to swell cellulose, and no glucose production was detected with these solvents. The bromide and triflate counterparts of these ionic liquids did swell cellulose, resulting in 4–5% glucose yields. On the other hand, the ionic liquids 1,3-dimethylimidazolium dimethylphosphate and [EMIM]OAc are excellent solvents for cellulose²²⁴. Upon addition of 20 wt% water, the cellulose in the dimethylphosphate ionic liquid formed a viscous gel, and analysis of the reaction mixture revealed no glucose. Although cellulose remained dissolved in [EMIM]OAc under the reaction conditions, no glucose was produced in this solvent as well. The HCl hydrolysis catalyst in each of these solvents is buffered by dimethylphosphate and acetate, forming conjugate acids with pK_a values of 1.29 and 4.76, respectively^{225,226}. These acids are probably too weak to accomplish cellulose hydrolysis under the reaction conditions²²⁰. In contrast to other ionic liquids, chloride-containing ionic liquids such as [BMIM]Cl, 1-butyl-4-methylpyridinium chloride, and 1-ethylpyridinium chloride both dissolved cellulose and supported hydrolysis with unoptimized glucose yields ranging from 66–73%. These results suggest that ionic liquid media for cellulose hydrolysis must balance both cellulose solubility and hydrolytic activity. Chloride alone achieves this goal through its strong interactions with cellulose coupled with its weak basicity.

Table 7.4 Hydrolysis of Cellulose in Ionic Liquids

ionic liquid	cellulose concentration (wt%)	glucose yield (%)
[EMIM]OAc	2	0
[EMIM]OAc	5	0
[EMIM]NO ₃	2	0
1,3-dimethylimidazolium dimethylphosphate	2	0
1,3-dimethylimidazolium dimethylphosphate	5	0
[EMIM]Br	2	4
[BMIM]BF ₄	2	0
[EMIM]OTf	2	5
[BMIM]Cl	5	66
1-butyl-4-methylpyridinium chloride	5	73
1-ethylpyridinium chloride	5	69
1-ethyl-2,3-dimethylimidazolium chloride	5	46

Cellulose was reacted in ionic liquid for 3 h at 105°C after mixing at 105°C for 6 h. HCl loading was 20 wt% relative to cellulose weight. The water content of the reaction began at 5 wt% and was increased as follows: 20% (10 min), 25% (20 min), 33% (30 min), 43% (60 min). Yields are molar yields based on HPLC analysis and are relative to the glucose monomers contained in the cellulose.

7.2.3 Hydrolysis of Lignocellulosic Biomass

Complex and heterogeneous, lignocellulosic biomass presents a more significant challenge for hydrolysis than does cellulose. In addition to intractable crystalline cellulose, lignocellulosic biomass such as corn stover includes protective hemicellulose and lignin, heterogeneous components that are major obstacles to many biomass hydrolysis processes^{174,199}. Nevertheless, chloride ionic liquids are excellent solvents for lignocellulosic biomass, suggesting that they would easily disrupt these polymeric barriers. Moreover, preliminary experiments demonstrated that xylan, a hemicellulose, was easily hydrolyzed under our conditions to produce xylose in 77% yield. Consequently, we found that our robust process for cellulose hydrolysis was easily extended to the hydrolysis of corn stover in two stages (Table 7.5). In the first stage,

untreated corn stover that had been mixed with [EMIM]Cl was hydrolyzed with 10 wt% HCl at 105 °C with the same water-dilution process used for pure cellulose. This process produced a 71% yield of xylose and 42% yield of glucose based on the xylan and cellulose content of the stover. Dilution of the reaction mixture to 70% water caused precipitation of unhydrolyzed polysaccharides and lignin. These residues were then dissolved in [EMIM]Cl and subjected to an identical second-stage hydrolysis, which released additional xylose and glucose, leaving behind lignin-containing solids. Combined, these two steps resulted in a 79% xylose yield and 70% glucose yield using only simple chemical reagents. Given the well-documented versatility of ionic liquids as biomass solvents, we anticipate that this process will be amenable to other biomass sources, such as wood and grasses.

Table 7.5 Hydrolysis of Corn Stover in [EMIM]Cl

stover (wt%)	stage	HCl (wt%)	water content (wt%)						time (h)	glucose yield (%)	xylose yield (%)
			0'	5'	10'	20'	30'	60'			
5	1	20	5	5	20	25	33	43	2.5	42	71
	2	20	5	5	20	25	33	43	3.0	28	8
	overall									70	79
10	1	10	5	5	20	25	33	43	3.5	19	74
	2	10	5	5	20	25	33	43	3.0	47	1
	overall									66	75
10	1	10	5	5	20	25	33	43	1.0	17	60
	1								1.5	21	73
	1								2.0	25	80
	1								2.5	27	82
	2	10	5	5	20	25	33	43	1.5	37	5
	2								2.0	42	5
	2								2.5	44	5
	2								3.0	48	5

Corn stover was reacted in [EMIM]Cl at 105 °C after its dissolution at 105 °C for 6 h. HCl loading is relative to stover weight. Yields are molar yields based on HPLC analysis and are relative to the glucose and xylose monomers contained in the stover.

7.2.4 Recovery and Fermentation of Hydrolyzate Sugars

A practical biomass hydrolysis process requires efficient means for sugar and reagent recovery. We found that ion-exclusion chromatography enables separation of the sugars and ionic liquid from the corn stover hydrolysis reaction mixture. In this technique, a mixture containing electrolyte and non-electrolyte solutes is separated by passing it through a charged resin²²⁷. Charged species, such as the ionic liquid, are excluded from the resin, while non-electrolytes, such as sugars, are retained. Passing the corn stover hydrolyzate through a column of [EMIM]-exchanged Dowex[®] 50 resin allowed laboratory-scale separation of the ionic liquid solvent from the sugars, with >95% recovery of the ionic liquid, 88% recovery of xylose, and 94% recovery of glucose. These yields are probably limited by the small scale of our demonstration separation and would be improved upon scale-up. Notably, very efficient ionic liquid recycling is possible, and the ionic liquid is not chemically incorporated into the biomass residue. This point is crucial to the economics of any process employing expensive ionic liquids.

To support bioconversion, biomass hydrolyzate sugars must be free of contaminants that inhibit microbial growth and fermentation. We found that sugars derived from corn stover through our process are excellent feedstocks for an ethanologenic bacterium and yeast. Whereas wild-type *Escherichia coli* ferments a range of sugars into a mixture of ethanol and organic acids, the engineered KO11 strain produces ethanol selectively²²⁸. Serving as the sole carbon source, a glucose-xylose-arabinose mixture from corn stover enabled aerobic growth of *E. coli* KO11 at a rate comparable to that of a control glucose-xylose mixture (**Figure 7.4A**). Moreover, under oxygen-deficient conditions, *E. coli*

KO11 produced a $79 \pm 4\%$ yield of ethanol from stover hydrolyzate sugars and a $76 \pm 3\%$ yield from pure xylose and glucose, demonstrating that sugars from our hydrolysis process can be readily converted into ethanol.

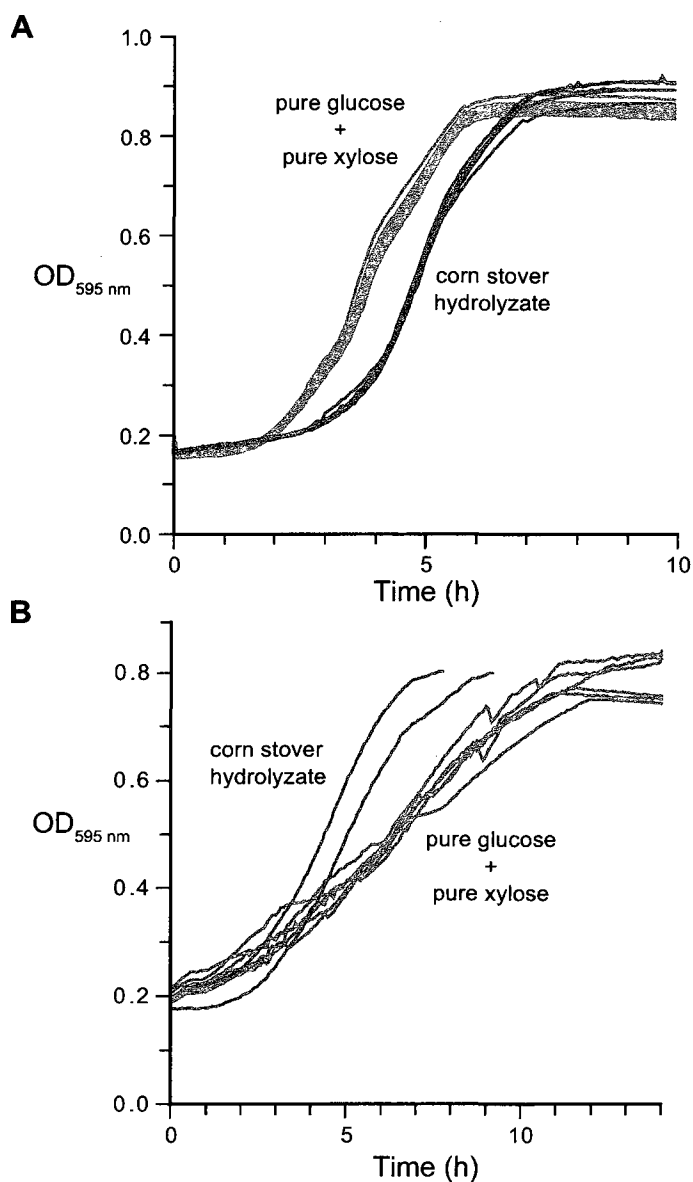


Figure 7.4 Aerobic growth of ethanologenic microbes on corn stover hydrolyzate sugars. The bacterium *Escherichia coli* (A) and yeast *Pichia stipitis* (B) grow rapidly on corn stover hydrolyzate sugars as their sole carbon source. On hydrolyzate, the mean doubling time for *E. coli* was 2.77 h; on pure sugars the doubling time was 2.95 h.

Engineered bacteria show promise for biofuel production, but yeast fermentation predominates today^{229,230}. *Pichia stipitis*, which has an innate ability to ferment xylose, is a yeast candidate for bioconversion of lignocellulose-derived sugars²³¹⁻²³³. Corn stover hydrolyzate sugars are an excellent carbon source for the growth of this yeast (**Figure 7.4B**), and *P. stipitis* efficiently converts hydrolyzate into ethanol. Fermenting xylose and glucose, the yeasts produced a $70 \pm 2\%$ yield of ethanol from hydrolyzate and a $72 \pm 1\%$ yield from pure sugars.

7.3 Discussion

We have demonstrated an efficient system for polysaccharide hydrolysis as well as means to separate and ferment the resulting sugars. By balancing cellulose solubility and reactivity with water, we produce sugars from lignocellulosic biomass in yields that are several times higher than those achieved previously in ionic liquids and approach those of enzymatic hydrolysis. Furthermore, the hydrolyzate products are readily converted into ethanol by microorganisms. Together, our results comprise an integrated process for chemical hydrolysis of biomass for biofuel production (Figure 4). First, lignocellulosic biomass such as corn stover is decrystallized through mixing with [EMIM]Cl. With their defense against chemical assault breached by the ionic liquid, the hemicellulose and cellulose are hydrolyzed by treatment with HCl and water. The residual lignin and cellulose solids are subjected to a second hydrolysis, while the liquid hydrolyzate is separated through ion-exclusion chromatography. Ionic liquid recovered in the ion exclusion step is stripped of water and recycled, while hydrolyzate sugars are fermented into fuels and other bioproducts.

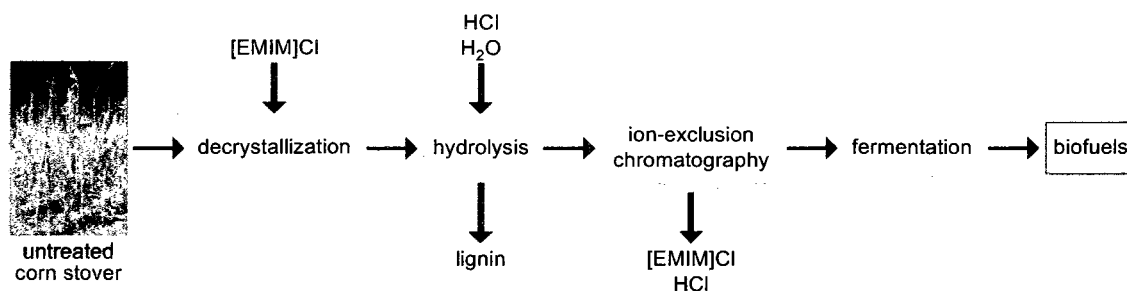


Figure 7.5 Integrated process for biofuel production using ionic liquid biomass hydrolysis. Ionic liquids solvents enable efficient biomass decrystallization and hydrolysis. Ion-exclusion chromatography separates the ionic liquids for recycling and the hydrolyzate sugars for fermentation. (Photograph courtesy of Department of Energy/National Renewable Energy Laboratory.)

In comparison to extant enzymatic and chemical approaches to biomass hydrolysis, this ionic liquid system has many attractive features. Like concentrated acid processes, it uses inexpensive chemical catalysts rather than enzymes and avoids an independent pretreatment step. Working in concert, [EMIM]Cl and HCl produce high sugar yields in hours at just 105 °C, whereas enzymatic hydrolysis can take days¹⁶³ and many pretreatment methods require temperatures of 160–200 °C²⁰⁰. Also, lignocellulose solubilization by the ionic liquid allows processing at high concentrations, which can be a problem in enzymatic hydrolysis. On the other hand, this ionic liquid process improves on typical acid hydrolysis methods by avoiding the use of hazardous concentrated acid. Using catalytic amounts of dilute acid removes the complexity and danger of recycling large volumes of concentrated acid. The ionic liquid used in its place is likely to be far easier to handle. Despite these differences, the ionic liquid process is similar to commercial processes using concentrated acid hydrolysis^{205,212}. Consequently, it can exploit proven engineering and equipment for facile scale-up.

Our chemical hydrolysis method offers flexibility for an integrated biomass conversion process. Because the ionic liquid solvent makes biomass polysaccharides readily accessible for chemical reactions, this process is likely to be compatible with a broad range of biomass feedstocks. Downstream, the sugars produced by ionic liquid hydrolysis are flexible feedstocks for production of a nearly infinite range of fuels and chemicals. *E. coli*, which readily use the hydrolyzate sugars, have been engineered to produce not only fuel ethanol but also 1-butanol, 2-butanol, branched alcohols, fatty acids, isoprenoids, and even hydrogen²³⁴⁻²³⁶. Furthermore, the aqueous stream of sugars can also be converted by catalytic processes into fuels²³⁷ or chemical intermediates. In contrast with enzymatic hydrolysis reactions that often require coupling to fermentation (simultaneous saccharification and fermentation) to prevent product inhibition, this chemical process can be paired with any downstream conversion. Finally, the lignin recovered from ionic liquid biomass hydrolysis could be a valuable coproduct. Jones and coworkers noted that the lignin residue from biomass hydrolysis in ionic liquids is relatively unmodified, suggesting that it could be an excellent feedstock for high-value lignin products^{238,218}. As a result, our process, which uses simple chemical reagents to overcome biomass recalcitrance and liberate valuable sugars, has the potential to unpin a versatile biorefinery.

7.4 Acknowledgements

This work was supported by the Great Lakes Bioenergy Research Center, a DOE Bioenergy Research Center. J.B.B. was supported by an NSF Graduate Research Fellowship. We are grateful to J. E. Holladay for helpful conversations on biomass

chemistry in ionic liquids, B. R. Caes and S. B. delCardayré for contributive discussions, J. J. Blank and A. V. Cefali for experimental assistance, B. E. Dale and B. Venkatesh for corn stover samples, W. D. Marner, G. N. Phillips, and T. J. Rutkoski for assistance with bacterial growth studies, and T.W. Jeffries and T.M. Long for assistance with yeast fermentation.

7.5 Experimental Section

7.5.1 General Considerations

Commercial chemicals were of reagent grade or better and were used without further purification. Reactions were performed in glass vessels heated in a temperature-controlled oil bath with magnetic stirring. The term “concentrated under reduced pressure” refers to the removal of water and other volatile materials using a Speed Vac concentrator system. Conductivity was measured with an Extech Instruments ExStik II conductivity meter. NMR spectra were acquired with a Bruker DMX-400 Avance spectrometer (^1H , 400 MHz; ^{13}C , 100.6 MHz) at the National Magnetic Resonance Facility at Madison (NMRFAM).

1-Ethyl-3-methylimidazolium chloride (99.5%, [EMIM]Cl) was from Solvent-Innovation (Cologne, Germany). 1-Ethyl-3-methylimidazolium tetrafluoroborate (97%, [EMIM]BF₄), 5-hydroxymethylfurfural, birchwood xylan (X0502, 98% xylose residues, ~95% dry solids) and Dowex® 50WX4 (200-400 mesh, H⁺ form) were from Aldrich (Milwaukee, WI). 1-Ethyl-3-methylimidazolium triflate (98.5%, [EMIM]OTf), 1-butyl-3-methylpyridinium chloride (97%, [BMPy]Cl), and 1-ethyl-3-methylimidazolium bromide (97%, [EMIM]Br) were from Fluka (Geel, Belgium). 1-Ethylpyridinium chloride (98%,

[EtPy]Cl), 1-ethyl-2,3-dimethylimidazolium chloride (98%, [MMEIM]Cl), and furfural were from Acros (Buchs, Switzerland). Cellulose (medium cotton linters, C6288, ~95% dry solids) was from Sigma (St. Louis, MO). Milled and sieved corn stover (~95% dry solids) was generously provided by B. E. Dale and co-workers (Michigan State University)¹⁵³ and was passed through a 40 mesh screen prior to use.

7.5.2 Analytical Methods

All reaction products were analyzed by HPLC and quantified with calibration curves generated from commercially available standards. Following a typical reaction, the product mixture was diluted with a known mass of deionized water, centrifuged or filtered to remove insoluble products, and analyzed. The concentrations of products were calculated from HPLC-peak integrations and used to calculate molar yields. HPLC was performed with an Agilent 1200 system equipped with refractive index and photodiode array detectors as well as a Bio-Rad Aminex HPX-87H column (300 × 7.8 mm; 5 mM H₂SO₄, 0.6 mL/min, 65 °C).

7.5.3 Representative Procedure for Hydrolysis of Cellulose

Cellulose (18.7 mg, 104 μmol glucose units) and [EMIM]Cl (380. mg) were mixed at 105 °C for 6 h to form a viscous solution. To this cellulose solution was added aqueous HCl (1.66 M, 23.2 μL, equivalent to 3.8 mg concd HCl), and the reaction mixture was vigorously stirred at 105 °C. During this time, the viscosity of the solution decreased dramatically. After 10 min, deionized water (80 μL) was added with stirring, followed by an additional 40 μL water at 20 min, 60 μL water at 30 min, and 100 μL water at 60 min.

After 3 h total reaction time, the solution was diluted with water (701 μL), centrifuged to sediment insoluble materials, and analyzed by HPLC (12.4 mg/g glucose, 88% yield; 0.34 mg/g HMF, 3% yield). In other cases, aliquots of the reaction mixture were removed periodically for HPLC analysis.

Reactions utilizing ionic liquids with melting points greater than 105 °C (1-butyl-4-methylpyridinium chloride, 1-ethylpyridinium chloride, 1-ethyl-2,3-dimethylimidazolium chloride) required slightly different handling. In these cases the ionic liquid and cellulose were heated together using a heat gun until dissolution of the cellulose was achieved. Then, the mixture was heated at 105 °C for 6 h prior to the hydrolysis reaction. While the 1-ethylpyridinium chloride solution remained liquid at this temperature, the other cellulose solutions solidified. Before addition of HCl, these solids were melted with a heat gun, and they remained liquid after the addition of aqueous HCl.

7.5.4 Representative Reaction of Glucose in [EMIM]Cl

Glucose (47.2 mg, 262 μmol) was dissolved in [EMIM]Cl (460 mg) and deionized water (50 μL). Conc'd H_2SO_4 (5.5 μL) was added, and the resulting solution was stirred at 100 °C. Aliquots of the reaction mixture were removed periodically for HPLC analysis.

7.5.5 Hydrolysis of Xylan

Xylan (9.4 mg, 66 μmol xylose units) and [EMIM]Cl (188 mg) were mixed at 105 °C for several hours to form a viscous solution. To this solution was added aqueous HCl (1.66 M, 11 μL), and the reaction mixture was vigorously stirred at 105 °C. After 10 min, deionized water (40 μL) was added with stirring, followed by an additional 20 μL water

at 20 min, 30 μL water at 30 min, 50 μL water at 60 min, and 50 μL water at 90 min.

After 3 h total reaction time, the solution was diluted with water (100 μL), centrifuged to sediment insoluble materials, and analyzed by HPLC (15.3 mg/g xylose, 77% yield).

7.5.6 Representative Procedure for Hydrolysis of Corn Stover.

Corn stover (26.7 mg, 54 μmol glucose units, 44 μmol xylose units) and [EMIM]Cl (502 mg) were mixed at 105 $^{\circ}\text{C}$ for 6 h. To this mixture was added aqueous HCl (1.66 M, 29 μL , equivalent to 5 mg concd HCl), and the reaction mixture was vigorously stirred at 105 $^{\circ}\text{C}$. After 10 min, deionized water (100 μL) was added with stirring, followed by an additional 50 μL water at 20 min, 75 μL water at 30 min, and 125 μL water at 60 min. After 2.5 h total reaction time, the solution was diluted with water (750 μL) and centrifuged to sediment insoluble materials. The solids were rinsed twice with water (200 μL) and dried. The liquid products (2.046 g) were analyzed by HPLC (2.0 mg/g glucose, 42% yield; 2.3 mg/g xylose, 71% yield).

The brown solids from the first hydrolysis were then heated with [EMIM]Cl (306 mg) at 105 $^{\circ}\text{C}$ for 4.5 h. To this mixture was added aqueous HCl (1.66 M, 14.5 μL , equivalent to 2.5 mg concd HCl), and the reaction mixture was vigorously stirred at 105 $^{\circ}\text{C}$. After 10 min, deionized water (50 μL) was added with stirring, followed by an additional 25 μL water at 20 min, 67.5 μL water at 30 min, and 70 μL water at 60 min. After 3 h total reaction time, the solution was diluted with water (300 μL) and centrifuged to sediment insoluble materials. The liquid products (770 mg) were analyzed by HPLC (3.56 mg/g glucose, 28% yield; 0.7 mg/g xylose, 8% yield). For the two-step process, the overall yield of glucose was 70% and the overall yield of xylose was 79%.

In other cases, aliquots of the reaction mixture were removed periodically for HPLC analysis.

7.5.7 Representative Procedure for Recovery of Sugars and [EMIM]Cl from Hydrolyzates

Dowex® 50WX4 (75 g, 0.128 eq) in a slurry with deionized water was placed in a jacketed column (120 cm x 1 cm, Kontes # 420870-1200) maintained at 65 °C, resulting in a resin bed approximately 100 cm in length. The resin was exchanged with [EMIM]⁺ by passing [EMIM]Cl (64 g, 0.44 mol) in water through the column. At the end of the exchange procedure, the column effluent was neutral, signifying complete exchange of H⁺ for [EMIM]⁺. Degassed, deionized water was then passed through the column to elute any solutes.

Hydrolyzate liquids (2.741 g, 8.5 mg glucose, 17.7 mg xylose, ~60% water) were obtained from the hydrolysis reaction of corn stover (102.3 mg) using [EMIM]Cl (1046 mg) under standard conditions. The solid residue from the reaction was reserved for a second hydrolysis reaction. A portion of the first hydrolysis liquids (2.591 g) was loaded on the top of the resin column and eluted with degassed, deionized water at a rate of 3 cm/min. Fractions were collected and analyzed by HPLC (7.5 mg glucose, 94%; 14.3 mg xylose, 86%). The fractions containing [EMIM]Cl were concentrated under reduced pressure, mixed with D₂O, and pooled, resulting in a D₂O/[EMIM]Cl solution (3.673 g). An aliquot (342.8 mg) of this solution was combined with *N,N*-dimethylacetamide (71.5 mg, 0.821 mmol), and the resulting solution was analyzed by ¹H NMR spectroscopy.

Integration of the spectra revealed a 0.708:1 molar ratio of [EMIM]Cl:DMA, indicating [EMIM]Cl recovery of 913 mg (92%).

The above process was repeated with the hydrolyzate liquids (1.684 g) from the reaction of the solid residue using [EMIM]Cl (471 mg). After chromatography of a portion of the liquids (1.534 g), the ionic liquid-containing fractions were concentrated under reduced pressure, mixed with D₂O, and pooled, resulting in a D₂O/[EMIM]Cl solution (3.261 g). An aliquot (528.4 mg) of this solution was combined with *N,N*-dimethylacetamide (79.6 mg, 0.914 mmol), and the resulting solution was analyzed by ¹H NMR spectroscopy. Integration of the spectra revealed a 0.532:1 molar ratio of [EMIM]Cl:DMA, indicating [EMIM]Cl recovery of 440 mg (103%). The combined [EMIM]Cl recovery from the two-step process was 96%.

Sugar-containing fractions from the separation process which were free of [EMIM]Cl were pooled and lyophilized to a brown residue. This residue was dissolved in deionized water (5 mL) and used for microbial growth and fermentation studies.

7.5.8 Bacterial Growth Studies

Escherichia coli KO11 was a gift from W.D. Marner and coworkers. In all cases *E. coli* were grown at 37 °C in media containing 40 mg/L chloramphenicol. A single colony was inoculated into 4 mL LB medium²³⁹ containing 0.4 wt % xylose. After incubation in a culture tube agitated at 250 rpm for 18 h, the cells were centrifuged and resuspended in 2 mL M9 minimal medium²³⁹ free of any carbon source.

In a polystyrene 96-well plate, 20 wells were prepared with M9 minimal medium (150 µL) containing 2.62 g/L xylose and 1.38 g/L glucose. 10 wells were prepared with

M9 minimal medium (150 μ L) supplemented with corn stover hydrolyzate sugars (2.62 g/L xylose, 1.38 g/L glucose, and 0.91 g/L arabinose). The remaining wells were filled with deionized water (200 μ L). Each well was inoculated with the above cell suspension (5 μ L), and the plate was capped with a low-evaporation lid and incubated with rapid agitation in a BioTek ELx808 Absorbance Microplate Reader. The OD_{595 nm} of each well was measured every 5 min for 25 h. Doubling times for each well were calculated from a fit of the OD measurements to a modified Gompertz function²⁴⁰.

7.5.9 Bacterial Fermentation Studies

To maintain a low-oxygen environment, fermentation with *E. coli* was performed in a glass test tube (13 mm x 100 mm) fitted with a rubber stopper which was pierced with a steel cannula. The other end of the cannula was immersed in water in a second glass test tube. The second test tube was fitted with a rubber stopper pierced with a needle for gas escape.

A single colony was inoculated into 4 mL LB medium containing 0.26 wt % xylose and 0.14 wt % glucose. After incubation in a culture tube agitated at 250 rpm for 11 h, the cells were centrifuged and resuspended in 4 mL LB medium. This cell suspension (10 μ L) was added to test tubes equipped for anaerobic growth containing LB medium (1.5 mL) supplemented with either 2.62 g/L xylose and 1.38 g/L glucose or corn stover hydrolyzate sugars (2.62 g/L xylose, 1.38 g/L glucose, and 0.91 g/L arabinose). Each medium was tested in triplicate. Following a purge with N₂(g), fermentation was performed with agitation at 250 rpm, and after 12 h the cultures were analyzed by HPLC for sugars and ethanol. In all cases the sugars were completely consumed. The ethanol

titer was compared to a theoretical yield of 0.51 g ethanol/g sugar (2.04 g/L for pure sugars or 2.25 g/L for corn stover hydrolyzate).

7.5.10 Yeast Growth Studies

Pichia stipitis CBS 6054 was a gift from T.W. Jeffries and coworkers. In all cases *Pichia* were grown at 30 °C. A single colony was inoculated into 6 mL in YP medium (10 g/L yeast extract and 20 g/L peptone) containing 1.2 wt % xylose and 0.8 wt % glucose. After incubation in a culture tube agitated at 225 rpm for 11 h, a 1 mL portion of the culture was centrifuged. The cells were resuspended in 500 μ L of synthetic minimal medium containing 6.7 g/L yeast nitrogen base without amino acids (Difco).

In a polystyrene 96-well plate, 10 wells were prepared with synthetic minimal medium (150 μ L) containing 1.82 g/L xylose, 2.18 g/L glucose, and 0.33 g/L arabinose. 5 wells were prepared with synthetic minimal medium (150 μ L) supplemented with corn stover hydrolyzate sugars (1.82 g/L xylose, 2.18 g/L glucose, and 0.33 g/L arabinose). The remaining wells were filled with deionized water (150 μ L). Each well was inoculated with the above cell suspension (10 μ L), and the plate was capped with a low-evaporation lid and incubated with rapid agitation in a BioTek ELx808 Absorbance Microplate Reader. The OD_{595 nm} of each well was measured every 5 min for 19 h.

7.5.11 Yeast Fermentation Studies

For fermentation experiments, *Pichia* were grown at 30 °C in YP medium (10 g/L yeast extract and 20 g/L peptone) containing the appropriate carbon source. A single colony was inoculated into 6 mL of medium containing 1.2 wt % xylose and 0.8 wt %

glucose. After incubation in a culture tube agitated at 225 rpm for 11 h, the yeast suspension was added to glass test tubes containing YP medium (1.5 mL) supplemented with either 3.24 g/L xylose, 3.88 g/L glucose, and 0.58 g/L arabinose or corn stover hydrolyzate sugars (3.24 g/L xylose, 3.88 g/L glucose, and 0.58 g/L arabinose). The sugar medium was tested in triplicate and the hydrolyzate medium, in duplicate. The test tubes were fitted with rubber stoppers pierced with needles and agitated at 150 rpm. After 52 h the cultures were analyzed by HPLC for sugars and ethanol. In all cases the sugars were completely consumed. The ethanol titer was compared to a theoretical yield of 0.51 g ethanol/g of glucose and xylose (3.63 g/L for pure sugars or 3.63 g/L for corn stover hydrolyzate).

CHAPTER 8***FUTURE DIRECTIONS**

Abstract: Rich possibilities exist for the extension of the catalytic chemistry illustrated in this dissertation. The olefin metathesis strategies described herein are poised for biological applications, while the biomass chemistry presents many opportunities for future mechanistic exploration and practical development.

8.1 Aqueous Olefin Metathesis

The olefin metathesis chemistry described in this dissertation, particularly the adaptation of conventional catalysts to aqueous media, offers opportunities for biological applications. Small molecules such as alkene-containing natural products (quinine hydrochloride) or peptides may be selectively modified in aqueous media. Moreover, olefin metathesis may be used as an orthogonal method to address alkenes incorporated into proteins either during protein synthesis²⁴¹⁻²⁴³ or by chemical modification of residues such as cysteine. This approach can enable protein labeling as well as more complex modifications. Cross metathesis between two proteins could produce protein dimers with enhanced functions. For example, the enzyme ribonuclease A (RNase A) selectively kills cancer cells if it is able to evade inhibitor proteins. One method for creating these cancer-killing proteins is to connect two ribonuclease molecules at the inhibitor-binding interface.^{244,245} Olefin metathesis on alkene-substituted RNase A might be used to create therapeutic inhibitor-evasive variants stitched together with strong carbon-carbon bonds.

Applications of aqueous olefin metathesis would also be aided by catalysts with enhanced water-tolerance. Though impressive, current aqueous olefin metathesis catalysts are much less effective than catalysts used in organic solvents. Investigations of the reaction mechanism, improved design of ligands, and even metathesis catalysis with alternative metals might allow high-performance olefin metathesis in water.

8.2 Transformation of Renewable Resources into Furan Intermediates

The chromium-catalyzed and halide-assisted transformation of sugars into furans is relatively unexplored. Chapters Four, Five, and Six described some initial mechanistic

investigations, including the influence of sugar, halide, and chromium concentrations on the rate of the reaction and the subtle effects of sugar structure. More extensive kinetic studies on glucose, xylose, mannose, and galactose would complement these. In addition, kinetic isotope effect analyses might illuminate the roles of proton transfer in the mechanisms of furan formation. While it is clear that chromium ions play an essential part in the conversion of aldoses into HMF, the redox state of the chromium is not known. Chromium(II) is known to catalyze ligand exchange of chromium(III),²⁴⁶ and the dissolution of chromium(III) under the reaction conditions suggests that some chromium(II) is present. On the other hand, chromium(II) can easily air-oxidize to chromium(III) under the reaction conditions used. Accordingly, either or both of the oxidation states may be relevant regardless of the initial oxidation state of the chromium ions. Related studies implicate chromium(III) complexes in carbohydrate transformations.^{247,248} In the future, EPR studies and careful control of the redox environment during reactions may elucidate the chromium species involved.

Greater knowledge of the reaction mechanism might inform future catalyst development. Although chromium ions are excellent catalysts for the isomerization of aldoses into ketoses in HMF synthesis, they have toxicity and recovery problems. Discovery of alternative catalysts would make this technology more practical. Additionally, yields of HMF from cellulose and furfural from xylan, though promising, are still low. Further investigation of these reactions and catalyst development might result in improved processes.

8.3 Processing of Lignocellulosic Biomass

The technologies described in this dissertation for direct conversion of lignocellulosic biomass into chemical intermediates and sugars rely on solvents that dissolve cellulose such as DMA–LiCl and chloride-containing ionic liquids. The same chloride ions which enable cellulose processing in these solvents also can cause corrosion and impair solvent recovery,²¹³ making them unattractive for industrial processes. Indeed, DMA–LiCl has not been used commercially since its discovery 28 years ago, in part because no practical means of recycling it has been invented.²⁴⁹⁻²⁵² Because ionic liquids are single-component cellulose solvents, their recycling may be simpler but is still likely to require costly removal of water from recovered aqueous–ionic liquid solutions. In addition, the chromatography used to recover sugars produced by biomass hydrolysis in ionic liquids is likely to be expensive. As polar, non-volatile compounds, current ionic liquid solvents have physical properties similar to those of sugars, making their separation difficult.

Novel cellulose solvents might overcome these challenges. Volatile yet tractable cellulose solvents would offer revolutionary advantages for biomass processing. For instance, HCl has been used industrially for the chemical hydrolysis of biomass, and can be recovered by vacuum distillation and spray drying of the hydrolyzate.²⁰⁵ A non-toxic and non-corrosive analog might be separated in the same fashion with far less expense. Switchable solvents, recently popularized by Eckert, Liotta, and Jessop, might be one answer.²⁵³⁻²⁶⁰ Properties of these solvent systems, such as polarity or volatility, may be altered dramatically by an external force, such as a change in pressure. A highly polar

cellulose solvent which could be switched to a nonpolar or volatile form might enable simple product and solvent recovery for biomass processing. Unfortunately, known switchable media do not dissolve cellulose, and many are not chemically inert. An alternative approach might be to design new ionic liquids with properties which are more favorable for physical separation from biomass transformation products.

8.4 Conclusions

As the foregoing discussion demonstrates, numerous opportunities exist for future exploration in the field of this dissertation, particularly in biomass chemistry. The transformation of renewable resources to supply the needs of human civilization has been a goal of chemistry for centuries. As Emil Fischer noted, “cellulose . . . is best hydrolysed by strong sulphuric acid and yields the reputed wood sugar which, it is not infrequently claimed in popular lectures, would one day solve the subsistence problem.”²⁶¹ Creative application of modern organic chemistry to these challenges will realize this dream.

REFERENCES

- (1) *Handbook of Metathesis*; Grubbs, R. H., Ed.; Wiley-VCH: Weinheim, Germany, 2003.
- (2) Metathesis reactions in total synthesis. Nicolaou, K. C.; Bulger, P. G.; Sarlah, D. *Angewandte Chemie, International Edition* **2005**, *44*, 4490-4527.
- (3) Multiple metal-carbon bonds for catalytic metathesis reactions (Nobel lecture). Schrock, R. R. *Angewandte Chemie, International Edition* **2006**, *45*, 3748-3759.
- (4) Olefin-metathesis catalysts for the preparation of molecules and materials (Nobel lecture). Grubbs, R. H. *Angewandte Chemie, International Edition* **2006**, *45*, 3760-3765.
- (5) Evolution and applications of second-generation ruthenium olefin metathesis catalysts. Schrodi, Y.; Pederson, R. L. *Aldrichimica Acta* **2007**, *40*, 45-52.
- (6) The remarkable metal-catalysed olefin metathesis reaction. Hoveyda, A. H.; Zhugralin, A. R. *Nature (London, United Kingdom)* **2007**, *450*, 243-251.
- (7) Chemistry in living systems. Prescher, J. A.; Bertozzi, C. R. *Nature Chemical Biology* **2005**, *1*, 13-21.

- (8) Simple synthesis of sex pheromones of the housefly and tiger moths by transition metal-catalyzed olefin cross-metathesis reactions. Rossi, R. *Chimica e l'Industria (Milan, Italy)* **1975**, 57, 242-243.
- (9) Synthesis of insect pheromones using metathesis catalysts. Kuepper, F. W.; Streck, R. *Chemiker-Zeitung* **1975**, 99, 464-465.
- (10) Synthesis of cell agglutination inhibitors by aqueous ring-opening metathesis polymerization. Mortell, K. H.; Gingras, M.; Kiessling, L. L. *Journal of the American Chemical Society* **1994**, 116, 12053-12054.
- (11) Bioactive polymers. Kiessling, L. L.; Strong, L. E. *Topics in Organometallic Chemistry* **1998**, 1, 199-231.
- (12) Romping the cellular landscape: Linear scaffolds for molecular recognition. Lee, Y.; Sampson, N. S. *Curr. Opin. Struct. Biol.* **2006**, 16, 544-550.
- (13) Activating B cell signaling with defined multivalent ligands. Puffer, E. B.; Pontrello, J. K.; Hollenbeck, J. J.; Kink, J. A.; Kiessling, L. L. *ACS Chem. Biol.* **2007**, 2, 252-262.

- (14) Single-step synthesis of cell-permeable protein dimerizers that activate signal transduction and gene expression. Diver, S. T.; Schreiber, S. L. *Journal of the American Chemical Society* **1997**, *119*, 5106-5109.

- (15) Synthesis of the Pro-Gly dipeptide alkene isostere using olefin cross-metathesis. Vasbinder, M. M.; Miller, S. J. *Journal of Organic Chemistry* **2002**, *67*, 6240-6242.

- (16) Peptide bond isosteres: Ester or (*E*)-alkene in the backbone of the collagen triple helix. Jenkins, C. L.; Vasbinder, M. M.; Miller, S. J.; Raines, R. T. *Organic Letters* **2005**, *7*, 2619-2622.

- (17) Alkene- and alkyne-bridged mimics of nisin as potential peptide-based antibiotics. Ghalit, N.; Rijkers, D. T. S.; Liskamp, R. M. J. *Journal of Molecular Catalysis A: Chemical* **2006**, *254*, 68-77.

- (18) Synthesis of bicyclic alkene-/alkane-bridged nisin mimics by ring-closing metathesis and their biochemical evaluation as lipid II binders: Toward the design of potential novel antibiotics. Ghalit, N.; Reichwein, J. F.; Hilbers, H. W.; Breukink, E.; Rijkers, D. T. S.; Liskamp, R. M. J. *ChemBioChem* **2007**, *8*, 1540-1554.

- (19) Synthesis of biologically active dicarba analogues of the peptide hormone oxytocin using ring-closing metathesis. Stymiest, J. L.; Mitchell, B. F.; Wong, S.; Vederas, J. C. *Organic Letters* **2003**, *5*, 47-49.
- (20) Synthesis of oxytocin analogues with replacement of sulfur by carbon gives potent antagonists with increased stability. Stymiest, J. L.; Mitchell, B. F.; Wong, S.; Vederas, J. C. *Journal of Organic Chemistry* **2005**, *70*, 7799-7809.
- (21) Highly efficient synthesis of covalently cross-linked peptide helices by ring-closing metathesis. Blackwell, H. E.; Grubbs, R. H. *Angewandte Chemie, International Edition* **1998**, *37*, 3281-3284.
- (22) Contemporary strategies for the stabilization of peptides in the α -helical conformation. Henchey, L. K.; Jochim, A. L.; Arora, P. S. *Current Opinion in Chemical Biology* **2008**, *12*, 692-697.
- (23) Harnessing helices. Drahl, C. *Chemical and Engineering News* **2008**, *86*, 18-23.
- (24) Catalytic organometallic chemistry in water: The aqueous ring-opening metathesis polymerization of 7-oxanorbornene derivatives. Novak, B. M.; Grubbs, R. H. *Journal of the American Chemical Society* **1988**, *110*, 7542-7543.

- (25) Synthesis of water-soluble, aliphatic phosphines and their application to well-defined ruthenium olefin metathesis catalysts. Mohr, B.; Lynn, D. M.; Grubbs, R. H. *Organometallics* **1996**, *15*, 4317-4325.
- (26) Ring-closing metathesis in methanol and water. Kirkland, T. A.; Lynn, D. M.; Grubbs, R. H. *Journal of Organic Chemistry* **1998**, *63*, 9904-9909.
- (27) Water-soluble ruthenium alkylidenes: Synthesis, characterization, and application to olefin metathesis polymerization in protic solvents. Lynn, D. M.; Mohr, B.; Grubbs, R. H.; Henling, L. M.; Day, M. W. *Journal of the American Chemical Society* **2000**, *122*, 6601-6609.
- (28) Benzyldiene-functionalized ruthenium-based olefin metathesis catalysts for ring-opening metathesis polymerization in organic and aqueous media. Roberts, A. N.; Cochran, A. C.; Rankin, D. A.; Lowe, A. B.; Schanz, H.-J. *Organometallics* **2007**, *26*, 6515-6518.
- (29) Highly active ruthenium catalysts for olefin metathesis: The synergy of *N*-heterocyclic carbenes and coordinatively labile ligands. Weskamp, T.; Kohl, F. J.; Hieringer, W.; Gleich, D.; Herrmann, W. A. *Angewandte Chemie, International Edition* **1999**, *38*, 2416-2419.

- (30) Olefin metathesis-active ruthenium complexes bearing a nucleophilic carbene ligand. Huang, J.; Stevens, E. D.; Nolan, S. P.; Petersen, J. L. *Journal of the American Chemical Society* **1999**, *121*, 2674-2678.

- (31) Increased ring closing metathesis activity of ruthenium-based olefin metathesis catalysts coordinated with imidazolin-2-ylidene ligands. Scholl, M.; Trnka, T. M.; Morgan, J. P.; Grubbs, R. H. *Tetrahedron Letters* **1999**, *40*, 2247-2250.

- (32) A recyclable Ru-based metathesis catalyst. Kingsbury, J. S.; Harrity, J. P. A.; Bonitatebus, P. J., Jr.; Hoveyda, A. H. *Journal of the American Chemical Society* **1999**, *121*, 791-799.

- (33) Efficient and recyclable monomeric and dendritic Ru-based metathesis catalysts. Garber, S. B.; Kingsbury, J. S.; Gray, B. L.; Hoveyda, A. H. *Journal of the American Chemical Society* **2000**, *122*, 8168-8179.

- (34) Unexpected results of a turnover number (TON) study utilizing ruthenium-based olefin metathesis catalysts. Maechling, S.; Zaja, M.; Blechert, S. *Advanced Synthesis & Catalysis* **2005**, *347*, 1413-1422.

- (35) Decomposition of ruthenium olefin metathesis catalysts. Hong, S. H.; Wenzel, A. G.; Salguero, T. T.; Day, M. W.; Grubbs, R. H. *Journal of the American Chemical Society* **2007**, *129*, 7961-7968.

- (36) A solid-supported phosphine-free ruthenium alkylidene for olefin metathesis in methanol and water. Cannon, S. J.; Blechert, S. *Bioorganic & Medicinal Chemistry Letters* **2002**, *12*, 1873-1876.
- (37) A neutral, water-soluble olefin metathesis catalyst based on an *N*-heterocyclic carbene ligand. Gallivan, J. P.; Jordan, J. P.; Grubbs, R. H. *Tetrahedron Letters* **2005**, *46*, 2577-2580.
- (38) Highly active water-soluble olefin metathesis catalyst. Hong, S. H.; Grubbs, R. H. *Journal of the American Chemical Society* **2006**, *128*, 3508-3509.
- (39) Amphiphilic ruthenium benzyldiene metathesis catalyst with PEG-substituted pyridine ligands. Breitenkamp, K.; Emrick, T. *Journal of Polymer Science, Part A: Polymer Chemistry* **2005**, *43*, 5715-5721.
- (40) A synthesis of PEG- and phosphorylcholine-substituted pyridines to afford water-soluble ruthenium benzyldiene metathesis catalysts. Samanta, D.; Kratz, K.; Zhang, X.; Emrick, T. *Macromolecules* **2008**, *41*, 530-532.
- (41) Salicylaldimine ruthenium alkylidene complexes: Metathesis catalysts tuned for protic solvents. Binder, J. B.; Guzei, I. A.; Raines, R. T. *Advanced Synthesis & Catalysis* **2007**, *349*, 395-404.

- (42) Small-molecule *N*-heterocyclic-carbene-containing olefin-metathesis catalysts for use in water. Jordan, J. P.; Grubbs, R. H. *Angewandte Chemie, International Edition* **2007**, *46*, 5152-5155.
- (43) A green catalyst for green chemistry: Synthesis and application of an olefin metathesis catalyst bearing a quaternary ammonium group. Michrowska, A.; Gulajski, L.; Kaczmarska, Z.; Mennecke, K.; Kirschning, A.; Grela, K. *Green Chemistry* **2006**, *8*, 685-688.
- (44) Activated pyridinium-tagged ruthenium complexes as efficient catalysts for ring-closing metathesis. Rix, D.; Clavier, H.; Coutard, Y.; Gulajski, L.; Grela, K.; Mauduit, M. *Journal of Organometallic Chemistry* **2006**, *691*, 5397-5405.
- (45) Highly recoverable pyridinium-tagged Hoveyda-Grubbs pre-catalyst for olefin metathesis. Design of the boomerang ligand toward the optimal compromise between activity and reusability. Rix, D.; Caijo, F.; Laurent, I.; Gulajski, L.; Grela, K.; Mauduit, M. *Chemical Communications (Cambridge, United Kingdom)* **2007**, 3771-3773.
- (46) A highly active aqueous olefin metathesis catalyst bearing a quaternary ammonium group. Gulajski, L.; Michrowska, A.; Naroznik, J.; Kaczmarska, Z.; Rupnicki, L.; Grela, K. *ChemSusChem* **2008**, *1*, 103-109.

- (47) Practical olefin metathesis in protic media under an air atmosphere. Connon, S. J.; Rivard, M.; Zaja, M.; Blechert, S. *Advanced Synthesis & Catalysis* **2003**, *345*, 572-575.
- (48) Olefin metathesis in homogeneous aqueous media catalyzed by conventional ruthenium catalysts. Binder, J. B.; Blank, J. J.; Raines, R. T. *Organic Letters* **2007**, *9*, 4885-4888.
- (49) Allyl sulfides are privileged substrates in aqueous cross-metathesis: Application to site-selective protein modification. Lin, Y. A.; Chalker, J. M.; Floyd, N.; Bernardes, G. J. L.; Davis, B. G. *Journal of the American Chemical Society* **2008**, *130*, 9642-9643.
- (50) Facile conversion of cysteine and alkyl cysteines to dehydroalanine on protein surfaces: Versatile and switchable access to functionalized proteins. Bernardes, G. J. L.; Chalker, J. M.; Errey, J. C.; Davis, B. G. *Journal of the American Chemical Society* **2008**, *130*, 5052-5053.
- (51) Olefin metathesis for chemical biology. Binder, J. B.; Raines, R. T. *Current Opinion in Chemical Biology* **2008**, *12*, 767-773.
- (52) Development of aqueous metathesis catalysts. Zaman, S.; Curnow, O. J.; Abell, A. D. *Australian Journal of Chemistry* **2009**, *62*, 91-100.

- (53) Aqueous olefin metathesis. Burtscher, D.; Grela, K. *Angewandte Chemie-International Edition* **2009**, *48*, 442-454.
- (54) Synthesis and applications of $\text{RuCl}_2(\text{:CHR})(\text{PR}_3)_2$: The influence of the alkylidene moiety on metathesis activity. Schwab, P.; Grubbs, R. H.; Ziller, J. W. *Journal of the American Chemical Society* **1996**, *118*, 100-110.
- (55) Synthesis and activity of a new generation of ruthenium-based olefin metathesis catalysts coordinated with 1,3-dimesityl-4,5-dihydroimidazol-2-ylidene ligands. Scholl, M.; Ding, S.; Lee, C. W.; Grubbs, R. H. *Organic Letters* **1999**, *1*, 953-956.
- (56) Advanced fine-tuning of Grubbs/Hoveyda olefin metathesis catalysts: A further step toward an optimum balance between antinomic properties. Bieniek, M.; Bujok, R.; Cabaj, M.; Lugan, N.; Lavigne, G.; Arlt, D.; Grela, K. *Journal of the American Chemical Society* **2006**, *128*, 13652-13653.
- (57) Application of ring-closing metathesis to the synthesis of rigidified amino acids and peptides. Miller, S. J.; Blackwell, H. E.; Grubbs, R. H. *Journal of the American Chemical Society* **1996**, *118*, 9606-9614.
- (58) Olefin metathesis in glycobiology: New routes towards diverse neoglycoconjugates. Leeuwenburgh, M. A.; van der Marel, G. A.; Overkleeft, H. *S. Current Opinion in Chemical Biology* **2003**, *7*, 757-765.

- (59) Metathesis reactions. General considerations. Van de Weghe, P.; Eustache, J.; Cossy, J. *Current Topics in Medicinal Chemistry (Sharjah, United Arab Emirates)* **2005**, 5, 1461-1472.
- (60) Recent applications of olefin ring-closing metathesis (RCM) in the synthesis of biologically important alkaloids, terpenoids, polyketides and other secondary metabolites. Gaich, T.; Mulzer, J. *Current Topics in Medicinal Chemistry (Sharjah, United Arab Emirates)* **2005**, 5, 1473-1494.
- (61) The application of olefin metathesis to the synthesis of biologically active macrocyclic agents. Van de Weghe, P.; Eustache, J. *Current Topics in Medicinal Chemistry (Sharjah, United Arab Emirates)* **2005**, 5, 1495-1519.
- (62) Ring closing metathesis in the synthesis of biologically interesting peptidomimetics, sugars and alkaloids. Martin, W. H. C.; Blechert, S. *Current Topics in Medicinal Chemistry (Sharjah, United Arab Emirates)* **2005**, 5, 1521-1540.
- (63) Olefin metathesis route to antiviral nucleosides. Agrofoglio, L. A.; Nolan, S. P. *Current Topics in Medicinal Chemistry (Sharjah, United Arab Emirates)* **2005**, 5, 1541-1558.

- (64) Application of olefin cross-metathesis to the synthesis of biologically active natural products. Prunet, J. *Current Topics in Medicinal Chemistry (Sharjah, United Arab Emirates)* **2005**, 5, 1559-1577.
- (65) Economic and ecological aspects in applied olefin metathesis. Streck, R. *Journal of Molecular Catalysis* **1992**, 76, 359-372.
- (66) Olefin metathesis in the ionic liquid 1-butyl-3-methylimidazolium hexafluorophosphate using a recyclable Ru catalyst: Remarkable effect of a designer ionic tag. Yao, Q.; Zhang, Y. *Angewandte Chemie, International Edition* **2003**, 42, 3395-3398.
- (67) *Aqueous-Phase Organometallic Catalysis*; 2nd ed.; Cornils, B.; Herrmann, W. A., Eds.; Wiley-VCH: Weinheim, Germany, 2004.
- (68) Rational design and convenient synthesis of a novel family of ruthenium complexes with *O,N*-bidentate ligands. Drozdak, R.; Ledoux, N.; Allaert, B.; Dragutan, I.; Dragutan, V.; Verpoort, F. *Central European Journal of Chemistry* **2005**, 3, 404-416.
- (69) Synthesis of Schiff base-ruthenium complexes and their applications in catalytic processes. Drozdak, R.; Allaert, B.; Ledoux, N.; Dragutan, I.; Dragutan, V.; Verpoort, F. *Advanced Synthesis & Catalysis* **2005**, 347, 1721-1743.

- (70) Ruthenium complexes bearing bidentate Schiff base ligands as efficient catalysts for organic and polymer syntheses. Drozdak, R.; Allaert, B.; Ledoux, N.; Dragutan, I.; Dragutan, V.; Verpoort, F. *Coordination Chemistry Reviews* **2005**, *249*, 3055-3074.
- (71) Assessing the scope of the introduction of Schiff bases as co-ligands for monometallic and homobimetallic ruthenium ring-opening metathesis polymerization and ring-closing metathesis initiators. De Clercq, B.; Verpoort, F. *Advanced Synthesis & Catalysis* **2002**, *344*, 639-648.
- (72) Synthesis and characterization of new ruthenium-based olefin metathesis catalysts coordinated with bidentate Schiff-base ligands. Chang, S.; Jones, L., II; Wang, C.; Henling, L. M.; Grubbs, R. H. *Organometallics* **1998**, *17*, 3460-3465.
- (73) Activity of a new class of ruthenium based ring-closing metathesis and ring-opening metathesis polymerization catalysts coordinated with a 1,3-dimesityl-4,5-dihydroimidazol-2-ylidene and a Schiff base ligand. De Clercq, B.; Verpoort, F. *Tetrahedron Letters* **2002**, *43*, 9101-9104.
- (74) Synthesis and evaluation of a new class of ruthenium-based catalytic systems for atom transfer radical addition and enol ester synthesis. De Clercq, B.; Verpoort, F. *Journal of Organometallic Chemistry* **2003**, *672*, 11-16.

- (75) Synthesis of highly active ruthenium indenylidene complexes for atom-transfer radical polymerization and ring-opening-metathesis polymerization. Opstal, T.; Verpoort, F. *Angewandte Chemie, International Edition* **2003**, *42*, 2876-2879.
- (76) Mechanism and activity of ruthenium olefin metathesis catalysts. Sanford, M. S.; Love, J. A.; Grubbs, R. H. *Journal of the American Chemical Society* **2001**, *123*, 6543-6554.
- (77) A versatile precursor for the synthesis of new ruthenium olefin metathesis catalysts. Sanford, M. S.; Love, J. A.; Grubbs, R. H. *Organometallics* **2001**, *20*, 5314-5318.
- (78) The first highly active, halide-free ruthenium catalyst for olefin metathesis. Conrad, J. C.; Amoroso, D.; Czechura, P.; Yap, G. P. A.; Fogg, D. E. *Organometallics* **2003**, *22*, 3634-3636.
- (79) Highly efficient Ru-pseudohalide catalysts for olefin metathesis. Conrad, J. C.; Parnas, H. H.; Snelgrove, J. L.; Fogg, D. E. *Journal of the American Chemical Society* **2005**, *127*, 11882-11883.
- (80) Ruthenium metathesis catalysts containing chelating aryloxide ligands. Monfette, S.; Fogg, D. E. *Organometallics* **2006**, *25*, 1940-1944.

- (81) Ru-aryloxide metathesis catalysts with enhanced lability: Assessing the efficiency and homogeneity of initiation via ring-opening metathesis polymerization studies. Conrad, J. C.; Camm, K. D.; Fogg, D. E. *Inorganica Chimica Acta* **2006**, 359, 1967-1973.
- (82) Novel reactivity of ruthenium alkylidenes in protic solvents: Degenerate alkylidene proton exchange. Lynn, D. M.; Grubbs, R. H. *Journal of the American Chemical Society* **2001**, 123, 3187-3193.
- (83) Synthesis, structure, and activity of enhanced initiators for olefin metathesis. Love, J. A.; Sanford, M. S.; Day, M. W.; Grubbs, R. H. *Journal of the American Chemical Society* **2003**, 125, 10103-10109.
- (84) Cis- and trans-effects of ligands. Hartley, F. R. *Chemical Society Reviews* **1973**, 2, 163-179.
- (85) Improved one-pot synthesis of second-generation ruthenium olefin metathesis catalysts. Jafarpour, L.; Hillier, A. C.; Nolan, S. P. *Organometallics* **2002**, 21, 442-444.
- (86) Synthesis and activity for romp of bidentate Schiff base substituted second generation Grubbs catalysts. Allaert, B.; Dieltiens, N.; Ledoux, N.; Vercaemst, C.;

Van Der Voort, P.; Stevens, C. V.; Linden, A.; Verpoort, F. *Journal of Molecular Catalysis A: Chemical* **2006**, *260*, 221-226.

- (87) In situ generation of highly active olefin metathesis initiators. Ledoux, N.; Allaert, B.; Schaubroeck, D.; Monsaert, S.; Drozdak, R.; Voort, P. V. D.; Verpoort, F. *Journal of Organometallic Chemistry* **2006**, *691*, 5482-5486.
- (88) A new highly efficient ruthenium metathesis catalyst. Wakamatsu, H.; Blechert, S. *Angewandte Chemie, International Edition* **2002**, *41*, 2403-2405.
- (89) Ruthenium olefin metathesis catalysts with modified styrene ethers: Influence of steric and electronic effects. Zaja, M.; Connon, S. J.; Dunne, A. M.; Rivard, M.; Buschmann, N.; Jiricek, J.; Blechert, S. *Tetrahedron* **2003**, *59*, 6545-6558.
- (90) Water-soluble ruthenium alkylidene complexes: Synthesis and application to olefin metathesis in protic solvents. Lynn, D. M. Ph.D. Thesis, California Institute of Technology, 1999.
- (91) Four or five coordinate metal complexes useful in metathesis and other reactions, supported catalyst manufacture, and catalyst intermediates. Walter, F.; De Clercq, B. US Pat. App. US 2005043541, 2005.

- (92) Synthesis, characterization, and catalytic activity of a ruthenium carbene complex coordinated with bidentate 2-pyridine-carboxylato ligands. Hahn, F. E.; Paas, M.; Froehlich, R. *Journal of Organometallic Chemistry* **2005**, *690*, 5816-5821.
- (93) Ruthenium carbene complexes with *N,N'*-bis(mesityl)imidazol-2-ylidene ligands: RCM catalysts of extended scope. Furstner, A.; Thiel, O. R.; Ackermann, L.; Schanz, H.-J.; Nolan, S. P. *Journal of Organic Chemistry* **2000**, *65*, 2204-2207.
- (94) Comparative investigation of ruthenium-based metathesis catalysts bearing *N*-heterocyclic carbene (NHC) ligands. Furstner, A.; Ackermann, L.; Gabor, B.; Goddard, R.; Lehmann, C. W.; Mynott, R.; Stelzer, F.; Thiel, O. R. *Chemistry--A European Journal* **2001**, *7*, 3236-3253.
- (95) Synthesis and reactivity of neutral and cationic ruthenium(II) tris(pyrazolyl)borate alkylidenes. Sanford, M. S.; Henling, L. M.; Grubbs, R. H. *Organometallics* **1998**, *17*, 5384-5389.
- (96) Control of multivalent interactions by binding epitope density. Cairo, C. W.; Gestwicki, J. E.; Kanai, M.; Kiessling, L. L. *Journal of the American Chemical Society* **2002**, *124*, 1615-1619.

- (97) Influencing receptor-ligand binding mechanisms with multivalent ligand architecture. Gestwicki, J. E.; Cairo, C. W.; Strong, L. E.; Oetjen, K. A.; Kiessling, L. L. *Journal of the American Chemical Society* **2002**, *124*, 14922-14933.
- (98) Synthetic multivalent ligands as probes of signal transduction. Kiessling, L. L.; Gestwicki, J. E.; Strong, L. E. *Angewandte Chemie International Edition* **2006**, *45*, 2348-2368.
- (99) Catalytic activities of salicylaldehyde derivatives. V. Syntheses and catalytic activities of some trimethylammonio derivatives of salicylaldehyde in the racemization of L-glutamic acid. Ando, M.; Emoto, S. *Bulletin of the Chemical Society of Japan* **1978**, *51*, 2433-2434.
- (100) New soluble-polymer bound ruthenium carbene catalysts: Synthesis, characterization, and application to ring-closing metathesis. Varray, S.; Lazaro, R.; Martinez, J.; Lamaty, F. *Organometallics* **2003**, *22*, 2426-2435.
- (101) The catalytic intramolecular Pauson-Khand reaction: 2,3,3 α ,4-tetrahydro-2-[(4-methylbenzene) sulfonyl]cyclopenta[c]pyrrol-5(1*H*)-one. Patel, M. C.; Livinghouse, T.; Pagenkopf, B. L. *Organic Syntheses* **2003**, *80*, 93-103.

- (102) Synthesis of *N*-heterocyclic diols by diastereoselective pinacol coupling reactions. Handa, S.; Kachala, M. S.; Lowe, S. R. *Tetrahedron Letters* **2004**, *45*, 253-256.
- (103) Catalytic asymmetric cyclocarbonylation of nitrogen-containing enynes. Sturla, S. J.; Buchwald, S. L. *Journal of Organic Chemistry* **1999**, *64*, 5547-5550.
- (104) A new cycloisomerization catalyst of enynes. One-step syntheses of 3,4-dialkylidenetetrahydrofurans from allyl propargyl ethers. Le Paih, J.; Rodriguez, D. C.; Derien, S.; Dixneuf, P. H. *Synlett* **2000**, 95-97.
- (105) SADABS v.2.05, SAINT v.6.22, SHELXTL v.6.10
& SMART 5.622 Software Reference Manuals. Bruker-AXS; Bruker-AXS: Madison, WI, USA, 2000-2003.
- (106) Insect pheromones from olefin metathesis. Banasiak, D. S. *Journal of Molecular Catalysis A: Chemical* **1985**, *28*, 107-115.
- (107) Synthesis of conformationally restricted amino acids and peptides employing olefin metathesis. Miller, S. J.; Grubbs, R. H. *Journal of the American Chemical Society* **1995**, *117*, 5855-5856.

- (108) Sustainable concepts in olefin metathesis. Clavier, H.; Grela, K.; Kirschning, A.; Mauduit, M.; Nolan, S. P. *Angewandte Chemie International Edition* **2007**, *46*, 6786-6801.
- (109) Synthesis of glycopolymers of controlled molecular weight by ring-opening metathesis polymerization using well-defined functional group tolerant ruthenium carbene catalysts. Fraser, C.; Grubbs, R. H. *Macromolecules* **1995**, *28*, 7248-7255.
- (110) Living ring-opening metathesis polymerization in aqueous media catalyzed by well-defined ruthenium carbene complexes. Lynn, D. M.; Kanaoka, S.; Grubbs, R. H. *Journal of the American Chemical Society* **1996**, *118*, 784-790.
- (111) Aqueous catalytic polymerization of olefins. Mecking, S.; Held, A.; Bauers, F. M. *Angewandte Chemie International Edition* **2002**, *41*, 544-561.
- (112) Synthesis of sulfated neoglycopolymers: Selective P-selectin inhibitors. Manning, D. D.; Hu, X.; Beck, P.; Kiessling, L. L. *Journal of the American Chemical Society* **1997**, *119*, 3161-3162.
- (113) Varying the size of multivalent ligands: The dependence of concanavalin A binding on neoglycopolymer length. Kanai, M.; Mortell, K. H.; Kiessling, L. L. *Journal of the American Chemical Society* **1997**, *119*, 9931-9932.

- (114) Controlled self-assembly triggered by olefin metathesis: Cross-linked graphitic nanotubes from an amphiphilic hexa-peri-hexabenzocoronene. Jin, W.; Fukushima, T.; Kosaka, A.; Niki, M.; Ishii, N.; Aida, T. *Journal of the American Chemical Society* **2005**, *127*, 8284-8285.
- (115) Entropically driven ring-opening metathesis polymerization (ED-ROMP) of macrocyclic olefin-containing oligoamides. Tastard, C. Y.; Hodge, P.; Ben-Haida, A.; Dobinson, M. *Reactive & Functional Polymers* **2006**, *66*, 93-107.
- (116) Smid, J. In *Ions and Ion-Pairs in Organic Reactions*; Szwarc, M., Ed.; Wiley Interscience: New York, 1972.
- (117) The effect of coordination on the optical spectra of alkali metal cation-electron pairs in ethers. Seddon, W. A.; Fletcher, J. W.; Catterall, R.; Sopchyshyn, F. C. *Chemical Physics Letters* **1977**, *48*, 584-586.
- (118) Towards a second-generation aqueous Grubbs metathesis catalyst: Understanding ruthenium methylidene decomposition in the presence of water. Jordan, J. P.; Hong, S. H.; Grubbs, R. H. *Abstracts of Papers, 229th ACS National Meeting, San Diego, CA, United States, March 13-17, 2005* **2005**, INOR-619.

- (119) A practical and highly active ruthenium-based catalyst that effects the cross metathesis of acrylonitrile. Love, J. A.; Morgan, J. P.; Trnka, T. M.; Grubbs, R. H. *Angewandte Chemie, International Edition* **2002**, *41*, 4035-4037.
- (120) Effect of 1,2-dimethoxyethane on potato phosphorylase for polysaccharide specificity. Miller, J. F.; Graves, D. J. *Biochemical and Biophysical Research Communications* **1981**, *99*, 1377-1383.
- (121) Do organic solvents affect the catalytic properties of lipase? Intrinsic kinetic parameters of lipases in ester hydrolysis and formation in various organic solvents. van Tol, J. B.; Stevens, R. M.; Veldhuizen, W. J.; Jongejan, J. A.; Duine, J. A. *Biotechnology and Bioengineering* **1995**, *47*, 71-81.
- (122) Penicillin acylase catalysed synthesis of ampicillin in hydrophilic organic solvents. van Langen, L. M.; Oosthoek, N. H. P.; van Rantwijk, F.; Sheldon, R. A. *Advanced Synthesis & Catalysis* **2003**, *345*, 797-801.
- (123) A comparison of the activities of three beta-galactosidases in aqueous-organic solvent mixtures. Yoon, J. H.; McKenzie, D. *Enzyme and Microbial Technology* **2005**, *36*, 439-446.

- (124) Design, synthesis, and conformational analysis of eight-membered cyclic peptidomimetics prepared using ring closing metathesis. Creighton, C. J.; Leo, G. C.; Du, Y.; Reitz, A. B. *Bioorganic & Medicinal Chemistry* **2004**, *12*, 4375-4385.
- (125) *Biorefineries—Industrial Processes and Products*; Kamm, B.; Gruber, P. R.; Kamm, M., Eds.; Wiley-VCH: Weinheim, Germany, 2006.
- (126) *Facing the Hard Truths about Energy*. US National Petroleum Council.; Washington, DC, 2007.
- (127) *Top Value-Added Chemicals from Biomass, Volume I: Results of Screening for Potential Candidates from Sugars and Synthesis Gas*. Werpy, T.; Petersen, G.; Aden, A.; Bozell, J.; Holladay, J.; White, J.; Manheim, A.; Report No. DOE/GO-102004-1992; U.S. Department of Energy, Office of Scientific and Technical Information: Oak Ridge, TN, 2004; www1.eere.energy.gov/biomass/pdfs/35523.pdf.
- (128) *Biomass as Feedstock for a Bioenergy and Bioproducts Industry: The Technical Feasibility of a Billion-Ton Annual Supply*. Perlack, R. D.; Wright, L. L.; Turhollow, A. F.; Graham, R. L.; Stokes, B. J.; Erbach, D. C.; Report No. DOE/GO-102995-2135; U.S. Department of Energy and U.S. Department of Agriculture: Oak Ridge, TN, 2005; feedstockreview.ornl.gov/pdf/billion_ton_vision.pdf.

- (129) Liquid-phase catalytic processing of biomass-derived oxygenated hydrocarbons to fuels and chemicals. Chheda, J. N.; Huber, G. W.; Dumesic, J. A. *Angewandte Chemie International Edition* **2007**, *46*, 7164-7183.
- (130) Synthesis, chemistry and applications of 5-hydroxymethylfurfural and its derivatives. Lewkowski, J. *ARKIVOC* **2001**, 17-54.
- (131) Unsaturated *O*- and *N*-heterocycles from carbohydrate feed-stocks. Lichtenthaler, F. W. *Accounts of Chemical Research* **2002**, *35*, 728-737.
- (132) The blending octane numbers of 2:5-dimethylfuran. Nisbet, H. B. *J. Inst. Petrol.* **1946**, *32*, 162-166.
- (133) Production of dimethylfuran for liquid fuels from biomass-derived carbohydrates. Roman-Leshkov, Y.; Barrett, C. J.; Liu, Z. Y.; Dumesic, J. A. *Nature* **2007**, *447*, 982-986.
- (134) Metal chlorides in ionic liquid solvents convert sugars to 5-hydroxymethylfurfural. Zhao, H.; Holladay, J. E.; Brown, H.; Zhang, Z. C. *Science* **2007**, *316*, 1597-1600.

- (135) One-pot, two-step, practical catalytic synthesis of 2,5-diformylfuran from fructose. Halliday, G. A.; Young, R. J., Jr.; Grushin, V. V. *Organic Letters* **2003**, 5, 2003-2005.
- (136) Phase modifiers promote efficient production of hydroxymethylfurfural from fructose. Roman-Leshkov, Y.; Chheda, J. N.; Dumesic, J. A. *Science* **2006**, 312, 1933-1937.
- (137) Production of 5-hydroxymethylfurfural and furfural by dehydration of biomass-derived mono- and poly-saccharides. Chheda, J. N.; Roman-Leshkov, Y.; Dumesic, J. A. *Green Chemistry* **2007**, 9, 342-350.
- (138) Dehydration of fructose and sucrose into 5-hydroxymethylfurfural in the presence of 1-*H*-3-methyl imidazolium chloride acting both as solvent and catalyst. Moreau, C.; Finiels, A.; Vanoye, L. *Journal of Molecular Catalysis A: Chemical* **2006**, 253, 165-169.
- (139) Methods for conversion of carbohydrates in ionic liquids to value-added chemicals. Zhao, H.; Holladay, J. E.; Zhang, Z. C. US Patent Application 20080033187, 2008.
- (140) Ionic liquids: Solvent properties and organic reactivity. Chiappe, C.; Pieraccini, D. *Journal of Physical Organic Chemistry* **2005**, 18, 275-297.

- (141) Reactivity of ionic liquids. Chowdhury, S.; Mohan, R. S.; Scott, J. L. *Tetrahedron* **2007**, *63*, 2363-2389.
- (142) Applications of ionic liquids in carbohydrate chemistry: A window of opportunities. El Seoud, O. A.; Koschella, A.; Fidale, L. C.; Dorn, S.; Heinse, T. *Biomacromolecules* **2007**, *8*, 2629-2647.
- (143) Solution studies of cellulose in lithium chloride and *N,N*-dimethylacetamide. McCormick, C. L.; Callais, P. A.; Hutchinson, B. H., Jr. *Macromolecules* **1985**, *18*, 2394-2401.
- (144) The cellulose solvent system *N,N*-dimethylacetamide/lithium chloride revisited: The effect of water on physicochemical properties and chemical stability. Potthast, A.; Rosenau, T.; Buchner, R.; Roder, T.; Ebner, G.; Bruglachner, H.; Sixta, H.; Kosma, P. *Cellulose* **2002**, *9*, 41-53.
- (145) Determination of dissociation constants for ion pairs from kinetic data of bimolecular nucleophilic substitutions. I. The importance of solvation and ion pairing on the nucleophilic reactivity of the halide anions. Weaver, W. M.; Hutchison, J. D. *Journal of the American Chemical Society* **1964**, *86*, 261-265.

- (146) Mechanism of formation of 5-(hydroxymethyl)-2-furaldehyde from D-fructose and sucrose. Antal, M. J., Jr.; Mok, W. S. L.; Richards, G. N. *Carbohydrate Research* **1990**, *199*, 91-109.
- (147) Thermolysis of sucrose in dimethyl sulphoxide solution. Poncini, L.; Richards, G. N. *Carbohydrate Research* **1980**, *87*, 209-217.
- (148) Hydrolysis of glycosides under reducing conditions. Garegg, P. J.; Lindberg, B. *Carbohydrate Research* **1988**, *176*, 145-148.
- (149) The behaviour of d-fructose and inulin towards anhydrous hydrogen fluoride. Defaye, J.; Gadelle, A. *Carbohydrate Research* **1985**, *136*, 53-65.
- (150) Method for manufacturing lactic acid, 5-hydroxymethylfurfural, and furfural. Kono, T.; Matsuhisa, H.; Maehara, H.; Horie, H.; Matsuda, K. Jpn. Patent Application 2005232116, 2005.
- (151) Direct, high-yield conversion of cellulose into biofuel. Mascal, M.; Nikitin, E. B. *Angewandte Chemie International Edition* **2008**, *47*, 7924-7926.
- (152) Chlorocarbons and chlorohydrocarbons. Marshall, K. A. In *Kirk-Othmer Encyclopedia of Chemical Technology*; 5th ed.; Wiley-Interscience: New York, 2004; Vol. 6, p 226-253.

- (153) Effect of particle size based separation of milled corn stover on AFEX pretreatment and enzymatic digestibility. Chundawat, S. P. S.; Venkatesh, B.; Dale, B. E. *Biotechnology and Bioengineering* **2006**, 96, 219-231.
- (154) *Biochemical Production of Ethanol from Corn Stover: 2007 State of Technology Model*. Aden, A.; Report No. NREL/TP-510-43205; National Renewable Energy Laboratory: Golden, CO, 2008; <http://www.nrel.gov/docs/fy08osti/43205.pdf>.
- (155) *The Chemistry and Technology of Furfural and its Many By-Products*. Zeitsch, K. J.; Elsevier: Amsterdam, 2000.
- (156) Degradation reactions of cellulose and lignocellulose. Blazej, A.; Kosik, M. In *Cellulose and its Derivatives: Chemistry, Biochemistry, and Applications*; Kennedy, J. F., Phillips, G. O., Wedlock, D. J., Williams, P. A., Eds.; Ellis Horwood Ltd.: Chichester, England, 1985, p 97-117.
- (157) *Reactions of Hydrogen with Organic Compounds over Copper-Chromium Oxide and Nickel Catalysts*. Adkins, H. B.; University of Wisconsin Press: Madison, WI, 1937.
- (158) Process for preparing pure 5-hydroxymethylfurfuraldehyde. Rapp, K. M. US Patent 4740605, 1988.

- (159) Principles and applications of ion-exclusion chromatography. Fritz, J. S.
Journal of Chromatography **1991**, 546, 111-118.
- (160) Hydrogen production reactions from carbon feedstocks: Fossil fuels and biomass.
Navarro, R. M.; Peña, M. A.; Fierro, J. L. *Chemical Reviews* **2007**, 107, 3952-3991.
- (161) *CRC Handbook of Chemistry and Physics*; 65th ed.; Weast, R. C., Ed.; CRC Press: Boca Raton, 1984.
- (162) Hydroxymethylfurfural. Middendorp, J. A. *Recueil des Travaux Chimiques des Pays-Bas et de la Belgique* **1919**, 38, 1-71.
- (163) *Lignocellulosic Biomass to Ethanol Process Design and Economics Utilizing Co-Current Dilute Acid Prehydrolysis and Enzymatic Hydrolysis for Corn Stover*.
Aden, A.; Ruth, M.; Ibsen, K.; Jechura, J.; Neeves, K.; Sheehan, J.; Wallace, B.; Montague, L.; Slayton, A.; Report No. NREL/TP-510-32438; National Renewable Energy Laboratory: Golden, CO, 2002;
www.nrel.gov/docs/fy02osti/32438.pdf.
- (164) *Man's Conquest of Energy: Its Ecological and Human Consequences*. Hubbert, M. K.; Report No. TID-25857; Atomic Energy Commission: Oak Ridge, TN, 1972.

- (165) Carbon dioxide emissions from fossil-fuel use, 1751–1950. Andres, R. J.; Fielding, D. J.; Marland, G.; Boden, T. A.; Kumar, N.; Kearney, A. T. *Tellus* **1999**, *51B*, 759-765.
- (166) Global biofuel use, 1850–2000. Fernandes, S. D.; Trautmann, N. M.; Streets, D. G.; Roden, C. a.; Bond, T. C. *Global Biogeochemical Cycles* **2007**, *21*, 1-15.
- (167) Synthesis and characterization of furanic polyamides. Mitiakoudis, A.; Gandini, A. *Macromolecules* **1991**, *24*, 830-835.
- (168) Synthesis and properties of polyesters based on 2,5-furandicarboxylic acid and 1,4:3,6-dianhydrohexitols. Storbeck, R.; Ballauff, M. *Polymer* **1993**, *34*, 5003-5006.
- (169) Furans in polymer chemistry. Gandini, A.; Belgacem, M. N. *Progress in Polymer Science* **1997**, *22*, 1203-1379.
- (170) New polymer systems from Baylis-Hillman chemistry and biorenewable feedstocks. Venkitasubramanian, P.; Hagberg, E. C.; Bloom, P. D. *Polymer Preprints (American Chemical Society, Division of Polymer Chemistry)* **2008**, *49*, 914-915.

- (171) Efficient catalytic system for the selective production of 5-hydroxymethylfurfural from glucose and fructose. Yong, G.; Zhang, Y.; Ying, J. Y. *Angewandte Chemie International Edition* **2008**, 47, 9345-9348.
- (172) Simple chemical transformation of lignocellulosic biomass into furans for fuels and chemicals. Binder, J. B.; Raines, R. T. *Journal of the American Chemical Society* **2009**, 131, 1979-1985.
- (173) Dissolution of cellulose with ionic liquids. Swatloski, R. P.; Spear, S. K.; Holbrey, J. D.; Rogers, R. D. *Journal of the American Chemical Society* **2002**, 124, 4974-4975.
- (174) *Polysaccharides: Structural Diversity and Functional Versatility*; 2nd ed.; Dumitriu, S., Ed.; Marcel Dekker: New York, 2005.
- (175) Dilute acid hydrolysis of loblolly pine: A comprehensive approach. Marziale, T.; Valenzuela Olarte, M. B.; Sievers, C.; Hoskins, T. J. C.; Agrawal, P. K.; Jones, C. W. *Industrial & Engineering Chemistry Research* **2008**, 47, 7131-7140.
- (176) Review of processes and products for utilization of lactose in deproteinized milk serum. Hobman, P. G. *Journal of Dairy Science* **1984**, 67, 2630-2653.

- (177) Lactose: Properties and uses. Zadow, J. G. *Journal of Dairy Science* **1984**, 67, 2654-2679.
- (178) Non-food applications of milk components and dairy co-products: A review. Audic, J.-L.; Chaufer, B.; Daufin, G. *Lait* **2003**, 83, 417-438.
- (179) Highly efficient catalytic activity of lanthanide(III) ions for conversion of saccharides to 5-hydroxymethyl-2-furfural in organic solvents. Seri, K.-i.; Inoue, Y.; Ishida, H. *Chemistry Letters* **2000**, 22-23.
- (180) Catalytic activity of lanthanide(III) ions for the dehydration of hexose. Seri, K.-i.; Inoue, Y.; Ishida, H. *Bulletin of the Chemical Society of Japan* **2001**, 74, 1145-1150.
- (181) Hydrothermal upgrading of biomass to biofuel; studies on some monosaccharide model compounds. Srokol, Z.; Bouché, a.; Vanestrik, a.; Strik, R.; Maschmeyer, T.; Peters, J. *Carbohydrate Research* **2004**, 339, 1717-1726.
- (182) The composition of reducing sugars in dimethyl sulfoxide solution. Angyal, S. J. *Carbohydrate Research* **1994**, 263, 1-11.
- (183) The ¹³C N.M.R. spectra of the hexuloses. Angyal, S. J. *Australian Journal of Chemistry* **1976**, 29, 1249-1265.

- (184) Furfural: Hemicellulose/xylose- derived biochemical. Lee, J.-M.; Kim, Y.-C.; Hwang, I. T.; Park, N.-J.; Hwang, Y. K.; Chang, J.-S. *Biofuels, Bioproducts, and Biorefining* **2008**, 2, 438-454.
- (185) Furan derivatives. Kottke, R. H. In *Kirk-Othmer Encyclopedia of Chemical Technology*; Wiley-Interscience: New York, 2004.
- (186) Industrial development of furfural. Brownlee, H. J.; Miner, C. S. *Industrial and Engineering Chemistry* **1948**, 40, 201-204.
- (187) Production of furfural from corn stover hemicellulose. Sproull, R. D.; Bienkowski, P. R.; Tsao, G. T. *Biotechnology and Bioengineering Symposium* **1985**, 15, 561-577.
- (188) Selective preparation of furfural from xylose over microporous solid acid catalysts. Moreau, C.; Durand, R.; Peyron, D.; Duhamet, J.; Rivalier, P. *Industrial Crops and Products* **1998**, 7, 95-99.
- (189) Acid-catalysed hydrolysis of rice hull: Evalulation of furfural production. Mansilla, H. D.; Baeza, J.; Urzua, S.; Maturana, G.; Villasenor, J.; Duran, N. *Bioresource Technology* **1998**, 66, 189-193.

- (190) Modified versions of sulfated zirconia as catalysts for the conversion of xylose to furfural. Dias, A. S.; Lima, S.; Pillinger, M.; Valente, A. A. *Catalysis Letters* **2007**, *114*, 151-160.
- (191) Energetics of xylose decomposition as determined using quantum mechanics modeling. Nimlos, M. R.; Qian, X.; Davis, M.; Himmel, M. E.; Johnson, D. K. *Journal of Physical Chemistry A* **2006**, *110*, 11824-11838.
- (192) Mechanism of formation of 2-furaldehyde from D-xylose. Antal, M. J.; Richards, G. N. *Carbohydrate Research* **1991**, *217*, 71-85.
- (193) The formation of 2-furaldehyde and formic acid from pentoses in slightly acidic deuterium oxide studied by ¹H NMR spectroscopy. Ahmad, T.; Kenne, L.; Olsson, K.; Theander, O. *Carbohydrate Research* **1995**, *276*, 309-320.
- (194) A bottom-up assessment and review of global bio-energy potentials to 2050. Smeets, E. M. W.; Faaij, A. P. C.; Lewandowski, I. M.; Turkenburg, W. C. *Progress in Energy and Combustion Science* **2007**, *33*, 56-106.
- (195) Raw materials. Peters, D. *Advances in Biochemical Engineering / Biotechnology* **2007**, *105*, 1-30.

- (196) Lignocellulose conversion: An introduction to chemistry, process and economics. Lange, J.-P. *Biofuels, Bioproducts, and Biorefining* **2007**, *1*, 39-48.
- (197) Bulk chemicals from biomass. Van Haveren, J.; Scott, E. L.; Sanders, J. *Biofuels, Bioproducts, and Biorefining* **2008**, *2*, 41-57.
- (198) The renewable chemicals industry. Christensen, C. H.; Rass-Hansen, J.; Marsden, C. C.; Taarning, E.; Egeblad, K. *ChemSusChem* **2008**, *1*, 283-289.
- (199) Biomass recalcitrance: Engineering plants and enzymes for biofuels production. Himmel, M. E.; Ding, S.-Y.; Johnson, D. K.; Adney, W. S.; Nimlos, M. R.; Brady, J. W.; Foust, T. D. *Science* **2007**, *315*, 804-807.
- (200) Features of promising technologies for pretreatment of lignocellulosic biomass. Mosier, N.; Wyman, C. E.; Dale, B. E.; Elander, R. T.; Lee, Y. Y.; Holtzapple, M.; Ladisch, M. R. *Bioresource Technology* **2005**, *96*, 673-686.
- (201) Comparative sugar recovery data from laboratory scale application of leading pretreatment technologies to corn stover. Wyman, C. E.; Dale, B. E.; Elander, R. T.; Holtzapple, M.; Ladisch, M. R.; Lee, Y. Y. *Bioresource Technology* **2005**, *96*, 2026-2032.

- (202) Sur la conversion du corps ligneux en gomme, en sucre, et en un acide d'une nature particuliere, par le moyen de l'acide sulfurique; conversion de la meme substance ligneuse en ulmine par la potasse. Braconnot, H. *Annales de Chimie et de Physique* **1819**, 12, 172.
- (203) X. Contributions to the chemistry of cellulose. I. Cellulose-sulphuric acid, and the products of its hydrolysis. Stern, A. L. *Journal Of The Chemical Society, Transactions* **1895**, 74-90.
- (204) Heterogeneous aspects of acid hydrolysis of α -cellulose. Xiang, Q.; Lee, Y. Y.; Pettersson, P. O.; Torget, R. W. *Applied Biochemistry and Biotechnology* **2003**, 105, 505-514.
- (205) Conversion of wood to carbohydrates. Bergius, F. *Industrial and Engineering Chemistry* **1937**, 29, 247-253.
- (206) The perfecting of wood hydrolysis in the Rheinau process. Schoenemann, K. *Chimie et Industrie (Paris)* **1958**, 80, 140-150.
- (207) The saccharification of agricultural residues: A continuous process. Dunning, J. W.; Lathrop, E. C. *Industrial and Engineering Chemistry* **1945**, 37, 24-29.

- (208) Production of ethanol and chemicals from cellulosic materials. Tsao, G. T.; Ladisch, M. R.; Voloch, M.; Bienkowski, P. R. *Process Biochemistry* **1982**, 34-38.
- (209) *Evaluation of Sulfuric Acid Hydrolysis Processes for Alcohol Fuel Production*. Wright, J. D.; D'Agincourt, C. G.; Report No. SERI/TR-231-2074; Solar Energy Research Institute: Golden, CO, 1984.
- (210) Comparative technical evaluation of acid hydrolysis processes for conversion of cellulose to alcohol. Wright, J. D.; Power, A. J. In *Energy from biomass and wastes*; Institute of Gas Technology: Chicago, 1987; Vol. 10, p 949-971.
- (211) Fuel alcohol production from agricultural lignocellulosic feedstocks. Farina, G. E.; Barrier, J. W.; Forsythe, M. L. *Energy Sources* **1988**, 10, 231-237.
- (212) Method of producing sugars using strong acid hydrolysis. Farone, W. A.; Cuzens, J. E. U.S. Pat. US5726046, 1998.
- (213) New developments in the manufacture of cellulose fibers with ionic liquids. Hermanutz, F.; Meister, F.; Uerdingen, E. *Chemical Fibers International* **2006**, 6, 342-343.

- (214) Dissolution of cellulose with ionic liquids and its application: A mini-review.
Zhu, S.; Wu, Y.; Chen, Q.; Yu, Z.; Wang, C.; Jin, S.; Ding, Y.; Wu, G. *Green Chemistry* **2006**, 8, 325-327.
- (215) Efficient acid-catalyzed hydrolysis of cellulose in ionic liquid. Li, C.; Zhao, Z. K. *Advanced Synthesis and Catalysis* **2007**, 349, 1847-1850.
- (216) Acid in ionic liquid: An efficient system for hydrolysis of lignocellulose. Li, C.; Wang, Q.; Zhao, Z. K. *Green Chemistry* **2008**, 10, 177-182.
- (217) Depolymerization of cellulose using solid catalysts in ionic liquids. Rinaldi, R.; Palkovits, R.; Schüth, F. *Angewandte Chemie International Edition* **2008**, 47, 8047-8050.
- (218) Ionic-liquid-phase hydrolysis of pine wood. Sievers, C.; Valenzuela-Olarte, M. B.; Marzioletti, T.; Musin, I.; Agrawal, P. K.; Jones, C. W. *Industrial & Engineering Chemistry Research* **2009**, 48, 1277-1286.
- (219) Conversion method: A process for the preparation of water-soluble cellulose hydrolysis products using an ionic liquid. Fanselow, M.; Holbrey, J. D.; Seddon, K. R. Eur. Patent Application 1860201, 2007.

- (220) Kinetic model for the hydrolysis of lignocellulosic biomass in the ionic liquid, 1-ethyl-3-methyl-imidazolium chloride. Vanoye, L.; Fanselow, M.; Holbrey, J. D.; Atkins, M. P.; Seddon, K. R. *Green Chemistry* **2009**, *11*, 390-396.
- (221) Acid hydrolysis of cellulose in zinc chloride solution. Cao, N. J.; Xu, Q.; Chen, L. F. *Applied Biochemistry and Biotechnology* **1995**, *51*, 21-28.
- (222) Limitations of the DNS assay for reducing sugars from saccharified lignocellulosics. Rivers, D. B.; Gracheck, S. J.; Woodford, L. C.; Emert, G. H. *Biotechnology and Bioengineering* **1984**, *26*, 800-802.
- (223) Side reaction of cellulose with common 1-alkyl-3-methylimidazolium-based ionic liquids. Ebner, G.; Schiehser, S.; Potthast, A.; Rosenau, T. *Tetrahedron Letters* **2008**, *49*, 7322-7324.
- (224) Extended dissolution studies of cellulose in imidazolium based ionic liquids. Vitz, J.; Erdmenger, T.; Haensch, C.; Schubert, U. S. *Green Chemistry* **2009**, *11*, 417-424.
- (225) The acid strength of mono and diesters of phosphoric acid. The *n*-alkyl esters from methyl to butyl, the esters of biological importance, and the natural guanidine phosphoric acids. Kumler, W. D.; Eiler, J. J. *Journal of the American Chemical Society* **1943**, *65*, 2355-2361.

- (226) Chemical constitution and the dissociation constants of monocarboxylic acids.
Part XVIII. Some acetic and propionic acids substituted with hydrocarbon radicals in 10% and 25%(w/w) acetone–water solutions. Dippy, J. F. J.; Hughes, S. R. C.; Rozanski, A. *Journal of the Chemical Society* **1959**, 1441-1446.
- (227) Sugar purification by ion exclusion. Asher, D. R. *Industrial and Engineering Chemistry* **1956**, 48, 1465-1466.
- (228) Bacteria engineered for fuel ethanol production: Current status. Dien, B. S.; Cotta, M. A.; Jeffries, T. W. *Applied Microbiology and Biotechnology* **2003**, 63, 258-266.
- (229) Successful design and development of genetically engineered *Saccharomyces* yeasts for effective cofermentation of glucose and xylose from cellulosic biomass to fuel ethanol. Ho, N. W. Y.; Chen, Z.; Brainard, A. P.; Sedlak, M. *Advances in Biochemical Engineering / Biotechnology* **1999**, 65, 163-192.
- (230) Development of efficient xylose fermentation in *Saccharomyces cerevisiae*: Xylose isomerase as a key component. Van Maris, A. J. A.; Winkler, A. A.; Kuyper, M.; De Laat, W. T. A. M.; Van Dijken, J. P.; Pronk, J. T. *Advances in Biochemical Engineering / Biotechnology* **2007**, 108, 179-204.
- (231) Emerging technology for fermenting D-xylose. Jeffries, T. W. *Trends in Biotechnology* **1985**, 3, 208-212.

- (232) Fermentation of acid-pretreated corn stover to ethanol without detoxification using *Pichia stipitis*. Agbogbo, F. K.; Haagensen, F. D.; Milam, D.; Wenger, K. S. *Applied Biochemistry and Biotechnology* **2008**, *145*, 53-58.
- (233) Cellulosic ethanol production using the naturally occurring xylose-fermenting yeast, *Pichia stipitis*. Agbogbo, F. K.; Coward-Kelly, G. *Biotechnology Letters* **2008**, *30*, 1515-1524.
- (234) Enhanced hydrogen production from glucose by metabolically engineered *Escherichia coli*. Maeda, T.; Sanchez-Torres, V.; Wood, T. K. *Applied Microbiology and Biotechnology* **2007**, *77*, 879-890.
- (235) Non-fermentative pathways for synthesis of branched-chain higher alcohols as biofuels. Atsumi, S.; Hanai, T.; Liao, J. C. *Nature* **2008**, *451*, 86-89.
- (236) Biofuel alternatives to ethanol: Pumping the microbial well. Fortman, J.; Chhabra, S.; Mukhopadhyay, a.; Chou, H.; Lee, T.; Steen, E.; Keasling, J. *Trends in Biotechnology* **2008**, *26*, 375-381.
- (237) Catalytic conversion of biomass to monofunctional hydrocarbons and targeted liquid-fuel classes. Kunkes, E. L.; Simonetti, D. A.; West, R. M.; Serrano-Ruiz, J. C.; Gartner, C. A.; Dumesic, J. A. *Science* **2008**, *322*, 417-421.

- (238) Recent industrial applications of lignin: A sustainable alternative to nonrenewable materials. Lora, J. H.; Glasser, W. G. *Journal of Polymer and the Environment* **2002**, *10*, 39-48.
- (239) *Molecular Cloning: A Laboratory Manual*. Sambrook, J.; Russell, D. W.; 3rd ed.; Cold Spring Harbor Laboratory Press: Cold Spring Harbor, New York, 2001; Vol. 3.
- (240) Modeling of the bacterial growth curve. Zwietering, M. H.; Jongenburger, I.; Rombouts, F. M.; van't Riet, K. *Applied and Environmental Microbiology* **1990**, *56*, 1875-1881.
- (241) The selective incorporation of alkenes into proteins in *Escherichia coli*. Zhang, Z.; Wang, L.; Brock, A.; Schultz, P. G. *Angewandte Chemie International Edition* **2002**, *41*, 2840-2842.
- (242) Prolegomena to future experimental efforts on genetic code engineering by expanding its amino acid repertoire. Budisa, N. *Angewandte Chemie, International Edition* **2004**, *43*, 6426-6463.
- (243) Stereoselective incorporation of an unsaturated isoleucine analogue into a protein expressed in *E. coli*. Mock, M. L.; Michon, T.; van Hest, J. C. M.; Tirrell, D. A. *ChemBioChem* **2006**, *7*, 83-87.

- (244) Structural basis for the biological activities of bovine seminal ribonuclease.
Kim, J.-S.; Soucek, J.; Matousek, J.; Raines, R. T. *Journal of Biological Chemistry* **1995**, *270*, 10525-10530.
- (245) Engineering ribonuclease-based cancer therapeutics. Rutkoski, T. J. Ph.D. Thesis, University of Wisconsin-Madison, 2008.
- (246) The kinetics of inorganic reactions in solution. Sutin, N. *Annual Review of Physical Chemistry* **1966**, *17*, 119-172.
- (247) Mechanism of lactic acid formation catalyzed by a macrocyclic chromium(III) complex. A comparison with the glyoxalase I enzyme. Bang, E.; Eriksen, J.; Monsted, L.; Monsted, O. *Acta Chemica Scandinavica* **1994**, *48*, 12-19.
- (248) Mechanism of metal ion catalyzed carbohydrate transformations. Stoichiometry of aldopentose rearrangement processes catalyzed by a macrocyclic chromium(III) complex. Eriksen, J.; Monsted, L.; Monsted, O. *Acta Chemica Scandinavica* **1995**, *49*, 713-721.
- (249) Novel cellulose solutions. McCormick, C. L. US Patent 4278790, 1981.
- (250) Separation of amide solvents. Uchiama, K.; Tagawa, K. Jpn. Patent 61218563, 1986.

- (251) The lithium chloride/dimethylacetamide solvent for cellulose: A literature review. Dawsey, T. R.; McCormick, C. L. *Review of Macromolecular Chemistry and Physics* **1990**, C30, 405-440.
- (252) Solvation in cellulose-LiCl-DMA. Morgenstern, B.; Kammer, H.-W. *Trends in Polymer Science* **1996**, 4, 87-92.
- (253) The dimethylamine-carbon dioxide complex dimcarb and its preparative chemistry. Schroth, V. W.; Andersch, J.; Schadler, H.-D.; Spitzner, R. *Chemiker-Zeitung* **1989**, 113, 261-271.
- (254) Self-associated, “distillable” ionic media. Kreher, U. P.; Rosamilia, A. E.; Raston, C. L.; Scott, J. L.; Strauss, C. R. *Molecules* **2004**, 9, 387-393.
- (255) Reversible nonpolar-to-polar solvent. Jessop, P. G.; Heldebrant, D. J.; Li, X.; Eckert, C. A.; Liotta, C. L. *Nature* **2005**, 436, 1102.
- (256) Piperylene sulfone: A recyclable dimethyl sulfoxide substitute for copper-catalyzed aerobic alcohol oxidation. Jiang, N.; Vinci, D.; Liotta, C. L.; Eckert, C. A.; Ragauskas, A. J. *Industrial & Engineering Chemistry Research* **2007**, 47, 627-631.

- (257) Piperylene sulfone: A labile and recyclable DMSO substitute. Vinci, D.; Donaldson, M.; Hallett, J. P.; John, E. A.; Pollet, P.; Thomas, C. A.; Grilly, J. D.; Jessop, P. G.; Liotta, C. L.; Eckert, C. A. *Chemical Communications* **2007**, 1427-1429.
- (258) Distillable ionic liquids for a new multicomponent reaction. Rosamilia, A. E.; Strauss, C. R.; Scott, J. L. *Pure and Applied Chemistry* **2007**, 79, 1869-1877.
- (259) Switchable-polarity solvents prepared with a single liquid component. Phan, L.; Andreatta, J. R.; Horvey, L. K.; Edie, C. F.; Luco, A.-L.; Mirchandani, A.; Darensbourg, D. J.; Jessop, P. G. *Journal of Organic Chemistry* **2008**, 73, 127-132.
- (260) Switchable solvents consisting of amidine/alcohol or guanidine/alcohol mixtures. Phan, L.; Chiu, D.; Heldebrant, D. J.; Huttenhower, H.; John, E.; Li, X.; Pollet, P.; Wang, R.; Eckert, C. A.; Liotta, C. L.; Jessop, P. G. *Industrial & Engineering Chemistry Research* **2008**, 47, 539-545.
- (261) Syntheses in the purine and sugar group. Fischer, H. E. *Nobel Lecture* **1902**.